

This electronic thesis or dissertation has been downloaded from the King's Research Portal at <https://kclpure.kcl.ac.uk/portal/>



The effect of oil structure on the diffusion of solutes across synthetic membranes and human epidermis

Najib, Omaima Naji Mahmoud

Awarding institution:
King's College London

The copyright of this thesis rests with the author and no quotation from it or information derived from it may be published without proper acknowledgement.

END USER LICENCE AGREEMENT



Unless another licence is stated on the immediately following page this work is licensed

under a Creative Commons Attribution-NonCommercial-NoDerivatives 4.0 International

licence. <https://creativecommons.org/licenses/by-nc-nd/4.0/>

You are free to copy, distribute and transmit the work

Under the following conditions:

- Attribution: You must attribute the work in the manner specified by the author (but not in any way that suggests that they endorse you or your use of the work).
- Non Commercial: You may not use this work for commercial purposes.
- No Derivative Works - You may not alter, transform, or build upon this work.

Any of these conditions can be waived if you receive permission from the author. Your fair dealings and other rights are in no way affected by the above.

Take down policy

If you believe that this document breaches copyright please contact librarypure@kcl.ac.uk providing details, and we will remove access to the work immediately and investigate your claim.

**THE EFFECT OF OIL STRUCTURE ON THE DIFFUSION OF
SOLUTES ACROSS SYNTHETIC MEMBRANES AND HUMAN
EPIDERMIS**

Omaina Naji Najib
(BSc, Pharm)

Institute of Pharmaceutical Science

King's College London

A thesis submitted in partial fulfilment of the
requirements for the degree of Doctor of Philosophy

January, 2015

ABSTRACT

Dermal and transdermal delivery offers a number of potential advantages for drug delivery. However the skin provides an efficient barrier, preventing both excessive water loss from the body and the ingress of xenobiotics. Nevertheless, the vehicle used in the topical formulation can enhance the diffusion of a drug through membranes and reduce the barrier properties. It is hypothesized that oils and oil blends may interact with membranes to different extents depending on the physicochemical properties of the oil(s) and membrane. The aim of this study was to investigate the interaction of oily vehicles with different synthetic membranes (silicone, polyurethane (PU), high density polyethylene (HDPE) and cellulose acetate nitrate (CAN)) and human epidermis with a view to understanding the effect of the co-administration of oil blends on the permeation of model solutes (methyl parabens (MP), butyl parabens (BP) and caffeine (CF)).

A gas chromatographic method was developed and validated to quantify the amounts of oil sorbed by silicone membrane (the principal membrane employed). High pressure liquid chromatography was used to quantify the amount of model solute that permeated the membranes contained within Franz diffusion cells. The uptake of different oils (isopropyl myristate (IPM), oleic acid (OA), hexadecane, isohexadecane (IHD) and light liquid paraffin) by the membranes was studied by monitoring the change in weight and thickness of the membranes after immersion in oil. Multivariate analysis (principal component analysis and quantitative structure-property relationship) was used with a view to identifying the key molecular properties of vehicle components, permeants and the barrier membrane that influenced the permeation of the compounds through different membranes. These mathematical tools were also employed to understand and predict compound permeation across human epidermis from the oily vehicles.

The permeation studies of model permeants through silicone membrane and CAN membrane were performed using systems having the same thermodynamic activity. The flux values achieved from different vehicles were different, which indicated vehicle sorption by the membrane potentially altering membrane properties. In solvent uptake studies the buffer showed a greater affinity for the more hydrophilic

CAN membrane but induced no swelling of the silicone membrane. The amounts of each oil sorbed by CAN were low; whereas oils were sorbed in different amounts by the hydrophobic membranes. Preferential uptake of one oil over the other component was observed for some blended oil mixtures (for example, this occurred for IHD from OA:IHD blends). Whereas using other blends (for example, those comprising IPM:IHD) both oils entered the membrane in a similar ratio to that applied to the surface. The diffusion of MP from buffer through silicone membrane pre-treated with different oils, showed that as the amount of oil sorbed into silicone membrane increased the diffusion of the subsequently applied MP also increased. Diffusion of the model permeants through different membranes from pure oils showed that oil uptake affected the amount of (model) compound permeated. The highest flux values through human epidermis for all three model permeants were obtained using IHD as a vehicle. Multivariate analysis confirmed that the nature of the vehicle, membrane and permeant affect the permeability of the latter; particularly highlighting the shape of the oil molecule with respect to its uptake into membranes.

Oils added into formulations or mixtures are sorbed into the membranes in different amounts. Membrane properties are subsequently modified and the thermodynamic activity of permeant within the formulation is likely to be altered due to preferential oil sorption from the vehicle by the membrane. The flux of the permeants through the membranes was shown to be related to the extent of oil uptake and a complex interaction of physicochemical properties of vehicle, membrane and permeant. The novel approach of using multivariate analysis was found to be promising approach to disassociate the relative importance of the various factors that might influence the interaction and diffusion behaviour of vehicles and permeants with synthetic membranes and human epidermis.

This thesis is dedicated to my parents

ACKNOWLEDGEMENTS

I am sincerely grateful to my supervisor Professor Gary P. Martin for his guidance, encouragement and understanding, and for his assistance in reviewing the manuscript. Gratitude is also due to Dr. Darragh Murnane for his support, intellectual contributions, insightful comments and his very constructive suggestions and discussions throughout the work.

I would like to thank my co-advisor Professor Al-Sayed Sallam for sharing his scientific knowledge, attention to details, and for the guidance he provided throughout the various stages of this work.

I would also like to thank Dr Stewart Kirton for his support in multivariate data analysis.

I am thankful for the management of the International Pharmaceutical Research Centre (IPRC) for their financial support and for providing the facilities and equipments needed for the research.

Most of all, I owe my deepest gratitude to my family; my father, Professor Naji Najib, my mother and my sister for their encouragement, love, support, and for believing in me. I could not have reached this stage without their constant care and attention. I am also grateful for my husband Dr. Ali Al-Asali and my lovely sons Naji and Kareem for their love and support throughout this journey.

TABLE OF CONTENTS

Abstract	2
Acknowledgment	5
Abbreviations	11
List of Figures	14
List of Tables	21

CHAPTER ONE: INTRODUCTION AND AIMS OF STUDY

1.1 Introduction to dermal and transdermal drug delivery	
1.1.1 Background	26
1.1.2 Structure and barrier properties of the skin	28
1.1.2.1 Epidermis	29
1.1.2.2 Stratum corneum	30
1.1.2.3 Dermis	35
1.1.2.4 Hypodermis	36
1.2 Routes of drug permeation across the skin	36
1.3 Advantages and limitations of dermal and transdermal drug delivery	38
1.4 Theoretical basis for passive absorption and its enhancement	39
1.5 Factors affecting drug permeation through the skin	41
1.6 Properties of drugs that affect diffusion	42
1.7 Passive approaches to overcome the barrier nature of the skin	44
1.7.1 Vehicle / chemical enhancers	44
1.7.1.1 Vehicle permeation enhancement by reducing the diffusional resistance of the skin	49
1.7.1.2 Vehicle permeation enhancement by increasing solubility of drug in the skin	52
1.7.2 Supersaturation	52
1.7.3 Prodrugs or metabolic approach	54
1.7.4 Lipid vesicles	54
1.8 Oils incorporated in topical formulations	56
1.9 Assessment of in vitro permeation techniques	59
1.9.1 Diffusion cell	60
1.9.2 Membrane type	60
1.9.3 Temperature	63
1.9.4 Receptor fluid	63

1.9.5 Finite or infinite dose	64
1.9.6 Open or occluded system	65
1.10 Aims and objectives	66
1.11 Model oily vehicles	67

CHAPTER TWO: VALIDATION OF ANALYTICAL METHODS

2.1. Introduction	71
2.1.1 Model permeants	71
2.1.2 Reverse phase high performance liquid chromatography (HPLC) for quantification of model permeants	73
2.1.3 Gas chromatography	75
2.2 Aims & Objectives	77
2.3 Methods	
2.3.1 Materials	78
2.3.2 HPLC assay method validation	79
2.3.2.1 HPLC chromatographic conditions for model permeants	79
2.3.2.2 Calibration curve (linearity and range)	79
2.3.2.3 Repeatability (intra-day variation) and intermediate precision	79
2.3.2.4 Limit of detection and quantification	80
2.3.3 UV assay method	80
2.3.4 GC assay method validation	81
2.3.4.1 Calibration curve (linearity and range)	81
2.3.4.2 Repeatability (intra-day variation) and intermediate precision and accuracy	83
2.3.4.3 Limit of detection and quantification	83
2.3.5 In vitro permeation method validation	83
2.3.5.1 Membrane vehicle interference study	83
2.3.5.2 Preparation of human epidermal sheets	83
2.3.5.3 Determination of permeant binding to filter paper	84
2.3.5.4 Effect of skin-filter paper composite	85
2.4. Results	
2.4.1 HPLC method validation	85
2.4.1.1 Calibration curve (linearity and range)	85
2.4.1.2 Precision (intra-and inter-day), accuracy, limit of detection and quantification	87
2.4.2 UV method validation	88
2.4.3 GC Analytical methods	89

2.4.3.1 Calibration curve (linearity and range)	89
2.4.3.2 Precision (intra- and inter-day), accuracy, limit of detection and quantification	92
2.4.4 In vitro permeation method validation	95
2.4.4.1 Membrane vehicle interference study	95
2.4.4.2 Permeant-filter paper binding study	95
2.4.4.3 Skin-permeant assay interference	96
2.5 Discussion	96

CHAPTER THREE: DIFFUSION OF MODEL PERMEANTS FROM OIL BLENDS

3.1 Introduction	102
3.1.1 Partition diffusion process	102
3.1.2 Formulation components affecting flux across membrane	102
3.2 Aims and Objectives	105
3.3 Methods	105
3.3.1 Materials	105
3.3.2 Solubility studies	105
3.3.3 Franz cell studies	106
3.3.3.1 Cellulose acetate nitrate membrane	106
3.3.3.2. Silicone membrane	107
3.4 Results	
3.4.1 Solubility studies of model permeants in donor/receptor fluid and deionised water	108
3.4.2 Franz cell studies	110
3.4.2.1 Cellulose acetate nitrate membrane diffusion studies from oils and oil combinations	110
3.4.2.2 Silicone membrane diffusion studies from oils and oil combinations	114
3.5 Discussion	120

CHAPTER FOUR: INTERACTION OF OILS WITH MODEL MEMBRANES

4.1 Introduction	131
4.1.1 Interaction with membranes	133
4.1.2 Factors effecting vehicle interactions with membrane	135

4.1.2.1 Molecular weight, shape and polarity	135
4.1.2.2 Hydrogen bond capacity	136
4.1.2.3 Solubility parameter	137
4.1.2.3.1 Hansen solubility parameter	139
4.2 Aims and objectives	141
4.3 Methods	
4.3.1 Materials	142
4.3.2 Membrane swelling experiments	142
4.3.2.1 Membrane weight	143
4.3.2.2 Kinetic study of membrane swelling	143
4.3.3 Quantification of oil uptake by silicone membrane from oil blends	144
4.3.3.1 Preliminary studies	144
4.3.3.2 Membrane extraction method	144
4.3.3.3 GC analysis	145
4.3.3.4 Calculation of amount absorbed	145
4.3.4 Determination of composition of the oil in donor compartment	145
4.3.5 Effect of membrane pre-treatment with oil on permeant diffusion	146
4.3.5.1 Franz cell experiment	146
4.3.5.2. HPLC analysis of MP	147
4.3.5.3 Calculation of enhancement ratio	147
4.3.6 Calculation of Hansen solubility parameter and spheres	148
4.3.7. Statistical analysis	148
4.4 Results	
4.4.1 Swelling data for model permeants in membranes	148
4.4.2 Kinetic study of silicone membrane swelling	149
4.4.3 Quantification of oil uptake by silicone membrane from oil blends	150
4.4.3.1 Change in membrane weight	150
4.4.3.2 Measurement of oil uptake by silicone membrane	152
4.4.4 Determination of composition of the oil in donor compartment	159
4.4.5 Effect of membrane pre-treatment on permeant diffusion	160
4.4.6 Hansen Solubility Parameter values and plots	161
4.5 Discussion	168

CHAPTER FIVE

THE APPLICATION OF MULTIVARIATE ANALYSIS ON THE UPTAKE AND PERMEATION STUDIES

5.1 Introduction	182
5.1.1 Multivariate analysis	182
5.1.2 Quantitative structure property relationships	183
5.1.3 Principal component analysis	186
5.1.4 Data pre-treatment	189
5.2 Aims and objectives	190
5.3 Methods	
5.3.1 Materials	192
5.3.2 Franz cells studies	192
5.3.2.1 Synthetic membranes	192
5.3.2.1.1 Diffusion through silicone membrane	192
5.3.2.1.2 Diffusion through high density polyethylene and polyurethane membranes	192
5.3.2.2 Human epidermis	193
5.3.2.2.1 Preparation of epidermal sheets	193
5.3.2.2.2 Diffusion through human epidermis	193
5.3.3 Statistical analysis	194
5.4 Results	
5.4.1 Synthetic membranes diffusion studies	196
5.4.2 Human epidermis diffusion studies	199
5.4.3 Statistical analysis	203
5.4.3.1 Data pre-treatment	203
5.4.3.2 Quantitative structure-property relationships	208
5.4.3.3 Principal component analysis	214
5.5 Discussion	227

CHAPTER SIX:

GENERAL DISCUSSION

6.1 General Discussion	248
Appendices	258
(I) Definitions of molecular descriptors used in PCA analysis	259
(II) Correlation matrix for different independent and dependent variables	263
References	267

ABBREVIATIONS

a_nC	Number of carbon atoms	C_s	Concentration of penetrant in vehicle
a_nH	Number of hydrogen atoms	C_v	Saturated solubility
a_nO	Number of oxygen atoms	D	Diffusion coefficient
ANOVA	a one-way analysis of variance	DIW	Deionised water
Azone	1-dodecylazacycloheptan-2-one	E_v	Energy of vaporization
BP	Butyl paraben	ER	Enhancement ratios
b_1rotN	Number of rotatable single bonds.	GC	Gas chromatography
b_1rotR	Fraction of rotatable single bonds	GRAS	Generally regarded as safe
b_ar	Number of aromatic bonds.	h	hour
b_count	Number of bonds	H-bond	Hydrogen bond
b_double	Number of double bonds..	HD	Hexadecane
b_rotN	Number of rotatable bonds	HDPE	High density poly ethylene
b_rotR	Fraction of rotatable bonds	HPLC	High performance liquid chromatography
b_single	Number of single bonds	HSP	Hansen solubility parameter
balabanJ	Balaban's connectivity topological index	HSPiP	Hansen solubility parameter in practice
CAN	Cellulose acetate nitrate	IHD	Isohexadecane
chi0	Atomic connectivity index	IPM	Isopropyl myristate
chi0_C	Carbon connectivity index (order 0).	Js	Steady state flux
chi1	Atomic connectivity index (order 1)	K'	Partition coefficient
chi1_C	Carbon connectivity index (order 1).	Kier1	First kappa shape index
chi0v	Atomic valence connectivity index (order 0)	Kier2	Second kappa shape index
chi0v_C	Carbon valence connectivity index (order 0).	Kier3	Third kappa shape index
CF	Caffeine		

Kierflex	Kier molecular flexibility index	opr_brigid	The number of rigid bonds
K_{o/w}	Octanol–water partition coefficient	opr_nring	The number of ring bonds
K_p	Permeability coefficient	opr_nrot	The number of rotatable bonds
L	Length of the diffusion pathway	P	Partition coefficient
lip_acc	The number of O and N atoms.	PC	Principal component
lip_don	The number of OH and NH atoms.	PCA	Principal Component Analysis
LOD	Limit of detection	PU	Poly urethane
LOQ	Limit of quantification	QSPR	Quantity structure-permeability relationship
LP	Liquid paraffin	Q_VSA_H	
m	Membrane	YD	Total hydrophobic van der
MP	Methyl paraben	PEOE_VS	Waals surface area
MPt	Melting point	A_HYD	
m_{upt}	Relative mass uptake of each oil of membrane	Q_VSA_F	Fractional polar van der
m_{GC}	Amount of oil quantified by GC	POL	Waals surface area
m_T	Total amount of oil sorbed	PEOE_VS	
m_{2GC}	Amount of second oil quantified by GC	A_FPOL	
Mvol	Molecular volume	Q_VSA_F	
Mwt	Molecular weight	HYD	Fractional hydrophobic van
n, N	number of observations	PEOE_VS	der Waals surface area
OA	Oleic acid	A_FHYD	
OECD	Organisation for Economic Co-Operation and Development	Q_VSA_P	
		OL	Total polar van der Waals
		PEOE_VS	Surface area
		A_POL	

R	Universal gas constant	W_b	Weight of membrane before soaking
RED	Relative energy difference	ΔH_v	Heat of vaporization
RSD	Relative standard deviation	a_v	Thermodynamic activity
sd, SD	Standard deviation	α	Hydrogen bond donor acidity
T	Absolute temperature	β	Hydrogen bond acceptor basicity
t_a	Thickness of membrane after soaking	δ_D	The dispersive component of HSP
t_b	Thickness of membrane before soaking	δ_P	The polar component of HSP
TPSA	Polar surface area	δ_H	The hydrogen bond component of HSP
UV	Ultraviolet	δ_T	Hildebrand solubility parameter
V_m	Molar volume	γ_v	Activity coefficient
vdw_are a	Area of van der Waals surface	τ	Membrane tortuosity
vdw_vol	Van der Waals volume.	ε	Membrane porosity
W	Weight		
W_a	Weight of membrane after soaking		

LIST OF FIGURES

Figure 1.1	Anatomy and physiology of the skin, showing the potential targets or site of action for cosmetics and drugs	27
Figure 1.2	Corneocyte lipid bilayers	31
Figure 1.3	Molecular organizations of stratum corneum lipids. Schemes of the chain conformation and lateral chain packing in orthorhombic, hexagonal and liquid-crystalline phases of long-chain lipids	34
Figure 1.4	Possible pathways through the stratum corneum	37
Figure 1.5	Schematic representation of the mechanisms by which a chemical enhancer may interact with stratum corneum intercellular lipids	46
Figure 1.6	Action of enhancers (particularly solvents) on the protein component of the stratum corneum, leading to fissuring of intercellular lipids, splitting of stratum corneum squames, keratin denaturation and vacuole formation in corneocytes	46
Figure 2.1	Structure of (a) methyl paraben (b) caffeine (c) butyl paraben	71
Figure 2.2	Schematic representation of Franz diffusion cell used for in vitro Permeation studies	84
Figure 2.3	HPLC Chromatogram of a standard comprising 20 $\mu\text{g mL}^{-1}$ CF in 15% v/v acetonitrile/ 85% phosphate buffer wave length 270 nm	86
Figure 2.4	Linearity of HPLC calibration curves showing mean peak areas (absorbance units $\times 10^{-4}$) as a function of concentration of methyl paraben, butyl paraben and caffeine in phosphate buffer	86
Figure 2.5	Calibration curves for UV method showing absorbance as versus concentration for methyl paraben butyl paraben and caffeine	89
Figure 2.6	GC Chromatogram generated after injecting a heptane solution containing 0.1 mg mL^{-1} IHD and 0.1 mg mL^{-1} IPM	90
Figure 2.7	GC Chromatogram generated after injecting a heptane solution containing 1 mg mL^{-1} IHD and 1 mg mL^{-1} HD	90

Figure 2.8	GC calibration curves showing mean peak areas (arbitrary units) as a function of concentration (mg mL^{-1}) of IHD and IPM	91
Figure 2.9	GC calibration curves showing mean peak areas (arbitrary units) as a function of concentration (mg mL^{-1}) of IHD and HD	91
Figure 2.10	GC calibration curves showing mean peak areas (arbitrary units) as a function of concentration (mg mL^{-1}) of IPM and HD	92
Figure 3.1	Solubility (mg mL^{-1}) in 100 % IHD, OA, IPM, LP, HD and different oil blends containing IHD or HD at 32°C (a) MP solubility in IHD blends (b) MP solubility in HD blends (c) BP solubility in IHD blends (d) BP solubility in HD blends (e) CF solubility in IHD blends (f) CF solubility in HD blends	109
Figure 3.2	The cumulative amount of MP diffusing through cellulose acetate nitrate membrane into the receptor compartment from the different vehicles as a function of time HD, IHD, LP, OA and IPM	110
Figure 3.3	The cumulative amount of BP diffusing through cellulose acetate nitrate membrane into the receptor compartment from the different vehicles as a function of time HD, IHD, LP, OA and IPM	111
Figure 3.4	The cumulative amount of CF diffusing through cellulose acetate nitrate membrane into the receptor compartment from the different vehicles as a function of time HD, IHD, LP, OA and IPM	111
Figure 3.5	Rates of permeation obtained for MP diffusion through cellulose acetate nitrate membrane from different oil combinations comprising IHD with LP, IPM, HD and OA	112
Figure 3.6	Rates of permeation obtained for BP diffusion through cellulose acetate nitrate membrane from different oil combinations comprising IHD with LP, IPM, HD and OA	113
Figure 3.7	Rates of permeation obtained for MP and BP diffusion through cellulose acetate nitrate membrane from different oil combinations comprising HD with LP	113

Figure 3.8	The cumulative amount of MP diffused across silicone membrane into the receptor compartment from the different vehicles as a function of time HD, IHD, LP, OA and, IPM	114
Figure 3.9	The cumulative amount of BP diffused across silicone membrane into the receptor compartment from the different vehicles as a function of time HD, IHD LP, OA and IPM	115
Figure 3.10	The cumulative amount of CF diffused across silicone membrane into the receptor compartment from the different vehicles as a function of time HD, IHD, LP OA and, IPM	115
Figure 3.11	Flux values obtained for MP diffusion through silicone membrane from different oil combinations comprising IHD with LP, IPM, HD and OA	117
Figure 3.12	Flux values obtained for MP diffusion through silicone membrane from different oil combinations comprising HD with LP and IPM	118
Figure 3.13	Flux values obtained for BP diffusion through silicone membrane from different oil combinations comprising IHD with LP, IPM, HD and OA	118
Figure 3.14	Flux values obtained for BP diffusion through silicone membrane from different oil combinations comprising HD with LP and IPM	119
Figure 3.15	Flux values obtained for CF diffusion through silicone membrane from different oil combinations comprising IHD with LP, IPM, HD and OA	119
Figure 3.16	Flux values obtained for CF diffusion through silicone membrane from different oil combinations comprising HD with LP	120
Figure 4.1	Structure of (a) isopropyl myristate (b) oleic acid (c) hexadecane (d) isohexadecane	131
Figure 4.2	An example of Hansen sphere: the orthogonal axes are the Hansen solubility parameters corresponding to; x-axis, $D=\delta_D$ (the dispersion force component), y-axis, $P=\delta_P$ (the polar component) and z-axis, $H=\delta_H$ (the hydrogen bonding component)	140
Figure 4.3	Percentage differences in weight of silicone membrane during soaking in IPM/IHD blends for 24 h at 32°C	150

Figure 4.4	Percentage weight changes in silicone membrane immersed in different oil combinations comprising IHD with HD, IPM, LP and OA for approximately 17 h at 32°C	150
Figure 4.5	Percentage weight changes in silicone membrane immersed in different oil combinations comprising HD with IHD, IPM, LP and OA for approximately 17 h at 32°C.	151
Figure 4.6	Percentage weight changes in silicone membrane immersed in different oil combinations comprising IPM with HD, IHD, LP and OA for approximately 17 h at 32°C	151
Figure 4.7	Percentage of individual oils extracted from silicone membrane after being incubated for approximately 17 h at 32°C in IPM/IHD blends expressed as a function of the percentage of IHD in solution	153
Figure 4.8	Percentage of individual oils extracted from silicone membrane after being incubated for approximately 17 h at 32°C in HD/IHD blends expressed as a function of the percentage of IHD in solution	153
Figure 4.9	Percentage of individual oils extracted from silicone membrane after being incubated for approximately 17 h at 32°C in LP/IHD blends expressed as a function of the percentage of IHD in solution	154
Figure 4.10	Percentage of individual oils extracted from silicone membrane after being incubated for approximately 17 h at 32°C in OA/IHD blends expressed as a function of the percentage of IHD in solution	154
Figure 4.11	Percentage of individual oils extracted from silicone membrane after being incubated for approximately 17 h at 32°C in IPM/HD blends expressed as a function of the percentage of HD in solution	155
Figure 4.12	Percentage of individual oils extracted from silicone membrane after being incubated for approximately 17 h at 32°C in LP/IPM blends expressed as a function of the percentage of IPM in solution	155
Figure 4.13	Percentage of individual oils extracted from silicone membrane after being incubated for approximately 17 h at 32°C in OA/IPM blends expressed as a function of the percentage of IPM in solution	156

Figure 4.14	Percentage of individual oils extracted from silicone membrane after being incubated for approximately 17 h at 32°C in LP/HD blends expressed as a function of the percentage of HD in solution	157
Figure 4.15	Percentage of individual oils extracted from silicone membrane after being incubated for approximately 17 h at 32°C in OA/HD blends expressed as a function of the percentage of HD in solution	157
Figure 4.16	Percentage of individual oils (HD/IHD blends) remaining in the donor compartment after six hours, expressed as a function of the percentage of IHD applied in solution	159
Figure 4.17	MP permeation profile through pre-treated silicone membrane showing the cumulative amount of MP in the receptor compartment from buffer as a function of time. Permeation was measured after pre-treatment of the membrane by soaking for approximately 17 h at 32°C in either IHD, HD, LP or buffer	160
Figure 4.18	Schematic of the Hansen Solubility sphere. Each axis is one of the three component Hansen solubility parameters, δ_D , δ_H , or δ_P . The centre of the sphere (green symbol) represents the three-dimensional solubility parameter for the silicone membrane. The blue symbols are the Hansen solubility parameters of oils used in this investigation	163
Figure 4.19	Schematic of the Hansen Solubility sphere. Each axis is one of the three component Hansen solubility parameters, δ_D , δ_H , or δ_P . The centre of the sphere (green symbol) represents the three-dimensional solubility parameter for the silicone membrane. The blue symbols are the Hansen solubility parameters of oils used in this investigation	163
Figure 4.20	Schematic of the Hansen Solubility sphere. Each axis is one of the three component Hansen solubility parameters, δ_D , δ_H , or δ_P . The centre of the sphere (green symbol) represents the three-dimensional solubility parameter for the silicone membrane. The blue symbols are the Hansen solubility parameters of oils used in this investigation	164
Figure 5.1	Data after mean-centering and unit variance scaling all variables will have equal length and mean value zero	190

Figure 5.3	An example of the cumulative amount of methyl paraben permeated across silicone, high density polyethylene and poly urethane membranes versus time when applied in IHD	196
Figure 5.4	Comparative flux data for methyl paraben across silicone, high density polyethylene and polyurethane membranes when applied in different oils and phosphate buffer	197
Figure 5.5	Comparative flux data for butyl paraben across silicone, high density polyethylene and polyurethane membranes when applied in different oils and phosphate buffer	198
Figure 5.6	Comparative flux data for caffeine across silicone and high density polyethylene membranes when applied in different oils and phosphate buffer	198
Figure 5.7	Comparative flux data for caffeine across polyurethane membrane when applied in different oils and phosphate buffer	199
Figure 5.8	Skin permeation profiles showing the cumulative amount of MP in the receptor compartment from the different vehicles as a function of time buffer, IPM, LP, IHD, OA and HD	200
Figure 5.9	Skin permeation profiles showing the cumulative amount of BP in the receptor compartment from the different vehicles as a function of time buffer, IPM, LP, IHD, OA and HD	200
Figure 5.10	Skin permeation profiles showing the cumulative amount of CF in the receptor compartment from the different vehicles as a function of time buffer, IPM, LP, IHD, OA and HD	201
Figure 5.11	(A) Score plot from the PCA of solvent uptake of vehicles into membranes showing the grouping of scores representing different vehicles. The two displayed PCs explain 76 % of the total variability; 45% and 31% of the variability are explained by PC1 and PC2 respectively. (B) Loading plots from the PCA of the solvent uptake of vehicles into membranes showing descriptors explaining the solvent uptake	216

- Figure 5.12 (A) Score plot from PCA showing the relationship between permeant-oily vehicle –membrane descriptors with flux. The two displayed PCs explain 54 % of the total variability; 33% and 21% of the variability are explained by PC1 and PC2 respectively. (B) Loading plots from PCA showing the relationship between permeant-oily vehicle –membrane descriptors with flux 220
- Figure 5.13 (A) Score plot from PCA showing the relationship between permeant-oily vehicle –membrane descriptors with K_p . The two displayed PCs explain 54 % of the total variability; 34% and 20% of the variability are explained by PC1 and PC2 respectively. (B) Loading plots from PCA showing the relationship between permeant-oily vehicle –membrane descriptors with K_p 222
- Figure 5.14 (A) Score plot from PCA showing the relationship between permeant- oily vehicles – membrane descriptors with lag time. The two displayed PCs explain 55 % of the total variability; 31% and 24% of the variability are explained by PC1 and PC2 respectively. (B) Loading plots from PCA showing the relationship between permeant- oily vehicles – membrane descriptors with lag time 224
- Figure 5.15 (A) Score plot from PCA showing the relationship between permeant-oily vehicles descriptor with epidermis flux. The two displayed PCs explain 33% and 26% of the variance, respectively. (B) Loading plots from PCA showing the relationship between permeant-oily vehicle descriptors with epidermis flux 226

LIST OF TABLES

Table 1.1	Examples of penetration enhancers used in commercial transdermal and topical products	48
Table 2.1	Physicochemical parameters of model permeants	72
Table 2.2	Materials used	78
Table 2.3	Analytical parameters for the GC quantification of IPM/IHD, IHD/HD and IPM/HD mixtures	82
Table 2.4	Intra- and inter-day repeatability and precision (%RSD) obtained from HPLC chromatograms for MP, BP and CF standards of different concentration prepared in phosphate buffer	87
Table 2.5	Linear regression analysis for calibration curves of MP, BP and CF on three different days, for peak area response ($\times 10^4$) plotted as a function of concentration	88
Table 2.6	Intra- and inter-day repeatability and precision (%RSD) obtained from GC chromatograms for IHD and HD standards of different concentrations prepared in heptane	92
Table 2.7	Intra- and inter-day repeatability and precision (%RSD) obtained from GC chromatograms for IHD and HD standards of different concentrations prepared in heptanes	93
Table 2.8	Intra- and inter-day repeatability and precision (%RSD) obtained from GC chromatograms for IPM and HD standards of different concentrations prepared in heptane	93
Table 2.9	Linear regression analysis for calibration curves of IHD and IPM on three different days, for peak area response ($\times 10^7$) plotted as a function of concentration	94
Table 2.10	Linear regression analysis for calibration curves of IHD and HD on three different days, for peak area response ($\times 10^6$) plotted as a function of concentration	94

Table 2.11	Linear regression analysis for calibration curves of IPM and HD on three different days, for peak area response ($\times 10^7$) plotted as a function of concentration	95
Table 2.12	The amount of MP, BP and CF expressed as a percentage (%) of the original standard concentration of model permeant recovered from receptor chamber of Franz cell after 8 h	96
Table 3.1	Solubility (mg mL^{-1}) of the model permeants in IPM, OA, IHD, HD, LP, deionised water and phosphate buffer at 32°C	108
Table 3.2	Silicone membrane permeation parameters permeability coefficients and fluxes for MP, BP and CF	116
Table 4.1	Properties of the oils used in this investigation	132
Table 4.2	Some parameters and properties of oils used in this investigation	133
Table 4.3	Physicochemical characteristics of membranes employed in this investigation	142
Table 4.4	Amount of oil indifferent membranes after being soaked in different vehicles for approximately 17 h at 32°C ($\text{mg oil/ g membrane}$)	149
Table 4.5	The percentage difference in weight of membranes after being soaked in different vehicles for approximately 17 h at 32°C	149
Table 4.6	Total amount of oil extracted and quantified by GC ($\text{mg oil/ g membrane}$) after incubation at 32°C for 17 h	158
Table 4.7	Amount of oil extracted from silicone membrane after immersion for 17 h at 32°C in various IHD oil blends and quantified by GC ($\text{mg oil/ g membrane}$)	158
Table 4.8	Amount of oil extracted from silicone membrane after immersion for 17 h at 32°C in various IPM oil blends and quantified by GC ($\text{mg oil/ g membrane}$)	158
Table 4.9	Amount of oil extracted from silicone membrane after immersion for 17 h at 32°C in various HD oil blends and quantified by GC ($\text{mg oil/ g membrane}$)	159
Table 4.10	MP fluxes from buffer through silicone membrane pre-treated with IHD, HD, LP and buffer	160

Table 4.11	Hansen Solubility Parameter values and molecular volume of oils used	161
Table 4.12	Relative energy differences (RED) values expressed for the oils when compared with different membranes	162
Table 4.13	Hansen solubility parameter (HSP) distance between the HSP of the oils and different membranes MPa ^{1/2}	162
Table 4.14	Hansen solubility parameters (HSP) values and distance between the HSP of the IHD/IPM oil blends and silicone membranes MPa ^{1/2}	164
Table 4.15	Hansen solubility parameters (HSP) values and distance between the HSP of the HD/IPM oil blends and silicone membranes MPa ^{1/2}	165
Table 4.16	Hansen solubility parameters (HSP) values and distance between the HSP of the IHD/HD oil blends and silicone membranes MPa ^{1/2}	165
Table 4.17	Hansen solubility parameters (HSP) values and distance between the HSP of the IHD/OA oil blends and silicone membranes MPa ^{1/2}	165
Table 4.18	Hansen solubility parameters (HSP) values and distance between the HSP of the HD/OA oil blends and silicone membranes MPa ^{1/2}	166
Table 4.19	Hansen solubility parameters (HSP) values and distance between the HSP of the IPM/OA oil blends and silicone membranes MPa ^{1/2}	166
Table 4.20	Hansen solubility parameters (HSP) values and distance between the HSP of the IHD/LP oil blends and silicone membranes MPa ^{1/2}	166
Table 4.21	Hansen solubility parameters (HSP) values and distance between the HSP of the HD/LP oil blends and silicone membranes MPa ^{1/2}	167
Table 4.22	Hansen solubility parameters (HSP) values and distance between the HSP of the IPM/LP oil blends and silicone membranes MPa ^{1/2}	167
Table 5.1	The in vitro skin permeation parameters permeability coefficients and fluxes for MP, BP and CF	202
Table 5.2	An example of a correlation matrix	204
Table 5.3	The final correlation matrix showing the descriptors that were included in the PCA and QSPR of epidermal permeation	205

Table 5.4	Physicochemical descriptors used in the PCA of solvent uptake, flux through membranes, permeability coefficient, lag time and flux through epidermis	206
Table A1.1	Descriptions of PCA and QSPR descriptors	259
Table A2.1	The final correlation matrix showing the descriptors that will be included in the flux through synthetic membranes PCA and QSPR	263
Table A2.2	The final correlation matrix showing the descriptors that will be included in the solvent uptake into synthetic membranes PCA and QSPR	264
Table A2.3	The final correlation matrix showing the descriptors that will be included in the permeability coefficient PCA and QSPR	265
Table A2.4	The final correlation matrix showing the descriptors that will be included in the lag time PCA and QSPR	266

CHAPTER ONE

INTRODUCTION

1.1 Introduction to dermal and transdermal drug delivery

1.1.1 Background

The skin has many essential functions, the most important being to form a physical barrier to the environment, allowing and limiting the inward and outward passage of water, electrolytes and various substances. A good knowledge of the skin penetration of xenobiotics is essential for a number of different purposes, for example, drug delivery to skin (dermatological treatments) and through skin (transdermal patches), skin care and ultraviolet radiation protection (sunscreen). It is also relevant when seeking to understanding the potential toxicity of cosmetics, anti-infectives or insect repellents. Skin also has the ability to regulate body temperature by means of both its blood flow and the mechanism of perspiration, and also serves as a sensory organ.

Topical and transdermal drug products are intended for external use. However dermal (topical) products are intended to be targeted to the pathological sites within the skin. The localized action on one or more layers of the skin is important in the treatment of dermatological conditions such as skin cancer, psoriasis, eczema, and microbial infections (Brown et al., 2006). However, although some active pharmaceutical ingredients from these topical products may also be absorbed beyond the dermal target site into the systemic circulation; it is usually in sub-therapeutic concentrations. On the other hand, in transdermal drug delivery systems a drug has to diffuse through the various layers of the skin and into the systemic circulation for a therapeutic effect to be exerted, despite the skin not being the primary target organ; for example as in the use of therapeutic patches (e.g. scopolamine). Further examples of possible target sites for drug action in skin therapy are shown in Figure 1.1.

Dermal and transdermal drug delivery provides a viable administration route for potent, low-molecular weight therapeutic agents which cannot withstand the hostile environment of the gastrointestinal tract and/or are subject to considerable first-pass metabolism by the liver. However, the barrier nature of human skin which confers its key protective function

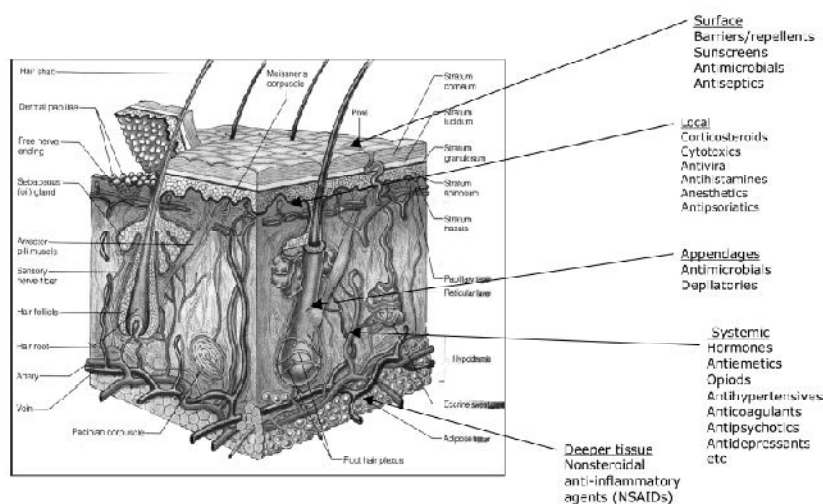


Figure 1.1 Anatomy and physiology of the skin, showing the potential targets or site of action for cosmetics and drugs (Brown et al., 2006).

also imposes physicochemical limitations on the type of penetrants that can traverse the barrier.

For a drug to be delivered passively via the skin it is generally accepted that it should have adequate lipophilicity and also a low molecular weight (Yano et al., 1986; Bos & Meinardi, 2000); and a molecular weight <500 Da is suggested to be preferable. These requirements have limited the number of commercially available products based on transdermal or dermal delivery. Thus, in order to exploit the potential advantages offered by this route of delivery, it would be desirable if the number of potential drug candidates could be increased. As such various strategies have begun to emerge over recent years to enhance the absorption of drugs that would otherwise not be absorbed in sufficient quantity to elicit a therapeutic response. A number of skin penetration enhancement techniques have been developed to improve bioavailability and increase the range of drugs for which topical and transdermal delivery is a viable option (Brown et al., 2006).

The principal rationale for the inclusion of oils within topical vehicles has historically been driven primarily by cosmetic requirements, involving ‘consumer feel’, emollience, and acceptable product appearance. Nevertheless, some consideration has also been given to the ability of blended oils to solubilize any incorporated drug and affect the release and

partitioning of drugs into the skin (Kreilgaard, 2002; Saroj et al., 2012). However it has been shown that a number of oils can partition into the skin and integrate within the lipid bilayers after application to the skin surface. This might in turn be expected to modify the partition behaviour into the epidermal layers of any concomitantly administered drugs. In addition, the partition of certain oils such as isopropyl myristate and oleic acid have been reported to promote membrane lipid fluidity (Pillai et al., 2004; Lane, 2013), which may contribute to the increased disorder of stratum corneum and thus enhance permeability of bilayers within the stratum corneum. Any oil residue remaining in contact with the skin can also confer barrier function, reduce epidermal water loss and possibly further modify the permeation properties of the skin.

However, the possible role of oils, which is incorporated and applied to the skin as supposedly inert vehicles/excipients in the modification of drug permeation, as a consequence of inducing an altered membrane structure has not been well-investigated. It is therefore the purpose of this study to study some of these factors. Accordingly it is appropriate to: review the structure of skin, consider the advantages; limitations and theoretical basis of transdermal delivery; and examine the vehicle effects on the skin, with an emphasis on the oils that have been previously incorporated in topically applied vehicles. It is also pertinent to assess the analytical and experimental techniques available for assessing permeation and appreciate the basis of techniques developed to predict permeability.

1.1.2 Structure and barrier properties of the skin

The skin is a very complex heterogeneous membrane and comprises the largest multifunctional organ of the body, accounting for more than 10% of the body mass. It is composed of tissue that grows, differentiates and renews itself constantly. The skin (Figure 1.1) consists of three anatomical layers: the epidermis, the dermis and a subcutaneous layer (hypodermis) (Schaefer et al., 1996; Williams, 2003; Cevic et al., 2004). The barrier function of the skin is thus reflected in its multilayered structure.

1.1.2.1 Epidermis

Epidermis is an epithelium divided into two distinct parts: the viable epidermis being a living hydrophilic layer (70% of water), and the stratum corneum, a hydrophobic layer (13% of water) made from dead cells which results in a horny texture. The epidermis is a thin, dry unvascularized and tough outer protective layer, consisting of cells which are differentiated from stem cells on the basal membrane at the interface between the epidermis and dermis. It has been reported that damage or removal of the epidermis allows diffusion of small water-soluble, non-electrolytes applied to skin surface to proceed approximately 1000 times faster than if applied to intact skin (Scheuplein & Blank, 1971). The epidermis, which is ~100 μm thick, is composed of four distinct regions, each representing a different phase of kartinocyte differentiation: the stratum basale, stratum spinosum, stratum ganulosum and stratum corneum (horny layer). Within the epidermis there are two distinct types of cells: the keratinocytes and the dendritic cells. The keratinocytes or keratin-forming cells are found in the basal layer. As keratinocytes divide and differentiate, they move from this deeper layer to the surface. There are three types of dendritic cells; melanocytes (melanin forming cells), Langerhans (immune) cells and Merkel (sensory) cells.

Keratinocytes were shown to be the major site of drug metabolism in the skin (Baron et al., 2001; Swanson, 2004; Oesch et al., 2007). The topically applied dermatological drugs and xenobiotics, to which the skin is exposed, may be toxified or detoxified by skin enzymes, which may result in dermatological disorders including skin sensitization or even skin carcinogenesis. Cytochromes P450 enzymes are important enzymes available in the viable epidermis. Many chemical compounds to which the human skin is exposed, (such as ingredients in cosmetics, toiletries, health-care products, as well as many allergens, toxicants, and carcinogens) are substrates of cytochrome P450 enzymes. Also most drugs used in dermatology are either a substrate or an inducer or an inhibitor of cytochrome P450 enzymes. In addition, cytochrome P450 enzymes act on many endogenous substrates including vitamin A and vitamin D; both these are also widely used in dermatological practice (Oesch et al., 2007). Other enzymes available in the viable epidermis are flavin-dependent monooxygenases, alcohol dehydrogenases,

aldehyde dehydrogenases, esterases/amidases, and epoxide hydrolases. In addition glucuronosyl transferase, sulfo-transferase, acetyl-transferase and methyl-transferase are also present. However, the specific activities of these cutaneous enzymes possess less than 10% activity as compared with the liver enzymes (Smith & Hotchkiss, 2001; Oesch et al., 2007).

Since there are no blood vessels in this layer of the skin, nutrients reach the epidermal cells by way of passive diffusion across the basement membrane at the dermal-epidermal border. The basement membrane physically separates the epidermis from the dermis. It acts as a permeability barrier, forming an adhesive interface between epithelial cells and the underlying matrix, and controlling cell organization and differentiation by mutual interactions between cell-surface receptors and molecules in the extracellular matrix, (the basement membrane is able to bind a variety of cytokines and growth factors, providing a reservoir for these compounds for subsequent controlled release during physiological remodeling or repair processes) (Iozzo, 2005; Masunaga, 2006; Breitkreutz et al., 2009). The passage of nutrients and other materials across the basement membrane is facilitated by the dermal papillae. The epidermal-dermal junction consists of papillae that project into the dermis. The papillae effectively increase the junctional surface area manifold in comparison to the area of the skin surface. Papillae at the dermal side are nearly completely filled with a cutaneous blood capillary plexus that is complemented with less abundant, small lymphatic vessels.

1.1.2.2 Stratum corneum

The final stage of keratinocyte differentiation is represented by the stratum corneum, the outermost layer of skin. Despite it being essentially dead tissue, diffusion through the stratum corneum is generally recognized as the rate limiting step to percutaneous absorption, although disruptions in the integrity of the other layers can also affect skin permeability (Schaefer & Redelmeier, 1996; Williams, 2003).

The stratum corneum is a 10–20 μm thick membrane composed of dead, flattened, keratin-rich cells: the corneocytes (Figure 1.2). These dense cells are surrounded by a complex mixture of intercellular lipids (Elias, 1988; Wertz, 1992; Menon et al., 2012).

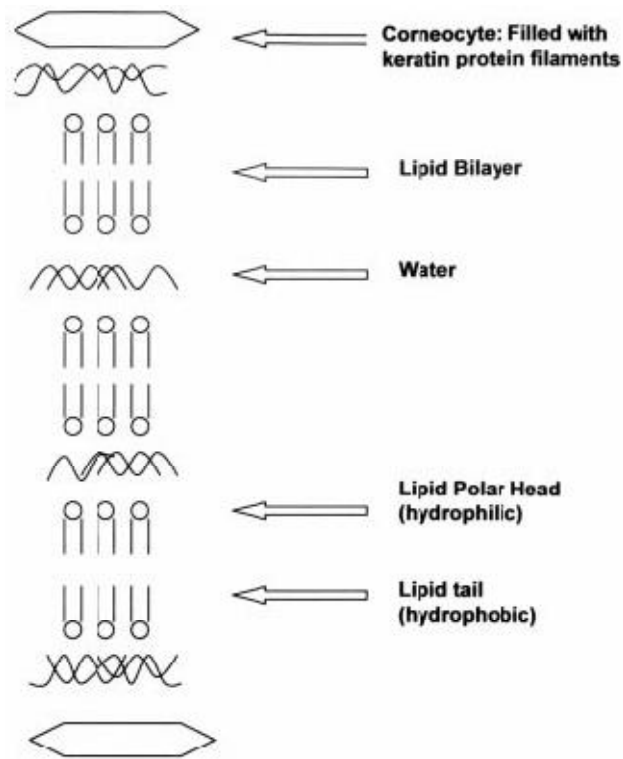


Figure 1.2 Corneocyte lipid bilayers (Bensouilah & Buck, 2006).

The most important feature of such lipids is that they are structured into ordered bilayer arrays and it is these that often provide the predominant diffusional path for a molecule crossing the stratum corneum (Albery & Hadgraft, 1979; Elias, 1983; Downing et al., 1987; Grubauer et al., 1989). Water also diffuses along this tortuous route (Potts & Francoeur, 1991) and the overall topography can be stylized as having a “brick-and-mortar” structure (Michaels et al., 1975; Elias, 1981; Shah, 1994). The corneocytes, (i.e. the “bricks”) are composed mainly of fibrous and water-insoluble keratin, which is about 20% cross-linked and packed tightly. Such cells are almost impermeable to most solutes, in contrast to the intercellular area of the stratum corneum. The latter can be considered as the “mortar”, comprising a complex lipoidal mixture in a uniquely arranged matrix which forms lamellar phases responsible for the skin’s natural barrier. Compared with the corneocytes, the intercellular lipid matrix has a looser structure and is relatively more permeable to solutes (Venkatraman, 1998). The diffusant therefore tends to follow a tortuous route and has to cross sequentially and repeatedly, a number of hydrophilic and

lipophilic domains (Suhonen et al., 1999; Hadgraft, 2001a). The corneocyte size and number of cell layers is the predominant reason for the variation in drug permeation due to body site. In other words as cell size gets bigger and the number of cell layers increase the skin barrier function becomes larger (Hadgraft & Lane 2009).

Corneocytes are linked together by protein structures termed corneodesmosomes, which continuing the 'brick and mortar structure' theme can be considered as being analogous to reinforcing 'rivets' within the mortar. Corneodesmosomes are important for the stratum corneum cohesion. When no longer functional, cells of the outer stratum corneum are shed in a process called desquamation. In desquamation, the desmosomes break down so the cells are no longer held together and can be shed from skin surface. Several enzymes degrade the desmosomes and allow non-functional cells to detach from each other and desquamate (shed). Alteration in the activity of these enzymes appears to be associated with skin barrier disturbances (Egelrud et al., 2005). This may partly be because of uncontrolled corneodesmolysis, which leads to weakening of the stratum corneum integrity and cohesion (Komatsu et al., 2005). Genetic differences in the amount or efficiency of these enzymes also determines the efficiency of this process. If the desmosomes are not degraded properly and the outer non-functional cells are held together longer than optimal, dry flaky sheets of skin develop in which the cells are still attached to one another.

The water content of normal stratum corneum comprises 15-20% of its dry weight (Plewig et al., 1983; Schätzlein & Cevic, 1998; Warner et al., 1988) but when it becomes hydrated, the water content can increase to about 400% of its dry weight (Williams & Barry, 2004). The stratum corneum receives water from the dermis and some from the environment. The hydration of the stratum corneum is important from a pharmaceutical, dermatological, and cosmetic point of view. Dry skin is mostly associated with dermatological conditions (e.g. atopic dermatitis), whilst increasing the hydration of the skin has been reported to promote the percutaneous absorption of certain solutes (Bouwstra et al., 2003; Williams & Barry, 2004) and also enhance skin appearance by providing the latter with a soft and fresh look. Ceramides are mainly responsible for generating the stacked lipid structures that trap water molecules in their hydrophilic

region. These stacked lipids surround the corneocyte and incorporate water into the stratum corneum, they also provide an impermeable barrier by preventing the movement of water out of the surface layers of the skin. After the age of 40 there is a sharp decline in skin lipids thus increasing a person's susceptibility to dry skin conditions (Bensouilah & Buck, 2006). Natural moisturizing factors present in the corneocytes in the stratum corneum are also responsible for keeping the skin moist and pliable by attracting and holding water, a property termed 'hygroscopicity'. Natural moisturizing factors are free amino acids, along with other physiological chemicals such as lactic acid, urea and salts, including sodium pyrrolidone carboxylate.

The major factor in the maintenance of a moist, pliable skin barrier is the presence of intercellular lipids (Figure 1.2). Generally all membrane lipids are amphiphilic *i.e.* they are constituted of a hydrophilic head group and a hydrophobic region. In human stratum corneum the major lipid classes are ceramides, cholesterol and saturated long chain free fatty acids. The ratio between these lipid classes is approximately equimolar (Weerheim & Poncet, 2001). Low levels of other lipid classes are also present, such as cholesterol sulphate, glucosylceramides and cholesterol esters. In human stratum corneum 11 subclasses of ceramides have been identified. The ceramides head groups are very small and contain several functional groups that can form lateral hydrogen bonds with adjacent molecules. The ceramides have a range of different structures, varying in head-group architecture and fatty acid chain length (Bouwstra et al., 2008).

The linear unsaturated nature of ceramides and free fatty acids in the stratum corneum are arranged in a bar-like form or a cylindrical form, which allow them to be tightly packed laterally and to form highly ordered gel phase domains. Apart from their lamellar organization, the lateral packing of lipids is of major importance for the barrier properties of skin. The lateral packing of lipids controls both the mobility within the lipid lamellae and the membrane. Cholesterol is an important membrane lipid. It can either increase the fluidity of membrane domains or make them more rigid, depending on the physical properties of the other lipids and on the relative proportion of cholesterol compared to the other components. A prime role of cholesterol in the epidermal barrier is to provide a

degree of fluidity to what would otherwise be a rigid, possibly brittle, membrane system. This may be necessary for the pliability of the skin (Wertz, 2000).

Three different phases have been observed in samples reconstituted from extracted lipids (Bolzinger et al., 2012). These phases are orthorhombic, hexagonal and fluid lamellar (Figure. 1.3). The orthorhombic phase is very densely packed with a very low permeability. In this phase the hydrocarbon chains responsible for the crystalline state are not equally distributed in the lattice and the molecules are not able to rotate, even along their longest axes. In contrast, the crystalline hydrocarbon chains in the hexagonal phase are equally spaced, which provides a much denser structure than the liquid packing and confers a much reduced permeability, often this phase is also referred to as a gel-phase. The lipids are in a liquid (molten) state in the fluid lamellar phase and the membrane is highly permeability to most substances (Bouwstra et al., 2008; Bolzinger et al., 2012).

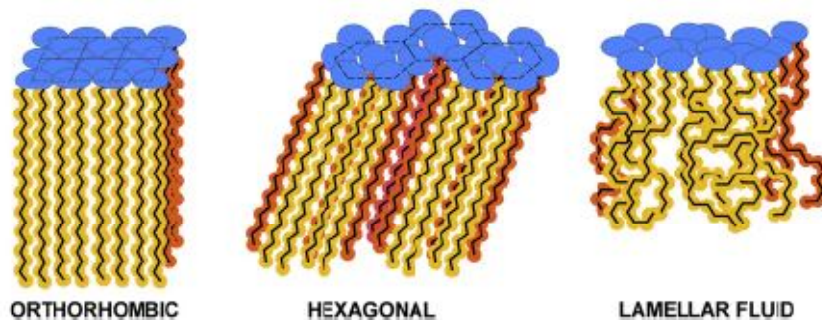


Figure 1.3 Molecular organizations of stratum corneum lipids. Schemes of the chain conformation and lateral chain packing in orthorhombic, hexagonal and liquid-crystalline phases of long-chain lipids (Bolzinger et al., 2012).

The unsaturated nature of ceramides enables phase transitions to occur at temperatures as low as skin temperature (32°C). Since there is a slight temperature gradient across the skin, the internal temperature of the body is 37°C as against 32°C at the skin surface. Lipid phase transitions taking place in this temperature range will cause a gradient of properties across the stratum corneum (Pilgram et al., 1999). These latter workers studied the temperature dependence of the phases in relation to stratum corneum depth. At room temperature the lipid packing is predominantly orthorhombic while the presence of hexagonal packing is more pronounced at 32°C. The transition from orthorhombic to

hexagonal occurs between approximately 35–40°C (and a fluid lamellar phase forms upon heating above 70°C). The lipid organization in human stratum corneum *in vivo* at 32°C is orthorhombic while in the inner layers of the stratum corneum the lipids are partly present in a hexagonal packing arrangement. However it has been shown that the lipid organization is non-homogeneous as a function of the stratum corneum depth, with results confirming the presence of predominantly orthorhombic phase at all depths (Damien & Bonchev, 2010). The presence of hexagonal and liquid phases was also detected, though only to a minor extent. The higher the extent of pure orthorhombic phase present, the lower the amount of water in the bilayers. The presence of the orthorhombic packing indicates that the lipids within the lamellae are very densely packed. This is considered to be very important for a proper skin barrier function.

1.1.2.3 Dermis

The dermis is a fibrous layer, which supports and strengthens the epidermis. The dermis is the thickest (1–3 mm) layer of the skin and comprises loose connective tissue consisting of fibrous proteins (collagen and elastin) embedded in an amorphous ground substance to form a matrix. The ground substance is composed primarily of water, ions, and complex carbohydrates such as glycosaminoglycans that are attached to proteins. The ground substance helps to hold the cells of the tissue together and allows oxygen and nutrients to diffuse through the tissue to cells. Elastin and collagen, present in this layer are responsible for the elasticity of the skin and the latter enables the skin to return to its original form after it has been stretched. Most of the appendages originate from the dermis, including the hair follicles, sebaceous glands, and sweat glands (Moser et al., 2001). The dermis also contains nerves and blood vessels, which help maintain “sink” conditions within the skin by efficiently transporting permeated compounds to the systemic circulation (Bolzinger et al., 2012). In addition, the vascular network of the dermis is responsible for supplying nutrients and oxygen to the skin and also plays a role in regulating body temperature. A system of lymphatic vessels comprises an additional dermal circulatory system. These vessels are involved in removing cellular waste and help regulate the volume of the interstitial fluid in the dermis (Schaefer & Redelmeier, 1996; Williams, 2003). Similar to the epidermis drug diffusion through the dermis is primarily a hindered diffusion through an aqueous-based medium. However, there are

important differences: the vascularization of the dermis contributes significantly to drug transport and distribution in the skin, as does the lymphatic system. Other functions of the dermis include acting as an anchor to the hypodermis.

1.1.2.4 Hypodermis

The deepest layer of the skin, the hypodermis, is primarily composed of adipose tissue and as such, it functions as an energy depot, a layer of insulation, and as a shock absorber and it supplies nutrients to the other two upper layers. The hypodermis serves as the entry point for the cutaneous nerves and the blood and lymph networks that service the skin. The bases of the hair follicles are also present in this layer, as are the secretory portions of the sweat glands. Since the loose connective tissue of the hypodermis is interwoven with that of the dermis, there is no distinct boundary between these two layers (Schaefer & Redelmeier, 1996; Williams, 2003).

1.2 Routes of drug permeation across the skin

Topically exposed drugs may permeate the skin via the intercellular, transcellular and appendageal (through either the eccrine (sweat) glands or hair follicles) routes (Barry, 1987; Cullander & Guy, 1992; Roberts et al., 2002; Lane 2013) (Figure 1.4). The net diffusion of a drug through the skin is the sum of the fractional contributions of each of the separate routes of permeation. The transport of the drug is controlled by its diffusion coefficient inside the stratum corneum lipids, the retention by adsorption to keratin of corneocytes, and the partition coefficient between the drug, formulation and the stratum corneum lipids.

The appendageal route is not considered to be a significant pathway for drug permeation due to the fact that sweat glands and hair follicles occupy only 0.1% of the total surface area of human skin, therefore the amount of any compound diffusing via this route does not contribute appreciably to the steady state flux (Scheuplein, 1967; Singh & Singh, 1993; Bolzinger et al., 2012; Lane, 2013). However it has been suggested

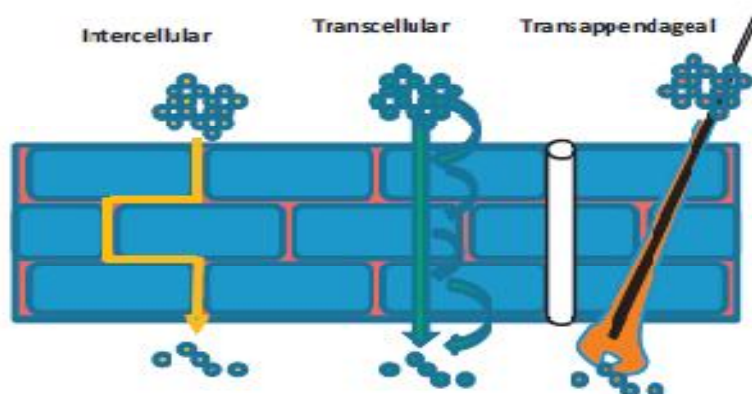


Figure 1.4 Possible pathways through the stratum corneum (Lane, 2013).

that this route may be important for the permeation of slowly diffusing compounds and very high molecular weight substances, such as nanoparticles (Lademann et al., 2011). It may also be important for ions and large polar molecules (Lauer et al., 1995), as well as contributing to the facilitated transport of charged molecules across the skin following application of a small electric current (iontophoresis) (Edwards et al., 1995). Additionally, the trans-appendageal route may be responsible for the rapid diffusion of compounds in the early stages of diffusion, before steady-state is achieved, and so might enable a loading dose to be delivered. Drug levels may then be subsequently sustained by slower diffusion of more of the compound through the epidermis (Scheuplein, 1967; Katz et al., 1971; Keister & Kasting, 1986; Meidan et al., 2005).

The transcellular route (via the hydrophilic keratinised cells) is another possible route of penetration. However its contribution to overall flux is usually considered to be only minor, involving sequential partitioning of the permeant into and out of cells. Therefore the predominant route of penetration for all molecules appears to be through the intercellular spaces (via the lipid channels), despite it being a more tortuous path in which the molecule diffuses within the intercellular lipid phase only (Boddé et al., 1989; Sharata & Burnette, 1989; Potts & Guy, 1992; Hadgraft, 2001 a&b). As a result, the majority of techniques to optimise permeation of drugs across the skin are directed towards manipulation of solubility in the lipid domain or alteration of the ordered structure of this region. An important consequence of the existence of a continuous lipid pathway across

the stratum corneum is its implication for the use of simple lipid membranes as model skin barriers (Houk & Guy, 1988; Feldstein et al., 1998).

1.3 Advantages and limitations of dermal and transdermal drug delivery

The skin can serve as an alternative route of drug delivery and offers various advantages in comparison to conventional methods such as oral administration. These advantages can lead to an optimization in therapy compared to the use of the latter route. The potential advantages of transdermal drug delivery may include: avoidance of first-pass metabolism by the gastrointestinal tract and liver in the case of oral delivery (Cleary, 1993; Kormic et al., 2003) and ease of use and withdrawal of drug (Payne et al., 1998). It provides direct access to the target or diseased site e.g. treatment of skin disorders such as psoriasis, eczema and fungal infections (Colin Long, 2002). The direct administration of the drug to the pathological site enables any adverse effects associated with systemic toxicity to be minimised. It also provides convenient and painless administration (Cleary, 1993; Henzel & Loomba, 2003) as well as conferring improved patient acceptance and compliance compared with some other routes. The route also enables ease of dose termination in the event of any adverse reactions; whether the latter are either systemic or local (Payne et al., 1998; Jarupanich et al., 2003; Archer et al., 2004). In addition transdermal delivery usually provides a means of obtaining a sustained and controlled delivery over a prolonged period of time (Yang et al., 2004). This can improve the therapeutic effect and reduce side effects resulting from alternating high-to-low plasma drug concentrations, characteristic of non-controlled release oral and parenteral drug delivery systems (Cramer et al., 1994; Kormic et al., 2003). The route also provides an alternative in circumstances where oral dosing is not possible (in unconscious or nauseous patients) (Kormic et al., 2003).

However, as with all other routes of delivering drugs, using the skin as a portal also has its disadvantages. For instance, a molecular weight less than 500 Da is preferable to ensure ease of diffusion across the stratum corneum (Bos & Meinardi, 2000). It is usually necessary for the diffusing species to have sufficient aqueous and lipid solubility, equating to a Log P (octanol/water) value of between 1-3 such that it might successfully

traverse the stratum corneum (Yano et al., 1986). Pre-systemic metabolism due to the presence of enzymes in the skin such as peptidases, esterases, glucuronyl transferases and sulphotransferases, which are present at relatively high levels, can occur (Steinsträsser & Merkle, 1995). For example glucocorticoids for dermal and transdermal application are susceptible to esterase activity (Lombardi et al., 2008, Wohlrab et al., 2010). However metabolism can also enhance the penetration of some drugs; for instance testosterone is activated by 5- α -reductase to generate dihydrotestosterone, which has a higher androgenic potency than testosterone. A low permeability of the skin may result in a low bioavailability of drugs delivered by this route and the amounts of percutaneously absorbed drugs may not reach minimum therapeutic levels even for many potent drugs (Venkatraman, 1998). Skin irritation and sensitization might occur due to exposure of certain drugs, excipients, or components of delivery devices resulting in erythema, oedema, etc. (Hogan & Maibach, 1990; Carmichael, 1994; Murphy & Carmichael, 2000; Toole et al., 2002; Hikima et al., 2005).

With respect to the physico-chemical and physiological limitations outlined above, it is clear that only relatively few drugs can be considered for formulation via this route of delivery, under passive conditions. Accordingly, there has been a consistent demand for novel and effective methods to enhance drug permeation through the skin (Iervolino et al., 2000).

1.4 Theoretical basis for passive absorption and its enhancement

Permeation of drugs through the skin or other membranes, as indicated by Higuchi (1960) is a process of passive diffusion and can be described by Fick's laws (Hadgraft, 2001a). In conditions of steady-state, the flux is given by:

$$J = DK C_v/L \quad \text{(Equation 1.1)}$$

Where J is the flux of drug, D the diffusion coefficient of the drug in the membrane, K the partition coefficient of the drug in the membrane, L the length of the diffusion pathway, C_v the concentration of drug in the vehicle

In non-steady state or finite dosing models where the diffusion causes the concentration to change with time. The changes of the concentration profile are predicted by Fick's second law:

$$\partial C / \partial t = -D (\partial^2 C / \partial x^2) \quad (\text{Equation 1.2})$$

Where, C is the concentration of the diffusing species in the membrane, D is the diffusion coefficient of the diffusing species, x is the diffusional pathlength, and t is time.

According to Fick's laws the most important factors that influence flux across the skin are the partition coefficient of the permeant, the diffusion coefficient, and the concentration gradient of the drug between the formulation and the skin, i.e. its thermodynamic activity in the formulation. Drug transport across a membrane can be considered to be a balance between driving forces and resistances. The diffusion coefficient D , directly correlates with the reciprocal of the viscosity of the barrier medium according to the Stokes-Einstein equation (Kokubo et al., 1991), and can be thought of as the kinetic resistance of the barrier to drug penetration.

In Equation 1.1, the ratio $C_v/C_{s,v}$, the degree of saturation or saturation ratio, represents the relative chemical potential of the donor system. Under sink conditions, this value reflects the gross chemical potential gradient across a target membrane. Thus, it can be regarded as the thermodynamic driving force. Therefore, the passive transport rate of a molecule through a homogeneous barrier is proportionally related to its degree of saturation in the applied vehicle, providing no significant vehicle-drug or drug-membrane interactions occur (Benaouda et al., 2012 a&b; Davis & Hadgraft, 1991; Higuchi, 1960; Pellett et al., 1994). Therefore, inducing drug supersaturation in topical formulations is one way to increase the flux and this can be achieved by variations in the pH, temperature or formulation vehicle or by using volatile excipients (Hadgraft, 2004).

Therefore, based on Equation 1.1, transdermal drug delivery is a thermodynamically favoured, but a kinetically suppressed process. To control the delivery of drugs into and across the skin the following strategies are possible:

- 1) Increase the drug diffusion coefficient, D , through reduction of barrier resistance by disordering the tightly packed lipid regions of stratum corneum, which consequently increases penetration through the intercellular lipid matrix (Barry, 1987; Moser et al., 2001; Thomas & Panchagnula, 2003).
- 2) Promote drug solubility, $C_{s,m}$, in the skin. This might be achieved by perhaps increasing the solubility of the drug in the skin caused by stratum corneum uptake of a cosolvent such as propylene glycol, 2-(2-ethoxyethoxy)ethanol (Transcutol), etc. (Moser et al., 2001; Thomas & Panchagnula, 2003). The increased solvent penetration may include increased drug solubility in the skin and increased skin penetration of the drug if the drug has a high affinity for the solvent (Yamada et al., 1987).
- 3) Increase the driving force for penetration. This might be induced either by increasing drug concentration in the vehicle, C_v or by decreasing the drug solubility, $C_{s,v}$ in the vehicle (Aungst et al., 1990, Moser et al., 2001).

Most of the strategies for enhancing transdermal permeation of drug utilise one or a combination of these mechanisms.

1.5 Factors affecting drug permeation through the skin

Several biological and physicochemical parameters may influence drug permeation across the skin (Barry, 1983). The passive diffusion of a molecule from a vehicle into and across the skin is mainly affected by the physicochemical properties of the molecule, vehicle and nature of the skin. Influencing biological factors include skin age, body region, health status, race, metabolism and hydration. At different body sites, the composition and finally barrier properties of the stratum corneum may vary; these include differences in the thickness, number of cells or, the density of skin appendages in the stratum corneum (Scheuplein, 1978; Bensouilah & Buck, 2006). The viable epidermis contains several enzyme systems that may catalyze processes such as oxidation, reduction, hydrolysis or conjugation (Section 1.3). Therefore skin metabolism may have additional impact on transdermal delivery of drugs (Storm et

al., 1990; Zhang et al., 2009). The effect of age is mainly attributable to the smaller surface-to-volume ratio in case of newborn infants compared with adults rather than an effect of lower barrier function of younger skin (Scheuplein, 1978; Yosipovitch et al., 2000). Skin hydration is a crucial and possibly the most frequently investigated factor affecting drug permeation.

1.6 Properties of drugs that affect diffusion

The characteristics of a drug that influence transport rates and permeability include: lipophilicity, hydrogen bonding capability and size (Camenisch et al., 1996). For a drug to penetrate well, it should have a small molecular size, adequate solubility in an oil phase, and a moderately high partition coefficient. Most drugs currently available in a patch formulation share three features that enable administration through a convenient area of skin, namely: a molecular mass <500 Da, a moderate lipophilicity and a low required daily dose (<10 mg.day⁻¹).

The lipophilicity of a drug is the most informative and successful single physicochemical property to predict its permeation in biological systems (Testa et al., 1996; Zhang et al., 2009). The lipophilicity of a drug is its tendency to prefer a lipidic or oil-like environment to an aqueous one. However, its magnitude depends on the summing of intermolecular interactions such as hydrogen bonding and dipole effects. Thus, although lipophilicity is a property ascribed to the drug compound, it is highly dependent on the choice of lipidic environment (Kaliszan, 1992). Drugs should possess a moderate lipophilicity if they are to diffuse through stratum corneum. Ideally, they should exhibit both lipoidal and aqueous solubilities: if too hydrophilic, the molecule will be unable to transfer into the stratum corneum; whereas if too lipophilic, the drug will tend to remain in the stratum corneum layer. Accordingly, an octanol water partition coefficient Log P 1-3 has been reported to be optimal (Yano et al., 1986; Naik et al., 2000). The lipophilicity of a compound dictates the partitioning behaviour into corneocytes and it has been postulated that hydrophilic compounds tend to partition into the corneocyte proteins, while the more lipophilic compounds

partition into the stratum corneum lipids (Raykar et al., 1988; Van der Merwe & Riviere, 2005).

The ordered lipid layers provide a finite number of hydrogen bonding groups located in the polar head groups. Therefore during the diffusion process the drug should be sufficiently lipophilic to overcome the hydrogen bonding with polar head groups, with generally the hydrogen bonding capacity having a negative effect on permeation (Su et al., 2010). Octanol is the most commonly used lipophilic phase in two-phase partition experiments carried out *in vitro*, one reason being that it can provide a good hydrogen bonding environment for solutes. A solute, which makes strong hydrogen bonds with water, will be able to make similar bonds in octanol (Conradi et al., 1991). The hydrogen bonding capacity of a solute can be expressed as the difference between its partition coefficient into octanol and a solvent devoid of forming hydrogen bonds, typically an alkane (Young et al., 1988). It is reported that the presence of 2 or 3 hydrogen bonding groups can successively reduce the diffusion coefficient, D , by an order of magnitude (Pugh et al., 1996). However in some cases where there is more than one hydrogen bond group, intramolecular hydrogen bonding between adjacent –OH groups and adjacent hydrogen groups can also act to modify the permeant diffusion (Plessis et al., 2001).

After the drug has partitioned into the membrane, it must be sufficiently ‘mobile’ to diffuse across it. The rate of diffusion is inversely proportional to the molecular volume (and hence molecular weight or size) of the ‘unit’ and the material through which it is diffusing; the smaller a molecule, the faster the rate of diffusion. This is due to larger molecules requiring more energy to diffuse. Various molecular dynamics simulations (Takeuchi, 1990; MüllerPlathe, 1991; Pant & Boyd, 1993) show that the mechanism of diffusion of permeants in polymers is a ‘hopping’ mechanism. In this mechanism, a permeant diffuses via ‘jumps’ between neighbouring free volume pockets and therefore the smaller the size the easier the diffusion (Marrink & Berendsen, 1996).

1.7 Passive approaches to overcome the barrier nature of the skin

The stratum corneum barrier can be altered passively to a degree using various strategies, some of which are outlined below:

1.7.1 Vehicle / chemical enhancers

As discussed in Section 1.2, the major route of drug penetration through the skin is through the intercellular channels (Albery, 1979), which contain a complex mixture of structured lipids (Elias, 1983). Generally the passage of compounds across the skin is divided into four steps: (1) the release of the penetrant from the vehicle then, (2) penetration, the entry of a substance into a particular skin layer, (3) permeation, the penetration through one layer into another, and finally (4) re-sorption, the uptake into the vascular system (Bolzinger et al., 2012). One of the major challenges for designing an effective (trans)dermal drug delivery system is the choice of vehicle in which the drug is entrapped in order to reach its target site i.e. the skin surface, the skin compartments or the systemic circulation. The partitioning behaviour of the drug from the vehicle into the lipid is therefore an important determinant in this first step of the absorption process. Also the solubility characteristics of the permeant in the lipids of the stratum corneum should be taken into account. This solubility could be influenced by components that diffuse out of the formulation into the skin. The diffusion of any applied potential permeant through the possibly modified structured lipids then follows. Therefore, the vehicle can have a significant impact on the rate at which a particular drug is delivered into and then through the skin i.e. the flux of the drug. This effect could occur as a consequence of changing the solubility of the penetrant in the skin, or by changing the thermodynamic activity of the formulation, or changing the resistance of the membrane for the penetration and diffusion.

A good vehicle for the skin is likely to be a vehicle which will readily enter the skin, swell the overall matrix and increase the diffusion of the permeant. Also it might 'drag' the permeant with it into the skin. The permeant molecules must dissolve in the vehicle in order to enable the former's diffusion through the vehicle to the vehicle-stratum corneum interface; therefore an appropriate vehicle should have the ability to

solubilize at least the minimum effective dose of the drug (Abbott, 2012). The diffusion through the skin depends on the concentration gradient and the diffusion coefficient. A high concentration in the vehicle on the stratum corneum sets the maximum possible concentration gradient across the stratum corneum; therefore the diffusion will be enhanced. Using supersaturated systems enhances drug flux (Section 1.7.2). The diffusion coefficient of the vehicle depends on the molecular shape, size and molecular weight. The Hansen solubility parameters values and the Hildebrand solubility parameter also affect the permeation of the vehicles into the skin. The smaller the difference between these values of the vehicle and skin, then the higher the rate of permeation (Abbot, 2012).

Vehicles or penetration enhancers have been suggested (Barry, 1988; Barry, 1991) to act on the skin via either one or combination of the following mechanisms: (1) interaction with the intercellular lipids of the stratum corneum resulting in disorganization of the highly ordered structures and increasing the lipid fluidity thus enhancing the paracellular diffusivity through the stratum corneum (Figure 1.5);(2) interaction with intracellular proteins of the corneocytes to increase transcellular permeation i.e. decreasing hydrogen-bonding between keratin and drug, increasing the porosity of the proteinaceous matrix via denaturation and formation of pores or vacuoles which serve as potential permeation pathways (Figure 1.6); and (3) increasing partitioning of the drug into the stratum corneum.

The overwhelming majority of a topical formulation is comprised of its vehicle, which can be modified to enhance the driving force for diffusion and/or increase skin permeability; also it can have a direct impact upon the therapeutic efficacy and tolerability of the formulation. Therefore the amount of drug diffusing into the skin can differ several-fold as a result of the vehicle alone (Hadgraft, 1991). The synergistic effect associated with using a combination of vehicle enhancers has also been reported (Mitragotri, 2000).

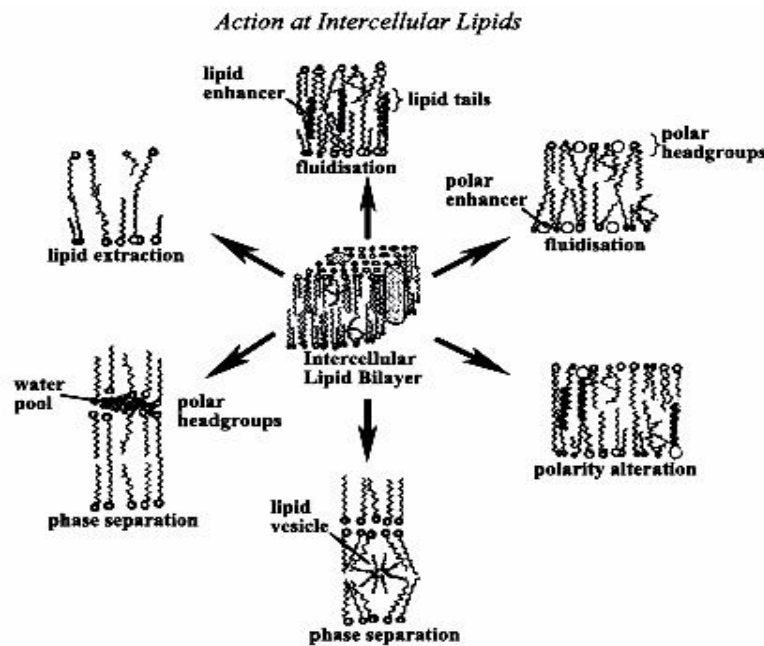


Figure 1.5 Schematic representation of the mechanisms by which a chemical enhancer may interact with stratum corneum intercellular lipids (Menon & Lee, 1998; Williams & Barry, 2004).

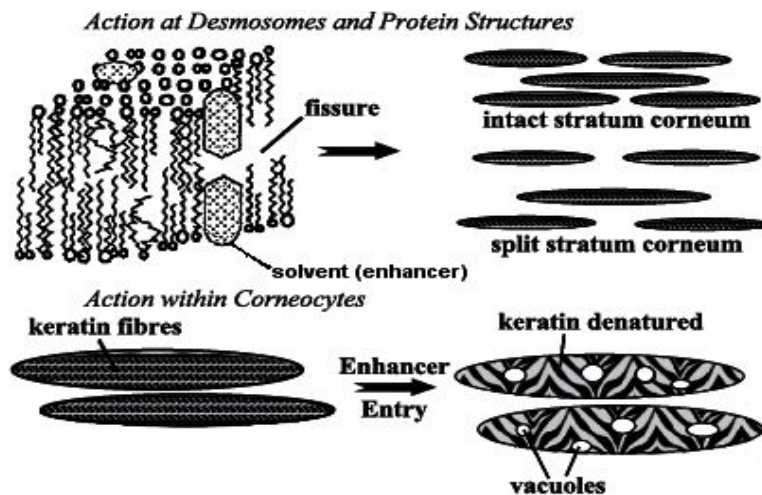


Figure 1.6 Action of enhancers (particularly solvents) on the protein component of the stratum corneum, leading to fissuring of intercellular lipids, splitting of stratum corneumsquames, keratin denaturation and vacuole formation in corneocytes (Menon & Lee, 1998; Williams & Barry, 2004).

Although many chemicals have been evaluated as penetration enhancers none has proven to be ideal. Some of the more desirable properties for a penetration enhancer acting within skin have been given (Barry, 1983) as:

- It should be non-toxic, non-irritating and non-allergenic.
- It should have no pharmacological activity within the body.
- It would ideally work rapidly, and the activity and duration of effect should be both predictable and reproducible.
- It should have no pharmacological activity within the body - i.e. should not bind to receptor sites.
- It should work uni-directionally, i.e. should allow therapeutic agents into the body whilst preventing the loss of endogenous material from the body.
- When it is removed from the skin, barrier properties should return both rapidly and fully.
- It should be appropriate for formulation into diverse topical preparations and thus should be compatible with both excipients and drugs.
- It should be cosmetically acceptable with an appropriate skin 'feel'.

Permeation enhancers currently represent the most widely studied approach to transdermal drug permeation enhancement on account of the potential advantages they offer over other methods. Chemical permeation enhancers are relatively inexpensive and easy to formulate, they offer flexibility in their design, are simple in application and allow the freedom of self-administration to the patient. Finally, chemical enhancers can be formulated with the active therapeutic as a topical cream or gel, or an adhesive skin patch that can be applied anywhere on the body for prolonged systemic delivery of the drug. In general, permeation enhancers may contain a wide variety of different chemical functional groups and act by a variety of different mechanisms in enhancing drug transport (Karande & Mitragotri, 2009). Table 1.1 shows examples of penetration enhancers used in commercial transdermal and topical products

Table 1.1. Examples of penetration enhancers used in commercial transdermal and topical products (*modified from Lane 2013*).

Active	Trade name	Enhancer
Buprenorphine	BuTrans	Oleyl oleate
Estradiol	Estraderm MX	Isopropyl palmitate
Estradiol	Prodynova	Ethyl oleate, Glycerol monolaurate, Isopropyl myristate
Estradiol	Sandrena	Ethanol, Propylene glycol
Estradiol	Vivelle-Dot	Dipropylene glycol, Oleyl alcohol
Estradiol	Divigel	Ethanol, Propylene glycol
Estradiol	Oestrogel	Ethanol
Ethinyl estradiol, norelgestromin	Evra	Lauryl lactate
Fentanyl	Fentalis	Ethanol
Oxybutynin	Anturol	Diethylene glycol monoethyl ether, Ethanol, Propylene glycol
Testosterone	Androgel	Isopropyl myristate
Testosterone	Axiron	Octyl salicylate, Ethanol, Isopropyl alcohol
Testosterone	Fortesta	Ethanol, Oleic acid, 2-Propanol, Propylene glycol
Testosterone	Testoderm	Ethanol
Testosterone	Testogel	Ethanol, Isopropyl myristate
Testosterone	Tostran	Ethanol, Isopropyl alcohol Oleic acid, Propylene glycol
Adapalene	Differin Gel	Propylene glycol
Diclofenac	Mobigel	Ethanol, Isopropyl alcohol
Diclofenac	Voltarol Emulgel	Isopropyl alcohol, Propylene glycol
Idoxuridine	Herpid	Dimethyl sulphoxide
Ketoprofen	Feldene	Ethanol

1.7.1.1 Vehicle permeation enhancement by reducing the diffusional resistance of the skin

As indicated in Section 1.4, an increase in the diffusion coefficient of the drug is one of the strategies to promote drug penetration through the skin. By disordering the lipid bilayers, many chemical enhancers can induce such an increase in the stratum corneum and thereby enhance penetration (Suhonen et al., 1999; Moser et al., 2001). The barrier function of intercellular lipids of the skin is attributed to several factors: a highly ordered multilamellar arrangement, a densely packed crystal-like structure, and solid phase at physiological temperature. Disturbances of these structures will result in a more disordered lipid matrix, thereby increasing the permeability of solutes. In general, the arrangement of a lipid bilayer can be affected at two locations, the polar head groups or the hydrophobic tails.

A simple example of a substance employed to enhance permeation is water, which can interact with the polar head groups of the lipid bilayer and thereby interfere with the molecular packing of the lipids (Roberts & Walker, 1993). Water cannot easily be applied directly to skin in order to enhance membrane hydration and therefore indirect methods of enhancing skin hydration are used. These include the use of moisturising factors, occlusive materials (such as hydrophobic base and patches) (Nardello et al., 2003), humectants, and hydrogels containing biopolymers such as hyaluronan (Neudecker et al., 2000).

Occlusion hydrates the keratin in corneocytes and increases the water content between adjacent intercellular lipid lamellae. It has been found that the limited amount of water located in the polar regions can induce a phase transition of the solid lipids and thereby enhance the mobility of the lipid acyl chains (Knutson et al., 1985). This will induce a loosening of the lipid packing, gelation or fluidization of the solid lipid phase and result in faster diffusion of hydrophobic compounds (Behl et al., 1980; Williams & Barry, 2004). On the other hand, adsorbed water that forms a separate water phase will provide a transport route for hydrophilic solutes with less resistance to the latter's penetration (as the partition coefficient between stratum corneum and the vehicle

increases towards unity) (Suhonen et al., 1999). Therefore, hydration of the stratum corneum enhances the penetration of both hydrophilic and hydrophobic compounds (Mak et al., 1991; Potts & Francoeur, 1991). Furthermore, skin temperature generally increases from 32°C to as much as 37°C under occlusive conditions (Hotchkiss et al., 1992). Of the various approaches employed to enhance the percutaneous absorption of drugs, occlusion is the simplest and perhaps one of the most common methods in use.

Hydrocarbons also have been used as vehicles or penetration enhancers to increase permeation of a variety of drugs across the skin. These permeation enhancers generally work by partitioning into the stratum corneum and disrupting the ordered lipid bilayer structure (Hori et al., 1991). Alkanes with 9–10 carbon atoms have been shown to induce the highest skin permeation enhancement of propranolol and diazepam, whilst shorter alkanes (5–6 carbon atoms) were most effective in enhancing the permeation of caffeine (Hori et al., 1991; Rahman et al., 1992).

Fatty acids and fatty alcohols are another class of enhancer and they function by interfering with the packing of lipid bilayers by inserting themselves between the hydrophobic tails of the lipids. They act by forming pools between the lipids rather than being distributed homogeneously throughout the bilayer structure (Ongpipattanakul et al., 1991). This disorder may induce alteration of the arrangement of polar head regions as well, so that diffusion of both hydrophilic and hydrophobic molecules can be enhanced. An example of such an enhancer is oleic acid, which has been shown to increase molecular mobility by inducing a phase transition in the lipid matrix by interacting with the hydrophobic tails of the lipids making them more fluid (Golden et al., 1987; Ongpipattanakul et al., 1991). The permeation enhancement effects of this class of enhancer are related to the length and conformation of the hydrocarbon chain. The maximum effect was achieved with chain lengths of about 12 carbon atoms (Aungst et al., 1986), and with the unsaturated double bonds in the middle of the chains with a *cis* conformation (Golden et al., 1987; Artusi et al., 2004). Since the lipids in the stratum corneum are primarily saturated (with the exception of small amounts of components such as linolenic acid) and therefore can form highly ordered structures, it is reasonable to assume that an unsaturated hydrophobic chain

inserted in the lipid bilayer may cause significant disruption to the bilayer structure (Golden et al., 1987; Harrison et al., 1996; Naik et al., 1995; Lane, 2013).

Similarly, 1-dodecylazacycloheptan-2-one (azone) can intercalate with the hydrophobic chains of the lipid bilayers and disturb the packing of the lipids (Okamoto et al., 1991). Additionally, it was found that azone and its chemically-related derivatives increased the diffusion coefficient of drug in the stratum corneum while the partition coefficient remained constant, showing that enhancement of diffusion accounted for the increased permeation (Schückler & Lee, 1992).

Esters, as isopropyl myristate, are another example of a vehicle that can disrupt the order of the arrangements of the lipids. The later solvent is capable of integrating into the lipid bilayers, inducing an increased membrane fluidity which may contribute to increased disorder of the stratum corneum and thus enhance the permeability of the lipids in the stratum corneum (Pillai et al., 2004).

Diffusion coefficients may be increased by mechanisms other than promoting disorder in the arrangement of lipids. Lipid extraction (delipidisation) may also provide an effective mechanism. For example, ethanol has been reported to selectively extract polar lipids from the lipid matrix, leading to a greater free volume in the lipid layer, thereby enhancing drug permeation (Bommannan et al., 1991). Further studies have also suggested that selective extraction of intercellular lipids may result in the formation of pores in the stratum corneum lipids (Peck et al., 1994). Ethanol has been used to enhance the skin permeation of solutes of differing physicochemical properties including: nitroglycerin (Berner et al., 1989) and estradiol (Megrab et al., 1995). The ethanol enhanced effect has been reported to be concentration dependent with the maximum fluxes occurring at an ethanol: buffer ratio of approximately 0.6 (Williams & Barry, 2004) beyond which a plateau or retardation in drug diffusivity across the epidermis might be expected to occur due to membrane dehydration.

Dimethylsulphoxide and urea not only have an effect on the stratum corneum lipids, but also interact with keratin in the corneocytes (Benson, 2005). When a surfactant penetrates the stratum corneum, it interacts and binds with the keratin filaments and

can change keratin conformation, resulting in a disruption within the corneocyte. This in turn causes an increase in the diffusion coefficient and permeability of any applied drug (Anigbogu et al., 1995; Benson, 2005).

1.7.1.2 Vehicle permeation enhancement by increasing solubility of drug in the skin

Many solvents can penetrate into the intercellular lipid matrix and change the solubility of an applied drug by transiently changing the solubility parameter of the skin. In turn, this results in an increase in the partition coefficient of some drugs in the stratum corneum. Consequently, there may be an improvement in the flux of the drug through the skin (Hadgraft, 1999; Hadgraft, 2004; Watkinson et al., 2009; Lane, 2013). For example the permeation of ibuprofen through skin from saturated propylene glycol–water mixtures increased with increasing volume fraction of propylene glycol. This was explained by an increase in the solubility of ibuprofen in the skin caused by the stratum corneum uptake of propylene glycol. However the solvent drag effect is also thought to participate in skin permeation enhancement of propylene glycol (Irwin et al., 1990; Bendas et al., 1995; Hadgraft & Pugh, 1998). Similarly, other solvents, such as ethanol, and *N*-methyl pyrrolidone, may also enhance drug permeation in a similar way (Hadgraft, 1999). Solvent drag can also account in part for the penetration enhancement effects of some solvents. For example, ethanol can pass rapidly through the stratum corneum and drag solute with it (Berner et al., 1989). However many chemical enhancers (e.g. propylene glycol and terpenes) act through a combination of several mechanisms, such as those which have been proposed for the effects of ethanol: causing alteration of the arrangement of the lipid polar head region (Granem et al., 1992), promoting extraction of polar lipids, enhancing drug solubility in the stratum corneum, and through exertion of the solvent drag effect.

1.7.2 Supersaturation

Supersaturated systems can be used to increase the concentration gradient beyond its maximum saturation level. This results in an increase in thermodynamic activity

leading to an improvement in drug flux across the skin as can be inferred from Fick's law of diffusion (Equation 1.1) (Hadgraft, 2001a). Supersaturated states can be prepared by loss of volatile solvent (Coldman et al., 1969), use of cosolvent mixtures (Davis & Hadgraft, 1991), temperature changes i.e. heating and cooling (Henmi et al., 1994) and uptake of water into the formulation from the skin (Kemken et al., 1992). The utility of the approach has also been demonstrated; for example, supersaturated systems of hydrocortisone (Davis & Hadgraft, 1991), estradiol (Megrab et al., 1995), piroxicam (Pellet et al., 1997) and fentanyl (Santos et al., 2011) have been studied. A major limitation of this approach is the subsequent physicochemical instability of the drug in the vehicle, since the drug often rapidly crystallizes leading to a decrease in the initial high activity (Hadgraft, 1999). This problem has been reportedly overcome by the use of antinucleant polymers such as hydroxypropyl methylcellulose to stabilize such systems; although the success of this method is dependent on the nature of the drug. It is possible that there are molecular interactions between the polymer and the drug molecules that prevent subsequent drug molecules interacting with each other (Pellet et al., 1994; Iervolino et al., 2000; Raghavan et al., 2001 a&b; Santos et al., 2009). Preparing drug administration systems using volatile solvents that induce drug supersaturation *in situ* (that is, only after dose actuation), is another way to achieve supersaturation (Leichtnam et al., 2006; Reid et al., 2008, 2009; Jones et al., 2009; Benaouda, 2012). The drug is prepared as a solution but, during dose actuation, it assembles into a micro fine occlusive film. In this technique a drug can be applied in a supersaturated form on the surface of human skin and stratum corneum transport will be enhanced without increasing the total loading of the compound in the topical product (Kondo et al., 1987). However, drug recrystallisation, remains a significant issue if solvents with low volatility are used to generate drug transient supersaturation (Santoso et al., 2010). Low boiling point propellant, such as a hydrofluoroalkane, is employed to form a transiently supersaturated system and provides the opportunity of reducing the applied volume of the formulation. The hydrofluoroalkane facilitates the storage of the active agent in a thermodynamically stable premix, whilst retaining the ability to form high levels of drug supersaturation upon dose ejection (Jones et al., 2009). Hydrofluoroalkane sprays have already been shown to be viable topical products, with MedSprayTM and MedthermTM being examples of available products

utilizing this technology (Leichtnam et al., 2006; Brown & Jones, 2007; Evans et al., 2010).

1.7.3 Prodrugs or metabolic approach

The permeability barrier properties of the skin are mediated by a series of lipid multilayers. Lipid synthesis is mediated by various enzymes (Steinsträsser & Merkle, 1995) and any alteration in enzyme activity will affect the barrier properties of the skin. The use of enzyme-inhibitors to enhance the permeation of hydrophilic and lipophilic drugs permeation has been investigated (Tsai et al., 1996; Elias et al., 2002, 2003; Babita & Tiwary, 2005). However another strategy to use a prodrug approach aimed at utilizing the enzyme function (Sloan & Wasdo, 2003). Such a prodrug approach depends on the ability of the available enzymes to metabolize the applied drug into its therapeutically active form. The prodrug design strategy generally involves addition of a promoiety to increase partition coefficient and hence solubility and transport of the parent drug across the stratum corneum. Upon reaching the viable epidermis, esterases (for example) can release the parent drug by hydrolysis thereby optimising solubility in the aqueous epidermis. The transdermal delivery of several compounds has been described in a number of studies, using such a prodrug approach for example oestradiol (Chien et al., 1985; Tojo et al, 1986 & 1991), indomethacin (Milosovich et al., 1989), theophylline, diclofenac (Bonina et al., 2001; Sloan et al., 2000; Majumda et al., 2012), 5-fluorouracil (Taylor & Sloan, 1998; Sloan et al., 2003; Milosovich et al., 1989), levodopa (Kushnir et al., 2008), acetaminophen (Thomas et al., 2009), bupropion (Kiptoo et al., 2009), naltrexone (Strasinger et al., 2008; Vaddi et al., 2009).

1.7.4 Lipid vesicles

Liposomes are colloidal particles formed as concentric biomolecular layers that are capable of encapsulating drugs. Vesicular carriers formed by the use of phospholipids have been shown to be very effective in enhancing the topical and transdermal delivery of solutes (Pierre, 2011). Phospholipids are amphiphilic molecules; having hydrophilic head groups and lipophilic tails. In aqueous solution the phospholipids are

arranged in bilayers, with the fatty acid tails being located on the interior of the vesicle, and the polar head groups pointed outwards. Phosphatidylcholine from soybean or egg yolk is the most common component (Touitou et al., 1994) and cholesterol is frequently added to the composition so as to stabilize the structure, thereby generating more rigid liposomes.

Liposomes are characterised by both their size and lamellarity (number of concentric lipid bilayers). A single bilayer enclosing an aqueous compartment is referred to as a unilamellar lipid vesicle, and according to size this is also known as either a small unilamellar vesicle (30-100 nm) or large unilamellar vesicle (100-3000 nm). If more than one bilayer is present, the liposome is referred to as a multilamellar vesicle (> 100 nm) (Gulati et al., 1998). The most effective liposomes employed to deliver drugs to the skin are claimed to be those composed of lipids similar to the stratum corneum lipids (Egbaria et al., 1990; Fresta & Puglisi, 1997; Sinico et al., 2005). This might be due to their ability to enter the stratum corneum lipid lamellae and fuse with endogenous lipids. Evidence suggests that liposomes do not enter the skin (Hope & Kitson, 1993; Moghimi & Patel, 1993; Schreier & Bouwstra, 1994; Badran et al., 2012). Standard liposomes exert their topical delivery by fusing with stratum corneum surface lipids and as a result enhance the partitioning of encapsulated material into the stratum corneum (Zellmer et al., 1995; Kirjavainen et al., 1996). It has also been postulated that phospholipids can affect stratum corneum lipid bilayer fluidity and enhance drug partitioning into the bilayers (Kirjavainen et al., 1996; Elmoslemany et al., 2012).

Another generation of vesicles has also been described and these have been termed 'ethosomes' and 'transferosomes'. These are claimed to be ultra-deformable liposomes, with an ability to penetrate into the skin i.e. squeeze themselves between the corneocytes in the stratum corneum to bypass the barrier (Cevc et al., 1993; Cevc, 1996; Godin & Touitou, 2003; Bragagni, 2012). Conventional liposomes remain near the skin surface, dehydrate and fuse with stratum corneum surface lipids and as a result can enhance the partitioning of encapsulated material into the stratum corneum (Zellmer et al., 1995; Kirjavainen et al., 1996, 1999 a&b). Transferosomes in

contrast are claimed to penetrate intact skin *in vivo*, carrying therapeutic concentrations of drugs (including macromolecules such as insulin (TransfersulinTM), with efficiency similar to subcutaneous administration, which only occurs when the elastic vesicles are topically applied in non-occlusive conditions (Cevc & Blume, 2001; Cevc et al., 1998, 2002). Transfersomes can act as carrier systems because of their high deformability and adaptability, which allow them to squeeze through small pre-existing channels in the stratum corneum despite their larger size (Cevc et al., 1998). The driving force for skin penetration of deformable vesicles is said to be the osmotic gradient across the skin. Topically applied Transfersomes become dehydrated on the skin surface by evaporation of the aqueous content and thus an osmotic pressure difference is created between the highly hydrated regions inside the skin and the dehydrated skin surface. This promotes the entrance of Transfersomes into the stratum corneum and they move into the deeper skin strata so as to avoid dehydration (Cevc & Blume, 2001; Cevc et al., 2002). Therefore, occlusive conditions are detrimental to the capability of Transfersomes to deliver drugs through the skin, as in this situation the osmotic effect would be removed.

Ethosomes are liposomes with a high alcoholic content that have been reported to be capable of enhancing penetration to deep tissues and the systemic circulation (Dayan et al., 2000; Touitou et al., 2000; Touitou et al., 2001; Godin & Touitou, 2003; Mao et al., 2013; Celia et al., 2012; Park et al., 2014). It is proposed that the ethanol ‘fluidises’ the ethosomal lipids and stratum corneum bilayer lipids and that this reduces the density of lipid multilayer and the barrier of the stratum corneum, allowing movement of the soft, malleable ethosomes into the skin. This process then results in fusion of the vesicles (ethosomes) with cell membranes in the deep layers of the skin allowing drug release and the subsequent absorption of the latter into the blood stream (Touitou et al., 2000; Godin & Touitou, 2003; Shi et al., 2012).

1.8 Oils incorporated in topical formulations

The topical application of oils and oil-based formulations in skin care and skin protection has been a common practice since ancient times. Such skin preparations

were originally comprised largely of animal fats and vegetable oils, especially sesame, olive and almond oils (Poucher, 1959). Oily vehicles are still currently widely used in cosmetics, for example in foundation creams, sun care creams, skin care creams, lip balms, deodorants, antiperspirant sticks, makeup removers and hair conditioners. Oils are also extensively used as moisturizers and emollients to improve skin quality and function in these formulations. A primary factor in selecting an oil for use on the skin is 'the feel' of the product on the skin. In addition, other factors may play a substantial role. For example the relative occlusivity on the skin is important for achieving an effective moisturizing function (Agner & Serup, 1993; Friebe et al., 2003; Förster et al., 2009; Hafeez et al., 2013). The occlusive effect traps water in the stratum corneum (preventing transepidermal water loss by evaporation) and there by mimics the role of natural emollients such as sebum and natural moisturising factor. Such an emollient effect can aid in the treatment of atopic eczema, since the prevention of water loss leads to a swelling of the stratum corneum, the closing of any cracks, and in so doing restores the epidermal barrier (Cork, 1997). Furthermore, the compatibility and the ability to solubilize other materials need to be considered, as does the ability of the final formulation to form stable emulsions. Odour and stability to light and oxygen are also critical to cosmetic formulation (Berdick, 1972). The oils incorporated in such topical formulations include: petrolatum, hexacecane, isohexadecane, lanolin, mineral oil, vegetable oils, fruit oils, essential fatty acids, eucalyptus oil, black currant seed oil, hazelnut oil, wheat germ oil, almond oil, sesame oil, coconut oil, hemp oil, squalane and synthetic oils such as polysiloxane (Müller et al., 2007; Pardeike et al., 2009 Karpanen et al., 2010; Fox et al., 2011; Sherry et al., 2013).

Oils also have been reported to enhance the percutaneous absorption of topically applied drugs (Dreher et al., 1997; Gallarate et al., 1999; Baroli et al., 2000; Alvarez-Figueroa & Blanco-Mendez, 2001; Wang et al., 2003; Rastogi & Singh, 2004; Sintov & Shapiro 2004; Kogan & Garti, 2006; Karpanen et al., 2010; Fox et al., 2011). This enhancement may involve a combination of mechanisms including fluidization of stratum corneum lipids, changes in the mechanical properties of the skin by rendering it more supple, lipid extraction or other means of barrier perturbation and occlusion.

The latter mechanism is often a consequence of the capacity of oils to moisturize the tissue. Lipid formulations work to moisturise the skin by increasing the amount of water held in the stratum corneum (Cork, 1997, Loden, 2003). Specifically, depending on the constituents of the oils, they work either by occlusion, ‘trapping’ moisture within the skin, by supplementing the properties of native stratum corneum lipids to provide a better barrier function as a consequence of reduced epidermal water loss (which results in an increase in skin hydration) (Lodén & Lindberg, 1991; Olsen et al., 1993; Blanken et al., 1989; Stamatas et al., 2008) , or in an ‘active’ way by drawing moisture into the stratum corneum from the dermis (Flynn et al., 2001, Rawlings & Harding, 2004). Formulations which involve the active movement of water from the dermis to the epidermis contain substances known as humectants, e.g. glycerine. These have a low molecular weight and water-attracting properties (Loden, 2003) and as they penetrate the epidermis they draw water from the dermis. Some cream and lotion emollients contain a mixture of occlusive and humectant substances; the humectant draws water into the epidermis while the occlusive element ensures that it is trapped there. The occlusive action of oils has been reported to increase the permeability and efficacy of drugs, due to the increasing presence of water, the swelling of corneocytes, possibly altering the intercellular lipid phase organization, as well as both increasing skin surface temperature and blood flow (Hotchkiss, 1992; Rawlings et al., 1994; Bucks & Maibach, 2005; Rawlings & Matts, 2005; Zhai & Maibach, 2005).

Lipid-based drug delivery systems (formulations containing lipids such as oils) have been demonstrated to be useful in enhancing the bioavailability of highly lipophilic compounds because they can maintain the drug in the dissolved state until it is absorbed (Rane et al., 2008). A number of cosmetic products now contain either solid lipid nanoparticles or nanostructured lipid carriers (Dingler et al., 1998; Jennings et al., 2000 a&b; Jennings & Gohla, 2001; Wissing & Müller, 2001 & 2002; Song & Liu, 2005; Jee et al., 2006; Joshi & Patravale, 2006; Liu et al., 2007; Pardeike & Müller, 2007; Shah et al., 2007; Pardeike et al., 2010). The cosmetic benefits of these lipid ingredients are reported to include an enhanced chemical stability and improved skin bioavailability of the active components, film-formation on the skin, skin hydration,

controlled occlusion, as well as an improved physical stability of the vehicle (Muller et al., 2007b; Barel et al., 2009).

Other examples of oils commonly in skin formulations include: isopropyl palmitate, octanol, triacetin, isostearyl isostearate, R(+)-limonene, and Mygliol 812[®] (medium chain length triglyceride), oleic acid, isopropyl myristate and Labrafil (Dreher et al., 1997; Gallarate et al., 1999; Rhee et al., 2001; Hiranita et al., 2003; Paolino et al., 2002; Escribano et al., 2003; Sintov et al., 2004; Kogan et al., 2006).

1.9 Assessment of in vitro permeation techniques

The methods for measuring skin absorption and dermal delivery can be divided into two categories: *in vivo* and *in vitro*. Ideally novel formulations or devices should be tested on humans in order to gain knowledge of the permeation, absorption and potential damage of the drug to the membrane. Practically, *in vivo* skin absorption measurement studies are rare due to ethical, economical, and analytical concerns. A shift in focus has been made over more recent years so as to develop and validate alternative *in vitro* test methods. There may be sufficient evidence to suggest that *in vitro* data are predictive for *in vivo* percutaneous absorption in both animals and man (Scott et al., 1992; Howes et al., 1996; Van Ravenzwaay & Leibold 2004; Williams, 2006; Lehman et al., 2011). Justification for the use of *in vitro* dermal absorption studies on isolated skin is based on the fact that the epidermis, in particular the stratum corneum, forms the principal *in vivo* barrier of the skin against penetration and uptake of xenobiotics in the body. *In vitro* methods measure the diffusion of chemicals into and across skin to a fluid reservoir and can utilise non-viable skin to measure diffusion only, or fresh, metabolically active skin to simultaneously measure diffusion and skin metabolism. Such methods have found particular use as a screen for comparing delivery of chemicals into and through skin from different formulations and can also provide useful models for the assessment of percutaneous absorption in humans (Howes et al., 1996; van de Sandt et al., 2004).

Several *in vitro* methods using excised skin have been developed for the evaluation of drug permeation. The use of Franz-type diffusion cells (Franz, 1975), also known as

vertical diffusion cells, is by far the most commonly used *in vitro* model for the study of percutaneous absorption, providing key insights into the relationships between skin, drug and formulation. This method is popular due to its simplicity, cost effectiveness, and the fact that the experimental conditions can be easily controlled by the investigator according to the purpose of investigation. Factors that need to be considered, when diffusion cells are required for *in vitro* testing, include: diffusion cell, membrane type, temperature, receptor fluid, finite or infinite dose, open or occluded testing.

1.9.1 Diffusion cell

In vitro permeation studies usually involve the use of *in vitro* diffusion cells which are made from inert, non-reactive materials such as glass, stainless steel and teflon (Friend, 1992). Diffusion cells comprise donor and receptor chambers between which the membrane is positioned. There are two different types of cells i.e. flow through systems and static type (Franz cell) systems (Franz, 1975; Bronaugh & Stewart, 1985; Van der Sandt et al., 2004).

1.9.2 Membrane type

Human skin for *in vitro* studies can be obtained from cadavers, or following cosmetic or plastic surgical procedures, and is subject to variability in the age, race, anatomical site, general health of the donor (Feldstein et al., 1998). Extreme care is necessary in the preparation of human skin membrane. There is a great deal of variability in human skin from donor to donor and hence studies should incorporate control experiments for each piece of skin to normalize the results. Due to biological variability a large number of measurements should be performed to obtain representative data (Gabbanini et al., 2009). The length and method of skin storage may also introduce variability (Swarbrick et al., 1982; Feldstein et al., 1998). There can be a problem with ensuring the availability of suitable quantities of human skin, especially if extensive experimentation is required. Due to such difficulties in obtaining skin and associated ethical considerations, simpler, better-characterized, readily available,

homogeneous, chemically pure and easier to handle membrane systems have been proposed to act as a model to investigate transdermal absorption (Scott, 1986; Feldstein et al., 1998). These include the use of artificial membranes including: silicone membrane which is a non-porous, hydrophobic, relatively inert and reproducible barrier. Silicone membrane is particularly useful to apply as a barrier, when factors, such as the effects of drug concentration on permeation are evaluated (Zadeh et al., 2008). Cellulose acetate and regenerated cellulose membranes are also used (Shah et al., 1989; Babar et al., 1991; Megrab et al., 1995; Ng et al., 2012).

Combining different polymers, such as silicone and cellulose acetate, has also been investigated as models to simulate the hydrophilic and lipophilic domains of the stratum corneum (Nastruzzi et al., 1993). Carbosil is a polydimethylsiloxane/polycarbonate block copolymer membrane, acting as a skin-imitating, permeation barrier (Feldstein et al., 1998). Other hydrophobic membranes, such as polyethylene, have, under certain circumstances, also proven to act as suitable models of the stratum corneum barrier function. However, the partitioning characteristics of both silicone and Carbosil membranes, lead to a much lower diffusional barrier when compared to polyethylene (Feldstein et al. 1998). Animal skin has also been used extensively in place of human skin, sources include the: mouse, rat, pig and snake (Babar et al., 1991; Dick & Scott, 1992; Schmook et al., 1993). More recently, the use of living skin equivalents i.e. reconstructed human epidermis (GraftskinTM, SkinethicTM) has also been reported (Lotte, 1997; Lotte et al., 2002; Schmook et al., 2001).

Synthetic membranes have been reported (Houk & Guy, 1988; Feldstein et al., 1998) to provide the most useful information about the *in vivo* process when:

- (1) The passive diffusional barrier imposed by the stratum corneum is the major resistance to transport.
- (2) The molecule of interest is known to be metabolically inert and not specifically bound in viable skin.

- (3) There is information available (taking into consideration the penetrant's physicochemical properties) concerning the probable importance of the possible penetration routes available *in vivo*.
- (4) *In vivo* experiments of similar design have been or can be performed and correlated with the *in vitro* results.

However, the use of artificial membranes also has its problems. In most instances, the membrane acts merely to separate physically the formulation from the receptor phase with the release rate being determined by the formulation, not the membrane. Although this might be adequate for developing therapeutic drug delivery systems, such studies do not provide appropriate relevant data when the skin controls drug input into the body.

Solute transport through a membrane that divides two compartments occurs either after the partitioning of the solute into, followed by diffusion through a distinct membrane phase (non-porous membrane), or by permeation through a continuous porous membrane. Cellulose acetate filtration and all dialysis membranes are examples of such porous barriers. Solutes (and some bulk solvent) may diffuse through the solution-filled pores, and the polymer and any immobilised solvent provides the only a physical barrier to free movement.

Partitioning membranes require solutes to partition into and to diffuse through a phase distinct from that of the donor and receptor solutions. Hydrophobic membrane systems such as silicone membrane have been used to model drug transport through biological lipid barriers and to correlate the transport rates with the physicochemical properties of the drugs studied. Specific molecular structure, absolute aqueous solubility, and the relative affinity of the molecule for the membrane versus the aqueous phase have been shown to be important determinants of permeability. If skin transport is determined by the lipophilic diffusional barrier of the stratum corneum, partitioning-membrane systems can provide a good correlation with skin models (Houk & Guy, 1988; Ottaviani et al., 2006; Sinko et al., 2009 & 2012; Joshi et al., 2012).

1.9.3 Temperature

The diffusion constant for diffusion processes across a homogenous membrane increases with increasing temperature (Clarys et al., 1998). Thus temperature should be maintained constant during permeation studies, at a temperature close to the normal topical skin temperature of 32°C. Any alteration in temperature will modify the flux of compounds across the membrane (Blank et al., 1967; Clarys et al., 1998; Akomeah et al., 2004). Increased xenobiotic penetration through the skin is associated with alterations in local blood flow (Sethna et al., 2005; Curry & Finkel, 2007; Sawyer et al., 2009). Four phase transitions in the structure of the stratum corneum, often defined as T1–T4, occur in the temperature ranges of 35–42, 65–75, 78–86 and 90–115 °C respectively (Silva et al., 2006). When heat is applied to a mixture of ceramides, fatty acids, cholesterol, cholesterol sulphate and esters, which constitute the lipid bilayers within the stratum coeneum, they become disrupted (Harrison et al. 1996). Wood et al. (2012) studied the effect of heat on the formulation release, drug partitioning and epidermal diffusion. Molecular mobility alterations in the vehicle, due to an increase in temperature to 45°C, led to higher drug release from the formulation. An increase in drug partitioning due to membrane mobility was also observed. A 5-fold increase in barrier diffusivity was attributed to lipidic bilayer structural rearrangement due to the fluidisation of the epidermis lipids in the temperature range of 37–45°C (Wood et al., 2012).

1.9.4 Receptor fluid

It is essential that during *in vitro* permeation studies, sink conditions are maintained to prevent significant back-diffusion of penetrant from the receptor phase into the donor chamber. Sink conditions may be defined as the provision of sufficient receptor phase to ensure that the thermodynamic activity in that compartment does not exceed 10% of the saturated solubility of penetrant in the receptor vehicle, in order to ensure an adequate driving force for diffusion is maintained (Higuchi, 1960 & 1961). Thus, the concentration of penetrant in the receptor should remain low throughout the diffusion study. The choice of a receptor fluid is influenced by the physicochemical properties

of the solute and the type of analytical method employed to determine the concentration. Also the receptor fluid should not alter the barrier properties of the membrane. Typically, aqueous solutions are used with polar solutes and ethanolic solutions with lipophilic solutes. The receptor fluid, preferably should be degassed in order to avoid formation of air bubbles during the experiment, and should be thoroughly stirred (static cells) or continuously replaced (flow through cells) during the entire experiment.

With regards to measuring skin integrity, the use of model markers covering a wide range of physicochemical properties is recommended. Possible candidates that have been proposed to act in this function include: hydrocortisone, theophylline, benzoic acid, salicylic acid, caffeine, water, mannitol, sucrose and testosterone (Howes et al., 1996). Increasing degree of skin damage causes an increase in the permeation of chemical markers. It is essential that the resulting permeability data recorded in the laboratory conducting the study agrees with that in the literature (performed under similar experimental conditions) to guarantee the fitness of the *in vitro* method employed.

1.9.5 Finite or infinite dose

The dose (finite or infinite) employed in permeation experiments should be considered depending on the type of information required. For *in vitro* studies requiring the determination of flux, or when investigating the effect of penetration enhancers on drug permeation through the skin, and other skin permeation parameters, an infinite dose is employed (Selzer et al., 2013). In infinite dose studies, the applied dose is so large that depletion of the permeant in the donor chamber caused by evaporation or diffusion into and through the barrier is negligibly small. Consequently, the dose is considered to be thermodynamically stable. In contrast, in the finite dose regime, only a limited amount of the donor formulation is applied to the skin surface. The application of a finite dose supposedly best resembles the *in vivo* situation when applying e.g. an ointment. In addition, special effects like the influence of evaporation of excipients can be observed

The Organisation for Economic Co-Operation and Development (OECD) guideline 428 (Howes, 1996), defines finite dose skin absorption experiments as those characterized by the application of $\leq 10 \mu\text{l}/\text{cm}^2$ of a liquid formulation to the skin. For semisolid and solid substances, values range from 1 to $10 \text{ mg}/\text{cm}^2$. The daily drug dose that can be systemically delivered through a reasonable ‘patch-sized’ area in contact with the skin is $\leq 10 \text{ mg}/\text{cm}^2$.

1.9.6 Open or occluded systems

Occlusion or the covering of the donor compartment of *invitro* diffusion cells, where the test substance or formulation resides during diffusion studies has been shown to enhance percutaneous absorption (Treffel et al., 1992; Cross & Roberts, 2000). Occlusion of the skin has been reported to increase the percutaneous absorption of various topically applied compounds (Bucks & Maibach, 2005) as a result of increase in temperature and stratum corneum water content as discussed previously.

1.10 Aims and objectives

In this study it is hypothesized that different oils interact with membranes depending on their inherent physicochemical properties. The aim of this study is to investigate the interaction of oily vehicles with synthetic membranes with a view to understanding the dermal delivery of concomitantly administered model permeant compounds. A further aim is to study the influence of mixed vehicle composition on the uptake of oil into silicone membrane and its influence on the diffusion of the model penetrants. Therefore the specific objectives were as follows:

- To identify a suitable range of oils for use as drug delivery vehicles based on their structure, molecular and physicochemical characteristics.
- To investigate the influence of blending different oil structures on the diffusion of model penetrants through silicone membrane.
- To investigate the interaction of oily vehicle formulations with model membrane barrier systems in order to understand the effect of structure and function of oil on the interaction with membranes.
- To study the influence of oil properties on the amount of oil that is sorbed by a membrane, from different oil blends applied to the membrane surface.
- To determine the flux of model compounds across a number of artificial membranes.
- To determine the flux of model penetrants across human epidermis from different oily vehicles.
- To model and identify the molecular properties that influence the permeation of different model compounds through different membranes and human epidermis by multivariate analysis of the data.

1.11 Model oily vehicles

In order to elucidate the factors affecting the amount of oils absorbed by membranes, five structurally unrelated oils with different solubility parameters, shape and size were required. The oils identified as suitable were isopropylmyristate (IPM) as an example of an ester oil, oleic acid (OA) as an example of *cis* fatty acid, isohexadecane (IHD) as a branched oil, hexadecane (HD) as an example of a linear oil and liquid paraffin (LP), which is comprised of mixed linear and branched oil molecules. All oils used are GRAS (Generally recognized as safe)

IPM is the ester of isopropyl alcohol and myristic acid. This oil is used in cosmetic and topical medicinal preparations where a high absorption through the skin is desired. IPM has been used extensively and over a prolonged time in commercial products including cosmetics and creams (Holzner, 1963; Campbell & Bruce, 1981). It has also been used in several *ex vivo* and *in vitro* drug permeation studies previously (Hadgraft et al., 1990; Alberti et al., 2001, Brinkmann & Müller-Goymann, 2003, Fang et al., 2002, Harada et al., 2005). IPM in combination with other solvents such as isopropyl alcohol, ethanol and triethanol amine has been shown to increase the drug permeation rate and bioavailability of these drugs (Alberti et al., 2001, Brinkmann & Müller-Goymann, 2003, Fang et al., 2002). It is suggested that IPM is capable of integrating into the lipid bilayers to promote membrane fluidity, which may contribute to an increased disorder of stratum corneum and thus enhance permeability of lipids within the stratum corneum (Pillai et al., 2004; Brinkmann & Muller-Goymann, 2005).

IHD is a light isoparaffin. It comprises a mixture of highly branched aliphatic hydrocarbon C₁₆ isoparaffins with a small proportion of C₁₂ and C₂₀ paraffins of similar structure (Nardello et al., 2003). The high degree of branching of IHD considerably shortens the overall molecular length, and this can enhance its interaction with other molecules (Nardello et al., 2003). It is widely used in cosmetics and personal care products since the sensory perception of the residue on the skin is 'non-greasy' in nature, but IHD has not been investigated as a vehicle in transdermal

delivery systems. It is a clear, colourless, slightly volatile, non-polar and hydrophobic liquid, which has very low toxicity and skin irritation. IHD forms particularly 'robust' emulsions (creams), which is an important feature for the product formulator. Foundation creams, sun-care creams, lip creams, deodorants and antiperspirant sticks, make up removers and hair conditioners are amongst the products that have been formulated with IHD.

OA is a monounsaturated omega-9-fatty acid and is present in various animal and vegetable sources; being the most abundant fatty acid in human adipose tissue. OA is a yellowish to pale brown, oily liquid with a characteristic lard-like odour and taste, comprised chiefly of (Z)-9-octadecenoic acid together with varying amounts of saturated and other unsaturated acids. Triglyceride esters of OA comprise the majority of olive oil, though there may be less than 2.0% as actual free acid in the virgin olive oil. Fatty acids promote skin permeation of various drugs (Cooper, 1984; Barry & Bennett, 1987; Larrucea et al., 2001; Nanayakkara et al., 2005). They interact with intercellular lipid domains and when intercalated in layers, they act to reduce the diffusional resistance to permeation and aid drug transport (Green & Hadgraft, 1987). The efficacy of fatty acids is related to their structures; there being differences between the efficacy of saturated and unsaturated forms and those of different hydrocarbon chain length (Tanojo et al., 1997; Kandimalla et al., 1999). The unsaturated fatty acids with *cis* conformation and C₁₈ chain length, have been shown to be more effective enhancers than their saturated counterparts, promoting the permeation of different drugs (Aungst et al., 1986; Chi et al., 1995). It is reported that oleic acid exists as a separate phase within the lipid domains of porcine stratum corneum and suggested that the mechanism of enhancement of OA is mediated by the formation of permeable defects within the stratum corneum lipids (Naik et al., 1995). This is a consequence of the conformation of the *cis* double bond, which favours the condensation of OA with other molecules of OA rather than distribute homogeneously within the skin lipid bilayers (Ongpipattanakulet al., 1991).

LP comprises a purified mixture of saturated hydrocarbons having the general formula C_nH_{2n+2}, with carbon chains generally greater than C₂₀, obtained from petroleum

(Rowe et al., 2006). It is employed as a topical vehicle, having no colour and only the faintest odour. LP is used in cosmetics due to its occlusive and moisturizing properties. Paraffin oil and vegetable oils (sweet almond oil, jojoba oil) have been reported to penetrate only the outermost layers of the stratum corneum (Stamatas, 2008). *In vivo* confocal Raman micro-spectroscopy was used to test the penetration and occlusion potential of the oils. The amount of petrolatum penetrated was 3-4 times more than vegetable oils and it penetrated deeper than the vegetable oils. There was no significant difference between the amounts of the three vegetable oils that penetrated. Paraffin oil and vegetable oils have the same occlusive potential, which is lower than petrolatum (Agero & Verallo-Rowell 2004; Stamatas, 2008).

HD is an alkane hydrocarbon. It is a colourless liquid, which does not mix with water. It is widely used in make-up, personal and skin care products due to its moisturizing and occlusive properties and non-greasy texture, although it is also reported to permeate well into the skin (Rossmiller & Hoekstra, 1966; Blank & McAuliffe, 1985; Singh et al., 2002).

CHAPTER TWO

**VALIDATION OF
ANALYTICAL METHODS**

2.1. Introduction

2.1.1 Model permeants

Permeants of different octanol/water partition coefficients and varying physicochemical properties, which are postulated to transverse the human skin through different routes, have been employed as suitable model permeants for transdermal research. For example, such permeants have been utilised for *in vitro* percutaneous absorption studies to: (i) determine the effect of possible penetration enhancement methods on the stratum corneum barrier (Ghanem et al., 1992) (ii) study the relationship between the physicochemical properties of the permeants and variability in their flux (Rougier et al., 1987; Williams et al., 1992; Liu et al., 1993) (iii) investigate any relationship between solvent and solute penetration (Cross et al., 2001) and (iv) validate *in vitro* skin permeation methods (Howes et al., 1996). In the current study, the model permeants: methyl paraben (MP), butyl paraben (BP) and caffeine (CF) were selected on the basis of their having a differing lipophilicity but similarity in molecular weight. Such a range of properties would enable some of the effects of partition on percutaneous absorption to be investigated discretely. These three compounds possess suitable stability over a range of pH and are reported to penetrate the skin via different routes (Akomeh et al., 2004) and have been employed by a number of formulation scientists to study transdermal penetration previously (Dias et al., 1999; Bock et al., 2002; Akomeah et al., 2004; Lopez et al., 2004; Akomeh et al., 2004; Nanayakkara et al., 2005; Oliveira et al., 2010; Oliveira et al., 2011). The chemical structure and some of the physicochemical properties the chosen permeants are shown in Figure 2.1 and Table 2.1 respectively.

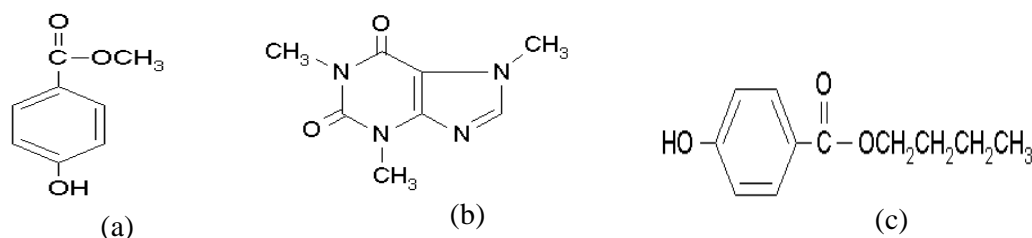


Figure 2.1 Structure of (a) methyl paraben (b) caffeine (c) butyl paraben.

Table 2.1 Physicochemical parameters of model permeants

	MP	CF	BP
Chemical Name	Methyl-4-hydroxybenzoate	1,3,7-Trimethylpurine-2,6(3H,1H)-dione;1,3,7-trimethylxanthine;7-methyltheophylline	Butyl 4-hydroxybenzoate
Molecular formula	C ₈ H ₈ O ₃	C ₈ H ₁₀ N ₄ O ₂	C ₁₁ H ₁₄ O ₃
Molecular weight	152.15	194.2	194.227
Log P _(o/w)	1.96	-0.07	3.57
δ _D ^a	17.9	19.5	17.3
δ _P ^b	5.9	10.1	4.9
δ _H ^c	13.5	13	10.4
Solubility parameter (MPa) ^{1/2}	24.13	28.83	22.29

*data determined by Hansen Solubility Parameters in Practice (HSPiP) software version 4.0.04 Copyright 2013 www.Hansen-Solubility.com

^adispersion component.

^bpolar component.

^chydrogen bonding component.

BP and MP are the butyl and methyl esters of p-hydroxybenzoic acid (termed parabens), respectively and they are frequently used in foodstuff, pharmaceuticals, cosmetic, toiletries and other personal care products; including shampoos, moisturizers, etc. They are considered good preservatives since they possess broad antimicrobial properties, relatively low toxicity, low volatility and high stability (Kang et al., 1997). However, studies suggest parabens may be carcinogenic and possess estrogenic disrupting activity, thereby disputing the notion of low toxicity for these compounds (Darbre et al., 2004; Harvey & Everett, 2004; Khanna et al., 2013). For example, it has been reported that the recommended intake of butyl and

propyl paraben (10 mg kg^{-1} body weight) was sufficient to cause adverse effects in male reproductive functions such as sperm production (Osihi, 2001 & 2002). In addition, both of these compounds have been reported to have the capacity to induce allergic contact dermatitis on topical exposure (Soni, 2002). Also the parabens have been reported to be implicated as a causative factor breast cancer (Khanna et al., 2013). However; such toxicological effects are of little relevance to the purpose of this study. Physically, MP and BP are white, crystalline powders, with a slight solubility in water but with a high solubility in ethanol (96%) and in methanol.

CF, a white crystalline powder is an alkaloid of the methylxanthine family, which also includes the similar compounds theophylline and theobromine. It occurs naturally in tea and coffee, but is prepared synthetically for commercial purposes. It sublimates readily and, in contrast to the parabens, is sparingly soluble in water and dehydrated alcohol. CF has been reported to be used as an anti-viral (Hamuy et al., 1998) and anti-cellulite (Bertin et al., 2001) and is claimed to be a mental stimulant (Benowitz, 1990; Kolega, 1993). The potential anticancer effects of CF upon oral administration have been reported (Sarkaria et al., 1999; Michal & Andrzej, 2008; Tomita & Tsuchiya, 2008). Orally administered and transdermally applied CF could protect the skin from ultraviolet light induced skin cancer (Huanget al., 1997; Lu et al., 2001; Lu et al., 2008; Shakeel & Ramadan 2010).

2.1.2 Reverse phase high performance liquid chromatography (HPLC) for quantification of model permeants

In order to monitor and quantify the amount of permeant traversing the membranes during diffusion studies, high performance liquid chromatography (HPLC) was used as the analytical method of choice. Model permeants used in this study could be analysed using several methods of analysis, for instance ultraviolet (UV) spectrometry, gas chromatography (GC) analysis, gas chromatography with mass spectrometry, liquid chromatography with mass spectrometry, ultra-high pressure liquid chromatography with mass spectrometry and HPLC analysis. HPLC separates various components in mixtures and can quantify them in a precise and

accurate way in short time with high sensitivity and specificity. These advantages in combination with the ease of operation and effectiveness of the method make it a popular analytical tool. HPLC affords simple preparation of many samples, avoiding extensive extractions usually necessary for ultraviolet or colorimetric assays. It avoids problems associated with thermal instability in gas chromatography and the occasional need for preparing volatile derivatives prior to analysis; and it overcomes the time factor and manipulative problems of quantitative thin-layer chromatography (Fitzpatrick et al., 1975). Separation in reverse phase HPLC chromatography depends on the reversible adsorption/desorption of solute molecules with varying degrees of hydrophobicity onto a hydrophobic stationary phase. It involves the partitioning of a solute molecule between mobile phase (e.g. acetonitrile, methanol, aqueous buffers or a mixture) and stationary phase filled with a solid adsorbent material (often octadecylsilane which is bonded to a silica support). The distribution of the solute between the two phases depends upon: the degree of interaction between the solute and adsorbent material in the column, the adsorption properties of the medium, the hydrophobicity of the solute and the composition of the mobile phase. The compounds can be detected most conveniently by monitoring the absorbance of ultraviolet (UV) radiation; assuming there is an appropriate chromophore in the molecule. UV detectors function by monitoring light absorbed by the solute molecules, each solute or, more specifically, its chromophore(s) may absorb light maximally at a characteristic wavelength, which allows identification of the solute. On the other hand if two or more solutes absorb light at the same wavelength, HPLC has the potential to separate them and quantify such analytes.

The HPLC method of analysis of all three permeants was adapted from the method described by Akomeah et al. (2004). HPLC was widely used previously to quantify the model permeants in transdermal studies (Twist & Zatz, 1986; Twist & Zatz, 1988 a&b; Bonina, 1993; Dias et al., 1999; Akomeah et al., 2004; Nanayakkara et al., 2005; Zhang et al., 2009; Oliveira et al., 2010; Zhang et al., 2011).

2.1.3 Gas chromatography

During diffusion studies permeants are expected to pass through the membranes, however the vehicle components may also enter the membrane. Since this thesis investigates oily vehicles, an appropriate analytical tool to quantify the amount of oil in the membrane is required. Oils are characterized by having non-polar and hydrophobic molecular skeletons. They are predominantly hydrocarbon-chain-containing organic compounds, having a wide range of structures. Oils can be analyzed using thin layer chromatography or HPLC with a refractive index detector. However gas chromatography (GC) is the primary and certainly one of the most suitable tools to analyze lipids (Mondello et al 2004; Brufau et al., 2006; Clement et al., 2010; Forchielli et al., 2010; Amusquivar et al., 2011).

GC comprises two phases: a stationary bed with a large surface area, and the other being a gas that passes through the stationary bed. The sample is vaporised and carried by the mobile gas (the carrier gas) through the column. Samples will partition into the stationary phase according to their solubility at a given temperature. The components of the sample separate from one another on the basis of their relative vapour pressure and affinity to the stationary bed. Classically, qualitative analysis with gas chromatography involves the comparison of retention data (retention time) of an unknown sample with that of a known one. Retention time is the time from the injection of the sample component until the recording of the peak maximum. The column temperature should be high enough for the sample components to pass through it at a reasonable speed. It needs to be higher than the boiling point of the sample, with higher temperature leading to decreased retention time and hence shorter analysis times.

GC analysis was chosen in order to separate and determine the amount of oils sorbed by the silicone membrane, since it provides a precise, accurate, sensitive, easy to operate and effective technique. Gas chromatography has several advantages as a physical method of separating gas mixtures (Matei et al., 2012) including: (1) resolution, the technique is applicable to systems containing components with very similar boiling points, (2) sensitivity, the detector based on

thermal conductivity of the component can detect picograms of sample, (3) convenience, it does not require highly qualified personnel to perform routine separation (4) low cost, (5) high separation power, (6) ease of recording data and (7) ready automation.

However GC has some disadvantages since it only detects volatile organic compounds; therefore it cannot be used for detecting semi-volatile compounds or thermally labile samples. The analytes should have a boiling point below 500°C (McNair & Miller, 1998). Operating under more extreme conditions may lead to short analysis intervals and incomplete use of the chromatographic column; for instance, many stationary phases undergo degradation or decomposition at operating temperatures above 250°C, resulting in a shorter operating life (Matei et al., 2012).

GC has been used previously to quantify lipids of different classes for instance free fatty acids, citrus oils, essential oils, olive oil, IPM, free sterols, squalene, palm oil, steryl esters, cholesterol, waxes, hydrocarbons (Bogusz et al., 2004; Fagan & Wijesundera, 2004 ; Mondello et al., 2004; Nang Lau et al., 2005; Brufau et al., 2006; Cardoso et al., 2006; Mondello et al., 2006; Isidorov, 2009 ; Liu et al., 2009; Clement et al., 2010; Forchielli et al., 2010; Amusquivar et al., 2011). Any GC method, in this case for the analysis for the oils, requires development and validation.

2.2 Aims & Objectives

The aim of the work described in this chapter was to develop suitable analytical methods to examine the influence of oily vehicles on barrier membranes and model permeant flux. In order to achieve this aim, the following were the objectives of this chapter:

1. Validate appropriate HPLC assay methods which would allow the precise quantification of the permeants being studied, in the presence of model membranes and human epidermis used in Franz cell diffusion studies.
2. Develop and validate appropriate GC assay methods which would allow the precise quantification of the oils being absorbed into silicone membrane.
3. Design a UV method which would allow the precise measurement of the solubility of model permeants in different oils.

During *in vitro* permeation methods, it was planned to conduct Franz cell diffusion studies. Franz diffusion experiments have evolved into one of the most important methods for investigating transdermal drug administration (Ng et al., 2010). The method requires the capability of monitoring the permeation of model diffusants through both synthetic membranes and human epidermis. Therefore a further objective of this chapter was to ensure lack of leaching of the membrane components (due to the interaction with the oils) which might interfere with the analysis. Another objective was to prepare human epidermal sheets such that they could be accommodated within Franz cells and to confirm that any leachable material from epidermis and the associated filter paper did not interfere with the utilised method.

2.3 Methods

2.3.1 Materials

The materials employed in the assay of the pentrants and oils are listed in Table 2.2.

Table 2.2 Materials used

Materials	Supplier
Methanol (HPLC grade) Acetonitrile (HPLC grade) Heptane (HPLC grade) Hexadecane	Merck Chemicals, Germany
Orthophosphoric acid	Riedel-de-Haen Chemical, Germany
Potassium hydroxide	Scharlau Chemical, Spain
Methyl paraben Butyl paraben Caffeine Triethylamine	Sigma Chemical Co., UK
Oleic Acid Liquid paraffin	Sigma, Germany
Isopropanol	BDH Laboratory Supplies, UK
Deionised water	Merck chemicals, Germany, and IPRC water treatment 0.22µm Millipak, Millipore, USA
Isopropyl myristate	Uniema, Malaysia
Isohexadecane	Uniema, UK
Whatman no. 1 filter paper	Whatman International Ltd, UK
Silicone membrane	Samco Ltd., UK
High density poly ethylene membrane	Pharmaceutical grade package material, donated from TQ Pharma, Jordan
Poly urethane membrane	Exopack, UK
Cellulose acetate nitrate membrane	Millipore, UK

2.3.2 HPLC assay method validation

2.3.2.1 HPLC chromatographic conditions for model permeants

A Class VP 2010 LC Pump with Auto sampler connected to a UV Absorbance Detector were employed (Shimadzu Japan). The column used for all permeants was a Symmetry 5 μ BDS (C18), 150 x 4.6 mm (5 μ m) (Waters, USA). The mobile phase for MP consisted of 35% v/v acetonitrile/65% phosphate buffer (50 mM KH₂PO₄ containing 1% w/v triethylamine, then adjusted to pH 3.5 with orthophosphoric acid). The mobile phase for the assay of BP was 50% acetonitrile/50% phosphate buffer (50 mM KH₂PO₄ adjusted to pH 3.0 with orthophosphoric acid) and for CF was 15% v/v acetonitrile/85% phosphate buffer (50 mM KH₂PO₄ adjusted to pH 3.0 with orthophosphoric acid). The flow rate and injection volume were maintained at 1 mL min⁻¹ and 50 μ L respectively, for all permeants. Samples were scanned using different wavelengths and the wavelength of detection (nm) was 254, 256 and 270 for MP, BP and CF respectively.

2.3.2.2 Calibration curve (linearity and range)

A stock solution (1.0 mg mL⁻¹) was prepared by dissolving 100 mg of the required solute (MP, BP or CF) to 100 mL volume in 50:50 v/v methanol:de-ionized water. A series of standard solutions with varying concentrations of each permeant was prepared by serial dilution using phosphate buffer (50 mM KH₂PO₄ adjusted to pH 7.0 with potassium hydroxide). Calibration curves were constructed by plotting the response (peak area) against concentration of the standards (0.2, 1.0, 5, 10, 15, 20 μ g mL).

2.3.2.3 Repeatability (intra-day variation) and intermediate precision

Three replicate series of the standard solutions were made from three stock solutions and then analysed on the day of preparation (day 1).

In order to determine the precision of the assay, the standards were stored at room temperature (25-27 °C) and analysed for the active content at different time intervals on three different days.

Accuracy was determined using the low (0.2 µg mL⁻¹), mid (10 µg mL⁻¹) and high (20 µg mL⁻¹) concentrations with three standard solutions of each concentration being employed for each point. The percent recovery and relative standard deviation (RSD) of the results were calculated.

2.3.2.4 Limit of detection and quantification

Calibration curves were constructed from the HPLC assay of the standard solutions, from which the limit of quantification (LOQ) and limit of detection (LOD) were calculated using equations 2.1 and 2.2, in accordance with ICH guidelines (2005).

$$\text{LOQ} = 10\delta / S \quad (2.1)$$

$$\text{LOD} = 3.3\delta / S \quad (2.2)$$

Where, δ is the standard deviation of the y-intercept and S the slope of the calibration curve.

2.3.3 UV assay method

The UV analytical method was carried out using Thermo electron vision pro software V4.20 (Thermo, Germany). A stock solution (1.0 mg mL⁻¹) was prepared by dissolving 100 mg of the required solute (MP, BP or CF) to 100 mL volume in isopropanol. A series of standard solutions with varying concentrations of each permeant was prepared by serial dilution using isopropanol. Using a 1mL volume quartz cell, calibration curves were constructed by plotting the response (absorbance) as a function of concentration of standards. The concentrations for the calibration curves were 1,2,4,6 and 10 (µg mL⁻¹) for BP, 1,2,4,5 and 8 (µg mL⁻¹) for MP and 1, 2,5,10 and 20 (µg mL⁻¹) for CF.

Samples were scanned spectrophotometrically at wavelengths between 200 and 400 nm to detect an appropriate wavelength for the assay of each permeant. The wavelengths of detection (nm) were: 254, 256 and 270 for MP, BP and CF respectively. Blank samples of isopropanol, and oils were scanned to determine whether there was any interference in the absorption of light at the wavelengths of assay.

2.3.4 GC assay method validation

The analytical method development and validation for the IPM/IHD and IHD/HD vehicles was carried out using a gas chromatograph model Varian CTC Analytic, (Varian,USA). A 0.53mm \times 30m fused silica capillary column bonded with a 1.0 μ m film of phase (G42) (Quadrex, USA) was employed with helium as the carrier gas and flame ionization detection.

For HD/IPM the analysis and validation were carried out using a Focus gas chromatograph (Thermo,Germany) with an auto sampler (Triplus, Germany) and the column was 0.53mm \times 30m fused silica capillary column bonded with a 1.0 μ m film (InertCap, Japan). The analytical parameters used to carry out the GC quantification of the oil mixtures are shown in Table 2.3.

2.3.4.1 Calibration curve (linearity and range)

A stock solution (100 mg mL⁻¹) was prepared by dissolving 2.50 g of the oil to 25 mL volume in heptane. A series of oil standard solutions containing varying concentrations of each were prepared by serial dilution using heptane. Calibration curves were constructed by plotting the response (peak area) against concentration of the standards (0.1-20 mg mL⁻¹) for the HD/IHD (0.1, 0.5, 1, 5, 20 mg mL⁻¹), IPM/IHD (0.1, 1, 5, 10, 20 mg mL⁻¹) and IPM/HD (0.1, 1, 5, 10, 20 mg mL⁻¹) blends of oils. Unknown concentrations of oils were then determined by reference to the appropriate calibration curves.

Table 2.3 Analytical parameters for the GC quantification of IPM/IHD, IHD/HD and IPM/HD mixtures

	IPM/IHD	IHD/HD	IPM/HD
Instrument temperature program			
Initial temperature (°C)	70	70	70
Initial time (min)	2	2	2
Rate (°C/ min)	7	8	7
final temperature (°C)	260	295	260
final time (min)	5	2	5
Injector temperature (°C)	220	220	220
Total time (min)	34.14	32.12	34.14
Inlet settings			
Mode split	Split	Split	Split
Split ratio	1:1	1:1	1:3
Injection volume (μL)	9.0	9.0	3
Flow rate (mLmin ⁻¹)	6	6	6

2.3.4.2 Repeatability (intra-day variation) and intermediate precision and accuracy

Three replicate series of the standard solutions were made from three stock solutions and then analysed on the day of preparation (day 1). In order to determine the precision of the assay, the standards were stored at room temperature (25-27°C) and analysed for the active content at different time intervals on three different days. The mean and RSD was calculated for each calibration point. Accuracy was determined using the low, mid and high concentrations with three standard solutions of each concentration being employed for each point. The percent recovery and RSD values were calculated.

2.3.4.3 Limit of detection and quantification

The LOD and LOQ were calculated as in section 2.3.2.4

2.3.5 In vitro permeation method validation

2.3.5.1 Membrane vehicle interference study

In order to determine the effect of synthetic membranes on the assay method employed in this study, 'simulated Franz cell' diffusion experiments were carried out. A piece of membrane was cut (the diameter being approximately 2 cm) and sandwiched between the donor and receptor chamber of the Franz cell (Figure 2.2). The receptor chamber was then filled with ~ 2 mL of phosphate buffer and 200 µL of oily vehicle introduced into the donor chamber. The assembled cell was then immersed into a water bath maintained at 37°C. Samples (200 µL) were only removed from the receptor compartment after 6 h and analysed via HPLC, the analysis was performed using the method described in section 2.3.2.

2.3.5.2 Preparation of human epidermal sheets

Fresh, surgically excised samples of human skin were obtained directly after abdomino plastic surgery with informed consent, from the patient attending a private clinic in Amman, Jordan. The board of directors and the ethics committee of the clinic reviewed

and approved the informed consent. Subcutaneous fat was carefully removed from the skin sample using forceps and a scalpel. Following removal of the fat, individual portions of skin were immersed in water at 60°C for 45 seconds (Kligman & Christophers, 1963; Nanayakkara, 2005). The skin was then pinned; dermis side down, on a corkboard and the epidermis (comprising stratum corneum and epidermal layer) gently removed from the underlying dermis by rolling the membrane using forceps. The dermis was then discarded and the epidermal membrane floated onto the surface of water and taken up onto a Whatman no.1 filter paper, the resultant epidermal sheets were blotted dry with tissue paper and stored flat, wrapped in aluminium foil and stored at -70 °C until use.

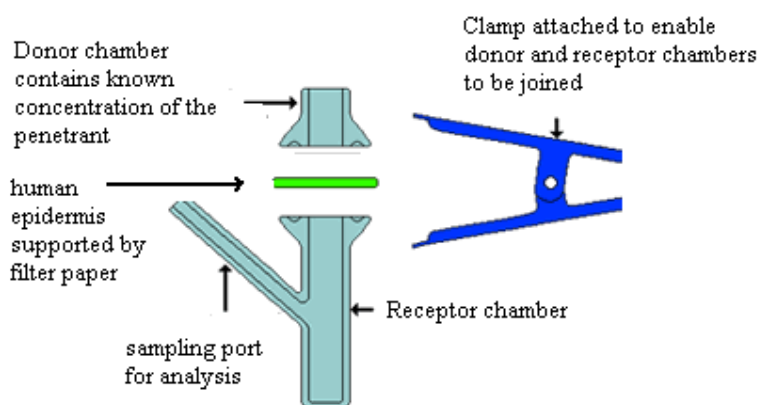


Figure 2.2 Schematic representation of Franz diffusion cell used for *in vitro* Permeation studies.

2.3.5.3 Determination of permeant binding to filter paper

During *in vitro* permeation studies (Figure 2.2), filter paper was used to support the epidermal membrane. However, a potential for some permeants to bind to the filter paper on which the epidermis is laid has been reported previously (Akomeah et al., 2004; Nanayakkara et al., 2005). This possibility was investigated by immersing circular pieces of filter paper, into a vial containing 5 mL of a standard solution (10 µg

mL⁻¹) of each permeant in phosphate buffer. Samples (200 µl) were removed from the vial after 0.5, 4, 6 and 8 h and assayed using the HPLC methods described in section 2.3.2.

2.3.5.4 Effect of skin-filter paper composite

In order to determine the effect of skin and filter paper on the assay method employed in this study, 'simulated Franz cell' diffusion experiments were carried out. A piece of human epidermal sheet (approximately 2 cm) was laid onto a filter paper and sandwiched between the donor and receptor chamber of the Franz cell (Figure 2.2). The receptor chamber was then filled with ~ 2 mL of a standard solution of the permeant in phosphate buffer.

100 µL of the same standard was also introduced into the donor chamber to ensure that no diffusional gradient was established. The assembled cell was then immersed into a water bath maintained at 37°C. Samples (200 µL) were removed from the receptor after 8 h only and analysed via HPLC. This experiment was performed using standard concentrations (µg mL⁻¹) of 0.5, 5, and 20 of each model permeant. Controls were also performed using phosphate buffer alone.

2.4. Results

2.4.1 HPLC method validation

2.4.1.1 Calibration curve (linearity and range)

A typical example of a standard HPLC/UV chromatograph (peak area against time (min)) generated in response to the injection of one of the model permeant is shown in Figure 2.3. The retention times were around 3.71 ± 0.07 min, 5.47 ± 0.08 min and 3.10 ± 0.07 min for MP, BP and CF respectively. Injections of phosphate buffer produced a steady baseline and no peaks were apparent which might coincide with the elution of any of the analytes (permeants) at the stated retention times. The data in Figure 2.4 show the linearity of the plots (between 0.2-20 µg mL⁻¹) of peak area as a function of concentration.

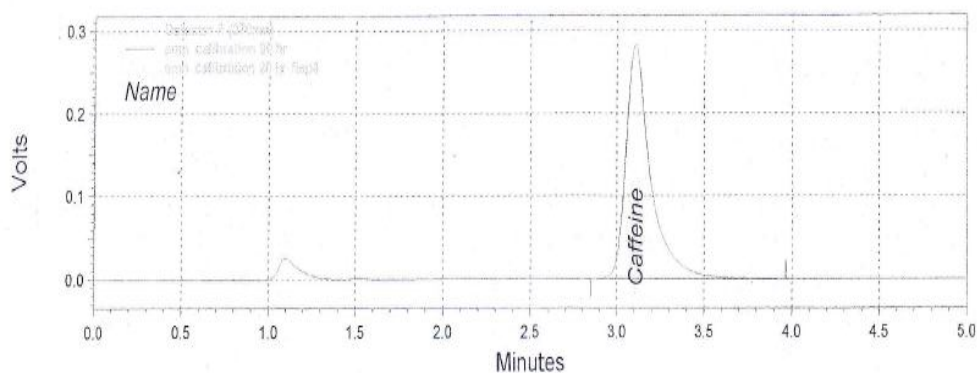


Figure 2.3 HPLC Chromatogram of a standard comprising $20 \mu\text{g mL}^{-1}$ CF in 15% v/v acetonitrile/ 85% phosphate buffer wave length 270 nm.

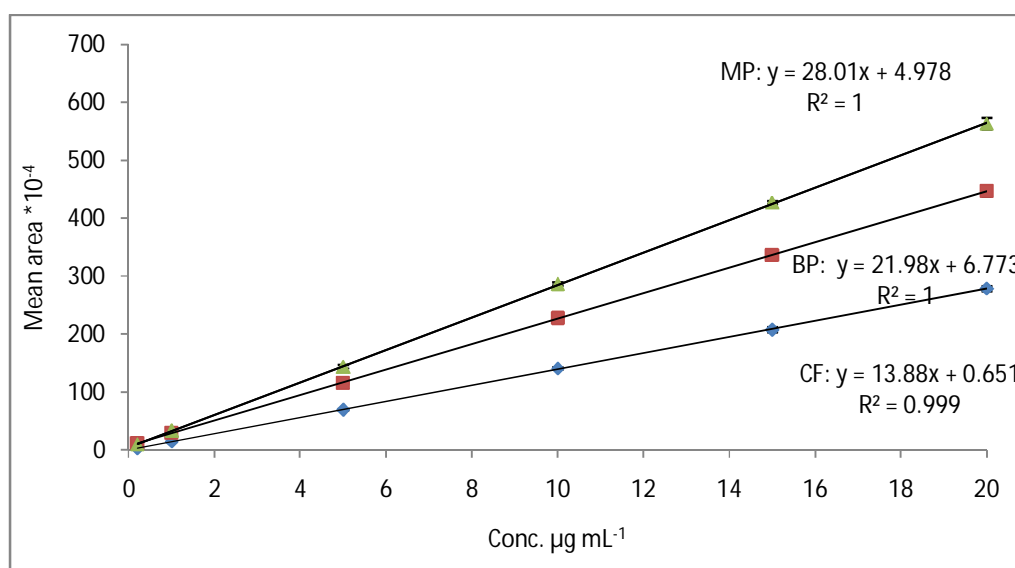


Figure 2.4 Linearity of HPLC calibration curves showing mean peak areas (absorbance units $\times 10^{-4}$) as a function of concentration of methyl paraben (▲), butyl paraben (■) and caffeine (◆) in phosphate buffer. The wavelength of detection (nm) was 254, 256 and 270 for MP, BP and CF respectively. Data represent mean \pm sd ($n=6$). Error bars lie within the symbols.

2.4.1.2 Precision (intra-and inter-day), accuracy, limit of detection and quantification

The relative standard deviation (% RSD) gives a measure of the precision of the analytical method (Table 2.4). The accuracy of the method was 95-105%. The repeatability (intra-assay variation) of the analytical method was found to be $\leq 5\%$ RSD on all occasions.

Table 2.4 Intra- and inter-day repeatability and precision (%RSD) obtained from HPLC chromatograms for MP, BP and CF standards of different concentration prepared in phosphate buffer

Concentration $\mu\text{g.mL}^{-1}$	% RSD intra-day (n=12)			% RSD inter-day (n=18)		
	MP	BP	CF	MP	BP	CF
0.2	1.43	1.3	1.67	1.87	1.71	1.94
1	0.71	1.28	1.63	1.93	1.64	1.86
5	0.33	1.13	0.43	0.92	1.17	1.72
10	0.11	1.04	1.00	1.03	1.38	1.56
15	0.21	0.45	1.82	1.23	1.13	1.12
20	0.13	1.35	0.48	0.54	1.23	1.05

There were no differences in the inter-day measurement of the slopes of the calibration curves for any of the model permeants employed (Table 2.5). These data also indicated the stability of the permeants in phosphate buffer at room temperature (25-27°C) over the duration of the experiment. The consistency observed in the measurement of both inter- and intra-day parameters implied that the employed HPLC conditions in the analytical determination of the permeants under investigation were “fit for purpose”. The assays were considered to have sufficient sensitivity to measure the likely levels of

each model permeant traversing the different membranes into the diffusion cell receptor.

Table 2.5 Linear regression analysis for calibration curves of MP, BP and CF on three different days, for peak area response ($\times 10^4$) plotted as a function of concentration

Compound	Day	Intercept	Standard deviation of the intercept	slope	Standard deviation of the slope	Correlation coefficient
MP	1	4.17	0.56	28.10	0.16	>0.999
	2	4.54	0.56	28.07	0.34	0.999
	3	4.14	0.43	28.05	0.25	>0.999
BP	1	6.61	0.44	22.17	0.12	>0.999
	2	7.00	0.40	21.99	0.18	>0.999
	3	7.30	0.38	21.95	0.19	>0.999
CF	1	0.62	0.30	13.87	0.22	>0.999
	2	0.83	0.25	13.78	0.23	>0.999
	3	0.79	0.25	13.81	0.14	0.999

2.4.2 UV method validation

Spectrophotometric scanning of the blank (control) samples of different oils and isopropanol did not yield any interference at the wavelengths selected to assay the permeants. Linear calibration curves comprising plots of absorbance as a function of concentration were obtained in all cases (Figure 2.5). The % RSD of the repeatability and reproducibility between all calibration points was ≤ 2 on different days. The LOD values obtained were 0.07, 0.04, 0.02 $\mu\text{g mL}^{-1}$ for MP, BP and CF, respectively.

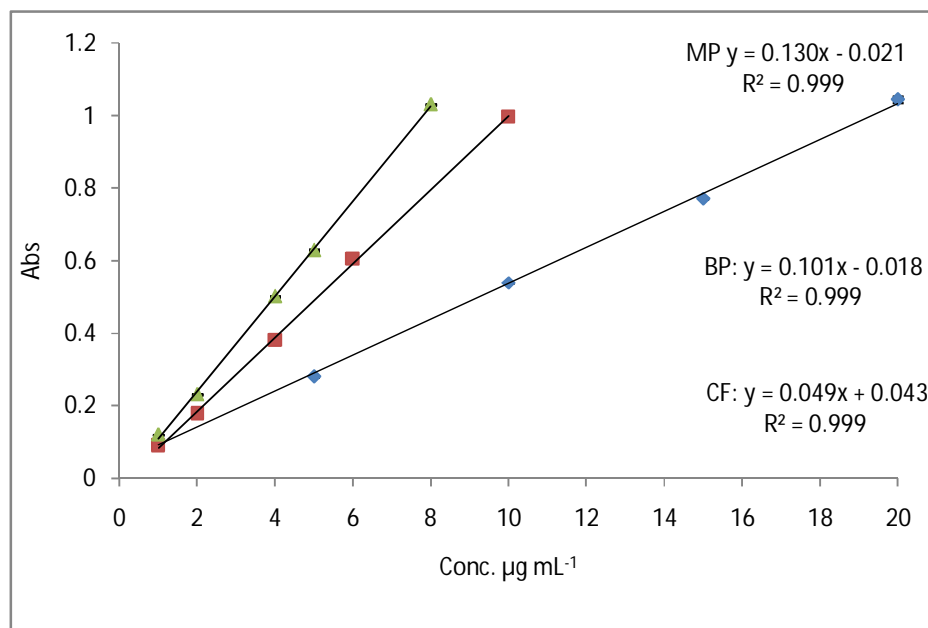


Figure 2.5 Calibration curves for UV method showing absorbance as versus concentration for methyl paraben (\blacktriangle) butyl paraben (\blacksquare) and caffeine (\blacklozenge). The wavelength of detection (nm) was 254, 256 and 270 for MP, BP and CF respectively. Data represent mean \pm sd ($n=6$). Error bars lie within the symbols.

2.4.3 GC Analytical methods

Three different methods were developed and validated for IHD/IPM, IHD/HD and IPM/HD.

2.4.3.1 Calibration curve (linearity and range)

When the mixtures of oils comprising IHD/IPM, IHD/HD and IPM/HD were injected onto the GC column, distinct separate and uniform peaks corresponding to the separate oils were obtained with retention times of IHD, IPM and HD at 12.48 ± 0.33 , 21.91 ± 0.35 and 16.61 ± 0.27 min, respectively. No other peaks were apparent which might coincide with the elution of the oils appeared when heptane was injected. Examples of chromatograms (peak height (arbitrary units) against time (min)) corresponding to the output obtained when standard solutions of IHD/IPM and IHD/HD were injected onto the GC column are shown in Figure 2.6 and 2.7.

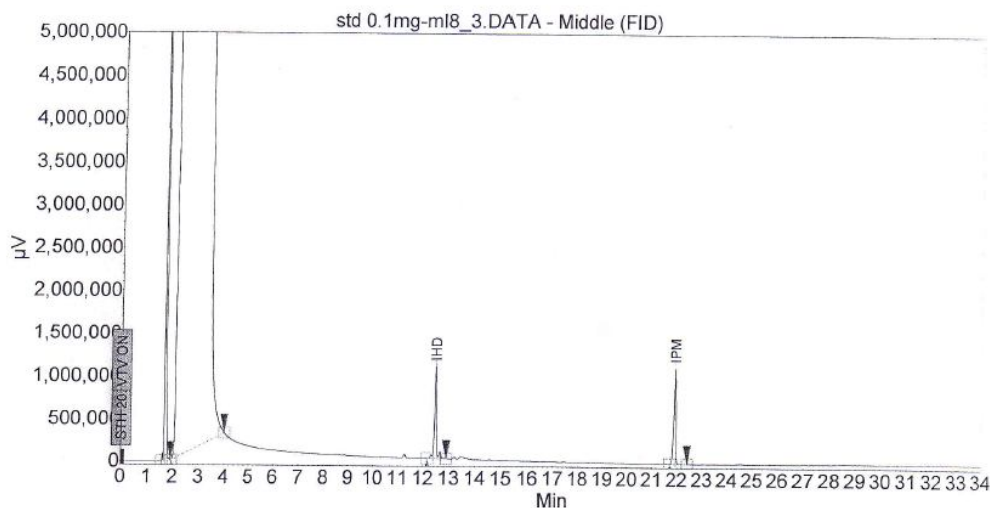


Figure 2.6 GC Chromatogram generated after injecting a heptane solution containing 0.1 mgmL^{-1} IHD and 0.1 mgmL^{-1} IPM.

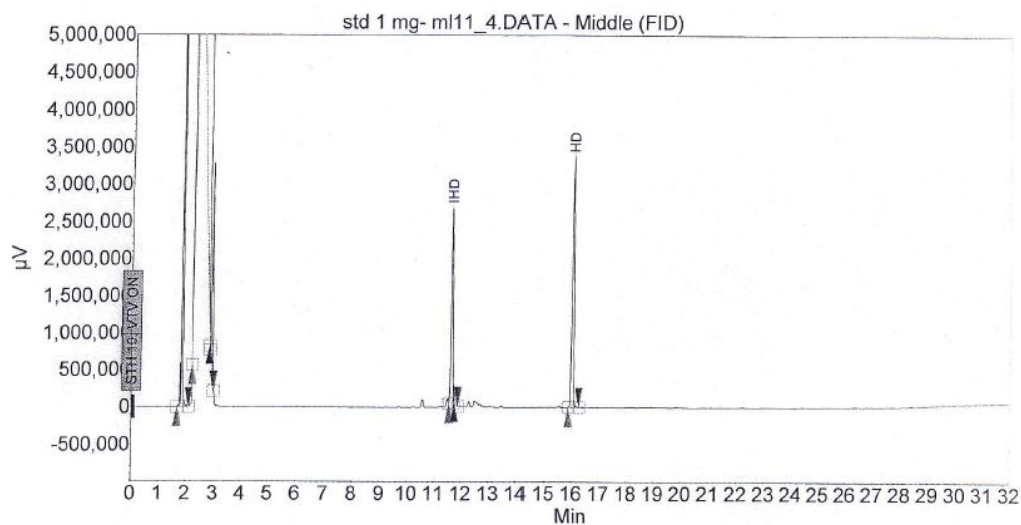


Figure 2.7 GC Chromatogram generated after injecting a heptane solution containing 1 mgmL^{-1} IHD and 1 mgmL^{-1} HD.

Intra-day analysis (day1) of the standards prepared in heptane for the three different methods yielded correlation coefficient (R^2) values exceeding 0.99 for IHD, IPM and HD (Figures 2.8, 2.9 and 2.10). The plots in Figure 2.8 show the linearity of the IHD/IPM method. Figure 2.9 shows the linearity of the IHD/HD method, and Figure 2.10 shows the linearity of HD/IPM method. The calibration curves were constructed (between $0.1\text{--}20 \text{ mg mL}^{-1}$) of oil.

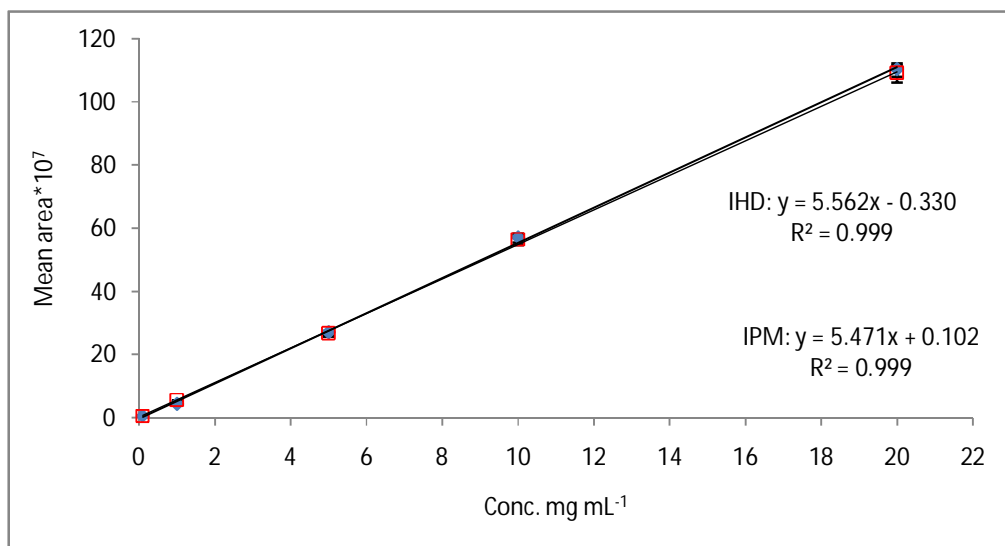


Figure 2.8 GC calibration curves showing mean peak areas (arbitrary units) as a function of concentration (mg mL^{-1}) of IHD (◆) and IPM (□). Data represent mean \pm sd ($n=6$). Error bars lie within the symbols.

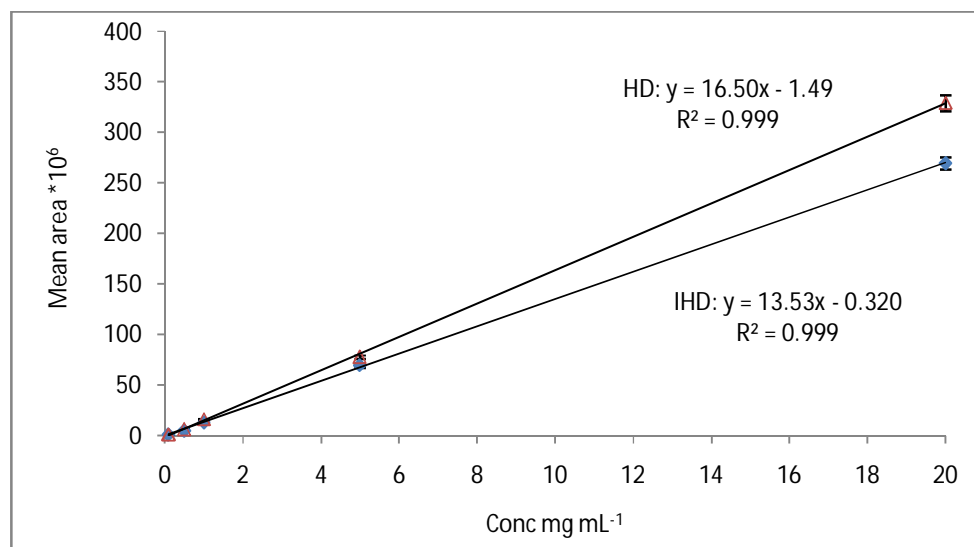


Figure 2.9 GC calibration curves showing mean peak areas (arbitrary units) as a function of concentration (mg mL^{-1}) of IHD (◆) and HD (△). Data represent mean \pm sd ($n=6$). Error bars lie within the symbols.

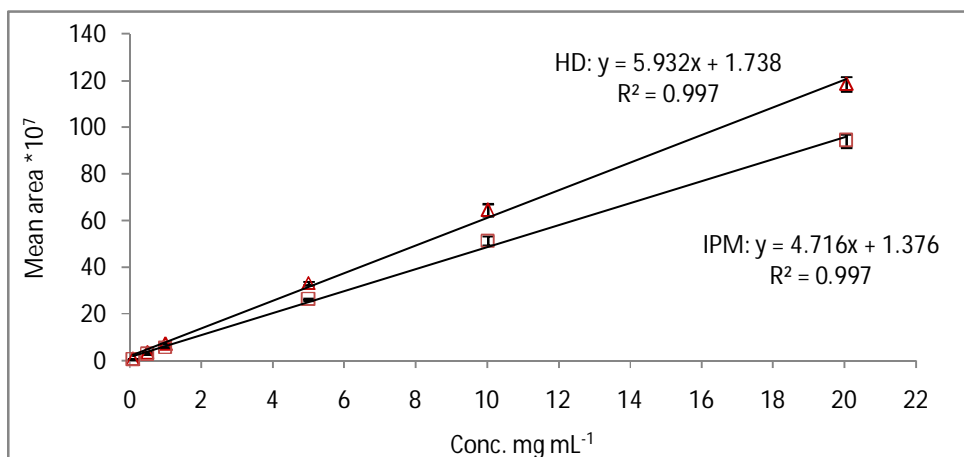


Figure 2.10 GC calibration curves showing mean peak areas (arbitrary units) as a function of concentration (mg mL^{-1}) of IPM (\square) and HD (Δ). Data represent mean \pm sd ($n=6$). Error bars lie within the symbols.

2.4.3.2 Precision (intra- and inter-day), accuracy, limit of detection and quantification

The % RSD provides a measure of the precision of the analytical methods for IPM/IHD (Table 2.6), IHD/HD (Table 2.7) and IPM/IHD (Table 2.8). The repeatability (intra-assay variation) of the analytical method was found to be $\leq 5\%$ RSD on all occasions. The accuracy of the methods was 95-105%.

Table 2.6 Intra- and inter-day repeatability and precision (%RSD) obtained from GC chromatograms for IHD and HD standards of different concentrations prepared in heptane

Concentration mg mL^{-1}	% RSD intra-day (n=12)		% RSD inter-day (n=18)	
	IHD	IPM	IHD	IPM
0.1	1.96	1.95	2.40	2.47
1	1.5	1.46	2.04	2.41
5	0.99	1.79	1.32	1.11
10	1.24	0.94	2.37	2.27
20	1.25	1.07	2.92	2.86

Table 2.7 Intra- and inter-day repeatability and precision (%RSD) obtained from GC chromatograms for IHD and HD standards of different concentrations prepared in heptanes

Concentration mgmL ⁻¹	% RSD intra-day (n=12)		% RSD inter-day (n=18)	
	IHD	HD	IHD	HD
0.1	2.52	1.63	2.66	2.50
0.5	1.83	1.10	1.70	1.73
1	1.25	1.62	1.60	2.35
5	1.04	1.89	1.92	1.75
20	1.79	2.11	1.80	2.70

Table 2.8 Intra- and inter-day repeatability and precision (%RSD) obtained from GC chromatograms for IPM and HD standards of different concentrations prepared in heptane

Concentration mgmL ⁻¹	% RSD intra-day (n=12)		% RSD inter-day (n=18)	
	IPM	HD	IPM	HD
0.1	2.55	2.36	2.75	2.90
0.5	1.76	1.78	2.02	2.12
1	1.88	2.70	1.95	1.96
5	1.54	1.55	1.98	2.01
10	1.11	1.06	2.50	2.12
20	2.14	2.02	2.78	2.58

There were also no differences in the inter-day measurement of the slopes of the calibration curves for any of the oils employed (Tables 2.9, 2.10 and 2.11). The assay was considered to have sufficient sensitivity for its application in this investigation.

Table 2.9 Linear regression analysis for calibration curves of IHD and IPM on three different days, for peak area response ($\times 10^7$) plotted as a function of concentration

Compound	Day	Intercept	Standard deviation of the intercept	slope	Standard deviation of the slope	Correlation coefficient
IHD	1	-0.69	0.12	5.76	0.55	0.999
	2	-0.50	0.09	5.49	0.29	0.999
	3	-0.71	0.12	5.48	0.17	0.999
IPM	1	-0.55	0.12	5.55	0.08	0.999
	2	-0.39	0.15	5.43	0.27	0.999
	3	-0.65	0.07	5.53	0.02	0.999

Table 2.10 Linear regression analysis for calibration curves of IHD and HD on three different days, for peak area response ($\times 10^6$) plotted as a function of concentration

Compound	Day	Intercept	Standard deviation of the intercept	slope	Standard deviation of the slope	Correlation coefficient
IHD	1	-0.59	0.68	13.13	1.02	>0.999
	2	-0.86	0.68	13.88	1.14	>0.999
	3	-1.23	0.61	13.49	1.02	0.999
HD	1	0.29	0.43	14.35	0.90	>0.999
	2	0.07	0.39	14.38	0.60	>0.999
	3	0.12	0.50	14.22	1.01	0.999

Table 2.11 Linear regression analysis for calibration curves of IPM and HD on three different days, for peak area response ($\times 10^7$) plotted as a function of concentration

Compound	Day	Intercept	Standard deviation of the intercept	slope	Standard deviation of the slope	Correlation coefficient
IPM	1	0.90	0.04	4.84	0.73	0.998
	2	1.17	0.11	4.75	0.66	0.998
	3	1.25	0.10	4.56	0.59	0.999
HD	1	1.20	0.14	6.09	0.78	0.998
	2	1.77	0.19	5.96	0.33	0.998
	3	1.49	0.10	6.01	0.82	0.999

2.4.4 In vitro permeation method validation

2.4.4.1 Membrane vehicle interference study

No additional peaks were detected in the chromatograms of any of the oil samples analysed after 6 h incubation with any of the membranes. Therefore it appears that none of the oily vehicles leached assay-interfering components in detectable amounts from the membranes. Accordingly, the analytical method appears to be 'fit for purpose' in assaying the proposed model permeants.

2.4.4.2 Permeant-filter paper binding study

Data from the permeant–filter paper binding experiments showed that 97.9-102% of each permeant could be recovered after 8 h incubation of any of the permeants with filter paper. These results are within acceptable range for this study, and the filter paper can be used as a support in the diffusion studies.

2.4.4.3 Skin-permeant assay interference

HPLC analysis of the permeant after 8 h at 37°C showed that there was no disappearance of model permeants from the receptor chamber when incubated with the filter paper and human epidermis composite in the Franz cell using low, medium and high concentrations of each permeant (Table 2.12). These results confirmed that there is no loss of the permeants when incubated with the skin and filter paper. In the control experiments using oily vehicles and phosphate buffer, no interfering peaks were noted at any of the retention times corresponding to the model permeants.

Table 2.12 The amount of MP, BP and CF expressed as a percentage (%) of the original standard concentration of model permeant recovered from receptor chamber of Franz cell after 8 h. Data represent mean \pm sd (n = 3)

Concentration $\mu\text{g mL}^{-1}$	MP	BP	CF
0.5	102.7 \pm 4.2	97.2 \pm 6.7	102.9 \pm 4.7
2	101.8 \pm 10.3	97.9 \pm 8.9	101.2 \pm 7.6
20	102.7 \pm 7.5	98.6 \pm 1.9	99.6 \pm 4.6

2.5 Discussion

The HPLC experimental results for assay validation of the model permeants demonstrated linearity, specificity, accuracy, repeatability and precision values, which were considered satisfactory and fit for the purpose of carrying out the proposed studies i.e. to quantify the model solutes involved in the *in vitro* permeation studies. The method was validated in the concentration range from 0.2 to 20 $\mu\text{g mL}^{-1}$, the correlation coefficients were $r^2 \geq 0.999$. The estimated lower detection limits were 0.05, 0.05 and 0.06 $\mu\text{g mL}^{-1}$ for MP, BP and CF respectively. The precision of an analytical procedure is an important parameter, and it is determined by the relative standard deviation (RSD). The experimental results indicate good repeatability and all the RSD values were no more than 2.00%. The

heat separation method used in this investigation to isolate the epidermis from the remaining skin tissues has been shown to result in the elimination of most of the skin's enzymatic activity (Wester et al., 1998). Accordingly, as expected the HPLC method, employed in this study did not identify or quantify p-hydroxybenzoic acid, which is the major metabolite when the parabens undergo hydrolysis due to the enzymes present in the skin.

Oils belong to a class of substance called lipids, and oils are usually liquid at room temperature. Gas chromatography is one of the most powerful analytical procedures for separating and analyzing the properties of lipids. It separates complex mixtures of different molecules based on their physical properties, such as polarity and boiling point. Gas chromatography in combination with flame ionization detection is the most commonly employed technique in the petrochemical and pharmaceutical industries for the assay of oils (Zeng et al., 2012). The operation of flame ionization detectors is based on the detection of ions formed during combustion of organic compounds in a hydrogen flame. The sample is passed into a hydrogen flame to oxidise (burn) organic molecules which produce electrically charged particles (ions). A polarizing voltage attracts these ions to a collector located near the flame producing an electrical signal, which is sensed by an electrometer. The generation of these ions is proportional to the concentration of organic species in the sample gas stream. The flame ionization detector is the most sensitive gas chromatographic detector for hydrocarbons (Yang et al., 2008; Matei et al., 2012).

Typically gas chromatography analysis is suitable for organic and inorganic compounds that are vaporized at 400°C or less. Due to the high boiling points of oils the injector, column and detector temperatures must be kept high. Most available GC methods allow for high detector and injector temperatures, but a limitation is likely to be conferred by the nature of the capillary column available. Most available columns have a maximum temperature limit of 320°C or less, and since oleic acid has a boiling point of 370°C, the available columns were unsuitable for the detection of this oil. Liquid paraffin is a mixture of hydrocarbons oils from C₁₀ to C₂₅, and therefore it is not easily quantifiable by gas chromatography with a flame ionization detector. It is not a selective technique for the LP components, and

the mixtures of hydrocarbons produce a broad hump of unresolved components. However, it can be used semi-quantitatively to determine the sum of the saturated hydrocarbons or aromatic hydrocarbon, with specified molecular mass ranges available in a sample (Biedermann et al., 2009).

The boiling points of IHD, HD and IPM are below 300°C and methods for mixtures of IPM/IHD, IHD/HD, and IPM/HD were designed, developed and validated. The chromatographic conditions (temperature programming) were optimized to achieve sufficient resolution of the analytes while maintaining the run-time as short as possible. To achieve full evaporation of the sample, the detector temperature was chosen to be higher than the boiling point of the two oils. Heptane was chosen as a solvent since it has the ability to dissolve the oils but is thermally stable and also volatile. Samples were found to be stable in heptane for one week (although, no further stability time points were completed after one week, since all analytical testing of samples was conducted within one week of sample preparation). Since the oils used were all hydrophobic the column employed was non polar silica, in order to achieve adequate separation. In GC analysis, in order to obtain the best peak shape and maximum resolution, a small sample size should be used; therefore a split mode was used to dilute the concentration of the sample. When a sample is introduced into the heated small chamber via a syringe through a septum, the heat facilitates volatilization of the sample. The carrier gas then either sweeps the entirety (splitless mode) or a portion (split mode) of the sample into the column. In split mode, a part of the sample/carrier gas mixture in the injection chamber is exhausted through the split vent. Split injection is preferred when working with samples with high analyte concentrations (>0.1%) whereas splitless injection is best suited for trace analysis with low amounts of analytes (<0.01%).

The complete separation of the compounds of interest is always the primary goal in any chromatographic separation method. The methods were validated in the concentration range from 0.1 to 20 mgmL⁻¹, with high correlation coefficients ($r^2 \geq 0.99$), and estimated lower detection limits of 0.05 and 0.05 mgmL⁻¹ for IHD and IPM respectively; 0.03 and 0.03mgmL⁻¹ for IHD and HD respectively; and 0.08 and 0.06 mgmL⁻¹ for HD and IPM respectively. The experimental results indicate good

repeatability and all the RSD values were not more than 5.00%. Generally branched alkanes elute first, followed by the normal alkanes (Zeng et al., 2012), which was demonstrated by the IHD having a shorter elution time than HD. The degree of resolution, between two peaks, appears to be a good measure of the separating power of capillary columns (Szopa et al., 2000). All the methods achieved high resolution between the two peaks. The retention times for the three different oils that formed components of binary mixtures being approximately 12.28 ± 0.33 16.61 ± 0.27 and 21.91 ± 0.35 min for IHD, HD and IPM, respectively. Therefore, analytical conditions such as column type, column temperature and carrier gas flow rate etc. allowed a baseline separation to be achieved. IPM was assayed using GC analysis in previous studies however different analysis conditions were used in this investigation (Klaffenbach & Kronenfeld, 1997; Liu et al., 2009). The designed GC method experimental results, for the validation of the assay of IHD, HD and IPM mixtures, were considered satisfactory to quantify the amount of oils sorbed by the silicone membrane.

It was planned to employ a series of synthetic and epidermal membranes to study the diffusion of model permeants from different oily vehicles; therefore it was necessary to check that there was no interference from the oily vehicles and membranes in the assay of model permeants. A simulated diffusion experiment was carried out, where an oily vehicle introduced to the donor compartment and the receptor solution was assayed after 6 h. It was shown that there is no interference due to components being solubilised from the membranes. No peaks appeared in the chromatograms.

During the skin permeation studies, filter paper was placed underneath the epidermis in order to facilitate handling. However there is the potential for permeants to be sorbed by the paper or for the epidermis to introduce components into the solution leading to interference with the assay. Such phenomena, if they occurred, would adversely affect the estimation of the *in vitro* skin permeation parameters. The potential for assay interference and sorption was investigated by incorporating a skin-filter paper composite in a Franz cell. Solution containing the same active concentration of each permeant was introduced into both the donor and

receptor compartments in order to simulate potentially the experimental design but also ensure that there was no diffusional gradient. Analysis of the permeant concentration after 8 h showed that there was no sorption of the permeants by the epidermis or the filter, and the loss of the permeants was negligible (recovery \geq 97%). Other authors have reported the lack of interference for the model permeants used with filter paper and human epidermis (Akomeah et al., 2004; Nanayakkara et al., 2005). The model permeants used in this study have been frequently used in skin permeation studies investigating the influence of permeant lipophilicity (Twist and Zatz, 1988 a&b; Kitagawa et al., 1997; Godwin & Michniak, 1999; Akomeah et al., 2004; Nanayakkara et al., 2005; Dias et al., 2007; Oliveira, 2010).

In conclusion, the Franz cell method appeared to provide a viable mean of assessing the *in vitro* diffusion of the selected model permeants. The assay methods would allow an adequate quantification of the diffusion of permeants from different vehicles through various membranes. The HPLC assay was found to be “fit for purpose”, and the GC method can be used to quantify the amount of oils sorbed by silicone membranes.

CHAPTER THREE

***DIFFUSION OF MODEL PERMEANTS
FROM OIL BLENDS***

3.1 Introduction

3.1.1 Partition diffusion process

In order for a topically applied drug to cross a membrane, the drug must first be dissolved in the vehicle/formulation; it then diffuses to a region where it can partition into the membrane from the vehicle, diffuses through the membrane and then partitions into the receiver fluid *in vitro* or *in vivo*, to lower dermal layers or the circulation. The physicochemical properties of the permeation barriers (i.e. the membranes) are one of the major rate determinants for transport (Higuchi et al., 1981; Martin, 1981). It includes the lipophilic character of the membrane, the presence of water pores and the membrane surface area available for absorption (Levine, 1970; Higuchi et al., 1981; Siepmann & Peppas, 2011). As discussed previously (Section 1.9.2) there is a requirement in certain studies to employ non-biological membranes. These are categorized generally into two classes: barrier membranes and porous membranes. As suggested by the name, barrier membranes have no pores and the drug will diffuse by "molecular permeation". Drug partitions into the membrane because it has some affinity for the membrane, then it will move from an area of high chemical potential to one with lower potential, and this ultimately leads to an equalisation of the chemical potential of the molecules throughout the membrane. Passive diffusion of a molecule through a membrane is controlled by several factors, including the solubility of the molecule, lipophilicity, molecular size and the concentration on either side of the membrane. A porous membrane allows small molecules to diffuse through the aqueous-filled pores, although the properties of the diffusing molecule, such as its size, shape, charge and aqueous solubility are critical determinants of the rate.

3.1.2 Formulation components affecting flux across membrane

The rate of transport of drugs from simple vehicles across the stratum corneum will often be insufficient to achieve therapeutic drug concentrations at the site of action. Simple vehicles are defined as those in which the drug is at or close to saturation solubility, and neither the vehicle nor the drug has any interaction with

the stratum corneum which might reduce the barrier function of the latter (Davis et al., 2002). In simple vehicle systems, a large difference in the rate of skin penetration can occur between two vehicles that contain a fixed drug concentration. Depending on the saturated solubility of the drug in each vehicle, vehicles in which the drug is at or near saturation will show enhanced drug penetration, compared with those in which the drug is sub-saturated (Ostrenga et al., 1971; Lippold, 1984). However, in many cases certain formulation components might also interact with the membrane, changing its physicochemical properties and consequently modulating solute transport. Hence, passive permeation enhancement can be achieved either by increasing the thermodynamic activity of the drug, or by using vehicles that could interact with membranes. A possible approach to increasing the thermodynamic activity of a drug is through the use of supersaturated systems, discussed in detail in Section 1.7.2, which was first proposed by Higuchi (1960). Supersaturated systems that are stabilized have been shown in a number of studies to enhance drug thermodynamic activity (Coldman et al., 1969; Davis & Hadgraft, 1991; Henmi et al., 1994; Pellett et al., 1994 & 1997; Raghavan et al., 2001 a&b; Santos et al., 2009).

A number of surfactants or solvents have been incorporated into transdermal delivery systems to act as permeation enhancers; for example low molecular weight alcohols, polysorbates, OA, azone, IPM, non-ionic surfactants, isopropyl palmitate, propylene glycol, hydrocarbon esters and urea (Embery & Dugard, 1971; Barry & Bennet, 1987; Hadgraft, 1993; Abraham, 1997; Paudel et al., 2010; Lane, 2013). Vehicles can therefore either promote an increase in diffusivity within the barrier membrane and/or enhance the partitioning properties into the membrane. Diffusion enhancement is mediated by vehicles that could intercalate with the lipid bilayers and disrupt their packing or fluidize them. Some of these penetration enhancers have also been employed as vehicles, they have been reported to exist as discrete phases in the intercellular lipid domains, these include for example OA, IPM, azone and alcohols (Wiechers et al., 1987; Hirvonen et al., 1994; Leopold & Lippold, 1995; Harrison et al., 1996; Clarys et al., 1998; Engblom et al., 1998; Degim et al., 1999; Ongpipattanakul et al., 1999; Lane, 2013).

Partition of permeants from vehicles will be dictated by the creation of a more favourable environment for increased solubility of the drug. The latter will be mediated by those solvents which are well taken up into the skin and/or which are also good solvents for the molecule of interest, for example propylene glycol (Lane, 2013). Synergy between these prime mechanisms has been demonstrated using a number of different systems including, for example, propylene glycol and terpenes, OA and propylene glycol and azone plus propylene glycol (Wotton et al., 1985; Davis et al., 2002; Rosado et al., 2003). The drug in the formulation can interact with the skin layers during percutaneous penetration, which might result in a slowed or more limited absorption. This interaction might be reversible or irreversible. However when the drug binds to a specific site in the skin, this might produce a physiological response, which can be either a therapeutic or non-therapeutic (i.e. unwanted or toxic) reaction. Also drugs might accumulate or be retained in the skin or membranes since this can occur as a result of relatively high drug partition, associated with slow drug diffusivity or drug crystallisation (Lane, 2013). These processes might contribute to the reservoir capacity of the skin for certain compounds. Lower layers of the skin comprise a metabolically active region and therefore some drugs may undergo metabolism during the process of permeation (Sections 1.1.2.1 and 1.7.3).

3.2 Aims and Objectives

Oils are generally assumed to be inert and not to interact with non-biological membranes. The aim of this study was to evaluate and compare the effect of oils and different oil blends on the solubility and diffusion of three model permeants of differing lipophilicity but similar molecular weight through a synthetic membrane. The diffusion of the respective compounds would be correlated with their physiochemical properties. In order to fulfil these aims the following objectives were developed:

1. To determine the solubility of model permeants in the receiver phase, oils and oil mixtures.
2. To study permeant release from oily vehicles using cellulose acetate nitrate (non-rate limiting) membranes.
3. To study permeant diffusion from oily vehicles using silicone (rate limiting) membrane.

3.3 Methods

3.3.1 Materials

The materials used in these studies are listed in Table 2.2

3.3.2 Solubility studies

Solubility studies were conducted by adding an excess amount of each model permeant separately to deionized water, phosphate buffer pH 7.0, IPM, IHD, LP, HD, OA and to different blends of oils. The suspensions were vortexed briefly and further agitated at 32°C in a shaking water bath at 110 rpm for around 48 h. After equilibration, the suspensions were filtered through 0.25 µm pore-size Teflon membrane filters (chosen to achieve minimal permeant adsorption) and the resultant solutions diluted. IPM, OA and IHD were diluted with isopropanol, HD

was diluted with n-hexane:isopropanol (50:50). LP was diluted with IHD:isopropanol co-solvent. This was because LP was not dissolved in isopropanol alone therefore IHD was added as a co-solvent (1500 mL isopropanol mixed with 300 mL IHD). The concentration of the permeant in each sample was determined using UV spectrophotometry (Section 2.3.3). Experimental data presented represent the mean (\pm SD) value ($n = 4$).

3.3.3 Franz cell studies

3.3.3.1 Cellulose acetate nitrate membrane

The release rate of MP, BP and CF through cellulose acetate nitrate membranes from the saturated suspensions was determined using individually (volume) calibrated Franz cells. The donor compartments were prepared by adding excess drug to 10 g of oil. The flask containing the suspension was placed in a shaker water bath overnight at 32°C. Diffusion experiments were carried out using (volume) calibrated Franz cells with a receptor phase of 20 mL and a diffusional area of 3.8 cm². Before the experiment the membrane was immersed and soaked in the receptor medium overnight. The membrane was cut into circular discs and placed between the donor and the receptor compartments of the Franz cell. The receptor compartment was carefully filled with phosphate buffer pH 7.0, after which the receptor temperature was maintained at 32°C by immersion in a temperature-controlled water bath. A small Teflon-coated magnetic bar (approximate length 5 mm) was included in the receptor compartment such that stirring occurred throughout the duration of the experiment. After allowing the membrane to equilibrate with the receptor fluid, 2 mL of the oily suspension (the sample contained undissolved/suspended solids of permeants at 32°C) of model permeant was then introduced into the donor. The experiments were conducted under occlusion (covering the donor compartment with parafilm) for 6 h using suspensions of MP, BP and CF respectively. At appropriate time intervals, 200 μ L samples were withdrawn from the receptor compartment and immediately replaced with an equal volume of fresh phosphate buffer, (pH 7.0). Each sample was analysed for drug by HPLC (Section 2.3.2). The concentration of the permeant in

the receptor solution at any time point was corrected for previous sample removal. Each experiment was conducted three times.

Fick's law of passive diffusion cannot be directly employed in porous membranes therefore, Hatanaka et al., (1990) modified Fick's Law to allow the fact that drug transport across a porous membrane was via the pores, thus the tortuosity and porosity factor of a membrane were included in a modified equation

$$J = D_v \cdot K' \cdot \varepsilon \cdot C_v / \tau \cdot h \quad \text{Equation 3.1}$$

Where J is flux, D_v is the diffusion coefficient of the permeant into the vehicle that fills in the membrane pore. K' is the partition coefficient of the permeant between the solvent in the membrane pore and the vehicle, ε is membrane porosity, τ is tortuosity, C_v is permeant concentration in vehicle and h is membrane thickness.

$$C_v = a_v / \gamma_v \quad \text{Equation 3.2}$$

Where a_v is the thermodynamic activity of the drug in the vehicle and γ_v the activity coefficient of the drug in the vehicle.

The cumulative amounts (per unit surface area of membrane) of permeant which diffused across cellulose acetate nitrate membrane were plotted against time (h). The slope of the linear plot was taken as the rate of permeation.

3.3.3.2. Silicone membrane

The diffusion of the model permeants from suspension was examined using silicone membrane. The permeation experiments were conducted as described previously (Section 3.3.3.1). However, calibrated Franz cells with a receptor phase of 2 mL and a diffusional area of 0.65 cm² were also used in some diffusion studies. The suspension volume applied in the small cells was 200 µL.

The cumulative amounts (per unit surface area of membrane) of permeant which diffused across silicone membrane were plotted against time (h). The slope of the

linear plot was taken as the flux of permeant permeation. The permeability coefficient (K_p , cm h⁻¹) for each solute was calculated as follows:

$$K_p = J_s / C_v \quad \text{Equation 3.3}$$

C_v is concentration of the penetrant in donor solution (saturated solubility of the penetrant in oil).

3.4 Results

3.4.1 Solubility studies of model permeants in donor/receptor fluid and deionised water

The solubility data of the model permeants in different oils, deionised water and buffer are shown in Table 3.1. The solubility of model permeants in different oil blends of IHD and HD are shown in Figure 3.1. The solubility of permeants in the aqueous vehicles was in the order of CF>MP>BP (mole.mL⁻¹), which is in accordance with the relative hydrophilicity of the permeants. While in oily vehicles the solubility of all permeants in OA and IPM was shown to be higher than in IHD, LP and HD. There was no significant difference in the solubility of each permeant, considered individually in HD, IHD or LP. Blending HD, LP or IHD with either OA or IPM increased the solubility of the permeants compared with IHD, HD and LP.

Table 3.1 Solubility (mg mL⁻¹) of the model permeants in IPM, OA, IHD, HD, LP, deionised water and phosphate buffer at 32 °C

Vehicle	BP	MP	CF
IPM	120.80 ± 2.60	35.04 ± 1.15	0.83 ± 0.02
OA	60.58 ± 1.16	6.58 ± 0.11	5.08 ± 0.20
IHD	1.32 ± 0.01	0.09 ± 0.01	0.07 ± 0.00*
HD	1.23 ± 0.01	0.08 ± 0.01	0.07 ± 0.00*
LP	1.21 ± 0.02	0.07 ± 0.01	0.08 ± 0.00*
buffer	0.25 ± 0.01	2.39 ± 0.07	25.72 ± 0.63
DIW	0.26 ± 0.01	2.01 ± 0.04	26.40 ± 0.32

Data are expressed as mean ± sd (n ≥ 4), * sd ≤ 0.009

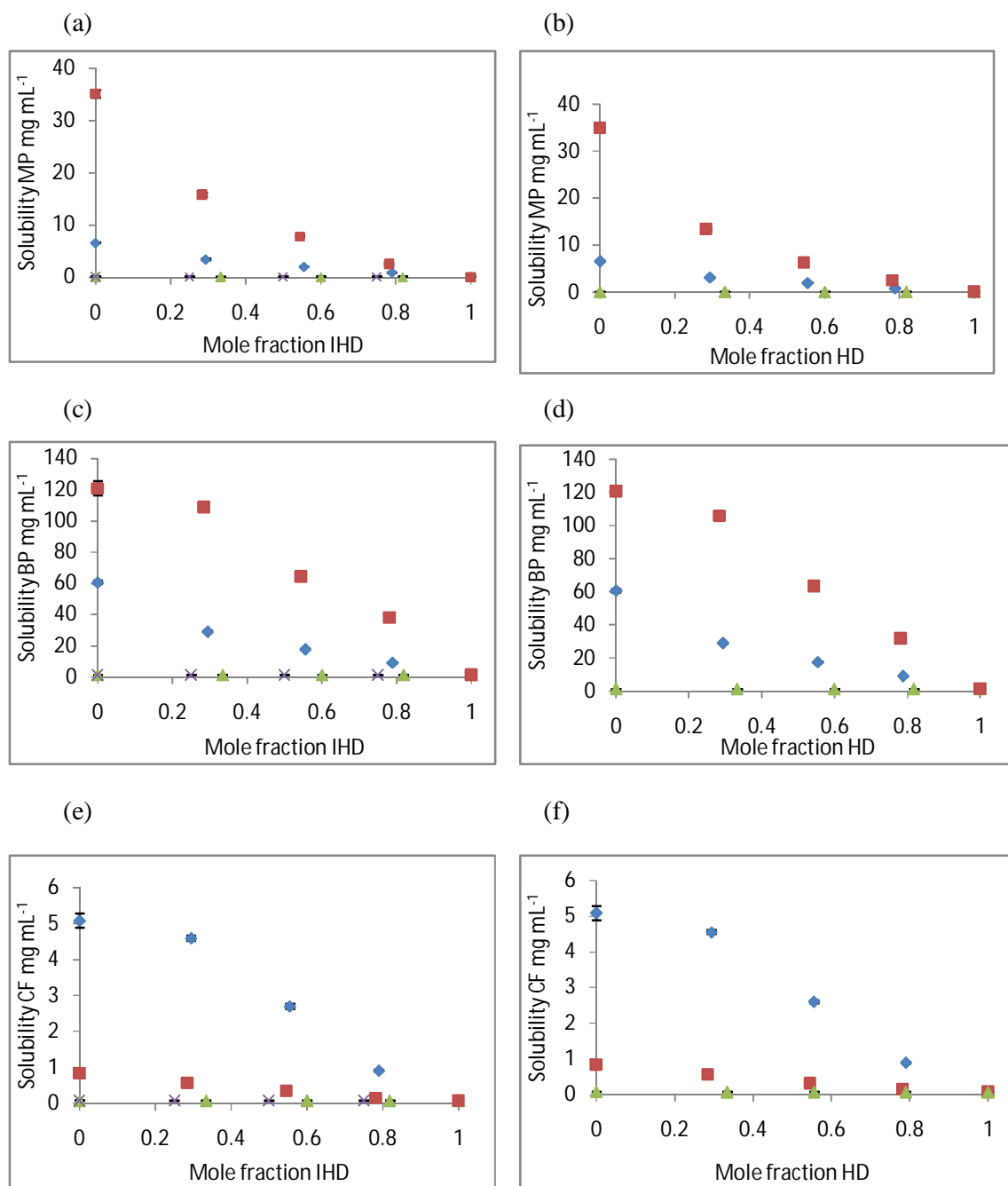


Figure 3.1 Solubility (mg mL⁻¹) in 100 % IHD, OA(♦), IPM(■), LP(▲), HD(×) and different oil blends containing IHD or HD at 32°C (a) MP solubility in IHD blends (b) MP solubility in HD blends (c) BP solubility in IHD blends (d) BP solubility in HD blends (e) CF solubility in IHD blends (f) CF solubility in HD blends. Data represent mean \pm sd ($n \geq 4$). Error bars lie within the symbols.

3.4.2 Franz cell studies

3.4.2.1 Cellulose acetate nitrate membrane diffusion studies from oils and oil combinations

The diffusion through the cellulose acetate nitrate membrane is predominantly through phosphate buffer filled pores. Therefore such diffusion depends on the relative affinity of the penetrant for the oily phase and phosphate buffer. The cumulative amounts of MP were higher than BP due to the higher affinity of MP into the buffer. Figures 3.2 and 3.3 show the cumulative amount of MP and BP permeated through cellulose acetate nitrate from pure oils. The cumulative amount of CF permeated through cellulose acetate nitrate membrane from different oils is shown in Figure 3.4, with the rate of permeation appearing to decrease after 3 h.

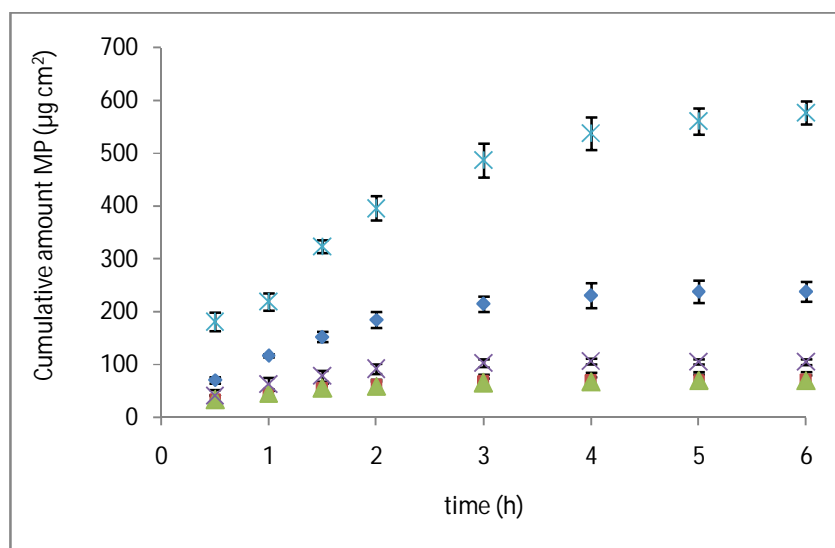


Figure 3.2 The cumulative amount of MP diffusing through cellulose acetate nitrate membrane into the receptor compartment from the different vehicles as a function of time (\blacktriangle) HD (\blacksquare) IHD (\times) LP ($*$) OA and (\blacklozenge) IPM. Data represent mean \pm sd ($n \geq 3$). Error bars lie within the symbols.

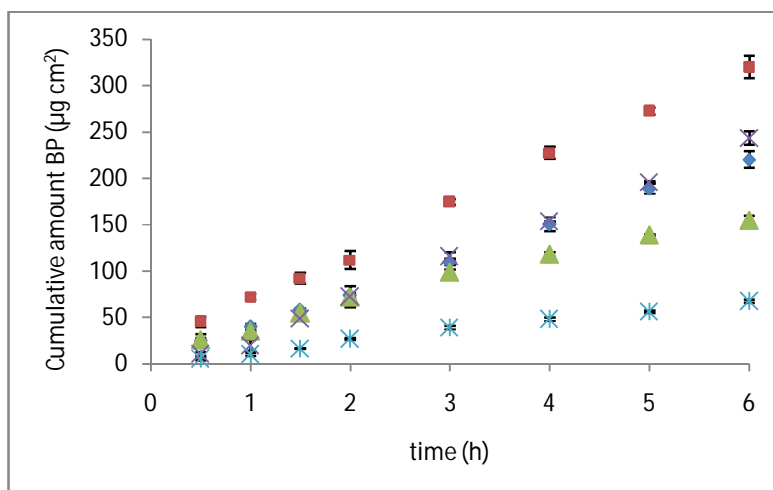


Figure 3.3 The cumulative amount of BP diffusing through cellulose acetate nitrate membrane into the receptor compartment from the different vehicles as a function of time (\blacktriangle) HD (\blacksquare) IHD (\times) LP ($*$) OA and (\blacklozenge) IPM. Data represent mean \pm sd ($n \geq 3$). Error bars lie within the symbols.

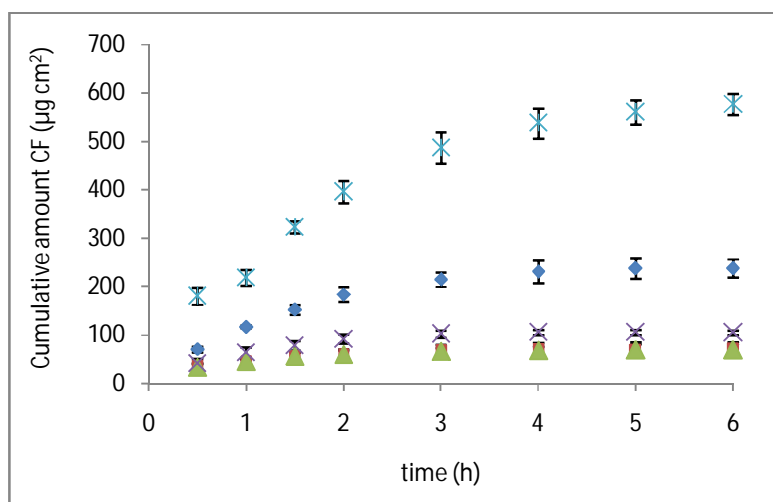


Figure 3.4 The cumulative amount of CF diffusing through cellulose acetate nitrate membrane into the receptor compartment from the different vehicles as a function of time (\blacktriangle) HD (\blacksquare) IHD (\times) LP ($*$) OA and (\blacklozenge) IPM. Data represent mean \pm sd ($n \geq 3$). Error bars lie within the symbols.

The derived permeation rates of MP and BP through cellulose acetate nitrate membrane from different oil blends are shown in Figures 3.5, 3.6 and 3.7. The data show that the highest amount of MP that permeated was from IPM/IHD blends, while the highest amount of BP was from LP/IHD blends. For both MP and BP, the lowest amounts that permeated were from OA/IHD blends.

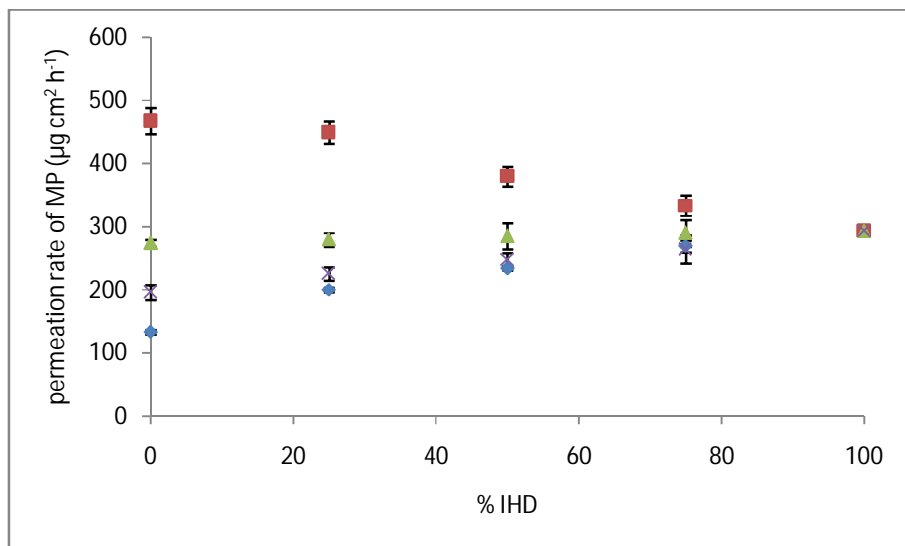


Figure 3.5 Rates of permeation obtained for MP diffusion through cellulose acetate nitrate membrane from different oil combinations comprising IHD with (▲) LP (■) IPM (×) HD and (◆) OA. Data represent mean \pm sd ($n \geq 3$). Error bars lie within the symbols.

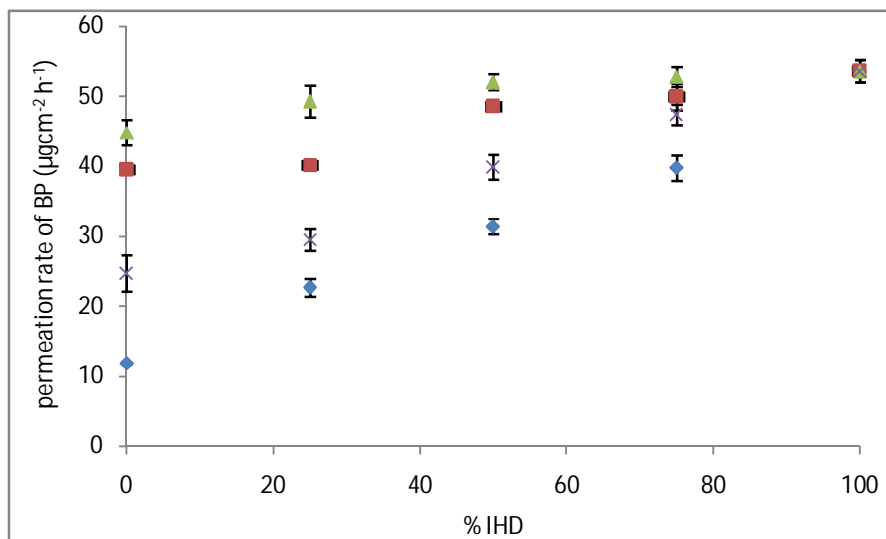


Figure 3.6 Rates of permeation obtained for BP diffusion through cellulose acetate nitrate membrane from different oil combinations comprising IHD with (▲) LP (■) IPM (×) HD and (◆) OA. Data represent mean \pm sd ($n \geq 3$). Error bars lie within the symbols.

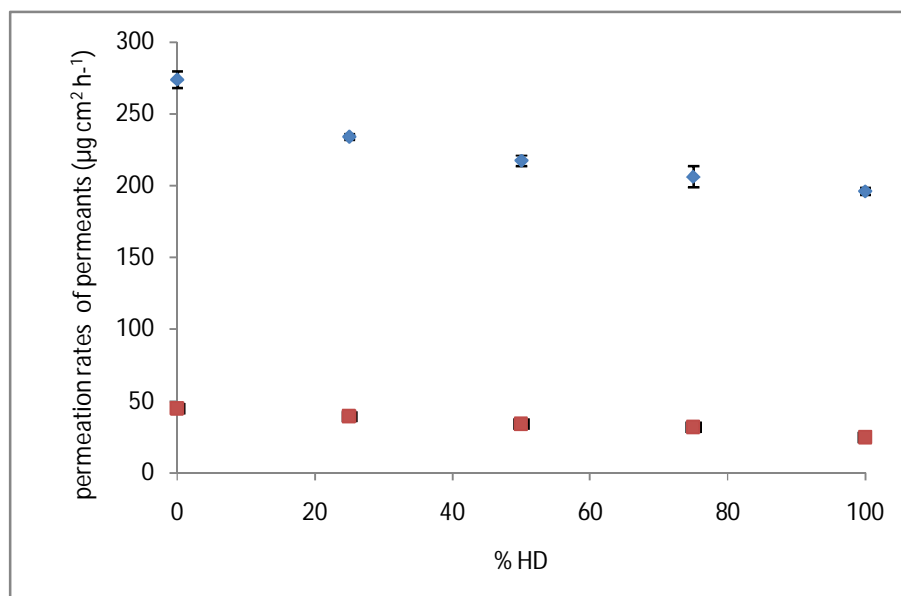


Figure 3.7 Rates of permeation obtained for (◆) MP and (■) BP diffusion through cellulose acetate nitrate membrane from different oil combinations comprising HD with LP. Data represent mean \pm sd ($n \geq 3$). Error bars lie within the symbols.

3.4.2.2 Silicone membrane diffusion studies from oils and oil combinations

The results obtained from the diffusion studies from different oil blends indicated that after a lag time, a linear correlation existed between the amount of penetrant and time. The linear portion of the curve was used to calculate a flux. The correlation coefficients (R^2), expressing the linearity of the plots were found to be ≥ 0.98 for the diffusion of permeants from all of the vehicles. The permeation profile of the model penetrants from the different vehicles across silicone membrane is depicted in Figures 3.8-3.10. The highest amounts of MP and CF that diffused through silicone membrane were from IPM, while the highest amount of BP was from IHD. The lowest amount of BP and CF were attained when OA was used as a vehicle, while the lowest amount of MP that diffused through silicone membrane was from LP as a vehicle.

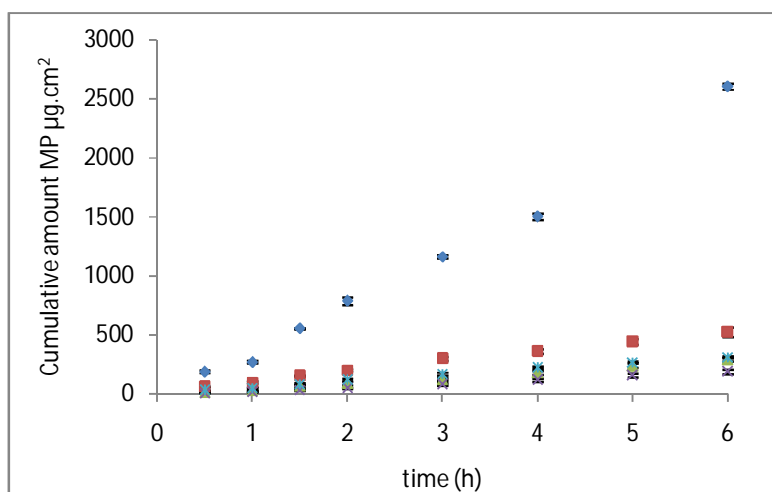


Figure 3.8 The cumulative amount of MP diffused across silicone membrane into the receptor compartment from the different vehicles as a function of time (▲) HD (■) IHD (×) LP (*) OA and (◆) IPM. Data represent mean \pm sd ($n \geq 3$). Error bars lie within the symbols.

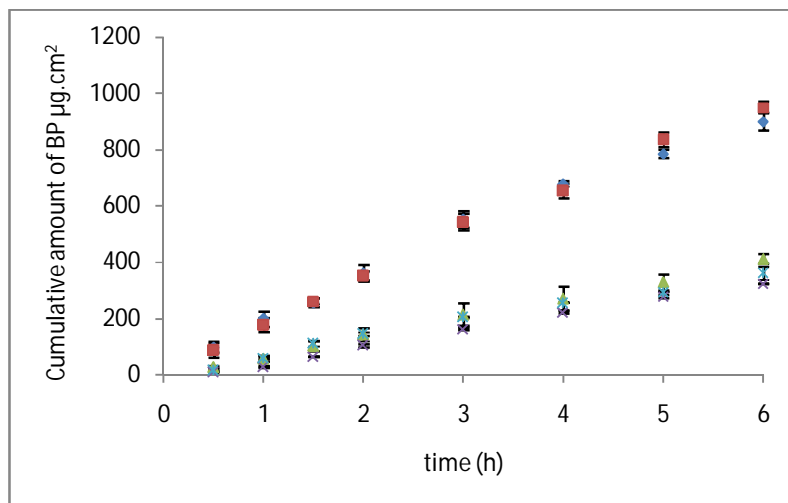


Figure 3.9 The cumulative amount of BP diffused across silicone membrane into the receptor compartment from the different vehicles as a function of time (▲) HD (■) IHD (×) LP (*) OA and (◆) IPM. Data represent mean \pm sd ($n \geq 3$). Error bars lie within the symbols.

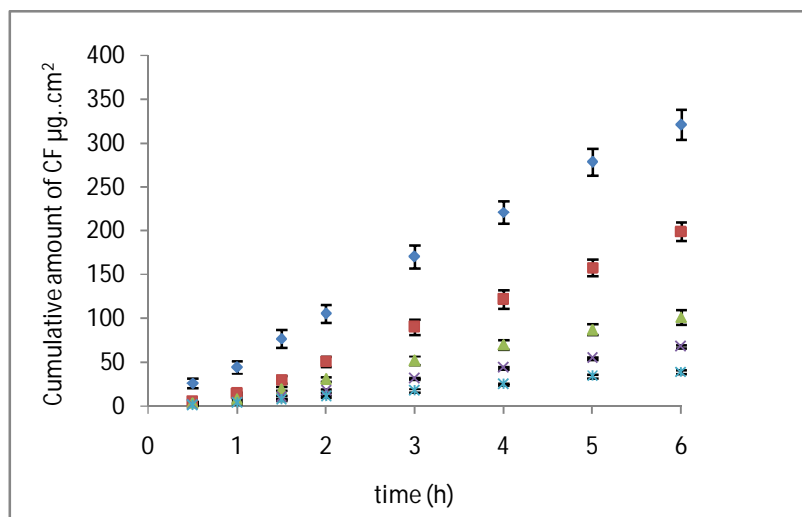


Figure 3.10 The cumulative amount of CF diffused across silicone membrane into the receptor compartment from the different vehicles as a function of time (▲) HD (■) IHD (×) LP (*) OA and (◆) IPM. Data represent mean \pm sd ($n \geq 3$). Error bars lie within the symbols.

Table 3.2 shows the calculated flux values and permeability coefficient (K_p) for the model permeants through silicone from different oils.

Table 3.2 Silicone membrane permeation parameters permeability coefficients and fluxes for MP, BP and CF

Permeant	Vehicle	$J_s(\mu\text{g cm}^{-2} \text{h}^{-1})$	$K_p(10^{-2} \text{ cm h}^{-1})$
<i>MP</i>	IHD	135.5 ± 3.3	139.7 ± 3.4
	IPM	560.5 ± 7.3	1.6 ± 0.02
	OA	56.7 ± 0.9	0.86 ± 0.01
	HD	68.4 ± 1.4	86.4 ± 1.8
	LP	39.1 ± 4.2	55.9 ± 6.01
<i>BP</i>	IHD	246.8 ± 9.1	18.70 ± 0.7
	IPM	161.6 ± 1.4	0.13 ± 0.002
	OA	65.8 ± 1.3	0.11 ± 0.003
	HD	89.8 ± 1.5	7.30 ± 0.12
	LP	66.7 ± 0.3	5.51 ± 0.02
<i>CF</i>	IHD	48.2 ± 1.7	65.1 ± 2.3
	IPM	69.3 ± 5.1	8.3 ± 0.4
	OA	7.9 ± 0.5	0.16 ± 0.01
	HD	25.3 ± 1.7	34.2 ± 2.3
	LP	13.8 ± 0.6	17.9 ± 0.8

The influence of IHD content when present in binary mixtures of oil on the flux of MP, BP and CF is shown in Figure 3.11, Figure 3.13 and Figure 3.15 respectively. Corresponding flux data for MP, BP and CF from HD binary blends

are shown in Figure 3.12, Figure 3.14 and Figure 3.16 respectively. The highest fluxes were attained by blending IPM with IHD. The highest flux of MP and CF was from 100% IPM and the flux decreased as IHD or HD was added. However the highest flux of BP was obtained when it was applied as a suspension in a 75% IHD/25% IPM mixture. The diffusion of MP from OA/IHD blends was at a maximum when suspended in a blend containing between 50 – 75% IHD (i.e. 50 – 25% OA) content (Figure 3.11). With CF the maximum flux was attained from a vehicle containing a blend of 75% IHD (25% OA) (Figure 3.15). The flux from all oils was higher than from the aqueous buffer for all model permeants through silicone membrane; the fluxes from phosphate buffer being 41.71 ± 1.01 , 27.88 ± 0.46 and $13.01 \pm 0.76 \mu\text{g cm}^{-2} \text{h}^{-1}$ for MP, BP and CF respectively.

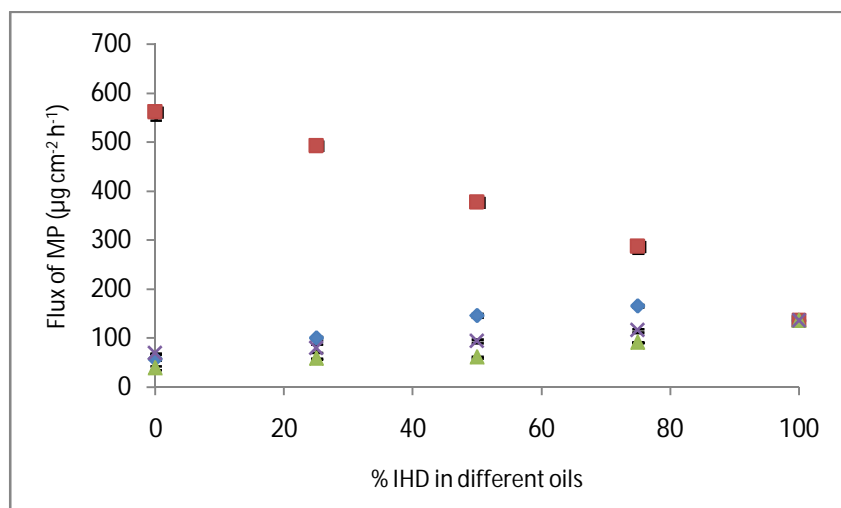


Figure 3.11 Flux values obtained for MP diffusion through silicone membrane from different oil combinations comprising IHD with (▲) LP (■) IPM (×) HD and (◆) OA. Data represent mean \pm sd ($n \geq 3$). Error bars lie within the symbols.

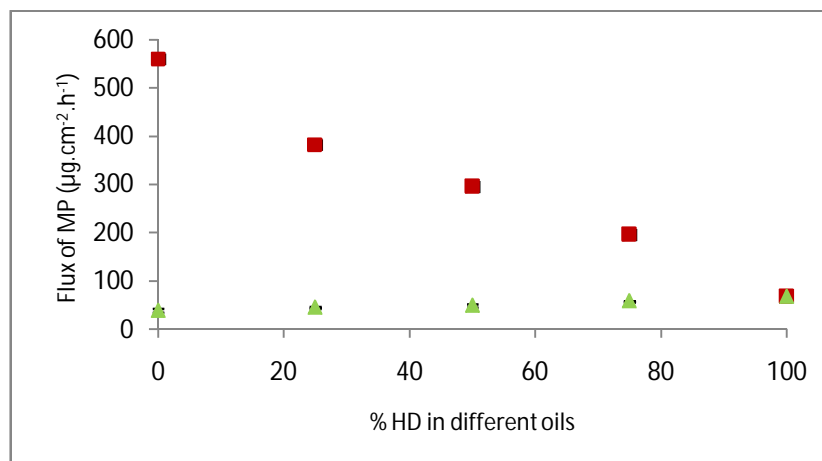


Figure 3.12 Flux values obtained for MP diffusion through silicone membrane from different oil combinations comprising HD with (▲) LP (■) IPM. Data represent mean \pm sd ($n \geq 3$). Error bars lie within the symbols.

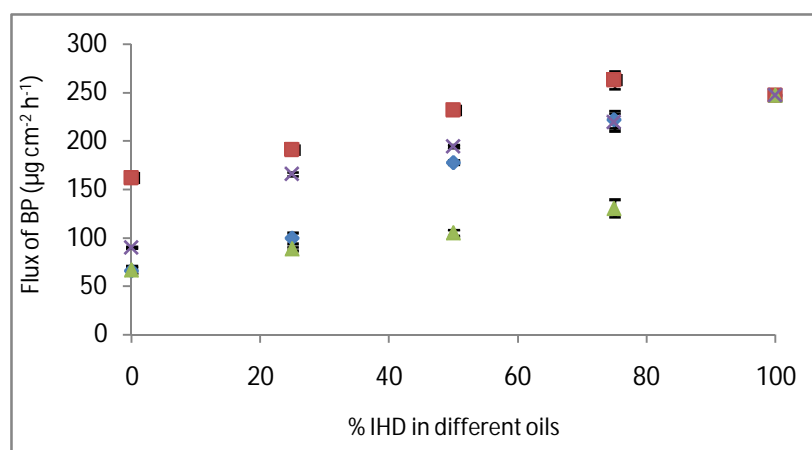


Figure 3.13 Flux values obtained for BP diffusion through silicone membrane from different oil combinations comprising IHD with (▲) LP (■) IPM (x) HD and (◆) OA. Data represent mean \pm sd ($n \geq 3$). Error bars lie within the symbols.

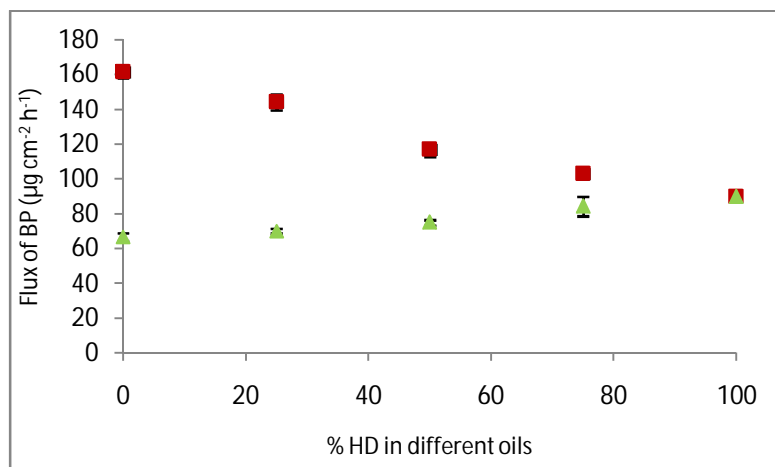


Figure 3.14 Flux values obtained for BP diffusion through silicone membrane from different oil combinations comprising HD with (▲) LP (■) IPM. Data represent mean \pm sd ($n \geq 3$). Error bars lie within the symbols.

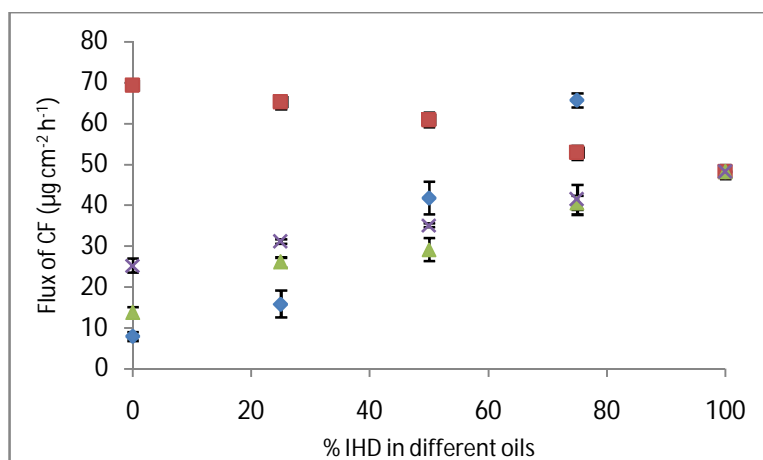


Figure 3.15 Flux values obtained for CF diffusion through silicone membrane from different oil combinations comprising IHD with (▲) LP (■) IPM (x) HD and (◆) OA. Data represent mean \pm sd ($n \geq 3$). Error bars lie within the symbols.

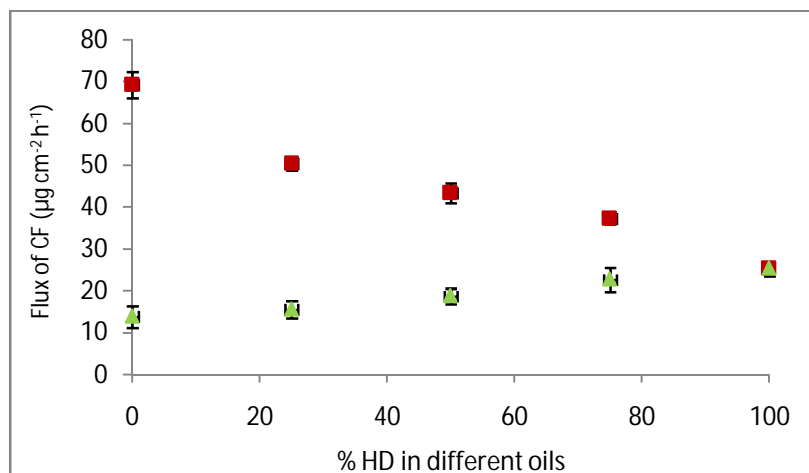


Figure 3.16 Flux values obtained for CF diffusion through silicone membrane from different oil combinations comprising HD with (▲) LP (■) IPM. Data represent mean \pm sd ($n \geq 3$). Error bars lie within the symbols.

3.5 Discussion

The measurement of the solubility of the permeants in phosphate buffer (pH 7.0) was essential in determining whether that medium could be used as receptor fluid, so as to ensure the maintenance of sink conditions during diffusion studies. Sink conditions should prevail throughout the Franz cell experiments, in order to maintain the concentration gradient as constant as possible without back-diffusion occurring (Higuchi, 1960). Thus, the concentration of permeant in the receptor fluid should remain low throughout the course of the diffusion study. Sink conditions have been defined practically as a situation when the thermodynamic activity in the receptor does not exceed 10% of the saturated solubility of permeant in the vehicle (Higuchi, 1960; Siepmann & Peppas, 2011). Accordingly, adequate solubility of the permeant in the receptor solution is essential so that its partition into the receptor fluid does not become dissolution- and diffusion-rate limiting. Earlier studies (Kitagawa et al., 1997; Dias et al., 1999; Akomeah et al., 2004; Lopez et al., 2004 & 2005; Chilcott et al., 2005) have confirmed the

suitability of using phosphate buffer as a receptor fluid in Franz cell studies in order to maintain sink conditions for the three model permeants.

Measurement of the solubility of drug in the vehicle is an important parameter for both the drug permeation studies and in determination of the degree of saturation. CF, a relatively hydrophilic molecule was shown to be more soluble in an aqueous solvent than in the oily vehicles; with CF solubility being in the order OA>IPM>LP, IHD and HD. Since MP has moderate lipophilicity compared to BP and CF it was found to have intermediate solubility in both the aqueous and oily vehicles. The order of solubility for MP and BP in oily vehicles was IPM>OA>IHD, HD and LP.

The solubility of each of the three permeants in LP, HD and IHD were not significantly different. Also no significant difference was found between their solubilities in oil combinations of IHD, HD and LP and the pure oil. These latter three oils are hydrocarbons and having similar chemical basis to their chemical structure and all form only either weak van der Waals forces or dispersion interactions with the model permeants. IPM is an ester with a long hydrophobic tail, and OA contains a *cis* unsaturated double bond and a carboxylic group within its structure (Figure 2.1). Therefore, IPM and OA have the ability of forming polar interactions as well as van der Waals interactions with the permeant. All permeants were found to have a higher solubility in IPM and OA compared with HD, IHD and LP. When OA and IPM were blended with any of the other oils the solubility of the model permeants generally were increased. The results are in general agreement with published results, for example the solubility of CF in IPM and OA has been reported previously as 0.93 ± 0.08 and 5.27 ± 0.06 mg/mL respectively at 32°C (Dias et al., 2007a). MP was found to have a solubility of 39.00 mg/mL in IPM at 32°C (Oliveira et al., 2008) and MP, BP and CF solubility in de-ionized water had reported values of 2.16, 0.22, 21.88 mg/mL in DIW at 25°C (Akomeah et al., 2004).

Artificial membranes may be used during the development of a formulation to aid in the process of selecting a vehicle and excipients or alternatively as a quality control tool (Flynn et al., 1999). There are potentially a large number of bi-component mixtures that can be generated from the oils used in the current study, and indeed the oils are frequently present as mixed blends in pharmaceutical and cosmetic products. Since the potential array of oil blend (and oil blend-permeant) combinations available to choose for study, the effects of selecting a few random, representative combinations on permeation of incorporated diffusants were examined. The use of cellulose acetate nitrate membrane allows the permeation through buffer-filled pores to be monitored, in the absence of a rate limiting continuous membrane. The permeants were all released readily from the vehicles and permeated the porous membrane relatively quickly.

The permeabilities of MP and BP through cellulose acetate nitrate membrane from different oil blends are shown in Figures 3.5, 3.6 and 3.7. According to Equation 3.1 and 3.2 the release of a permeant through a porous membrane depends on the partition coefficient, diffusion coefficient, the thickness of the membrane, membrane porosity and tortuosity and also on the thermodynamic activity of the permeant in the vehicle which in turn are determined by the concentration and activity coefficient of the drug in the vehicle. It might be assumed that the properties of the cellulose acetate nitrate membrane are affected primarily by the buffer rather than the oily vehicles. Since buffer was present in all permeation experiments then it is possible that the membrane thickness, porosity and tortuosity will remain reasonably constant between experiments. However this would not be the case if the vehicle does interact with the membrane matrix. Another factor which affects the diffusion through the pores of the membrane is the activity coefficient of the drug in the vehicle, which also might result in the differences in the partitioning of the drugs into the buffer.

Differences between the diffusion of MP (Figure 3.2) and BP (Figure 3.3) through cellulose acetate nitrate membrane, are partly attributable to the differences in the

partitioning of the drug from the oil into the buffer which fills the membrane pores (since the membranes were soaked in the buffer before initiating the experiment). The difference in the amounts of penetrant diffusing was therefore related to magnitude of its aqueous solubility, its partitioning properties between the vehicle and buffer, and the activity coefficient of the drug in the vehicle. Also an interaction between the vehicle and membrane matrix has to be considered. In addition oils may perhaps displace the bound water within the pores of the cellulose acetate nitrate membrane, or interact with the unbound water in the pores (OA and IPM) which in turn would affect the pore structure and shape, or the matrix of the membrane (Kamo et al., 1992; Barbe et al., 2000; Wang et al., 2004). Any of these effects might influence the permeation of the penetrant through a 'modified' membrane.

The important factors influencing the release of permeants from a vehicle into the receptor phase are the solubility in the vehicle and the partition coefficient between the vehicle and the receptor phase (Coldman et al., 1969). Higuchi (1960) predicted that the drug solubilising capacity of the vehicle in excess of that needed to dissolve the desired dose of drug can lead to a decrease in the rate of the drug delivery from that vehicle, i.e. as the solubility of the drug in the vehicle increases, the partition coefficient into a receptor phase decreases; the two effects tending to cancel each other (Poulsen et al., 1968). The higher release rate of MP compared with BP and CF is due to the mid-range partition coefficient of MP that will aid in its partition into the buffer. The partition coefficient of BP between oil and buffer was predicted to be lower than MP, due to its lower solubility in the buffer. The low partition coefficient reflects the higher tendency BP to remain in the vehicle, such that the flux values of BP were lower than those of MP.

The amount of CF released was in the order of OA>IPM>LP>IHD, HD. The highest amount of CF that permeated through the porous membrane was from OA. This might be attributed to the higher ability of OA to dissolve CF compared with other oils; therefore more drug is likely to be solubilised by OA entrapped

within the pores, such that CF from OA might have a shorter diffusion path to the receptor phase compared with other oils. There were no significant differences in either the solubility of CF in HD and IHD or its partitioning properties between the oil and the buffer. This is likely to account for the finding that there was no difference in the release of CF from the two oils.

The results of CF permeation (Figure 3.4) through cellulose acetate nitrate membrane correlated well with the solubility of CF in the oil. When the CF molecules partition from the donor to the receptor through the membrane pores, the amount lost should be compensated by the dissolution of un-dissolved drug from the excess particles suspended in the donor compartment. The viscosity of the oil may influence the dissolution rate of the drug, its diffusion through the donor vehicle, and its diffusion through the oil-filled regions of the membrane pores. However due to the high solubility of CF in the buffer and low solubility in the oils, the amount released may not have been quickly restored by the suspended particles, therefore the concentration of CF in the donor compartment (C_v) decreased with time such that the permeation slowed after the third hour.

In vitro experiments were performed using systems having the same thermodynamic activity. The flux of a permeant across a non-porous barrier membrane (Equation 3.3) is known to be directly proportional to its applied concentration as a consequence of the thermodynamic activity or ‘leaving potential’ of the permeant (Equation 3.2) (Hadgraft et al., 2001). Previous experiments (Twist & Zatz, 1986) using rate-limiting (silicone) membranes have shown that the flux of permeant from saturated aqueous systems of different solubilities will yield the same flux as long as the vehicle and its components do not interfere (or interact to a similar extent) with the membrane. This was observed by permeation of a series of parabens across silicone membranes (Twist & Zatz, 1986). Using non-interactive solvents and mixtures of non-interactive solvents, the latter authors observed that saturated solutions produced similar fluxes of parabens, despite the differences in parabens solubility within these

vehicles. Saturated systems were therefore used in this investigation to ensure equal thermodynamic activity of the permeant in the chosen vehicles, with excess solute being present so as to maintain saturation throughout the experiment. Thus, any drug lost from the solution by diffusion was replenished by dissolution of the excess drug. This methodology allows any effects of the vehicle on the diffusion of permeants through the membrane to be determined. The use of silicone (rate-limiting) membranes to study diffusion kinetics has been employed previously in permeation studies as a means of mimicking the lipoidal component of the stratum corneum membrane (Hatanaka et al., 1990; Cappel & Kreuter, 1991; Hayashi et al., 1992; Maitani et al., 1995; Pellett et al., 1997a; Müller & Kreuter, 1999; Valenta et al., 2000; Du Plessis et al., 2001, 2002; Dias et al., 2003).

The highest fluxes were achieved using MP as a permeant, which has mid-range physicochemical properties (when compared with BP and CF), as indicated by both the solubility data, as well as the octanol-water partition constant (Log P in Table 2.1). Its moderate lipophilicity promotes its permeation through the hydrophobic silicone membrane. Also its high solubility in the oil will quickly restore any amount lost by diffusion. The higher log P of BP enhances the partitioning of the compound into the hydrophobic silicone membrane, but the smaller size of MP maximises the diffusion of the compound through the membrane (Magnusson et al., 2004). According to the rule 'like dissolves like' the solubility parameter of BP is the closest to the solubility parameter of silicone membrane (Tables 2.1 and 4.2), therefore the former might be expected to partition favourably into the membrane, but its lower partitioning (compared with MP) into the buffer decreases the overall net flux. The higher diffusion rates recorded for MP in comparison to BP and CF may occur as a result of its adequate solubility both in oil and water.

When there is no interaction between the vehicles and the membrane, all saturated solutions of the same permeant should produce the same steady state flux through the membrane. This would be expected to occur regardless of the nature of the

vehicle used (Higuchi, 1960; Siepmann & Peppas, 2011). Hence, the flux of a permeant from saturated solutions from any of the vehicles might be expected to be constant. In this study the diffusion of permeants through the membrane was changed and since the thermodynamic activity is constant in all blends, this indicated that the vehicles were probably not inert and interacted with the membrane.

The diffusion studies conducted using model permeants, showed that the highest fluxes of model permeants were obtained from pure IPM, IHD and blends of the two oils (Figures 3.11-3.16). In addition, MP and BP have a higher solubility in IPM and IPM/IHD combinations compared with the solubility in other oils (Figure 3.1). The high solubility helps quickly restore the amount of permeant lost by diffusion which keeps the thermodynamic activity constant. Each model permeant has a specific activity coefficient in different oils (γ); therefore the leaving potential of the drug will be different for each vehicle. The enhanced permeation through the membrane might be due to the enhanced partitioning or diffusion of the compound through the membrane, or indeed a combination of both effects. The flux of model permeants from IPM/IHD combinations was in the order MP>BP>CF. This order is likely to be attributable to the relative magnitude of the partition coefficients with MP more readily partitioning from oil to silicone membrane to buffer than the more hydrophobic BP or the more hydrophilic CF.

Despite the higher solubility of BP in IPM and OA compared with IHD, the flux from IHD was significantly higher than all other oils. Qualitative changes in the membrane dimensions (swelling and expansion) were noticed visually after diffusion studies which employed IHD as a vehicle. This suggested that IHD was possibly taken up by the membrane and this might lead to an enhanced BP partitioning and diffusion through membrane with the vehicle molecules. Blending oils with IHD significantly enhanced the flux of BP (Figure 3.13). In the case of BP, blends of IPM with IHD were found to affect the diffusion in a

manner that was not linearly dependent upon IHD content (Figure 3.13). A blend of 75 % IHD in IPM was found to be the combination that gave the highest flux of BP.

The diffusion of MP and CF from OA/IHD blends formed parabolic curves with the peak at blends containing 25% OA for CF (Figure 3.15), while with MP the maximum flux was attained between 25 – 50% OA content (Figure 3.11). A parabolic relationship was also seen with OA uptake and enhanced of flux of piroxicam into and through porcine skin and silicone membrane from a series of ethanol:water vehicles (Francoeur et al., 1990). The maximum flux was attained with the vehicle containing 40% ethanol, as the OA was completely solubilised at 40% or higher levels of ethanol. The authors suggested that the uptake of OA by silicone and porcine stratum corneum membranes was therefore controlled by the thermodynamic activity of OA in the applied ethanolic vehicle (Francoeur et al., 1990).

A comparison of the fluxes of model permeants from IHD and HD blends provides an indication on the effect of the chemical structure and shape of the oil on the diffusion of the model permeant. Thus the difference in the flux values through the silicone membranes could possibly be related to the shape and degree of branching, since HD and IHD have similar solubility and partitioning properties. The results suggest that as the degree of branching increases and the shape becomes more spherical and compact, this in turn might enhance the partitioning of the vehicle into the membrane and its interaction with the membrane. The flux of the permeant through the modified membrane would consequently be altered. The fluxes of three model permeants from the spherical branched IHD were significantly higher than the linear oval HD; regardless of their respective Log P values (i.e. their partitioning tendency).

Blending IPM with HD led to lower flux results of the model permeants compared with those obtained for the same permeants dissolved in IPM/IHD

blends. As stated previously, HD and IHD differ only in the structure and shape of the molecules. There was no significant difference in the solubilities of any of the penetrants in 100% HD, IHD or the blends of either of these with IPM (Figure 3.1). In the current study, the fluxes of BP from HD/IHD blends were higher than from the equivalent HD/IPM blends. In contrast, the fluxes of MP and CF were higher from HD/IPM blends than IHD/HD blends. These diffusion results indicate that there is possibly difference in the partitioning properties of the oils into the membrane, which might have led to the difference in the diffusion results.

Diffusion studies of the model permeants were also carried out using the HD/LP and IHD/LP blends in order to investigate further the effects of a branched molecular structure and different molecular sized oil (LP) on the flux. The three oils are hydrocarbons with similar physicochemical properties and there was no significant difference in the solubility of permeants in the IHD/LP and HD/LP blends (Figure 3.1). The viscosity of LP is higher than IHD and HD and it has been reported that the viscosity of the vehicle does have an effect upon the release rate of a number of different dissolved solutes from the medium. The lower the viscosity of the vehicle the faster is the release (Malzfeldt et al., 1989; Kriwet & Müller-Goymann, 1995; Clément et al., 2000; Trotta et al., 2003; Yener et al., 2009). However the effect of viscosity of a vehicle on the diffusion rate of a permeant through a membrane might be minimal when compared to other potential factors, since most vehicles used are oils with similar viscosity. The flux of permeants depends mainly on the thermodynamic activity of the drug and the partitioning properties of the drug and possibly vehicle components into the membrane. Since all the systems were thermodynamically uniform, the significantly higher flux of specific model permeants, through silicone membrane from the IHD/LP blends compared with the HD/LP blends, is likely to be primarily attributed to a difference in the vehicle partitioning into the membrane.

In the current studies, the diffusion of BP through silicone membrane displayed an increase in the flux of BP as the % of IHD increased (Figure 3.13). The order

of flux of BP, from the different vehicles was IHD>IPM>HD>LP>OA (Figure 3.8). Since the thermodynamic activity of the system is constant there might be a difference in the interaction and uptake of oils into the membrane. BP and silicone membrane are hydrophobic therefore if there is any uptake of oils into the membrane, it might modify BP (and consequently, other hydrophobic permeants) partitioning and diffusion through the silicone membrane.

In conclusion, it has been shown that oils (even those that are GRAS listed) have the potential to modify the membrane. The modified membrane can affect 'drug' diffusion in two ways (1) it acts to modify the barrier to the diffusion of many drugs, and (2) since the oils (from blends) may be taken up in different ratios this could modify the composition of the applied vehicle such that the thermodynamic activity of the applied drug is altered. Therefore the flux of the applied drug might be enhanced. The amounts of oil sorbed by silicone membrane require determination and it is planned to do this in the next phase of the study.

CHAPTER FOUR

***INTERACTION OF OILS
WITH MODEL MEMBRANES***

4.1 Introduction

The penetration of a permeant through membranes is generally controlled by the chemical structure and physicochemical properties of that permeant. Generally the lipophilicity, hydrogen bonding ability and molecular size plays a major role on its absorption profile (Pugh et al., 1996; El Tayar et al., 1991). However in some cases, the delivery and penetration of the vehicle to the membrane can be as important as that of the drug itself. This is because the permeated vehicle can alter the penetration of a concomitantly applied drug either by changing the partition of the latter into the membrane or by affecting the barrier properties of the membrane, with the consequent modulation of drug transport (Dias et al., 2001). Therefore, penetration of the drug can depend not only on the nature of the drug but also on the nature of the other components present in the formulation. Many of the previous studies which have investigated vehicle uptake into membranes and its effect on drug diffusion employed single aqueous and alcoholic vehicles (Twist & Zatz, 1988; Flynn, 1990; Twist & Zatz, 1990; Dias et al., 2007; Oliveira et al., 2010). Few studies have addressed the influence of oily vehicles and their blends. In this chapter the uptake of different oily vehicles by membranes and blends of oils into silicone membrane will be investigated. A general description of the oily vehicle is in section 1.11. The structures of these oils are demonstrated in Figure 4.1, the physical properties of these oils (including the molecular connectivity index to approximate molecular branching and shape) are shown in Tables 4.1 and 4.2.

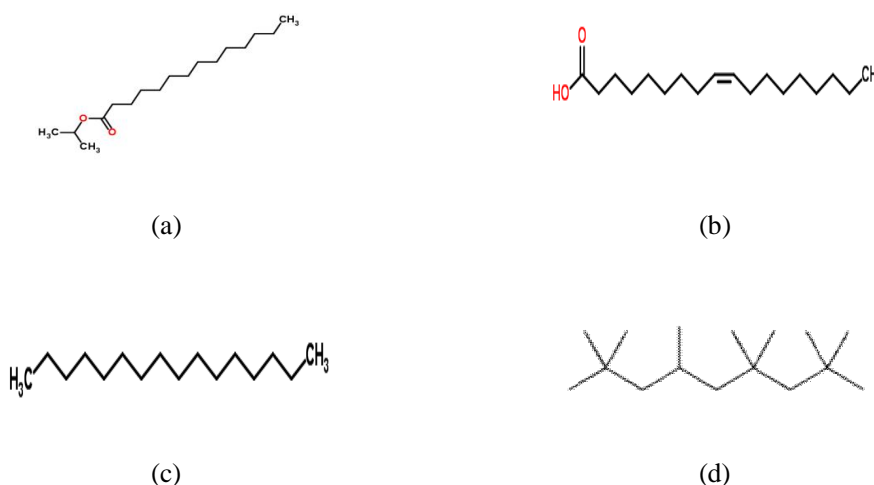


Figure 4.1 Structure of (a) isopropyl myristate (b) oleic acid (c) hexadecane (d) isohexadecane.

Table 4.1 Properties of the oils used in this investigation

	IPM	OA	HD	IHD	LP
Description	Ester of isopropanol and tetradecanoic (myristic) acid	monounsaturated omega-9-fatty acid	alkane hydrocarbon	highly branched aliphatic hydrocarbon C16 isoparaffins	purified mixture of saturated hydrocarbons obtained from petrolatum
Molecular formula	$C_{17}H_{34}O_2$	$C_{18}H_{34}O_2$	$C_{16}H_{34}$	$C_{16}H_{34}$	C_nH_{2n+2}
Mwt $g\ mol^{-1}$ *	270.4	282.5	226.4	226.4	340.0
Log P	6.32	6.08	10.24	9.77	
Molecular connectivity index*	9.61	9.77	7.91	6.81	
Log K_{ow} *	7.35	7.73	8.25	7.46	>6

*data determined by Hansen Solubility Parameters in Practice (HSPiP) software version 4.0.04 Copyright 2013 (www.Hansen-Solubility.com).

Table 4.2 Some parameters and properties of oils used in this investigation

	IPM	OA	HD	IHD
Molar volume *	315	319.7	294.2	295.3
Boiling point °C*	167	360	210	240
Melting point °C*	15	13	18	-75
Ovality *	1.8	1.9	1.8	1.7
Solubility parameter* (MPa) ^{1/2}	16.4	17.4	16.3	14.7

*data determined from HSPiP software version 4.0.04 Copyright 2013 (www.Hansen-Solubility.com).

4.1.1 Interaction with membranes

Permeation of a molecule through a membrane is influenced mainly by its activity gradient across the membrane thickness, and also by its mobility within the membrane. Solvent interactions with the membrane can alter the membrane physicochemical properties. This might lead to modified permeation of a co-formulated drug through the membrane. The degree to which solvents affect and interact with the skin will depend on the uptake kinetics. Increasing the ethanol content of a vehicle was found to increase the diffusion rate of 4-aminopropiophenone through silicone membrane from saturated water/ethanol solutions (Garrett & Chemburkar, 1968). Mulder et al. (1985) showed that the component of a solution that is sorbed preferentially into the membrane will permeate preferentially. Paraben permeation from a series of alcohols through silicone membrane was shown not to be constant, with the degree of uptake of alcohol into silicone membrane being well correlated with the flux data (Twist & Zats, 1988b). In general the amount of solvent absorbed by the membrane is related to the solubility parameter, molecular weight and hydrogen bonding capacity of the solvent (Cross et al., 2001). The latter workers showed that the log of hydrocortisone flux was linearly

related to the amount of vehicle sorbed by silicone membrane, although solvents with higher sorption did not cause a higher retention of hydrocortisone by the membrane. These same investigators also observed that solvent that was sorbed to the membrane changed both the diffusivity and the membrane solubility of solutes. The maximum flux of phenolic compounds was found to be related to the vehicle stratum corneum solubility which in turn was related to the amount of vehicle absorbed into the stratum corneum and the amount of phenolic compounds dissolved in that absorbed vehicle (Zhang et al., 2011). It is thus well documented that vehicles that are highly sorbed by the membrane affect the diffusional characteristics and alter the properties of the membrane thereby changing the partitioning and diffusion properties of the permeant across the membrane (Mulder et al., 1986; Twist & Zatz, 1988; Cross et al., 2001; Dias et al., 2007; Zhang et al., 2011; Oliveira et al., 2012).

The mode of action of enhancers and the molecular interactions between enhancers and components of stratum corneum had been investigated using various techniques including Fourier transform infrared spectroscopy (Jain et al., 2002; Vaddi et al., 2002; Tokudome & Sugibayashi, 2003) and Raman spectroscopy (Caspers et al., 1998 & 2000; Stamatas, 2006; Olsztyńska-Janus et al., 2012). These methods offer a non-invasive way to study cutaneous biochemical events at the molecular level. They give information about protein conformation and lipid structures. In general, changes in the absorbance frequency reflect changes in the conformational arrangement of functional groups. The greatest benefits of these spectroscopic techniques lie in their high sensitivity to biochemical changes, as well as in non-destructive application (Olsztyńska-Janus et al., 2012).

The use of synthetic membranes has been found to be ideal in certain instances for studying topical formulations. Synthetic membranes have two functions: simulation of skin (Twist & Zatz, 1988 a&b) and quality control (Carbo et al., 1993). The membrane employed to simulate the skin should be broadly hydrophobic and possess rate limiting properties similar to skin. Synthetic membranes for quality control should have minimum resistance to the diffusion of the drug and act to separate the formulation from the receptor medium. Such synthetic membranes often have incorporated pores (Ng et al., 2010). A major advantage of such systems is that they

eliminate the requirement to obtain human or animal skin (Shin & Byun, 1996; Pellett et al., 1997b) and such membranes have been used to study both transdermal and dermal drug permeation (Fang et al., 1999; Sinico et al., 2005). Synthetic membranes are used in interaction studies since they are more homogenous, therefore data analysis is simplified, and they provide insight into the potential difficulties when more complex membranes such as skin are examined. Polydimethylsiloxane (silicone), high density poly ethylene (HDPE) and poly urethane (PU) membranes are examples of partitioning-membranes which have been used in these studies, where transport through the polymeric matrices is controlled by parameters similar to those of the stratum corneum. In contrast cellulose acetate nitrate membranes and all dialysis membranes are examples of porous barriers.

4.1.2 Factors effecting vehicle interactions with membrane

Many factors can influence the overall effect of vehicle interaction with the membranes and skin. These include its chemical structure, molecular weight and polarity, its hydrogen bonding capacity and the solubility parameter of the vehicle (Scheuplein et al., 1969; Sloan et al., 1986 a&b; Green et al., 1988; Okamoto et al., 1990).

4.1.2.1 Molecular weight, shape and polarity

The molecular shape and polarity are important factors in any enhancement induced by a vehicle component (Hadgraft, 1991). For example, azone and oleic acid, have been found to interact with the intercellular lipids making them more fluid (Golden et al., 1987) and thereby facilitate the diffusion of topically applied drugs. Such activity is probably attributable to the polar regions within the vehicle interacting with the polar regions of the lipids, and the hydrophobic tail inserting into the ordered alkyl chain region of the lipids. The presence of the *cis* (Z) double bond of oleic acid creates a 'kinked' structure (Green et al., 1988), which imposes disorder on the regular packing of the lipids and imparts greater fluidity to the bilayer. Azone, however, does not possess a 'kinked' structure and computer graphic representations and monolayer experiments suggest that when it is incorporated into the lipid layer, the seven membered ring lies in the plane of the lipid polar head groups. These

groups are then forced apart which prevents the alkyl chains packing efficiently also imparting disorder and facilitating diffusion of concomitantly applied drug (Beastall et al., 1987; Beastall et al., 1988).

The enhancement of membrane transport of estradiol by alcohols has been shown to be dependent upon the chain length of the latter, the dependence exhibiting a bell-shaped curve, peaking at C₁₀ (Santus & Baker, 1993). Also branched short chain alcohols blended with IPM have been shown to produce the highest estradiol flux compared with either linear short chain alcohols (alone or incorporated within the vehicle) or water (Goldberg-Cettina et al., 1995). Branched molecules are more compact than straight chain molecules of the same molecular formula and they are therefore hypothesized to penetrate into the stratum corneum more easily. Their penetration is expected to induce destabilization of the stratum corneum structure, and hence render it more susceptible to penetration by concomitantly applied active pharmaceutical ingredients (Rowe, 2006; Stamatas et al., 2008).

The molecular weight of the solvent has an important effect on the mobility of the solvent inside the membrane; higher molecular weight solvents have restricted movement in bulky polymers and have been shown to exhibit lower permeation rates when compared with solvents of lower molecular weights having the same solubility parameters (Most, 1970). The uptake of a series of aliphatic alcohols with 2–10 carbon numbers into silicone membranes at different temperatures was investigated (McAuley et al., 2010). An increase in alcohol membrane sorption with carbon number from ethanol to butanol (4 carbon atoms), was observed after which sorption decreased exponentially with increasing aliphatic chain length.

4.1.2.2 Hydrogen bond capacity

When a drug or a solvent partitions into the skin, there is the potential for hydrogen bonding to occur between that species and the polar head groups of the lipids. Mainly this hydrogen bonding would be primarily with the –COOH of the fatty acid, or the –OH group and amide group of the ceramides (Hadgraft et al., 1996). The stratum corneum is predominantly an H-bond donor environment with donor/acceptor effects in the ratio 0.6:0.4 (Pugh et al., 1996). Therefore the number and type of H-bonding

groups is an important factor when considering the potential of candidates for transdermal delivery. Pugh et al. (1996) showed that the presence of a –COOH group reduced the diffusion coefficient by a factor of about 50; while an ether group reduced it by about 5. The H- bond donor/acceptor properties in the acids are more similar to the H- bond properties of the stratum corneum compared with the ether derivatives. Increasing the number of hydrogen bonding groups in a diffusing species increases the chances of interaction between the permeant and the skin or membranes, providing the membranes are capable of such an interaction (Pugh et al., 1996; Plessis et al., 2001).

4.1.2.3 Solubility parameter

The solubility parameter of the vehicle is an important predictor of the flux of the drug through the membrane (Cross et al., 2001; Dias et al., 2007b). The concept of solubility parameter was first developed by Hildebrand and Scott (1950) based on regular solution theory. Solubility parameters are related to the cohesion energy, as they derive from the energy required to convert a liquid to a gas state. All types of bonds holding molecules together are broken in the vaporization process. Thus the energy of vaporization is a direct measure of the total cohesive energy holding the liquid molecules together and both can be considered as being identical to each other.

The solubility parameter (δ) is defined as the square root of the cohesive energy densities, which corresponds to the energy of vaporisation per unit volume (Equation 4.1).

$$\delta = (\Delta E_v/V_m)^{1/2} \quad \text{Equation 4.1}$$

Where V_m represents the molar volume and E_v is the energy of vaporization.

$$\Delta E_v = \Delta H_v - RT \quad \text{Equation 4.2}$$

The energy of vaporization is usually calculated by Equation 4.2 where ΔH_v is the heat of vaporization, R is the universal gas constant, and T is the absolute temperature.

For two materials to be mutually soluble, their cohesive energy densities must be similar, since this energy must be overcome to separate the molecules of the solute to allow the molecules of solvent to insert. For materials such as crosslinked polymers that do not dissolve, solubility can be measured by the degree of swelling (Lee et al., 2003).

If the solubility parameter of the vehicle is close to the solubility parameter of the skin, permeation may be enhanced (Dias et al., 2007b). Similarly, permeants with a solubility parameter close to that of the skin will have a higher permeation rate through the skin. The relationship between permeability coefficient of a series of alkanolic acids through porcine skin and solubility parameter was reported to take the form of a parabola with a maximum permeability near a solubility parameter of $20.46 \text{ (MPa)}^{1/2}$ (Liron & Cohen, 1984). Also the relationship between the solubility parameter of a series of narcotic analgesics and their permeation through cadaver skin was studied. It was found that narcotics with a solubility parameter close to $20.46 \text{ (MPa)}^{1/2}$ had higher permeability coefficients (Roy & Flynn, 1989). For vehicles or mixture of vehicles exhibiting solubility parameters in the range of $\delta = 16.36\text{--}24.55 \text{ (MPa)}^{1/2}$ large increases in fluxes of drug were reported in comparison to those obtained in the range $\delta = 24.55\text{--}36.82 \text{ (MPa)}^{1/2}$. This was attributed to vehicle effects on the modified skin as a consequence of the similarity in the solubility parameters of the vehicles to that of skin (Sloan et al., 1986 a&b). Qualitatively, fluxes and permeability coefficients were found to be inversely dependent on drug solubility in the vehicles with a minimum corresponding approximately to the point where solubility parameter of the drug = solubility parameter of the vehicle (Sloan et al., 1986a). The penetration of theophylline, salicylic acid and 6-mercaptopurine was investigated from various vehicles and the permeability coefficient was found to be minimized when the solubility parameter of the vehicle was close to that of the permeant (Sloan et al., 1986 a&b; Waranis et al., 1987). The maximum flux of benzocaine through various silicone rubber membranes occurred when the solubility parameter of the vehicle was intermediate between the solubility parameter of the permeant and solubility parameter of the membrane, providing that the vehicle had a low molecular volume and high mobility in the membrane (Most, 1972).

4.1.2.3.1 Hansen solubility parameter

Hansen parameters (Hansen, 1967) divide the total Hildebrand value (δ) into three parts: a dispersion force component (δ_D), hydrogen bonding component (δ_H) and a polar component (δ_P).

$$\delta^2 = \delta_D^2 + \delta_P^2 + \delta_H^2 \quad \text{Equation 4.3}$$

Dispersion forces are the weakest of the intermolecular forces. They occur between all molecules and they are the main forces that act in neutral, non-polar molecules. Polar forces or dipole-dipole interactions act to produce medium to weak bonds. They occur between neutral, polar molecules where the positive end of one molecule is attracted to the negative end of another molecule. Hydrogen bonding acts to form the strongest bonds, when compared with the dispersion and polar bonds. In hydrogen bonds, the positively charged hydrogen end of one molecule is attracted to the negatively charged end of another molecule, which must be an extremely electronegative element for example oxygen or nitrogen

As shown by Figure 4.2, any molecular substance can be represented by a point in a tridimensional space, called a Hansen sphere, whose orthogonal axes are Hansen solubility components (HSPs: $x=\delta_D$, $y=\delta_P$, $z=\delta_H$). In the exact centre is a green symbol. This shows the position of a particular molecule with values $\delta_D = 18.5$, $\delta_P = 9.9$, $\delta_H = 7.9$ in Figure 4.2.

There is a set of blue cubes, which are located at the HSPs of solvents which dissolve this molecule; these all lie inside the sphere. All substances qualified as good solvents for the solute should stay within this sphere and those considered as bad solvents (or nonsolvents) should lie outside. Accordingly, the red cubes show the solvents outside the sphere which do not dissolve this molecule.

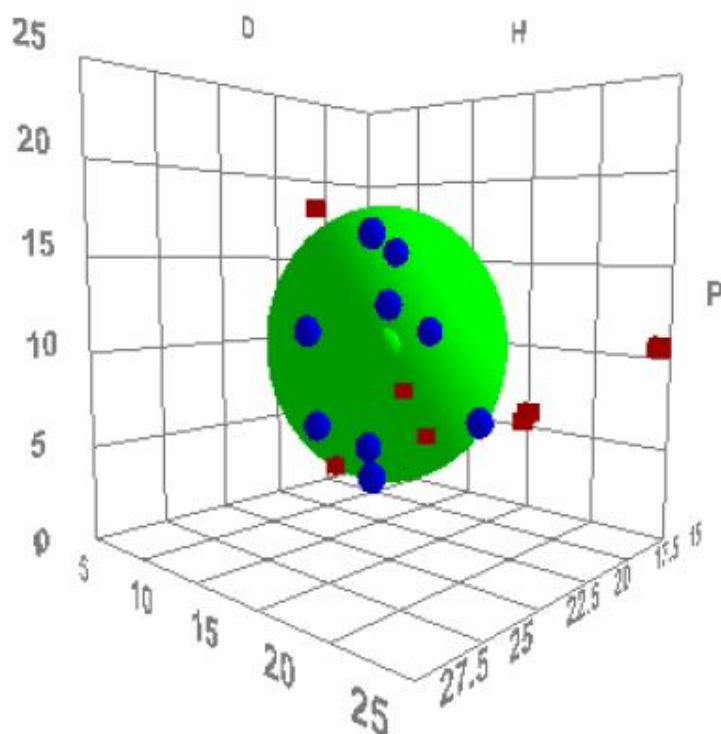


Figure 4.2 An example of Hansen sphere: the orthogonal axes are the Hansen solubility parameters corresponding to; x-axis, $D=\delta_D$ (the dispersion force component), y-axis, $P=\delta_P$ (the polar component) and z-axis, $H=\delta_H$ (the hydrogen bonding component).

A useful parameter for comparing two substances is the solubility parameter distance based on their respective HSP components:

$$\text{Distance}^2 = 4(\delta_{DA} - \delta_{DB})^2 + (\delta_{PA} - \delta_{PB})^2 + (\delta_{HA} - \delta_{HB})^2 \quad \text{Equation 4.4}$$

where δ_{DA} , δ_{DB} are the energy of the dispersion forces of compound A and B respectively, δ_{PA} , δ_{PB} are the energy of the dipolar forces of compound A and B respectively, δ_{HA} , δ_{HB} are the energy of the hydrogen bonds forces of compound A and B respectively,

A high affinity between a solvent and solute requires the distance to be less than the interaction radius of the sphere. The radius is the distance from the centre to the

border of the sphere. A RED (Relative Energy Difference) number is often used to quantify distances relative to the interaction radius. A perfect solvent has a RED of 0 which indicates no energy difference. A RED <1 indicates a high solute-solvent affinity, whereas a RED >1 indicates low affinity and a RED=1 (or around 1) reflects a boundary condition.

4.2 Aims and objectives

The interaction of vehicles employed in drug delivery systems with the membrane/skin is an important consideration in developing a suitable topical formulation. The importance of solubility parameter and structure of an oily vehicle when considering its potential to interact with membrane/skin has not been fully elucidated. The use of stratum corneum to interpret data correctly for the purpose of creating predictive models is difficult, due to the complexity of the membrane and therefore the nature of the possible interactions. Accordingly the use of simple membranes with different solubility parameters and homogenous structures might provide a means of identifying key factors that might be extrapolated later to human skin. When using blends of vehicles, one vehicle might partition to a greater extent into the membrane than the other, therefore the ratio of vehicle in the membrane could differ from the original ratio in the donor solution. The aim of this chapter was to investigate the nature and extent of interactions between a range of physicochemically diverse oily vehicles with membranes possessing heterogeneous physicochemical properties. The objectives of the work carried out in this study were to:

1. Investigate the effect of solubility parameter and different physicochemical properties on the uptake of a range of oils by different membranes.
2. Quantify the amount of oil(s) absorbed by silicone membrane from different oil blends, and compare these values with the oil ratio applied in the donor solution.
3. Quantify where possible the oil depletion from donor compartment.
4. Compare the effects of different oil blends on the permeation of MP across (silicone) membranes.

4.3 Methods

4.3.1 Materials

The suppliers of materials employed in this study have been reported previously and are listed in Table 2.2.

4.3.2 Membrane swelling experiments

Silicone, HDPE, PU and cellulose acetate nitrate membranes were used in the swelling experiments. The membranes employed in this study and some of their physicochemical characteristics are listed in Table 4.3.

Table 4.3 Physicochemical characteristics of membranes employed in this investigation

	Silicone	HDPE	PU	Cellulose acetate nitrate
Thickness (mm)	0.32	0.2	0.25	0.25
Porosity (μm)	non porous	non porous	non porous	0.025
Repeated monomer	$[\text{Si}(\text{CH}_3)_2\text{O}]_n$	$(\text{CH}_2\text{-CH}_2)_n$	$(\text{-R-O-C-NH-R}_2\text{-NH-C-O-})_n^{**}$	
δ_D^{*a}	17	18	18.1	
δ_P^{*b}	2.9	0	9.3	
δ_H^{*c}	2.6	2	4.5	
Solubility parameter ($\text{MPa}^{1/2}$)	17.4	18.1	20.8	28.6

*Determined from HSPiP software version 4.1.0.3

a dispersion force component

b polar component

c hydrogen bonding component

** Where n is the number of repetitions and R2 is a hydrocarbon chain. R represents a hydrocarbon containing the OH group.

4.3.2.1 Membrane weight

Uptake of vehicles into silicone, HDPE, PU and cellulose acetate nitrate membrane was determined gravimetrically. Membranes were cut to size (the diameter being approximately 2 cm) and the samples were then immersed in vehicle in a sealed glass vial, and soaked overnight (approximately 17 h) in a temperature-controlled water bath at around 32°C. The membranes were blotted dry with tissue paper and reweighed. The percentage weight difference (% ΔW) was calculated according to Equation 4.5.

$$\% \Delta W = \frac{(W_a - W_b)}{W_b} * 100 \quad \text{Equation 4.5}$$

Where W_a is the weight of membrane after soaking and W_b is the weight of membrane before soaking.

The amount of oil (mg per gram) in each membrane was calculated according to Equation 4.6

$$m_{\text{upt}} = \frac{\Delta \text{weight of membrane weight (mg)}}{\text{original weight of membrane (g)}} \quad \text{Equation 4.6}$$

4.3.2.2 Kinetic study of membrane swelling

The experiment described in Section 4.3.2.1 was repeated using silicone membrane with different oil blends, except that the weight and thickness of silicone membrane was measured at 0, 1, 3, 6 and 24 h.

The thickness was measured using callipers (Mitutoyo, Digimatic Calliper resolution 0.01mm, accuracy $\pm 0.02\text{mm}$ and repeatability 0.01mm). The thickness of membranes was measured before their immersion in vehicle at room temperature. The membranes were blotted dry with tissue paper after each set time interval and the thickness was re-measured. The percentage difference in membrane thickness (% ΔT) was calculated according to Equation 4.7.

$$\% \Delta T = \frac{(T_a - T_b)}{T_b} * 100 \quad \text{Equation 4.7}$$

Where T_a is the thickness of membrane after soaking and T_b is the thickness of membrane before soaking.

4.3.3. Quantification of oil uptake by silicone membrane from oil blends

4.3.3.1 Preliminary studies

Silicone membranes were cut into circular pieces (the diameter was approximately 2 cm) weighed and immersed in the vehicle in a sealed glass vial, approximately 17 h at 32°C (maintained in a temperature-controlled water bath). The following day, the membranes were blotted dry with tissue paper and reweighed. Samples were then soaked in 9 mL of heptane for 3 h, or soaked 3 mL of heptane for 1 h, replaced hourly for three hours (total 9 mL after pooling) to extract any sorbed oils from the membrane. After each hour the 3 mL of heptane was replaced with fresh solvent. Some samples were left for 5 h in heptane.

4.3.3.2 Membrane extraction method

The amount of oil taken up by the silicone membrane was quantified using GC analysis. Membranes were cut into circular pieces (the diameter was around 2 cm) weighed and immersed in the vehicle in a sealed glass vial, approximately 17 h at 32°C maintained in a temperature-controlled water bath. The following day, the membranes were blotted dry with tissue paper and reweighed. Samples were soaked in 3 mL of heptane for 1 h, replaced hourly for three hours (total 9 mL after pooling) to extract any sorbed oils from the membrane. After each hour the 3 mL of heptane was replaced with fresh solvent.

A control experiment was performed by soaking the membrane for 3 h in heptane. A sample of the heptane used to soak the membrane was subsequently assayed by GC to check whether the assay employed to determine the amount of extracted oil was

prone to possible interference with any potential extractable material present in the membrane.

4.3.3.3 GC analysis

Chromatographic measurements were carried out as described previously in section 2.3.4.

4.3.3.4 Calculation of amount absorbed

The percentage of amount of any specific oil absorbed by silicone membrane from the oil blends was calculated according to Equation 4.8.

$$\% m_{\text{upt}} = \frac{(m_{\text{GC}})}{m_{\text{T}}} * 100 \quad \text{Equation 4.8}$$

Where m_{upt} is the amount of oil sorbed, m_{GC} amount of oil quantified by GC and m_{T} the total amount of oil sorbed by silicone membrane

Since OA and LP were not detected by GC analysis the amount of (LP or OA in the membrane from the blends) was calculated according to Equation 4.9.

$$\text{Amount of LP or OA} = m_{\text{T}} - m_{2\text{GC}} \quad \text{Equation 4.9}$$

Where m_{T} is the total amount of oil sorbed by silicone membrane and $m_{2\text{GC}}$ the amount of second oil quantified by GC

4.3.4 Determination of composition of the oil in donor compartment

In order to determine the ratio of the oils remaining in the donor compartment after diffusion experiments, silicone membrane was cut to an appropriate size and immersed overnight in phosphate buffer pH 7.0. On the following day the receptor compartment, of Franz cell having a receptor phase of 2 mL and a diffusional area of 0.65 cm², was carefully filled with phosphate buffer, after which the receptor

temperature was maintained at 32°C by immersion in a temperature-controlled water bath. The membrane was then allowed to equilibrate with the receptor fluid for 1 h, after which time 200 µL of 75:25, 50:50 or 25:75% w/w IHD/HD solution was introduced into the donor compartment. After 6 h any oil remaining in the donor compartment was removed for assay. The sample was diluted appropriately with heptane and analysed using the GC method described in section 2.3.4.

Equations 4.10 and 4.11 were employed to calculate the percentage ratio of the oil applied and the oil remaining in the donor compartment after 6 h:

$$\%m_{oil a} = \frac{(m_{oil a})}{m_{Ta}} * 100 \quad \text{Equation 4.10}$$

$$\%m_{oil r} = \frac{(m_{oil r})}{m_{Tr}} * 100 \quad \text{Equation 4.11}$$

Where $m_{oil a}$ is the amount of one the component oil applied (i.e. either IHD or HD), m_{Ta} the amount of both oils applied into the donor compartment. $m_{oil r}$ the amount of that component oil remaining after 6 hours and m_{Tr} the total amount of oil remaining in the donor compartment (i.e. the total amount of HD+IHD applied

4.3.5 Effect of membrane pre-treatment with oil on permeant diffusion

4.3.5.1 Franz cell experiment

The donor suspension was prepared by adding an excess amount of MP to 6g of phosphate buffer pH 7.0. The suspension was shaken overnight in a water bath at 32°C. Before the experiment the membrane was cut into circular discs (around 0.8 cm²), immersed and soaked in the HD, IHD and LP overnight at 32°C. As a control, a sample of the membrane was immersed and soaked in phosphate buffer overnight, rather than oil. Diffusion experiments were carried out using calibrated (for volume) Franz cells with a receptor phase of 2 mL and a diffusional area of 0.65 cm². The membrane was cut to the appropriate size (around 2 cm) and placed between the donor and the receptor compartments of the Franz cell. The receptor compartment was carefully filled with phosphate buffer pH 7.0 and the cell placed on a stirring

plate submerged in a water-bath maintained at 32°C. A small Teflon coated magnetic bar (around 5 mm) was included in the receptor compartment such that stirring was maintained throughout the duration of the experiment. After allowing the membrane to equilibrate with the receptor fluid, 200 µL of the buffer suspension (the sample contained undissolved/suspended solid of MP at 32°C) was added to the donor compartment. At appropriate time intervals, 200 µL samples were withdrawn from the receptor compartment and immediately replaced with an equal volume of fresh phosphate buffer, (pH 7.0). The cumulative amounts (per unit surface area of membrane) of MP which diffused across membrane were plotted against time (h). The slope of the linear plot was taken as the flux of MP permeation. Each experiment was conducted five times.

4.3.5.2. HPLC analysis of MP

The MP concentrations of receptor samples were analysed by HPLC methods (section 2.3.2). The values at each time were corrected for previous sample removal and the replacement of the previous samples with fresh media.

4.3.5.3 Calculation of enhancement ratio

Enhancement ratios (ER) were derived from:

$$ER = J_s(E)/J_s(C) \quad \text{Equation 4.12}$$

Where $J_s(E)$ and $J_s(C)$ are the flux values of the MP following pre-treatment of the membrane with oils (enhanced) or phosphate buffer (control), respectively. Results were expressed as the mean \pm standard deviation (SD) of 4–5 determinations.

4.3.6 Calculation of Hansen solubility parameter and spheres

Hansen Solubility Parameters in Practice HSPiP software version 4.1.0.3 was used to calculate the Hansen solubility parameter (HSP) values and derive a graphical plot of the Hansen spheres. The HSP distance from the centre of the sphere to the oil is calculated by Equation 4.4.

The HSP values for the oil blends were calculated using the linear mixing rule.

4.3.7. Statistical analysis

Data reported in this study are usually the mean of $n \geq 3$ with the standard deviation (sd) given. In order to establish differences in the parameters measured in this study, statistical tests were conducted. The analysis of variance (ANOVA) method and student's t- test were used as the major statistical tests where applicable. Post hoc comparisons of the means of individual groups were performed using Tukey's test, and the level of significance was taken at $p \leq 0.05$ in all cases.

4.4 Results

4.4.1 Swelling data for model permeants in membranes

The absolute amount of oils sorbed into the different membranes is shown in Table 4.4. The percentage weight increases in the silicone, HDPE, PU and cellulose acetate nitrate membranes due to solvent uptake are shown Table 4.5. Membranes sorbed oils in different ratios with the order being silicone>HDPE>PU for IPM, HD and IHD. OA was highly sorbed into PU; however it acted as a plasticizer for the membrane and PU lost its consistency, becoming sticky when soaked in the oil. Generally the difference in membrane weight after being soaked in the buffer was the lowest, when compared with the resultant weight gain after incubation with oils. However the reverse was found when cellulose acetate nitrate membrane was employed and weight gain was greatest in buffer. The difference between membrane weight after incubating with buffer at 32°C was 0.06 ± 0.05 % for silicone

membrane, 18.16 ± 0.72 % for HDPE, 1.01 ± 0.40 for PU and 70.14 ± 16.16 % for cellulose acetate nitrate.

Table 4.4 Amount of oil indifferent membranes after being soaked in different vehicles for approximately 17 h at 32°C (mg oil/ g membrane).

Membrane	IHD	IPM	HD	OA	LP
Silicone	1048.6 ± 17.6	662.1 ± 19.8	464.6 ± 9.2	31.2 ± 1.3	137.5 ± 5.2
HDPE	364.0 ± 24.1	188.7 ± 11.7	262.7 ± 9.6	297.0 ± 19.5	300.7 ± 17.2
PU	22.4 ± 1.1	51.7 ± 1.9	20.4 ± 0.98	885.8 ± 27.2	23.4 ± 0.98

Data represent mean \pm sd ($n \geq 3$).

Table 4.5 The percentage difference in weight of membranes after being soaked in different vehicles for approximately 17 h at 32°C.

Membrane	IHD	IPM	HD	OA	LP
Silicone	105.6 ± 1.1	64.2 ± 1.4	43.9 ± 0.7	3.1 ± 0.1	13.8 ± 1.8
HDPE	36.2 ± 2.0	18.3 ± 2.1	25.3 ± 3.1	29.1 ± 2.2	29.1 ± 2.9
PU	2.3 ± 0.2	5.1 ± 0.4	2.2 ± 0.1	88.1 ± 5.1	2.2 ± 0.2
Cellulose acetate nitrate	20.3 ± 2.1	25.4 ± 2.0	16.2 ± 0.7	14.1 ± 0.8	13.2 ± 3.2

Data represent mean \pm sd ($n \geq 3$).

4.4.2 Kinetic study of silicone membrane swelling

A kinetic study was carried out to monitor oil uptake by incubating the membrane at 32°C, over a 24 h period. Generally most of the eventual total weight increase occurred in the first hour. Also there was no significant difference in the thickness of the membrane between that measured after the first and that at hour 24; any change in thickness occurring during the first hour. Figure 4.3 provides a typical example of rate of oil uptake; in this instance the change in membrane weight after different

time intervals is shown after immersion in IPM/IHD blends. Immersion of silicone membrane in other oils/oil combinations produced similar profiles.

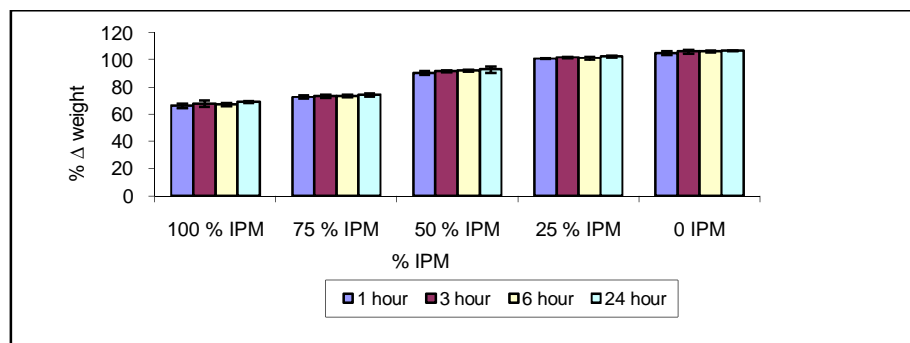


Figure 4.3 Percentage differences in weight of silicone membrane during soaking in IPM/IHD blends for 24 h at 32°C.

4.4.3. Quantification of oil uptake by silicone membrane from oil blends

4.4.3.1 Change in membrane weight

Distinct differences were found in the weight increase of samples of silicone membrane when incubated with different combinations of oil in different ratios (Figures 4.4, 4.5 and 4.6). The highest amount sorbed was when the membrane was incubated with IPM/IHD blends. The lowest amount of oil uptake was determined to occur from HD/OA blends.

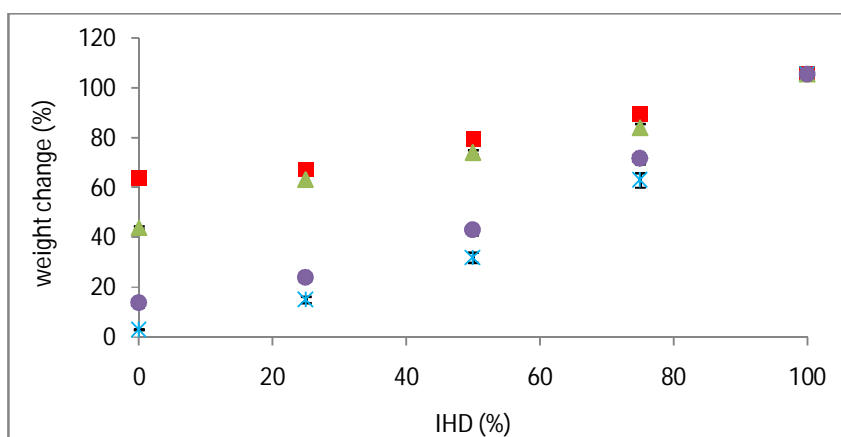


Figure 4.4 Percentage weight changes in silicone membrane immersed in different oil combinations comprising IHD with (▲) HD (■) IPM (●) LP and (*) OA for approximately 17 h at 32°C. Data represent mean \pm sd ($n \geq 3$). Error bars lie within the symbols.

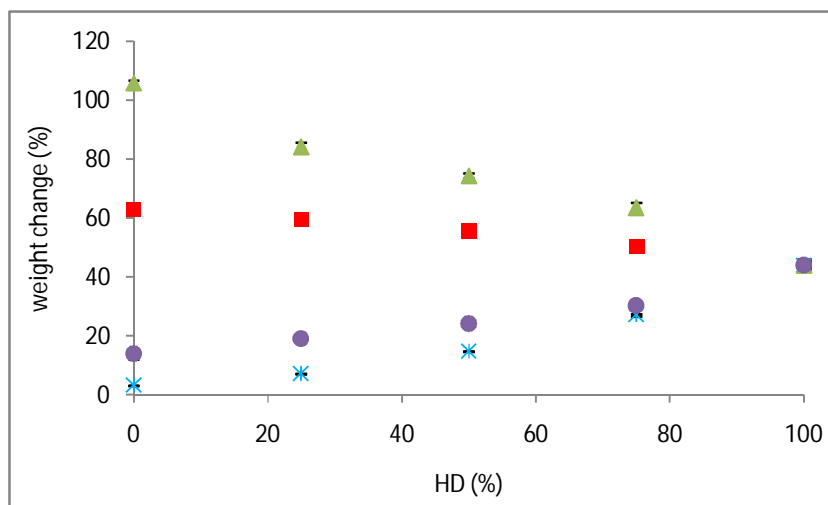


Figure 4.5 Percentage weight changes in silicone membrane immersed in different oil combinations comprising HD with (▲) IHD (■) IPM (●) LP and (*) OA for approximately 17 h at 32°C. The IHD blend is also presented in Figure 4.4. Data represent mean \pm sd ($n \geq 3$). Error bars lie within the symbols.

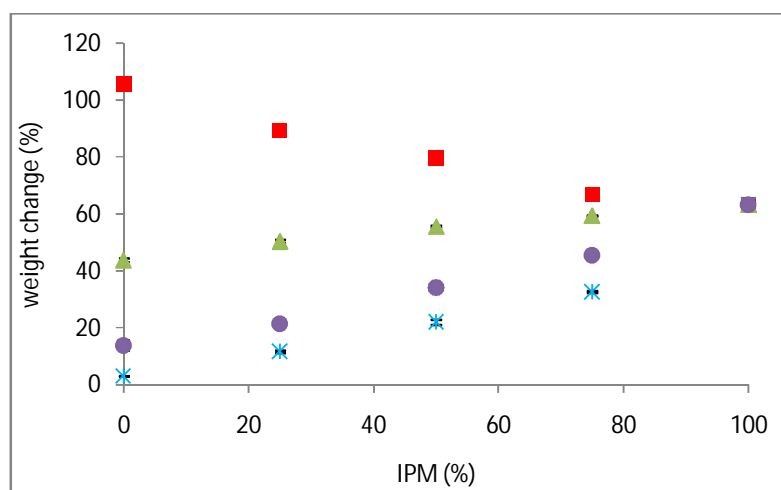


Figure 4.6 Percentage weight changes in silicone membrane immersed in different oil combinations comprising IPM with (▲) HD (■) IHD (●) LP and (*) OA for approximately 17 h at 32°C. The IHD and HD blends are also presented in Figure 4.4 and 4.5 respectively. Data represent mean \pm sd ($n \geq 3$). Error bars lie within the symbols.

4.4.3.2 Measurement of oil uptake by silicone membrane

The amount of oil taken up by silicone membrane was analysed by GC chromatography. The quantity extracted from the membrane using heptane was then related to the ratio of oil originally present in the oil solution. The efficiency of recovery of all oils using the extraction technique described was shown to be $\geq 97\%$ in preliminary studies. Figures 4.7 – 4.15 show the composition of oil extracted versus the composition of the oil blend at the start of incubation. Please note, that only mean composition values are presented in the bar charts, below. However, in Tables 4.7 – 4.9, the total amount (including measures of variability) are presented from which the data for Figures 4.7 – 4.15 have been calculated. The extraction results for IHD with other oils showed that IPM and IHD were sorbed to the same extent, and hence the composition of the amount of oil absorbed from the different ratio blends was close to the ratio present in the starting blend (Figure 4.7). On the other hand when IHD was blended with HD, LP or OA, then the IHD appeared to be absorbed preferentially in comparison to the other oil present in the blend (Figures 4.8-4.10). There was no significant difference in the amount of HD and IPM sorbed as a function of starting composition (Figure 4.11), whilst when IPM was blended with either LP or OA then less of the latter two oils was sorbed by the membrane than was present in the original mixture (Figures 4.12 and 4.13). In all blends the RSD between the samples was ≤ 5 , which was deemed to be within acceptable limits for the GC method employed.

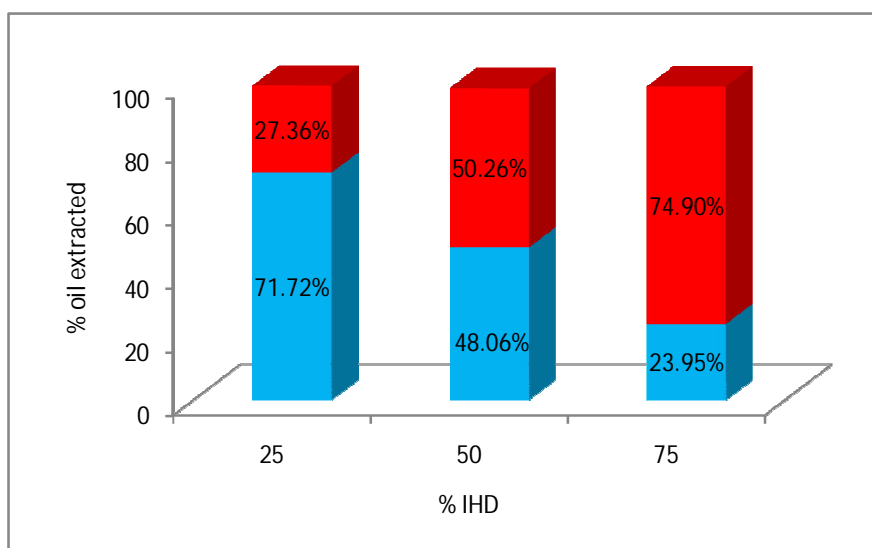


Figure 4.7 Percentage of individual oils extracted from silicone membrane after being incubated for approximately 17 h at 32°C in IPM/IHD blends expressed as a function of the percentage of IHD in solution (■) IHD (■) IPM.

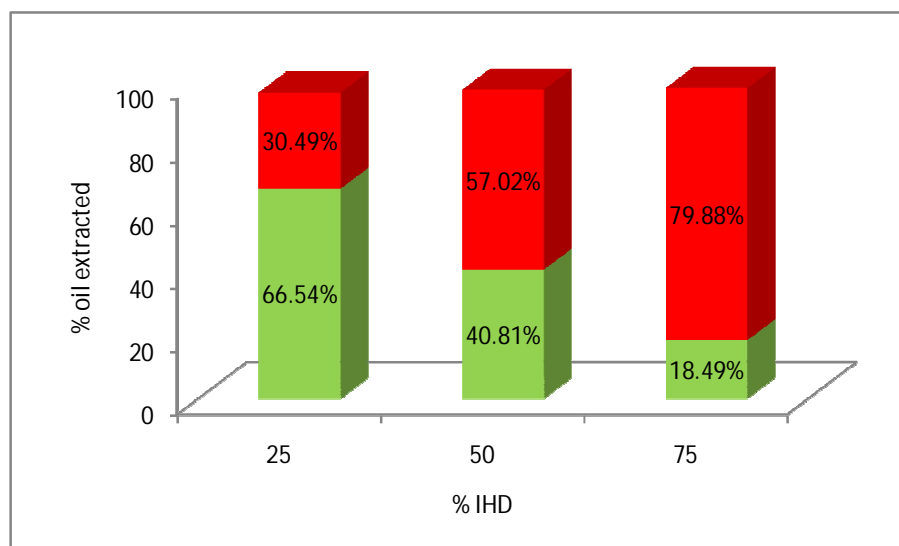


Figure 4.8 Percentage of individual oils extracted from silicone membrane after being incubated for approximately 17 h at 32°C in HD/IHD blends expressed as a function of the percentage of IHD in solution (■) IHD (■) HD.

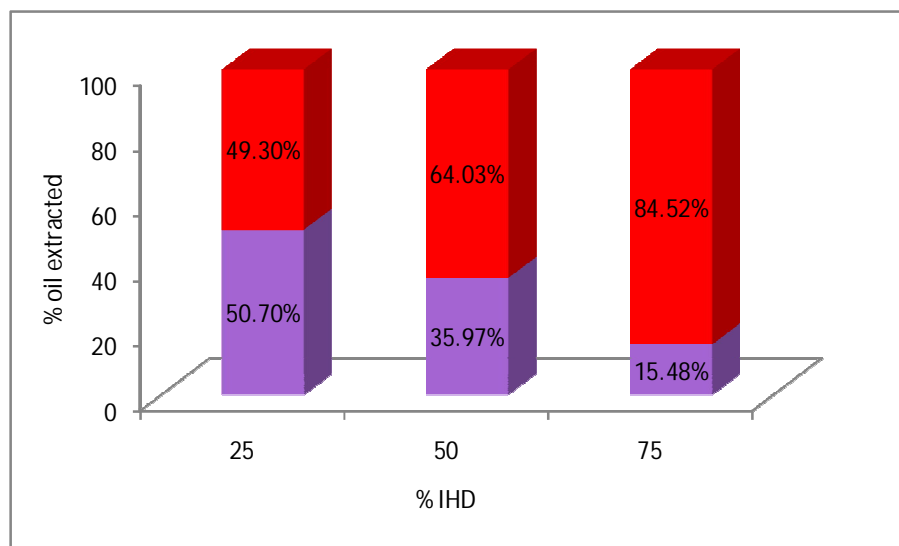


Figure 4.9 Percentage of individual oils extracted from silicone membrane after being incubated for approximately 17 h at 32°C in LP/IHD blends expressed as a function of the percentage of IHD in solution (■) IHD (■) LP.

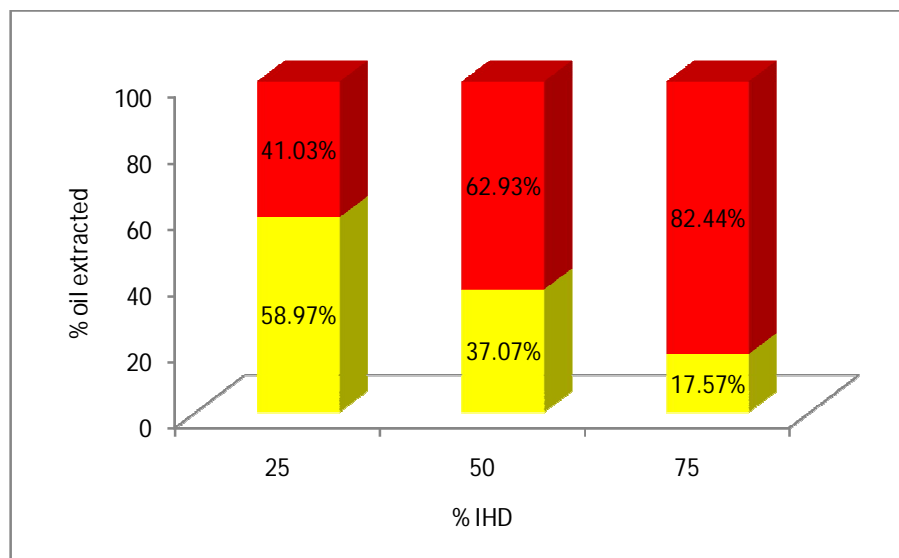


Figure 4.10 Percentage of individual oils extracted from silicone membrane after being incubated for approximately 17 h at 32°C in OA/IHD blends expressed as a function of the percentage of IHD in solution (■) IHD (■) OA.

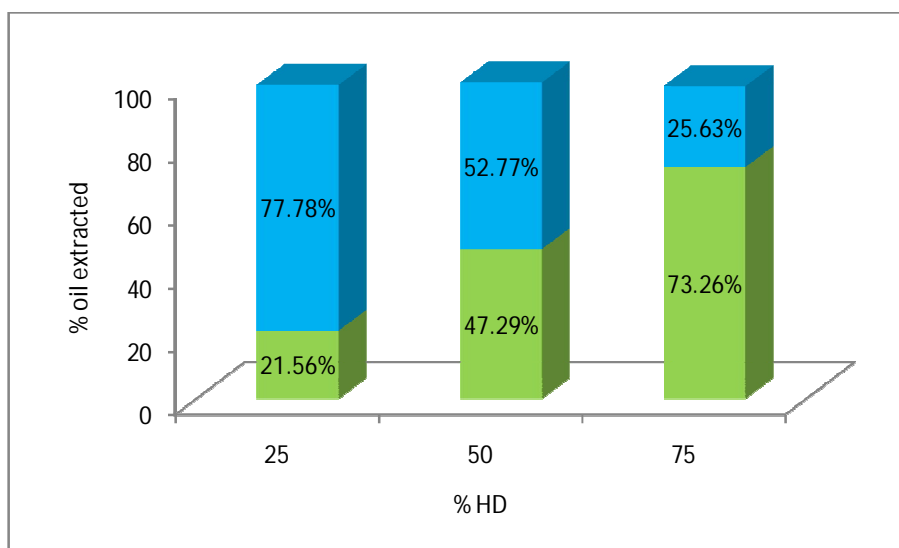


Figure 4.11 Percentage of individual oils extracted from silicone membrane after being incubated for approximately 17 h at 32°C in IPM/HD blends expressed as a function of the percentage of HD in solution (■)HD (■) IPM.

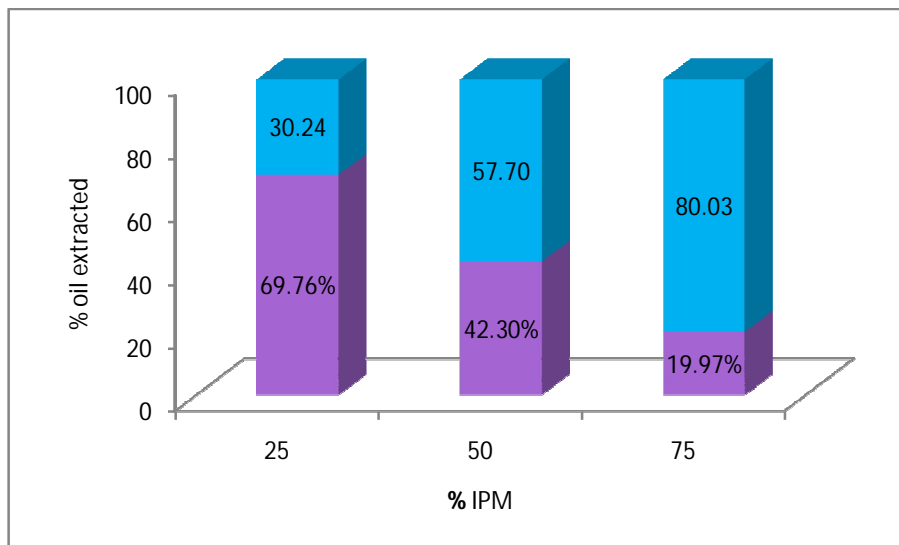


Figure 4.12 Percentage of individual oils extracted from silicone membrane after being incubated for approximately 17 h at 32°C in LP/IPM blends expressed as a function of the percentage of IPM in solution (■)LP (■) IPM.

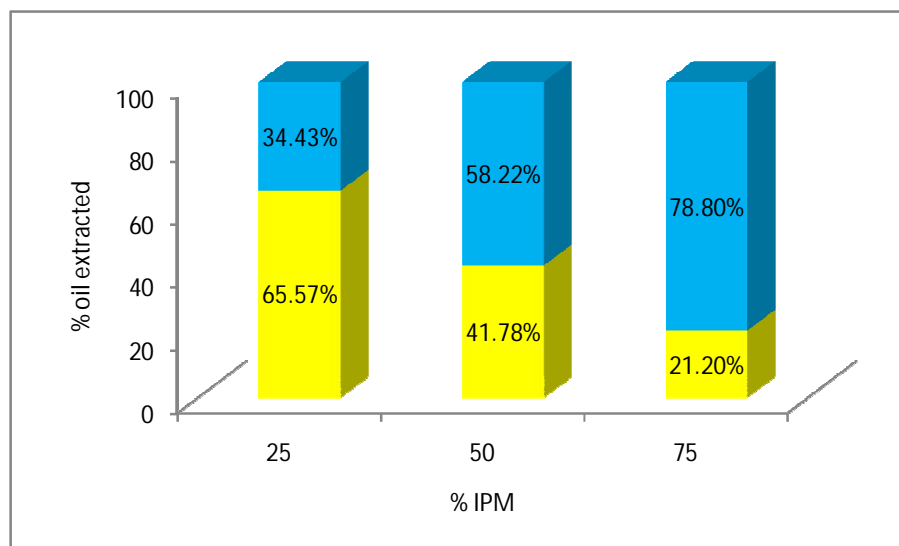


Figure 4.13 Percentage of individual oils extracted from silicone membrane after being incubated for approximately 17 h at 32°C in OA/IPM blends expressed as a function of the percentage of IPM in solution (■)OA (■) IPM.

There were no significant differences between the percentages of HD and LP extracted and that present in the original blend (Figure 4.14). However the percentage of HD in the extracted oil was significantly higher than the percentage OA recovered (Figure 4.15) in comparison to the ratios present in the original vehicle.

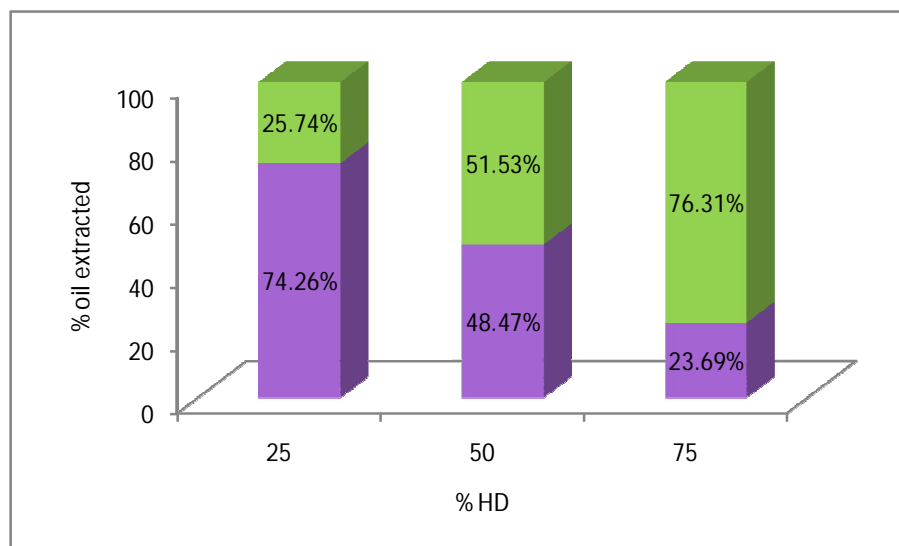


Figure 4.14 Percentage of individual oils extracted from silicone membrane after being incubated for approximately 17 h at 32°C in LP/HD blends expressed as a function of the percentage of HD in solution (■)HD (■) LP.

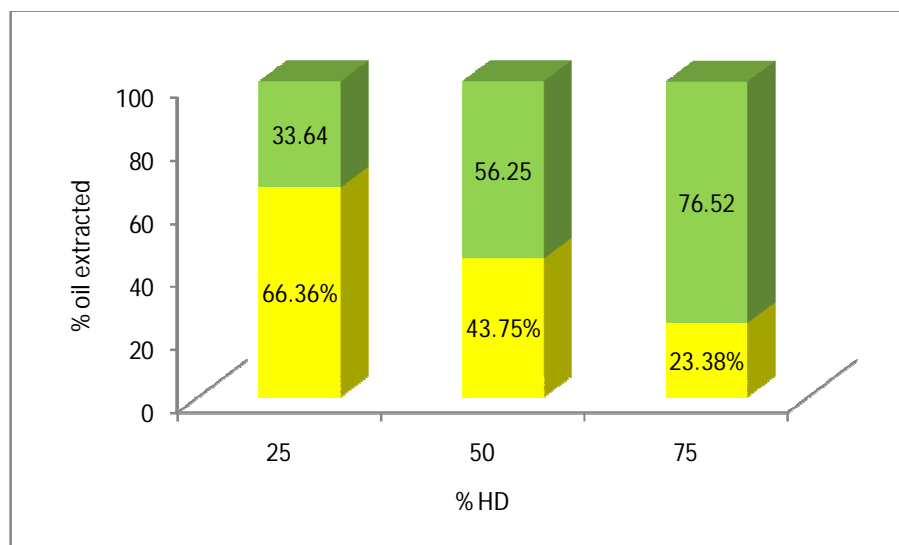


Figure 4.15 Percentage of individual oils extracted from silicone membrane after being incubated for approximately 17 h at 32°C in OA/HD blends expressed as a function of the percentage of HD in solution (■)HD (■) OA.

Table 4.6 shows the amounts of IHD, IPM and HD that were extracted from silicone membrane in each of the separate oils. The amount of IHD sorbed to/in the membrane was significantly higher than that of HD and IPM. Tables 4.7-4.9 shows the absolute amount of oils extracted from the silicone membrane when it was

incubated in different oil blends. Generally blending oils incorporating IHD were taken up by the membrane in higher amounts than similar blends containing either HD or IPM.

Table 4.6 Total amount of oil extracted and quantified by GC (mg oil/ g membrane) after incubation at 32°C for 17 h

Oil	Amount extracted by GC (mg oil/ g membrane)
IHD	1026.4 ± 20.7
IPM	648.8 ± 13.7
HD	449.1 ± 12.8

Table 4.7 Amount of oil extracted from silicone membrane after immersion for 17 h at 32°C in various IHD oil blends and quantified by GC (mg oil/ g membrane)

%IHD	IHD/IPM		IHD/HD		IHD/LP		IHD/OA	
	IHD	IPM	IHD	HD	IHD	LP	IHD	OA
25	195.2 ± 7.1	502.7 ± 11.9	188.5 ± 5.2	425.4 ± 10.6	122.6 ± 7.1	126.1 ± 6.9	60.7 ± 2.4	87.8 ± 3.0
50	437.7 ± 13.8	418.4 ± 3.4	425.5 ± 7.5	304.5 ± 3.8	281.9 ± 5.2	158.2 ± 5.3	197.2 ± 9.3	116.5 ± 2.1
75	722.1 ± 15.7	230.9 ± 2.8	724.5 ± 18.4	168.5 ± 5.7	637.3 ± 10.6	116.7 ± 3.1	522.8 ± 3.8	111.3 ± 2.0

Table 4.8 Amount of oil extracted from silicone membrane after immersion for 17 h at 32°C in various IPM oil blends and quantified by GC (mg oil/ g membrane)

%IPM	IPM/HD		IPM/LP		IPM/OA	
	IPM	HD	IPM	LP	IPM	OA
25	138.2 ± 4.1	403.0 ± 6.0	64.8 ± 1.8	149.6 ± 2.8	20.6 ± 0.2	39.5 ± 0.5
50	313.4 ± 6.8	280.8 ± 5.5	196.6 ± 3.5	144.1 ± 2.7	73.6 ± 2.1	52.9 ± 1.4
75	449.3 ± 4.0	124.5 ± 1.2	364.3 ± 10.8	90.9 ± 1.5	202.6 ± 5.8	54.5 ± 2.0

Table 4.9 Amount of oil extracted from silicone membrane after immersion for 17 h at 32°C in various HD oil blends and quantified by GC (mg oil/ g membrane)

%HD	HD/LP		HD/OA	
	HD	LP	HD	OA
25	36.2 ± 0.6	104.5 ± 3.7	23.7 ± 0.98	46.8 ± 2.3
50	108.7 ± 4.2	103.2 ± 1.7	82.4 ± 3.9	64.8 ± 2.1
75	223.0 ± 2.1	69.3 ± 2.4	207.3 ± 1.1	62.5 ± 2.2

4.4.4 Determination of composition of the oil in donor compartment

Oil (200 µL) was added to the donor compartment of a Franz cell containing silicone membrane and a sample of the oil remaining in the donor compartment after 6 h (the duration of the diffusion experiments) was analysed. The results in Figure 4.16 show the calculated (Section 4.3.4) percentage of oil applied and the percentage of oil remaining in the donor compartment after 6 h. These results indicate that the composition of the applied vehicle in the donor compartment is changing significantly within the time that the experiment was conducted ($p \leq 0.05$). In addition it indicated that one oil is being sorbed preferably compared to the other. Accordingly, therefore both the thermodynamic activity of any incorporated permurant might be altered, and the membrane structure could be modified.

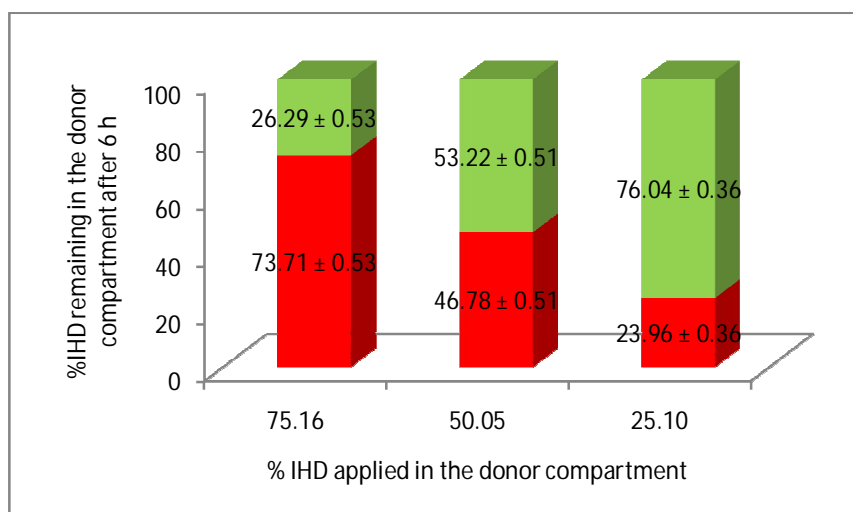


Figure 4.16 Percentage of individual oils (HD/IHD blends) remaining in the donor compartment after six hours, expressed as a function of the percentage of IHD applied in solution (■) IHD (■) HD (mean ± SD).

4.4.5 Effect of membrane pre-treatment on permeant diffusion

The permeation profiles of the MP through silicone membrane pre-treated with different oils in comparison to a control comprising membrane pre-treated with buffer are shown in Figure 4.17. Steady state fluxes were in the order of IHD>HD>LP, as shown in Table 4.10. Generally, the flux of MP from pre-treated silicone membrane was found to be significantly higher than that of MP flux through silicone membrane soaked in buffer. These results indicate that the membrane is modified by the oil that has partitioned into the matrix, leading to the modification of the flux of drug presented at the same thermodynamic potential.

Table 4.10 MP fluxes from buffer through silicone membrane pre-treated with IHD, HD, LP and buffer

Pre-treatment	Flux ($\mu\text{g cm}^{-2} \text{h}^{-1}$)	ER
IHD	113.46 ± 1.83	2.62 ± 0.03
HD	75.60 ± 1.43	1.74 ± 0.03
LP	56.87 ± 1.99	1.31 ± 0.04
Buffer	43.25 ± 0.94	1.00 ± 0.03

Data are expressed as mean \pm sd ($n \geq 4$)

(ER) Enhancement ratio

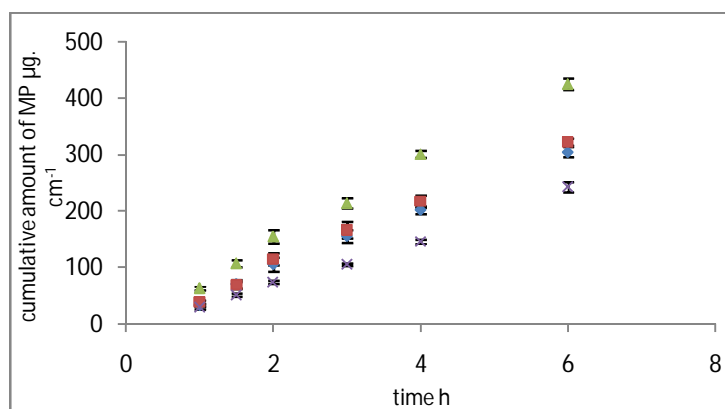


Figure 4.17 MP permeation profile through pre-treated silicone membrane showing the cumulative amount of MP in the receptor compartment from buffer as a function of time. Permeation was measured after pre-treatment of the membrane by soaking for approximately 17 h at 32°C in either (▲) IHD, (■) HD, (◆) LP or (x) buffer. Data represent mean \pm sd ($n \geq 3$).

4.4.6 Hansen Solubility Parameter values and plots

The various HSP parameters and the molar volume of the different oils are shown in Table 4.11. LP displays the highest molar volume (Mvol), while HD and IHD have the lowest Mvols. The δ_D values for all oils were of similar magnitude. IHD and HD are pure hydrocarbons therefore the δ_P and δ_H are zero. OA displays a higher value of δ_H compared with other oils.

Table 4.11 Hansen Solubility Parameter values and molecular volume of oils used

Oil	δ_D^a	δ_P^b	δ_H^c	Mvol ^d
OA	16.0	2.8	6.2	319.7
IPM	16.0	2.7	2.7	315.0
HD	16.3	0	0	294.2
IHD	14.7	0	0	295.3
LP*	16.1	1.8	3.7	424.1

^adispersion component

^bpolar component

^chydrogen bonding component

^d molecular volume

*values from Abbott, 2012

The Relative Energy Difference (RED) is the ratio of the distance between the HSP values of the solvent and membrane to the radius of the Hansen sphere. The RED values for the oils calculated by the HSPiP software are shown in Table 4.12. Table 4.13 shows the distance between the HSP values of membranes and oils. Generally if two components are chemically similar then it would be expected that their HSP values would be the same; and when the sum of the absolute differences of the three HSP values is calculated, then difference would be zero. If the two components are chemically fairly similar then it would be expected that their HSP values would be similar, and the differences would be small. So the definition of a perfect solvent is the one that has the difference of 0 MPa^{1/2}.

Table 4.12 Relative energy differences (RED) values expressed for the oils when compared with different membranes

Oil	OA	IPM	HD	IHD
Silicone	0.72	0.39	0.72	1.05
HDPE	3.40	2.55	2.25	3.75
PU	0.99	1.06	1.36	1.55

Table 4.13 Hansen solubility parameter (HSP) distance between the HSP of the oils and different membranes MPa^{1/2}

Oil	OA	IPM	HD	IHD	LP
Silicone	4.1	2.2	4.1	6.0	2.4
HDPE	6.8	5.1	4.5	7.5	5.1
PU	7.9	8.5	10.9	12.4	8.5

The plots of the Hansen spheres for the different oils and membranes are shown in Figures 4.18-4.20. If a solvent blend is inside the sphere then it is likely to be miscible with the polymer and the closer it is to the centre, the more effective it is in its solvency. Figure 4.18 shows that the solubility parameter of all the oils lay inside the Hansen sphere generated for silicone membrane consequently they are all expected to swell the silicone membrane. It should be borne in mind that the radius of the Hansen sphere is also a function of the experimental data used for their calculation in the HSPIP software. Failure to study a sufficient range of solvents may underestimate the true radius of the sphere, where a more extensive range of solvents studied. Whereas the same solubility parameters of the oils were sited outside the spheres for HDPE (Figure 4.19) and PU (Figure 4.20, this indicates that these oils are not perfect for the membranes. However the blue colour of the cubes indicates that these solvent still possess solvency power on the selected membranes.

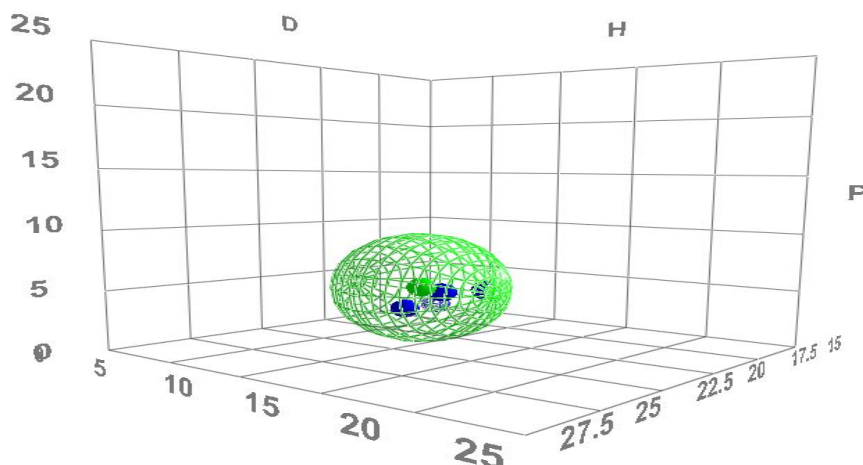


Figure 4.18 Schematic of the Hansen Solubility sphere. Each axis is one of the three component Hansen solubility parameters, δ_D , δ_H , or δ_P (representing the magnitude of the dispersive or van der Waals forces, the hydrogen bonding, and the polar bonding, respectively). The centre of the sphere (green symbol) represents the three-dimensional solubility parameter for the silicone membrane. The blue symbols are the Hansen solubility parameters of oils used in this investigation. The radius of the sphere is $5.7 \text{ MPa}^{1/2}$.

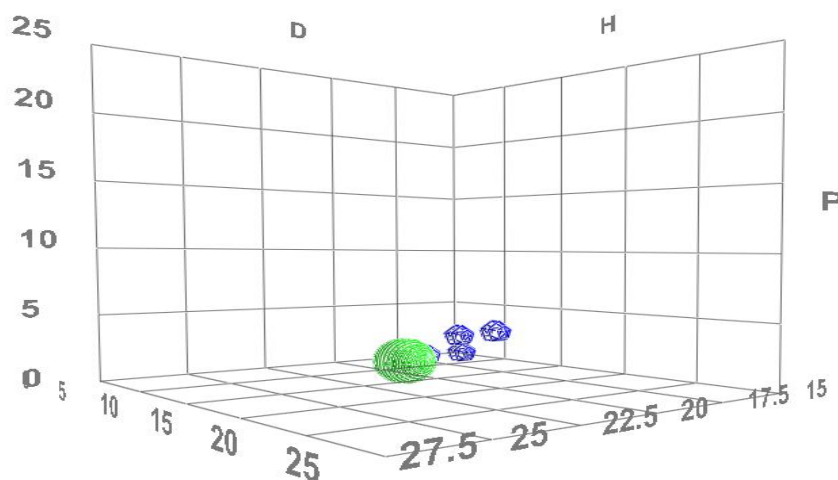


Figure 4.19 Schematic of the Hansen Solubility sphere. Each axis is one of the three component Hansen solubility parameters, δ_D , δ_H , or δ_P (representing the magnitude of the dispersive or van der Waals forces, the hydrogen bonding, and the polar bonding, respectively). The centre of the sphere (green symbol) represents the three-dimensional solubility parameter for the HDPE membrane. The blue symbols are the Hansen solubility parameters of oils used in this investigation. Radius of the sphere is $2 \text{ MPa}^{1/2}$.

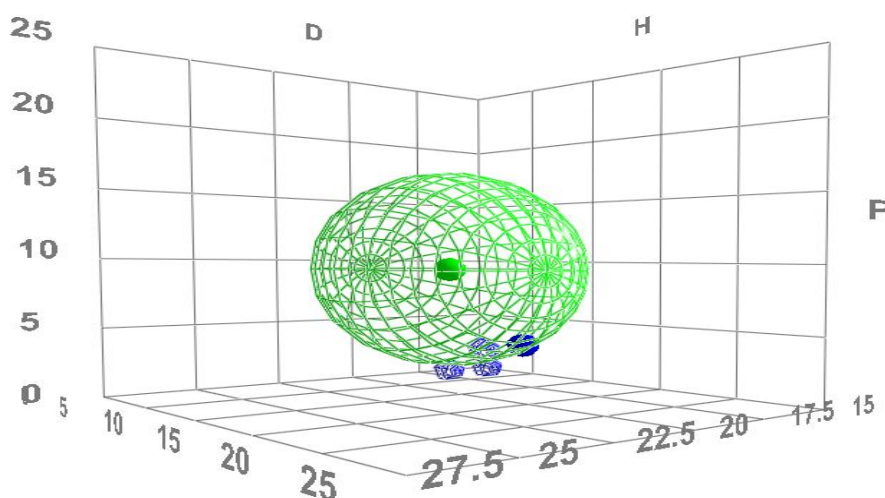


Figure 4.20 Schematic of the Hansen Solubility sphere. Each axis is one of the three component Hansen solubility parameters, δ_D , δ_H , or δ_P (representing the magnitude of the dispersive or van der Waals forces, the hydrogen bonding, and the polar bonding, respectively). The centre of the sphere (green symbol) represents the three-dimensional solubility parameter for the PU membrane. The blue symbols are Hansen solubility parameters of the oils used in this investigation. Radius of the sphere is $8 \text{ MPa}^{1/2}$.

The HSP values for the different oil blends and the distance between HSP of oils and silicone membrane are shown in Tables 4.14-4.22. OA blends were found to display low distance value comparatively, while IHD blends were associated with the highest values. The highest distance values for the mixtures were obtained when the IHD was mixed with HD (Table 4.16).

Table 4.14 Hansen solubility parameters (HSP) values and distance between the HSP of the IHD/IPM oil blends and silicone membranes $\text{MPa}^{1/2}$

% IHD/IPM	δ_D	δ_P	δ_H	Distance
25/75	15.7	1.6	2.0	3.0
50/50	15.4	1.1	1.4	4.0
75/25	15.0	0.5	0.7	5.0

Table 4.15 Hansen solubility parameters (HSP) values and distance between the HSP of the HD/IPM oil blends and silicone membranes MPa^{1/2}

% HD/IPM	δ_D	δ_P	δ_H	Distance
25/75	16.1	1.6	2.0	2.4
50/50	16.2	1.1	1.4	2.8
75/25	16.2	0.5	0.7	3.4

Table 4.16 Hansen solubility parameters (HSP) values and distance between the HSP of the IHD/HD oil blends and silicone membranes MPa^{1/2}

% IHD/HD	δ_D	δ_P	δ_H	Distance
25/75	15.9	0	0	4.5
50/50	15.5	0	0	4.9
75/25	15.1	0	0	5.4

Table 4.17 Hansen solubility parameters (HSP) values and distance between the HSP of the IHD/OA oil blends and silicone membranes MPa^{1/2}

% IHD/OA	δ_D	δ_P	δ_H	Distance
25/75	15.7	2.1	4.7	3.4
50/50	15.4	1.4	3.1	3.7
75/25	15.0	0.7	1.6	4.6

Table 4.18 Hansen solubility parameters (HSP) values and distance between the HSP of the HD/OA oil blends and silicone membranes MPa^{1/2}

% HD/OA	δ_D	δ_P	δ_H	Distance
25/75	16.1	2.1	4.7	2.9
50/50	16.2	1.4	3.1	2.3
75/25	16.2	0.7	1.6	2.9

Table 4.19 Hansen solubility parameters (HSP) values and distance between the HSP of the IPM/OA oil blends and silicone membranes MPa^{1/2}

% IPM/OA	δ_D	δ_P	δ_H	Distance
25/75	16.0	2.6	5.3	3.4
50/50	16.0	2.5	4.5	2.8
75/25	16.0	2.3	3.8	2.3

Table 4.20 Hansen solubility parameters (HSP) values and distance between the HSP of the IHD/LP oil blends and silicone membranes MPa^{1/2}

% IHD/LP	δ_D	δ_P	δ_H	Distance
25/75	15.8	1.4	2.8	3.0
50/50	15.4	0.9	1.9	3.9
75/25	15.1	0.5	0.9	4.9

Table 4.21 Hansen solubility parameters (HSP) values and distance between the HSP of the HD/LP oil blends and silicone membranes MPa^{1/2}

% HD/LP	δ_D	δ_P	δ_H	Distance
25/75	16.2	1.4	2.8	2.3
50/50	16.2	0.9	1.9	2.7
75/25	16.3	0.5	0.9	3.3

Table 4.22 Hansen solubility parameters (HSP) values and distance between the HSP of the IPM/LP oil blends and silicone membranes MPa^{1/2}

% IPM/LP	δ_D	δ_P	δ_H	Distance
25/75	16.1	1.9	3.5	2.3
50/50	16.1	2.0	3.2	2.2
75/25	16.0	2.0	3.0	2.2

4.5 Discussion

Stratum corneum comprises a complex molecular and supramolecular structure composed primarily of a mixture of lipids and proteins (Section 1.2.2). The extent to which a vehicle is sorbed and interacts with these structures, can affect the penetration kinetics of any topically applied drug. However (due to the complex number and diverse nature of types of interactions possible between vehicles, stratum corneum and drug), the interpretation of transcutaneous diffusion data with a view to identifying the key factors affecting these interactions is not simple. The use of simpler membranes, with distinctive properties such as silicone, polyethylene and polyurethane membranes might provide one means of identifying some of the prime parameters controlling the overall transport process through the markedly more complex stratum corneum. The permeation process consists of initial partition of the solute into, and then diffusion through, the polymer matrix (Roberts & Anderson, 1975; Roberts & Horlock, 1978; Jiang et al., 1998). Silicone membranes are extensively used to characterize interaction and drug transport processes because of: their ease of preparation (Most, 1970), hydrophobic character and the relatively high diffusivities of drugs through the core matrix (Most, 1970; Flynn et al., 1971). Silicone membranes have been used extensively to study the influence of topical and transdermal formulation components on solute transport (Scott, 1986; Nakano & Patel, 1970; Pellett et al., 1997; Twist & Zatz, 1990; Schwarb et al., 1999; Iervolino et al., 2001; Geinoz et al., 2002; Dias et al., 2007a ; McAuley et al., 2009; Watkinson et al., 2009 a&b; Wasdo et al., 2009; Sloan et al., 2013), despite their failure in providing an analogous model for the complexity of the stratum corneum (Hatanaka et al., 1992; Cronin et al., 1998; Moss et al., 2006).

It is well established that transdermal drug absorption is influenced by the vehicle in which the applied drug is incorporated (Twist & Zatz, 1986; Cross et al., 2001). One commonly used method to improve the absorption of a drug molecule across the skin is to formulate the active agent in an appropriate vehicle which could enhance the former's permeation. There is a large range of vehicles which have the capacity to fulfill this function including alcohols, esters and fatty acids (Friend, 1991; Friend et al., 1991; Liu et al., 1991; Ogiso et al., 1995; Oh et al., 1998; Gorukanti et al., 1999 ;

Takahash et al., 2002; Brinkmann & Muller-Goymann, 2003; Artusi et al., 2004; Hadgraft, 2004; Brinkmann & Muller-Goymann, 2005; Liu et al., 2009; Watkinson et al., 2009 a&b; Williams & Barry, 2012; Lane, 2013). The drug solubility in the formulation and its partition coefficient between formulation and epidermis are factors that affect the diffusion of drug from the vehicle and the subsequent sorption of the drug by the skin. In addition some of the formulation components can interact with the skin to modify the delivery of drugs to the stratum corneum, epidermis or beyond (Cross et al., 2001). The greater the degree of interaction of the vehicle with the stratum corneum then the greater is the potential of that vehicle to alter the physicochemical properties of the membrane matrix. This could occur due to modification of the packing of the constituent lipids and protein, leading to a modified permeation of any concomitantly administered topical agent through the membrane due to the modified diffusivity and partitioning of the drug in the altered membrane. However in some cases when the drug solubility is low, the solvent might permeate into the skin leaving the drug on the surface. Therefore an understanding of the interaction of vehicles or mixture of vehicles with the membranes might be expected to assist in the optimization of the design of a topical formulation.

The uptake of different oils by the silicone, HDPE, PU and cellulose acetate nitrate membranes was studied by monitoring the change in weight of the membranes after immersion in oil. The gravimetric method, although simple, has been shown by many other workers to yield reliable results (Aithal & Aminabhavi, 1990; Dias et al., 2007; Oliveira et al., 2011). The membranes selected in this study have a range of solubility parameters 17.4-28.6 (MPa)^{1/2} and the oils, which by definition are hydrophobic in nature, have solubility parameters in the range of 14.5-17.4 (MPa)^{1/2}. The order of interaction with the silicone on the basis of swelling parameters was IHD>IPM>HD>LP>OA. While for HDPE it was IHD>LP≥OA≥HD>IPM, the order of interaction with PU was OA>IPM>IHD≥HD≥LP and the order of uptake into cellulose acetate nitrate was IPM>IHD>HD>OA≥LP. These results indicate that membranes interact with oils differently depending on the properties of both the membrane and oil. The uptake of the buffer by the membranes was in the order of cellulose acetate nitrate>HDPE>PU>silicone. The buffer is much more hydrophilic

than any of the oils and might be expected to have a solubility parameter close to that of water $48 \text{ (MPa)}^{1/2}$ which is markedly higher than the oils. It thus showed a greater affinity for the more hydrophilic cellulose acetate nitrate membrane but induced no swelling in the silicone membrane and relatively little swelling in the PU and HDPE membranes. The amount of different oils sorbed into cellulose acetate nitrate was possibly as a consequence of the porous structure of the membrane's polymer matrix, since the originally open pores of the membrane are likely to fill with oil, contributing to the overall weight increase of the membrane.

The transport process of drugs and oils (if interaction occurs) can be rationalised by considering diffusion in terms of a net jump of a permeant occurring when an adjacent "hole" large enough to accommodate it exists in the polymer matrix (Aminabhavi & Khinnavar, 1993). The molecular size of a permeant is expressed in terms of molar volume (Table 4.2), which can only be described as an average value due to changing bond angles, rotations and chain conformations. To describe the vehicle properties the size, shape, HSP values and total solubility parameter and relative interactions (with itself and with the polymer matrix) should be taken into account. The solubility parameter is directly proportional to the extent to which a material coheres to itself upon vaporization. Based upon the familiar rule of "like-dissolves-like", the solubility parameter of the vehicle and membrane should match in order to enhance the compatibility between them. Accordingly swelling might be expected to be a maximum when the difference between the solubility parameter of membrane and the solubility parameter of vehicle is zero.

A Hansen plot for the HDPE membrane and oils (Figure 4.19) showed that the membrane has a small radius compared with the other membranes, and all the oils were located outside the sphere. Such a small radius lowers the chances of finding a good solvent for the membrane. This is also confirmed by the high RED values and the large distance between the HSP values of the solvents and membrane. Therefore generally only small amounts of the oils were taken up by the HDPE membrane when compared with silicone membrane. Nevertheless, IHD was sorbed in the highest amounts by HDPE membrane, whilst IPM was sorbed in the lowest quantity. This occurred despite IHD having the highest RED value and distance from the HSP

of the membrane, its greater uptake might be due to physicochemical factors including molecular shape, flexibility, volume and homogeneity of polarity. OA shape and high molecular volume hinders its sorption into the HDPE membrane. LP is a viscous mixture of different hydrocarbons; comprising linear and branched alkanes and a small amount of naphthenes (consisted of alkyl-substituted cyclo-alkanes) (European food safety authority, 2012). It may also include minor amounts of nitrogen- and sulphur-containing compounds. Within each of these classes of hydrocarbon compounds, there are enormous numbers of individual components, which will each partition with varying degrees of affinity depending upon their specific molecular structures. The distance between the HSP values of LP and the membranes is similar to the distance of IPM; however the size and viscosity of LP might hinder its uptake into different membranes. The distance between the HSP of HDPE and HD is the smaller than the distance between the membrane and IHD. HD, therefore, was expected to be taken up in greater quantities than IHD since both molecules possess the same molecular size. However it would appear that the sphericity in structure of IHD compared with HD promotes the sorption by the membrane of the former to a greater extent than the latter. These results show that the HSP indicates if there is a tendency of sorption, but other molecular properties may dictate the extent to which this actually occurs. HDPE membrane is comprised of hydrocarbons with a low degree of branching. The absence of branching in a closely packed structure, being formed with a higher density leads to somewhat high stability and excellent chemical resistance (Harper, 2002; Berins 1991). The differences in membrane structure are most likely to contribute to the significant differences between the amounts of oil sorbed by silicone and HDPE membranes.

PU is a relatively hydrophilic, non-porous, membrane; it has a solubility parameter of $20.84 \text{ (MPa)}^{1/2}$. Despite the PU membrane possessing a comparatively large Hansen Solubility sphere (with a radius of $8 \text{ MPa}^{1/2}$), the oils (with the exception of OA) did not lie within the sphere (Figure 4.20). As indicated above, an increased interaction between vehicle and membrane might be expected to occur for any membrane structure where the solubility parameter of the vehicle approaches the solubility parameter of the membrane. Being a comparatively (to silicone and HDPE) hydrophilic membrane so the distance between the HSP values of the oils

and PU was high. Accordingly the affinity of the oils for PU membrane was, perhaps, predictably low with the amounts of most oils sorbed being small. However as can be seen from Figure 4.20 the position and colour of the symbols relating to the oils, indicate that the latter still possess some degree of solvency power on the membrane. IPM contains a free ester group within its structure that might have the potential to interact with and might even ‘dissolve’ the PU membrane. HD, IHD and LP, in contrast, are hydrocarbons and therefore the aliphatic nature of these latter oils might only be expected to lead to the involvement of van der Waals and dispersion forces between oil and membrane. This lowers the chances of a strong interaction between vehicle and solid matrix. However the amount of IPM sorbed into the membrane is still very low (compared with other membranes), in agreement with the differences between its solubility parameter and that of the membrane, as compared to the differences in the solubility parameter value of IPM and those for other membranes. OA in contrast to the other oils was located inside the Hansen solubility sphere and displayed the lowest HSP distance. Consequently, it was associated with polymer chain dissolution-type interactions with PU membrane, behaving as an effective plasticizer of the membrane and indeed changed the properties and shape of the latter. As a consequence of this plasticization, a large increase in weight of the membrane was recorded when it was soaked in OA (this corresponded to an increase of around 885.8 mg. g⁻¹ of membrane).

Silicone membrane is cross-linked in structure, and it is likely that the weight gain observed following equilibration with a specific oil is more associated with chain solvation and subsequent membrane swelling interactions rather than polymer dissolution which can occur with non-cross-lined barriers. Figure 4.18 shows the Hansen sphere for silicone membrane and the oils. All the oils are located inside the sphere. This indicated that all the oils can be considered good solvents for this polymer. Therefore since there were differences in the amounts of oil uptake then other factors must also affect the extent and degree of interaction with silicone membrane such as the molecular size, shape and the HSP distance of the different oils.

IPM and OA have similar molecular weights (270 g/mol and 282 g/mol respectively) and molecular volume (315 and 319.5 respectively), but the effect of each on the hydrophobic membranes was different. Almost three times as much IPM was sorbed to silicone membrane than OA, thus the differences in sorption could not be attributed to the differences in molecular weight. The HSP distance for IPM was lower than that for OA. This suggests that both the distance and the molecular nature (e.g. shape, polarity, molecular flexibility) are also key factors affecting the interactions between the solvent and the membrane. For example, the low interaction of OA with the membrane may be related to its molecular shape since oleic acid contains a *cis* double bond which provides OA with a 'kinked' structure (Green et al., 1988). Such molecular geometry will lead to a less flexible molecule which requires a greater expenditure of energy to penetrate into the membrane. The presence of carboxylic acid group in oleic acid may also contribute to the decreased uptake of this oil by the silicone membrane (Cross et al., 2001). The $-\text{COOH}$ group will increase the polarity of the oil and this moderate polarity would be anticipated to decrease its uptake by the silicone membrane (Lee et al., 2003).

The lower the HSP distance value, the more alike the polymer and solvent, therefore the vehicle that has similar partial components to the partial components of the membrane might be expected to induce the greatest swelling of the membrane. The values for solubility parameters reported previously for IPM were for the Hildebrand (or total) solubility parameter. The previously reported values for IPM are $17.2 (\text{MPa})^{1/2}$ (Dias et al., 2007), $16.4 (\text{MPa})^{1/2}$ (Cross et al., 2001) and $16.8 (\text{MPa})^{1/2}$ (Oliveira et al., 2012). The values reported for silicone membrane are: $15.3 (\text{MPa})^{1/2}$ (Most, 1972; Liron et al., 1984; Cross et al., 2001) and $16.4 (\text{MPa})^{1/2}$ (Dias et al., 2007). Comparing the Hildebrand solubility parameter of OA and IPM (Table 4.2) to the Hildebrand solubility parameter of silicone membrane shows that the solubility parameter value for OA is closer to the value of the membrane than the corresponding value for IPM. Hence the preferential uptake of IPM compared with OA is hypothesized to derive from the distance between partial HSP components and not the total solubility parameter. Therefore the HSP values and distance between the Hansen solubility sphere values oils and membranes should both be taken into account. It can be concluded therefore, that the HSP distance, combined with the

shape, polarity and other physicochemical properties of OA most likely explain these observed differences in IPM and OA uptake by the membrane. The results of this study confirmed the findings of an earlier study (Dias et al., 2007a), when it was also reported that OA was taken up in lower amounts than IPM by silicone membrane..

IHD was the oil that was taken up in greatest quantity by the silicone membrane, an amount that was significantly higher than all the other oils studied. HD has the same molecular formula as IHD but in contrast to the latter comprises a linear hydrocarbon structure. The solubility parameter of HD is higher than the solubility parameter of IHD but since both oils are hydrocarbons, they interact almost entirely through dispersion forces. The magnitude of the dispersion forces is related to the surface area of the molecule; the larger the molecule, the greater the number of temporary dipoles, and the greater the intermolecular attractions. Molecules with straight chains contain more surface area, and thus greater dispersion forces, than branched-chain molecules of the same molecular weight.

Despite both oils having the same molecular size, the molecular shape of IHD is almost spherical, while the shape generated by HD is oval (Table 4.2). Both oils are inside the Hansen sphere which means both oils are good solvents for the membrane. In spite of this occurrence, the RED value and the HSP distance of HD are lower than IHD value, although IHD was sorbed in greater amounts than HD. Indeed, the amount of IHD that was sorbed by the silicone membrane was more than twice that of HD (Table 4.4). In addition, IHD uptake by other membranes was in most cases significantly higher than HD (Table 4.5). This suggests that again the chemical structure and shape of the vehicle might be of relevance to the degree of swelling. Silicone membrane is polydimethylsiloxane which itself comprises branched chain molecules. Cross-linked polymers generally are less compact than their linear counterparts and small spaces will exist between the polymer chains. Thus the branched structure of IHD along with its compact spherical shape could enable a greater partitioning of the oil into the space between the branched cross-linked membrane structure. If this occurs in stratified membranes composed of non-covalently linked molecules then this could affect the packing of those membranes.

All other oils had smaller RED values and HSP distances, when compared with that of IHD.

The kinetic study which was aimed at determining the vehicle interaction with silicone membrane indicated that the swelling of the silicone membrane in all oils was complete after the first hour of soaking. There was no significant difference in either the measured thicknesses of the membrane between 1 and 24 h of immersion. Therefore the thickness of the membrane was not expected to be changed after the first hour of the diffusion study.

Binary mixtures of some vehicles have been reported previously to offer synergistic effects in terms of leading to higher epidermal drug transport and reduced skin irritation (Cooper et al., 1985; Catz & Friend, 1990). If binary formulations exhibit a pure additive effect of the composite vehicles, a good correlation between the ratio of vehicles and the effect on the permeation of drugs through the membrane should be apparent. However this has not proved to be the case for a number of transdermal formulations (Karande et al., 2006). It has been shown previously that permeation of a molecule through a barrier membrane can (and does) occur independently of permeation of a co-applied molecule (Dias et al., 2001; McAuley et al., 2009). However, this has not been shown in the case of co-administered oils nor to differentiate between other co-applied vehicle components. When two oils are mixed and applied to a membrane, it has not been established whether the oils are sorbed in the same ratio as that in the applied solution. Different oily vehicles were blended together and the amount of swelling was measured by weight increase and then subsequently the partitioned oils were extracted and quantified by gas chromatography. All of the studied oil blends exhibited total miscibility with each other. The results presented in Figures 4.4 - 4.6 show the percentage amount of oil absorbed by silicone membrane from different oil blends.

There was no significant difference in the total weight of oil sorbed when IHD was blended with either IPM or HD (Figure 4.4). However when the partitioned oil was extracted there was a significant difference between the relative amount of IHD absorbed compared with HD (Figure 4.8). IHD was absorbed into the silicone

membrane in a greater proportion than the ratio present in the original applied blend. In contrast the ratio of IHD/IPM sorbed from different ratios of the two oils was the same as that in the applied vehicle. The amounts of IPM and IHD extracted from the membrane were superimposable and correlated linearly with the amounts of each in the original solution (Figure 4.7). Similar results were obtained for HD/IPM blends (Figure 4.11). IPM displayed a lower HSP distance value compared to that of HD relative to silicone membrane. On the other hand HD displays a smaller molecular size than IPM (Table 4.2). All these factors might be expected to affect the solvent uptake and the swelling of the silicone membrane; nevertheless both oils were sorbed in similar amounts. Koszinowski (1986) studied the diffusion behaviour of linear alkanes, linear alcohols and substituted phenols in polyolefins. The results showed that as the number of carbon atoms increased, both the alcohols and phenols approached the behaviour of the alkanes as a consequence of the increased shielding of the –OH group. This is due the high degree of rotational freedom about the carbon–carbon bond of the longer chains, leading to chains folding back upon themselves, as a consequence of intramolecular interactions through the flexible methylene groups composing the carbon chain. These methylene moieties are able to form ‘ring’ structures with an adjacent moiety on the molecule (ester group) (Nisbet, 1977; Forster et al., 1991), whilst still retaining the linear structure. IPM could be behaving in the same way. IPM comprises a molecule containing a polar ester head group at the end of a relatively long hydrocarbon chain. As the number of carbon atoms is increased, the polarity is “diluted” by the presence of a longer hydrophobic tail, and this in turn leads to a lowering of the solubility parameter of any long ester. When blending IPM with HD or IHD, the partition behaviour of the blends into a silicone membrane was the same, indicative of the weak specific interactions between silicone membrane and the ester group of IPM. The long alkyl chain attached to the ester group dominates the overall size and shape of the molecule and diffusion occurs preferentially along the direction of greatest length of the molecule.

Blends of OA with IHD, HD or IPM, showed that there were resultant significant differences in the amounts and the ratios of oleic acid sorbed to the membrane (compared to that present in the original applied blended oil). IHD appeared to be sorbed preferentially in comparison to both IPM and HD (in descending order) from

blends of each with OA. From the values determined using the HSPIP software, OA has a solubility parameter ($17.4 \text{ MPa}^{1/2}$) that is similar to that of silicone membrane ($17.4 \text{ MPa}^{1/2}$). OA and HD display similar distance value relative to silicone membrane which is lower than the distance between IHD and silicone membrane. Therefore although OA might have been expected to be taken up into the silicone membrane in greatest quantity, it was in fact the less preferentially sorbed oil from the different blends. This is likely to be a consequence of both the higher molecular weight of OA in comparison to other oils as well as its larger molecular shape, discussed above. It has been reported that OA in conjunction with a polar solvents such as propylene glycol has been shown to be a more potent penetration enhancer (Mahjour et al., 1989; Larrucea et al., 2001). The proposed explanation for this synergistic effect was the facilitated incorporation of OA into the stratum corneum lipid alkyl domains by the interaction of propylene glycol with the polar head groups (Oh et al., 1998). It was also reported that short chained fatty acids were able to disrupt lipids when applied in a lipophilic mineral oil-based formulation, while the uptake of long chained fatty acids, such as OA were enhanced when applied with hydrophilic, polar solvents such as propylene glycol (Wang et al., 2004). In this study blending IHD with OA enhanced the uptake of OA into the membrane. IHD swelled the silicone membrane and this affected the packing of the cross-linked polymer chains, which might allow chain extension resulting in extra free volume, and facilitate OA uptake. This enhancement did not occur to the same extent as with HD or IPM blends with OA. Blending OA with HD, IPM and IHD produced the same trends where the amount of OA taken up by the membrane did not change between 50 and 75% (Tables 4. 7 - 4.9).

Blending LP with IHD, HD and IPM, led to an increase in the total amount of oil sorbed by the silicone membrane and this amount was larger as the ratio of the IPM, HD and IHD present in the blend increased (Figures 4.4 - 4.6). The amount of oil sorbed by silicone membrane of both oils was the highest when LP was blended with IHD and lowest when blended with HD. The results of GC analysis after oil extraction show that the amount of IHD and IPM extracted was significantly greater than the amount of LP (Figures 4.9 and 4.12). The solubility parameter of LP is $14.5 \text{ (MPa)}^{1/2}$, which is close to the solubility parameter of IHD $14.7 \text{ (MPa)}^{1/2}$. Light liquid

paraffin consists of a mixture of alkanes, the latter comprising single-bonded carbon and hydrogen atoms, which renders them relatively inert to interacting with matrices. HD and IHD are present in small amounts as natural components of LP. It has been reported that the paraffinic hydrocarbon mixture consist of 87.9 w/w% normal alkanes and 12.1 w/w% isoalkanes from C₁₀ to C₂₅ (Postnov, 1972). The amount of LP sorbed by the membrane is low compared with the IPM, HD and IHD, possibly due in part to the content of molecules having a high molecular weight and a high molecular volume; the higher molecular volume decreases the ability of the oil to be sorbed into the membrane. IPM and IHD were preferentially taken up by silicone membrane since they are smaller in size and have a higher affinity to the membrane. LP viscosity is around 30 mPas, whilst the viscosities of IPM, HD and IHD viscosities are 5 mPas at 20°C, 3.34 mPas at 25°C and 5.2 mPas at 20°C respectively. The higher viscosity of LP may also reduce its tendency to be sorbed into silicone membrane as a consequence of the lower diffusion coefficient of viscous liquids. The percentage of oil sorbed by silicone membrane when soaked in HD/LP was lower compared with IHD and IPM blends (Figures 4.4 - 4.6). When the oil was extracted there was no significant difference in the ratio of HD and LP sorbed in comparison to the ratio present in the applied oil (Figure 4.14). Hence both the total amount of oil sorbed was low, and the affinity of the hydrocarbons in the LP mixture to the membrane appears to be comparable with that of HD affinity to silicone membrane.

In diffusion studies the silicone membrane was soaked in buffer overnight, then it was sandwiched between the donor and receptor chamber of the Franz cell. Oily vehicles were introduced into the donor compartment, whilst the receptor contained phosphate buffer. In order to determine the ratio of the oil remaining in the donor compartment under such conditions, blends of HD/IHD were added to the donor compartment and a sample of the applied and remaining oils in the donor compartment were analysed. HD/IHD blends were employed since both oils have close physicochemical characteristics and the ratio of the two oils sorbed by silicone membrane from the blends was found to be significantly different in the uptake studies, to that present originally in the solution applied to the membrane. Also both oils could be readily detected and quantified by gas chromatography analysis, rather

than the method being dependent upon a gravimetric analytical factor (as with some oils). The results show that the composition of the oil has changed. IHD was sorbed to greater extent compared with HD over a period of six hours therefore altering the original weight ratio. These results were comparable to those obtained in the silicone membrane uptake studies. These results indicated that since one vehicle was preferably sorbed compared to the other from this particular blended vehicle, then the thermodynamic activity of any applied drug in that vehicle would also be likely to be changed as a function of time. It would be either enhanced or reduced, depending on the drug solubility in the two vehicles and the amount of vehicle sorbed by the membrane. In addition the nature of the membrane might also change and possibly present an environment in which the agent is more soluble – promoting the potential uptake into the membrane, alternatively if the oil that is preferentially absorbed is one in which the agent is less soluble then uptake may be reduced. Karande et al. (2006) studied the effect of pure penetration enhancers and mixtures on the skin's barrier properties and concluded that a random combination of two penetration enhancers was not necessarily more effective at enhancing transport than the individual components. The results of the current study indicate that this might be due to the preferential uptake of one penetration enhancer into the membrane compared to the other. Also fatty acids were found to produce a significantly lower enhancement ratio compared to many other categories of 'enhancer' (Karande et al., 2006). Herein, OA was often found to be the oil sorbed into the membrane in lowest amounts.

In order to assess the effect of oils on silicone membrane, the membrane was soaked in LP, HD and IHD and the diffusion of MP from buffer across such membranes was studied. These three oils were selected for study since they were sorbed into the membrane in different ratios from oil binary blends. However the three oils have similar solubility parameters, and physicochemical characteristics, but comprise hydrocarbons that differ in the shape. MP was selected because it has moderate hydrophilic/hydrophobic characteristics with an intermediate partition coefficient and exhibits relatively high diffusivity through silicone membranes (Twist & Zatz, 1986; Romonchuk & Bunge, 2006; Oliveira et al., 2012 a&b). Therefore any pre-treatment solution that increased the MP permeation is likely to modify the

permeation of other compounds (Nanayakkara et al., 2005). The pre-treatment of the silicone membrane with any of the oils was found to increase MP flux from all oils in comparison with the use of buffer (Table 4.10). The amount of oil sorption into silicone membrane correlated well with the enhancement ratio, the order of enhancement being IHD>HD>LP. The highest enhancement of IHD might be due to its higher sorption and presumably more favourable interactions with silicone membrane, leading perhaps to a greater disruption of its barrier properties. It might also by its presence in the membrane enhance the partition of MP into the oil-containing matrix of the membrane. It can be concluded from the results that as the amount of oil sorbed into silicone membrane increases, the diffusion of the applied drug was promoted. Since the solubility of MP in the oils, and the physicochemical properties of HD and IHD are the similar, it appears that the branching of IHD and the spherical shape of the molecule produce a positive enhancement in the uptake and subsequently on the penetration of MP. Figure 4.17 shows that the cumulative amount of MP that penetrated the silicone membrane was highest when the membrane was pretreated with IHD. This indicates that the membrane properties have been changed and silicone membrane diffusional resistance might have changed. Therefore as the degree of solvent uptake increases the diffusional behaviour of the membrane will change, depending on the membrane and sorbed solvent properties.

In conclusion this study has shown that oils interact with membranes to different extents depending on the molecular size, shape and structure. The results also suggest that the Hansen solubility parameter values and distance are factors that may require consideration when studying the membrane interaction with different vehicles. It would appear that oils that are highly sorbed by membrane might either affect the packing of the membrane or provide a modified matrix into which a drug might more favourably partition, thereby influencing drug permeation.

CHAPTER FIVE

***MULTIVARIATE ANALYSIS OF VEHICLE UPTAKE BY
MEMBRANES AND PERMEATION DATA***

5.1 Introduction

Recently there has been much interest in computer models to investigate the relationship between the structure of a molecule and its dermal penetration (Mitragotri et al., 2011; Chen et al., 2013; Hathout, 2014). Molecular permeation across the epidermis has previously been demonstrated to be determined by a number of physicochemical properties, for example, the lipophilicity, molecular weight and hydrogen bonding ability of the permeant. In the current work it has also been shown that interactions between the membrane and some oily vehicles (previously unreported to modify membrane barriers) can occur. Therefore there are several physicochemical parameters that may determine the rate and degree of permeation of any compound formulated within a topical vehicle across a membrane. As such it is likely that permeant, vehicle and membrane descriptors will be integral components of any model that seeks to understand the significant factors that influence the process of membrane permeation. Should it be possible to identify a correlation between the chemical structures and physicochemical properties of vehicles and permeant to membrane penetration it might be possible to define the desirable features of both compound and vehicle that might promote transport. This would enable a better approach to formulation and lead to a reduction in the amount of screening, involving *in vitro* and *in vivo* testing, that is currently required to identify suitable topical agents and vehicles.

5.1.1 Multivariate analysis

Multivariate data analysis can be defined as: '*the investigation of many variables simultaneously, in order to understand the relationships that may exist between them*'. A univariate approach only provides part of the overall picture. For example an examination of the mean with standard deviation describes one variable, but provides no information on how that one variable is related to the others. Therefore a univariate approach provides an over-simplistic assessment of the data. Moreover it fails to detect any relationship that may exist between the

variables being studied because it treats all such variables as being independent of each other (Rencher, 2002). This latter phenomenon is known as covariance or correlation and it forms a central theme in multivariate analysis. The term covariance is a measure of the joint variance of two variables and it describes the influence that one variable has on other variables. Multivariate data analysis can be classified into three main areas (Wold & Sjostrom, 1998):

- *Exploratory data analysis*: sometimes this is termed ‘data mining’. Such action is useful for gaining deeper insights into large complex data sets. It enables any hidden structure which results from the influence of all variables acting together to be extracted. This will show the data-specific patterns or groups and such patterns enable new data to be classified into similar groups.
- *Regression analysis*: is the process of developing a model from the relationship between the variables in the available data to predict response. These models can be used later to predict a new and future event.
- *Classification*: is the separation (or sorting) of a group of objects into one or more classes based on distinctive features. This could be used to separate the objects according to their behaviour or composition.

5.1.2 Quantitative structure property relationships

The *in vitro* and *in vivo* experimental measurement of skin permeability is a difficult and complex process, due in part to ethical difficulties with respect to human and animal experimentation. In addition, there are a high number of chemicals that come in contact with the skin; also it is costly and time consuming. There are also difficulties in obtaining excised human skin, which is the best membrane to use for *in vitro* measurements. As a consequence, there has been a great interest over the past years to avoid unnecessary and costly *in vitro* testing

and develop models that would allow the formulation scientist to predict the ability of a compound to cross the skin using its physicochemical characteristics. A number of attempts have been made to develop quantitative structure–permeability relationship (QSPR) models based on the skin permeation of compounds derived from *in vitro* experiments, with skin permeability linearly correlated to the physicochemical properties and/or molecular structure parameters of the chemical compounds (Flynn, 1990; Potts & Guy, 1992; Wilschut et al., 1995; Pugh et al., 1996; Moss et al., 2002; Mitragotri, 2003; Yamashita & Hashida, 2003; Mitragotri et al., 2011). Such models have been used by environmental agencies for safety assessment of dermal exposure to industrial and environmental hazards, and also by pharmaceutical companies to screen and select drugs for possible transdermal delivery potential.

The physicochemical descriptors most employed in QSPR include hydrophobicity, molecular size or weight and hydrogen bonding. Such models are expected to be consistent with the transport mechanisms by which permeants traverse the skin barrier (Potts & Guy, 1992). For the development of QSPR models, a key feature is that all data must be consistent and reliable. Ideally all experiments should be performed under standardised conditions (i.e. employing the same skin type from the same anatomical region and constant laboratory conditions (such as temperature, concentration and receptor medium, for example)). However, practically this has not been the case, and therefore a limitation of QSPR models is that the data used in most QSPR models are derived from an extensive database from different investigators and laboratories using different experimental protocols. Controlled studies involving inter- and intra-laboratory measurement of the diffusion of MP across a synthetic membrane using a defined protocol produced a variability of 35% with a fourfold difference between the highest and lowest flux values (Chilcott et al., 2005). A much larger inter- and intra-subject variability in the skin permeation of exogenous materials has also been previously reported (Tsai et al., 2003). Accordingly nearly all QSPR models are inherently subject to experimental error (Moss et al., 2002).

Many of the developed QSPR models are based on a data base assembled by Flynn (1990). This comprised 97 human skin permeability coefficients for 94 compounds obtained *in vitro* through human skin, from 15 different literature sources. However other investigators have shown that Flynn's data set contains a high degree of experimental error resulting from combined inter- and intra-laboratory error as well as variation due to the skin being from different sources and locations on the body (Johnson et al., 1995; Abraham et al., 1997; Degim et al., 1998; Moss et al., 2002).

The main focus of the development of QSPRs has been with a view to assessing the permeability coefficient (K_p) of compounds untested either *in vitro* or *in vivo*. The K_p of a compound is the ratio of steady-state flux expressed as a function of the concentration of the test compound with units of m.s^{-1} (Wilkinson & Williams, 2002). K_p is therefore generally constant over a range of concentrations. In addition over time, a substantial database of experimentally determined K_p values from aqueous vehicles has built up, allowing theoretical predictions to be directly compared with real measurements (Mitragotri et al., 2011).

One of the most widely used empirical models is that developed by Potts and Guy (Equation 5.1), which predicts permeability coefficient (K_p) based on Log octanol water partition coefficient (Log K_{oct}) and molecular weight (Mwt) (Potts & Guy, 1992):

$$\text{Log } K_p = 6.3 + 0.71 \text{ Log } K_{\text{oct}} - 0.0061 \text{Mwt} \quad \text{Equation 5.1}$$

These workers studied more than 90 chemicals with MWs ranging from 18 to over 750 and Log K_{oct} values from -3 to $+6$ applied in different vehicles. The r^2 of the multiple regressions was 0.67 suggesting that approximately two thirds of the variability in the data was explained by the model. In Equation 5.1, the rate-limiting transport barrier of the skin is implicitly assigned to the lipophilic stratum

corneum and, as a result, the model can generate unfeasible values of K_p for compounds that are extremely lipophilic (Mitragotri et al., 2011).

Later, Potts and Guy attempted to describe the effects of descriptors for the solute hydrogen bond acidity ($\Sigma\alpha_2^H$) and the solute hydrogen bond basicity ($\Sigma\beta_2^H$) and the molecular volume (MV) on K_p (Potts & Guy, 1995):

$$\text{Log } K_p = 0.0256MV - 1.72 \Sigma\alpha_2^H - 3.93\Sigma\beta_2^H - 4.85 \quad \text{Equation 5.2}$$

These workers used 37 samples and the r^2 of the multiple regressions was 0.94 indicating an improved fit to the model.

Several QSPRs have been derived since the publication of Potts and Guy's model. However Moss et al. (2011) have shown that there were significant differences between permeability values measured experimentally and those determined using the Potts and Guy (and other QSPRs) equations. They showed that the greatest difference between experimental and predicted values was found at high Log K_{oct} values.

5.1.3 Principal component analysis

Principal component analysis (PCA) is a descriptive or exploratory technique for reducing the amount of dimensionality in complex data when there is a correlation between variables (Han et al., 2006; Reid & Spencer, 2009). PCA reduces the dimensionality by extracting the smallest number of components or factors that account for most of the variation in the original data, and summarizes the data with little loss of information. It is not a useful technique if the variables are uncorrelated (Miller & Miller, 2010). In addition, it aids in the visualization of the relationship and correlation among different variables; by graphing the variables in different groups or patterns and removing the noise (un-useful information) from the data (Abdi & Williams, 2010). This results in more easily interpretable

output which contains relevant information (Barcelo & Petrovic, 2011). PCA separates the data into principal components (PCs). Each principal component (PC) contributes to explaining the total variability in the observed results in a data set. However, the PCs are also chosen so that the first PC (PC1), accounts for most of the variation in the data set, the second (PC2), accounts for the next largest variation and so on (Wold, 1987). Hence, when a significant correlation occurs the number of useful PCs is much less than the number of original variables.

In mathematical terms the PCs are the eigenvectors of the covariance matrix and the technique for finding these eigenvectors is called eigenanalysis. Corresponding to each PC (i.e. eigenvector) is an eigenvalue, which gives the amount of variance in the data set that is explained by that specific PC. Therefore obtaining the PCs is entirely equivalent to finding the eigenvectors of the covariance matrix: each eigenvector generating one PC. The corresponding eigenvalue provides the variance of that PC, and the PCs with the largest variances are the most important (Miller & Miller, 2010). The PCs are derived by finding the projections which maximize the variance, with the first PC being the direction in feature space along which projections have the largest variance. The second PC is the direction which maximizes variance among all directions orthogonal to the first. The k^{th} component is the variance-maximizing direction orthogonal to the previous $k-1$ components.

PCA uses two graphical visualization tools that must be displayed together to map the co-variance structure in the data. These comprise a:

- scores plot: which provides a map of the samples, showing a summary of the relationship between the samples. Score plots can reveal patterns, such as clusters, trends and outliers in the data (Idborg-Björkman, 2003).

- loadings plot: which provides a map of the variables, showing a summary of the variables. It is useful for identifying the important variables. Loading plots reveal covariances among variables and can be used to interpret patterns observed in the score plot (Idborg-Björkman, 2003).

Applications of PCA have found widespread use in most stages of pharmaceutical research and industry. For example it has been used in distinguishing, quantifying and predicting the compression behavior of pure excipients and binary blends on tablet formation and properties (Haware et al., 2009). Other research workers have used PCA to gain a general overview of the relationship between four groups of excipients (filler, binder, disintegrant and lubricant) with respect to desirable tablet properties (i.e. good mechanical strength and short disintegration time) (Gabrielsson et al., 2000 & 2004). The effect of powder properties on the segregation tendency has also been studied using PCA (Xie et al., 2008). Other formulation scientists have used PCA analysis for characterizing the performance of nebulizers (Shi et al., 2009). In addition, it has been used to study the relative importance of certain structural characteristics in terms of their contribution to transdermal permeation (Ghafourian et al., 2010; Hathout, 2014). It has also been employed in connection with studies concerned with the: accumulation of essential oil in herbs (Shiyab et al., 2012); characterization of pharmaceutical solids (Laitinen et al., 2004; García-Muñoz & Carmody, 2010); investigation of drug and excipient content in pharmaceutical formulations (powders and tablets) (Sarraguça & Lopes, 2009); evaluation of dissolution profiles (Tsong et al., 1997; Adams et al., 2001, 2002; Maggio et al., 2008); the analysis and differentiation of polymorphic forms (Jorgensen et al., 2006; Kogermann et al., 2007, 2008; Maggio et al., 2009); and classification of drugs according to their mode of action (Yi et al., 2007).

5.1.4 Data pretreatment

Data for PCA and QSPR should be arranged into a table (matrix) in such a way that each row represents one sample and each column represents one measured variable (e.g. molecular size). The matrix is presented in two co-existing spaces, variable space and object space, which together contain all available data (Kvalheim, 1988). Subsequent to the analysis, constant descriptors are eliminated, since such descriptors cannot provide useful statistical information.

Also prior to analysis, data are often pre-treated, in order to transform the data into a form suitable for analysis. The first step of pretreatment is data scaling. Variables often have substantially different numerical ranges and a variable with a large range has a large variance, whereas a variable with a small range has a small variance. Unless the data are scaled, a variable with a large variance will dominate. The most common scaling technique employed is unit variance scaling. Unit variance scaling shrinks the long variables and stretches the short ones. Therefore no variable is allowed to dominate over another because of its length (Figure 5.1) (Eriksson et al., 2006). In some instances, if all the data are on the same scale, no scaling for the data is needed for example spectroscopic data.

The second part of data treatment is to effect ‘mean-centering’. In mean-centering the average value of each variable is calculated and subtracted from the data (Figure 5.2). The subtraction of the averages from the data corresponds to a repositioning of the system such that the average point is the origin (Geladi & Kowalski, 1986).

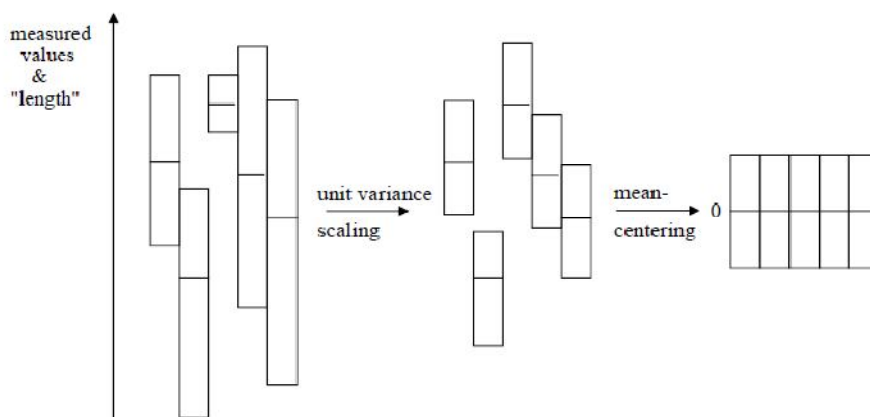


Figure 5.1 Data after mean-centering and unit variance scaling all variables will have equal length and mean value zero (Eriksson et al., 2006).

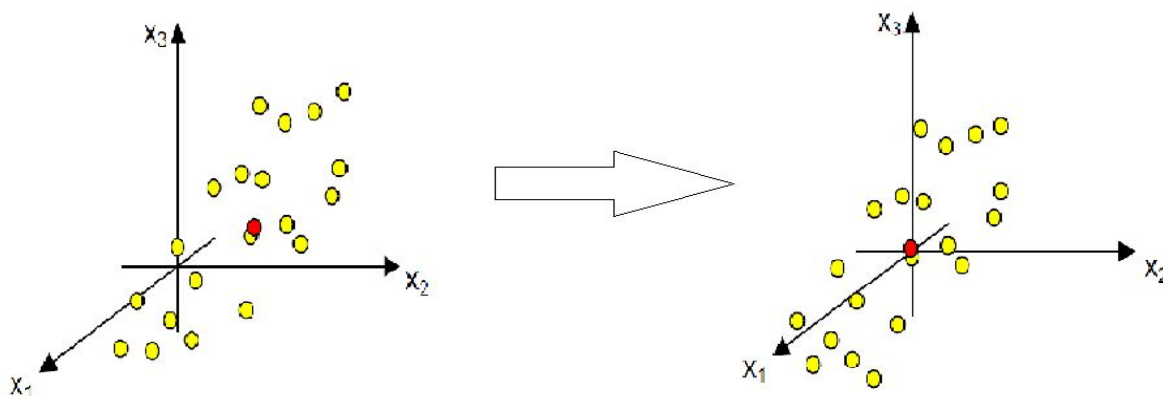


Figure 5.2 The mean-centering procedure corresponds to moving the origin of the co-ordinate system to coincide with the average point (Eriksson et al., 2006).

5.2 Aims and objectives

One important goal for the pharmaceutical industry is the identification of an appropriate vehicle which could enhance the diffusion of the administered drug. To reduce the risk, cost and workload, it is useful if a relationship between chemical/structural properties and diffusion parameters could be found. One approach to find this relation is the use of multivariate analysis. The application of multivariate analysis to data derived using synthetic membranes and relating the

analytical results to data obtained employing epidermis, may provide the knowledge to enhance dermal delivery, develop new therapeutic formulations, boost the cosmetic industry, whilst additionally lead to a reduction in toxicity and irritancy (caused by dermal exposure of chemical substances).

The permeability through skin is controlled by the properties of the permeant and the vehicles, which are related to the molecular descriptors of both. The chemical structure of a vehicle can determine the effect that it will have on the membranes or on the partitioning of the penetrant, leading to the observed changes in the skin penetration profile of the penetrant. Most previous models have largely concentrated on the chemical structure of the drug; they did not take into account the effect of vehicle or membrane on the diffusion process. The vehicle is as important as the drug itself, since it could enhance or retard the permeation of the administered drug. Therefore in this study the permeant, vehicle and membrane descriptors were all considered in the statistical analysis. The aim of this study was to seek to understand the influence of chemical/structural descriptors of permeants, oily vehicles and membranes on solvent uptake by the membrane, flux and permeability coefficient of the compounds through the membrane, and the lag time before diffusion of the compound can be detected.

In order to fulfill these aims the following objectives were identified:

- Detect the important descriptors of oily vehicles which enhance solvent uptake into membranes having different characteristics.
- Extract the main descriptors of the vehicles and permeants responsible for identifiable patterning of behaviour in the uptake or diffusion studies.
- Examine the range of descriptors for permeants, vehicles and membranes to determine if a statistical relationship exists between the properties of all three, and dermal absorption.

5.3 Methods

5.3.1 Materials:

Materials used in this study have been reported previously and are listed in Table 2.2.

5.3.2 Franz cells studies

The fluxes of the model permeants through synthetic membranes (silicone, HDPE and PU) and human epidermal sheets were assessed as described below.

5.3.2.1. Synthetic membranes

5.3.2.1.1 Diffusion through silicone membrane

The diffusion through silicone membrane was carried as described previously (Section 3.3.3.2).

5.3.2.1.2 Diffusion through high density polyethylene and polyurethane membranes

The diffusion of the model permeants from the suspensions was examined using HDPE and PU membranes. Each suspension was prepared by adding excess permeant to 6 g of oil and was incubated at 32°C in a shaker water bath overnight. Diffusion experiments were carried out using calibrated Franz cells with a receptor phase of 2 mL and a diffusional area of 0.65 cm². Before the experiment the membrane was immersed and soaked in the receptor media overnight. The membrane was cut into circular discs and placed between the donor and the receptor compartments of the Franz cell. The receptor compartment was carefully filled with phosphate buffer pH 7.0 and the cell placed on a stirring plate submerged in a water-bath maintained at 32°C. A small teflon-coated magnetic bar (about 5 mm length) was included in the receptor compartment such that

stirring occurred throughout the duration of the experiment. After allowing the membrane to equilibrate with the receptor fluid, 200 μL of the oily suspension (the sample contained undissolved/suspended solids of permeants at 32°C) of model permeant was then introduced into the donor chamber. At appropriate time intervals, 200 μL samples were withdrawn from the receptor compartment and immediately replaced with an equal volume of fresh phosphate buffer, (pH 7.0). The duration of the experiment was 7 h through HDPE and 6 h through PU. Each sample was analysed for permeant using the HPLC method described previously (Section 2.3.2). The concentration of the permeant in the receptor solution at any time point was corrected for previous sample removal. Each experiment was conducted five times.

The cumulative amounts (per unit surface area of membrane) of permeant which diffused across membrane were plotted against time (h). The slope of the linear plot was taken as the flux of permeant permeation.

5.3.2.2 Human epidermis

5.3.2.2.1 Preparation of epidermal sheets

The preparation of epidermal sheets was carried as described previously (section 2.3.5.2).

5.3.2.2.2 Diffusion through human epidermis

The permeation of MP, BP and CF from the oily vehicle and buffer pH 7.0 was determined using Franz cells. The receptor compartment was carefully filled with phosphate buffer, after which the receptor temperature was maintained at 32°C . The epidermal membrane was then allowed to equilibrate with the receptor fluid for 1 h, after which 200 μL of the oily suspension (as prepared in Section 5.3.2.1.2) was then introduced onto the stratum corneum (i.e. donor

compartment). At appropriate time intervals 200 μL of the receptor phase were withdrawn and immediately replaced by an equal volume of fresh receptor solution. The duration of the skin permeation experiments was 8 h for MP and BP and 10 h for CF. A minimum of four cells was used for each vehicle, and the permeant concentration of receptor samples was analysed by HPLC methods (Section 2.3.2).

The concentration of the permeant in the receptor solution at any time point was corrected for previous sample removal. The cumulative amount of permeant permeating per unit skin surface area was plotted as a function of time, and the slope of the linear portion of the plot was determined and taken as a measure of the average flux (between 4&8h for MP and BP, 4-10h for CF) (J , $\mu\text{g cm}^{-2} \text{h}^{-1}$). The permeability coefficient (K_p , $\text{cm}^{-2} \text{h}^{-1}$) for each solute was calculated as follows:

$$K_p = J_s / C_v \quad \text{Equation 5.3}$$

Where C_v is saturated solubility of the permeant in the applied vehicle.

5.3.3 Statistical analysis

Data reported in this study are usually the mean of $n \geq 3$ with the standard deviation (sd) given. In order to establish differences in the parameters measured then statistical analysis of the data was undertaken using either analysis of variance (ANOVA) or student's t- test, as appropriate. Post hoc comparisons of the means of individual groups after carrying out ANOVA were performed using Tukey's test. ANOVA and Post hoc Turkey's test were performed using SYSTAT version 5.0 (SYSTAT Software Inc., CA, USA), and the level of significance was taken at $p \leq 0.05$ in all cases.

QSPR models were generated using Microsoft Excel[®] software regression analysis. Data were evaluated by multivariate analysis PCA using The

Unscrambler[®] (CAMO Software, Oslo, Norway). The analysis was performed to identify both the most important factors that affect, and to quantify the influence on, the solvent uptake and diffusion of compounds through model membranes and human epidermis. An important factor in the strategy is to characterise the materials in terms of multiple variables. A separate PCA was calculated to identify patterns in the dependent variables due to the range of input descriptors for each of the following dependent variables: membrane solvent uptake, flux, K_p , lag time through synthetic membranes and flux through epidermis. In order to carry out the analysis, data were scaled and mean-centered using Microsoft Excel[®] software.

The correlation was performed on the following descriptors: solvent uptake into membranes and solubility of the permeant in the oil with various molecular descriptors, such as: δ_D , δ_P , δ_H , solubility parameter $\text{MPa}^{1/2}$, Mvol, Mwt, density, Mpoint, Log $K_{o/w}$, ovality, molecular connectivity index, weight, Log P, TPSA, vdw_vol, vdw_area, a_nH, a_nC, a_nO, b_1rotN, b_1rotR, b_count, b_double, b_rotN, b_rotR, b_single, lip_acc, lip_don, opr_brigid, opr_nrot, chi0, chi0_C, chi1, chi1_C, chi0v, chi0v_C, Kier1, Kier2, Kier3, Kier flex, balabanJ, Q_VSA_HYD_PEOE_VSA_HYD, being used. However some descriptors were eliminated from the analysis since they had the same value therefore they would not have any statistical contribution on the analysis. The descriptors eliminated were: b_ar, opr_nring, Q_VSA_POL_PEOE_VSA_POL, Q_VSA_FHYD_PEOE_VSA_FHYD, Q_VSA_FPOL_PEOE_VSA_FPOL). An account of the meaning of these abbreviated descriptors is given in Appendix I. The molecular descriptors used in PCA analysis were determined using Molecular Operating Environment 2012, produced by Chemical Computing Group Inc., Montreal, Canada, and by HSPiP software version 4.0.0.4. The solubility and solvent uptake were determined experimentally.

5.4 Results

5.4.1 Synthetic membranes diffusion studies

The cumulative amount of permeant diffused across the synthetic membranes was plotted versus time; and the flux was derived from the slope of the linear portion of the curve. Figure 5.3 shows an example of the cumulative amount of MP permeated across silicone, HDPE and PU from saturated solutions in IHD as a function of permeation time. The fluxes through the membranes from IHD were in the order silicone>PU>HDPE. The curve shows a typical lag time phase followed by a linear portion corresponding to the steady state flux. The shapes of the cumulative amount of BP and CF against time were similar to MP.

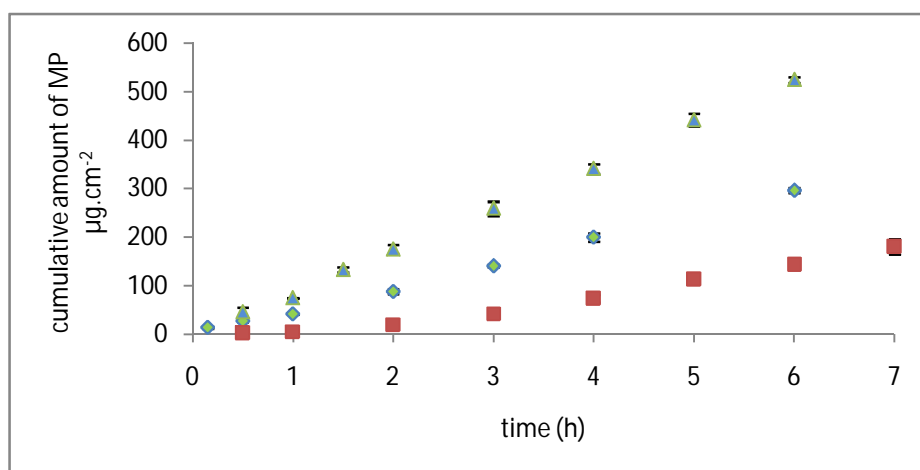


Figure 5.3 An example of the cumulative amount of methyl paraben permeated across ▲silicone, ■high density polyethylene and ◆poly urethane membranes versus time when applied in IHD. Data represent mean \pm sd ($n=3-5$). Error bars lie within the symbols.

The derived flux results of the *in vitro* diffusion studies of the three model permeants across different membranes are shown in Figures 5.4 and 5.5 for MP

and BP respectively and 5.6 and 5.7 for CF, due to scaling issues CF results are shown in two figures. The highest measured fluxes of BP from oils were obtained for diffusion of the compound through silicone membrane. In contrast, the highest fluxes recorded for MP and CF were those obtained for its diffusion through PU. There was no significant difference between the fluxes of MP from either LP or buffer through silicone membrane. All oils enhanced the permeation of MP through HDPE compared with buffer. The fluxes of MP from LP and OA through HDPE were not significantly different from each other (Figure 5.4), and although low in magnitude, flux of MP from both was higher than from buffer. All oils enhanced BP permeation through silicone and HDPE membranes compared with the buffer. However, with PU, the flux of BP from the buffer was higher than its flux from OA (Figure 5.5). There were no significant differences in the fluxes of CF from OA, LP and buffer through silicone membrane. In addition, there were no differences in the fluxes of CF from either OA or HD through HDPE. Generally all oily vehicles enhanced the permeation of CF through HDPE membrane compared with the buffer (Figure 5.6). However the flux of CF from saturated buffer solutions was higher than from oily solutions through PU membrane (Figure 5.7).

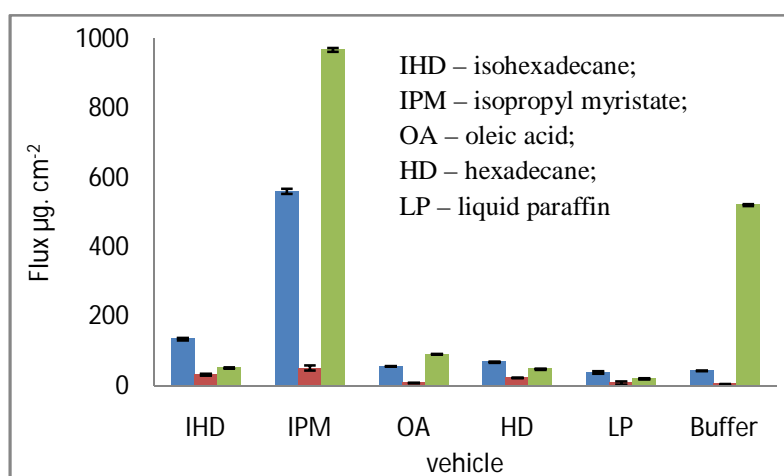


Figure 5.4 Comparative flux data for methyl paraben across ■ silicone, ■ high density polyethylene and ■ polyurethane membranes when applied in different oils and phosphate buffer. Data represent mean \pm sd ($n=3-5$).

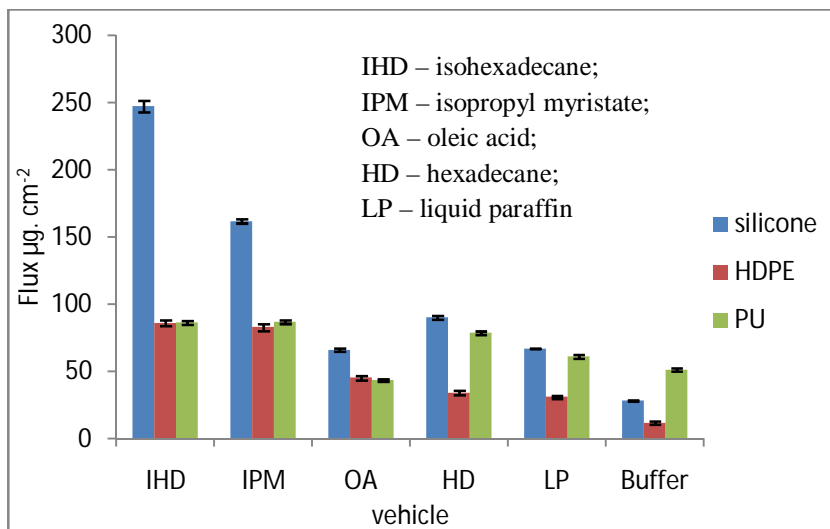


Figure 5.5 Comparative flux data for butyl paraben across ■ silicone, ■ high density polyethylene and ■ polyurethane membranes when applied in different oils and phosphate buffer. Data represent mean \pm sd (n=3-5).

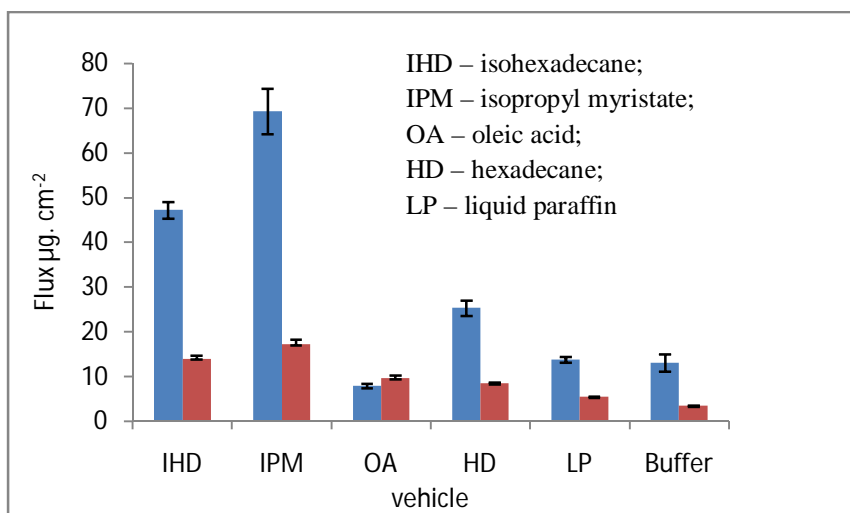


Figure 5.6 Comparative flux data for caffeine across ■ silicone and ■ high density polyethylene membranes when applied in different oils and phosphate buffer. Data represent mean \pm sd (n=3-5).

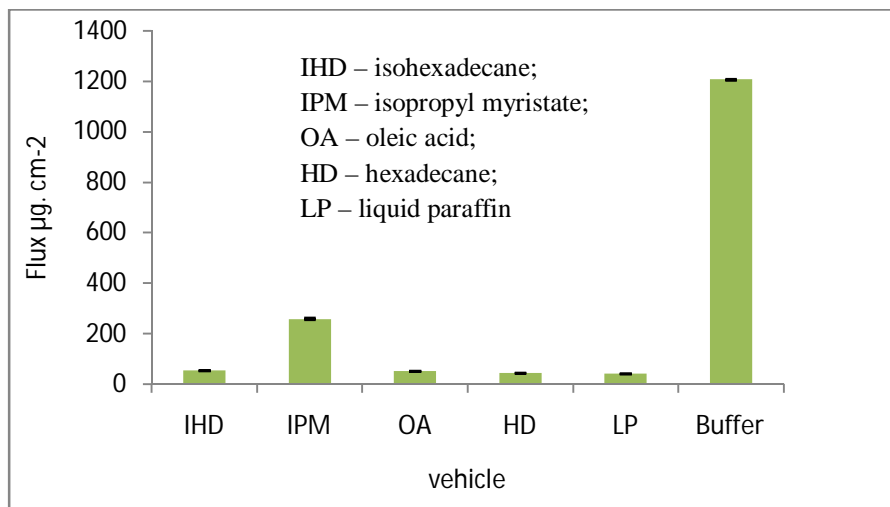


Figure 5.7 Comparative flux data for caffeine across polyurethane membrane when applied in different oils and phosphate buffer. Data represent mean \pm sd ($n=3-5$).

5.4.2. Human epidermis diffusion studies

The diffusion profile of the model permeants from the different vehicles across human epidermis is depicted in Figures 5.8, 5.9 and 5.10 for MP, BP and CF respectively. The amounts of model permeants penetrating the skin when the compounds were applied in IHD as a vehicle were found to be significantly higher when compared to those amounts which diffused from any other vehicle $p \leq 0.05$.

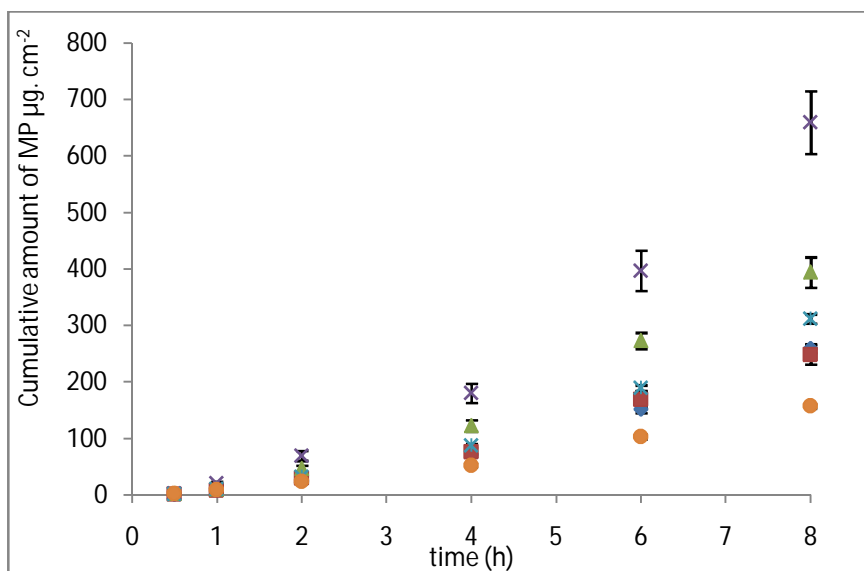


Figure 5.8 Epidermal permeation profiles showing the cumulative amount of MP in the receptor compartment from the different vehicles as a function of time (●) buffer (▲) IPM (■) LP (×) IHD (*) OA and (◆) HD. Data represent mean \pm sd ($n=4-5$). Error bars lie within the symbols.

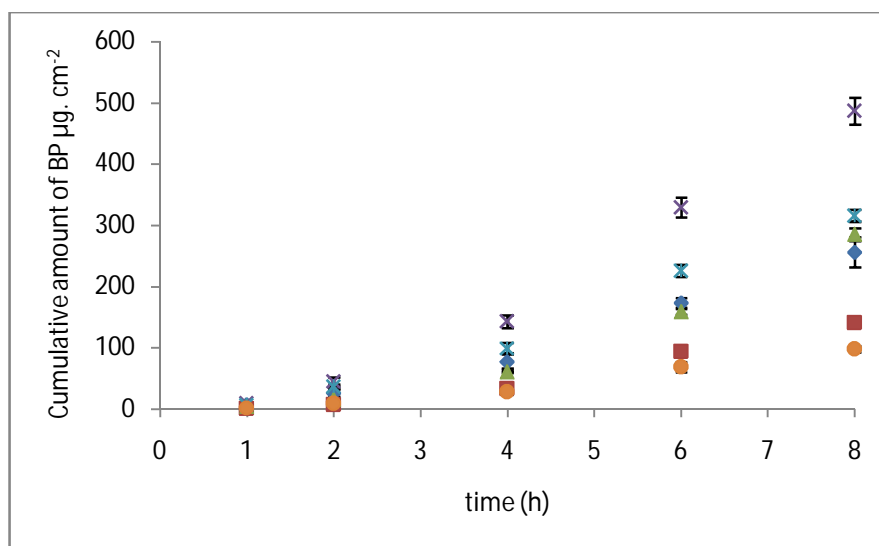


Figure 5.9 Epidermal permeation profiles showing the cumulative amount of BP in the receptor compartment from the different vehicles as a function of time (●) buffer (▲) IPM (■) LP (×) IHD (*) OA and (◆) HD. Data represent mean \pm sd ($n=4-5$). Error bars lie within the symbols.

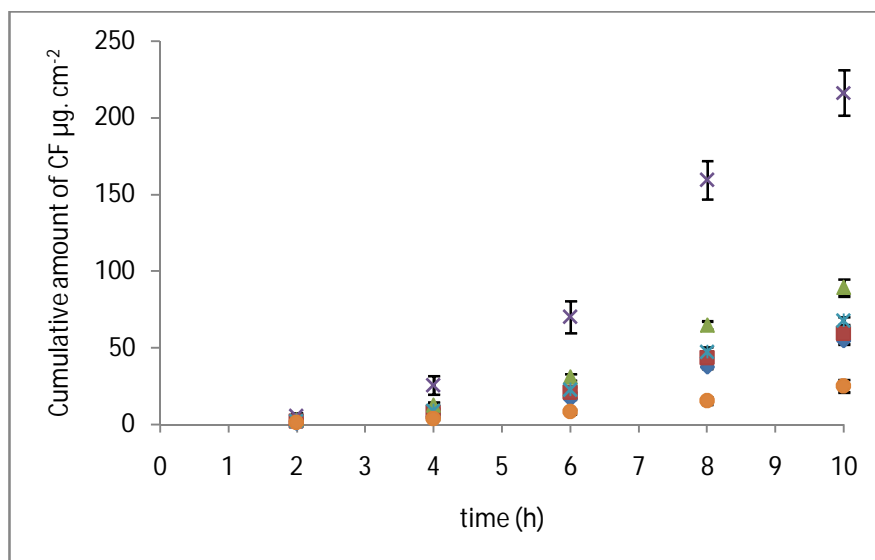


Figure 5.10 Epidermal permeation profiles showing the cumulative amount of CF in the receptor compartment from the different vehicles as a function of time (●) buffer (▲) IPM (■) LP (x) IHD (*) OA and (◆) HD. Data represent mean \pm sd ($n=4-5$). Error bars lie within the symbols.

The parameters derived from the *in vitro* epidermal diffusion studies are shown in Table 5.1. The mean fluxes (calculated between 4-8h for MP and BP, 6-10h for CF) were in the order of MP (Log P 1.96) >BP (Log P 3.57) >CF (Log P -0.07). Generally, all oils significantly enhanced the diffusion of model permeants through the human epidermis compared with phosphate buffer ($p \leq 0.05$). BP and CF have Log P values which fall outside the generally reported range required for optimal transdermal delivery (Log P values 1-3). The highest flux for all model permeants was achieved using IHD.

Table 5.1 The *in vitro* eipdermal permeation parameters permeability coefficients and fluxes for MP, BP and CF Data represent mean \pm sd ($n= 4-5$).

Permeant	Vehicle	J_s ($\mu\text{g cm}^{-2} \text{h}^{-1}$)	K_P (10^{-2}cm h^{-1})
MP	Buffer	26.28 ± 0.42	1.09 ± 0.02
	IHD	115.6 ± 10.54	152.61 ± 13.9
	IPM	67.82 ± 2.49	0.19 ± 0.007
	OA	56.27 ± 1.06	0.86 ± 0.02
	HD	47.78 ± 2.51	60.47 ± 3.17
	LP	43.24 ± 2.94	61.77 ± 4.19
BP	Buffer	17.60 ± 0.57	7.04 ± 0.22
	IHD	86.02 ± 3.80	11.03 ± 0.49
	IPM	56.11 ± 2.27	0.06 ± 0.002
	OA	54.05 ± 1.49	0.09 ± 0.002
	HD	44.61 ± 4.61	5.95 ± 0.61
	LP	26.98 ± 1.20	3.70 ± 0.16
CF	Buffer	4.22 ± 0.69	0.02 ± 0.002
	IHD	36.60 ± 1.41	49.47 ± 1.90
	IPM	14.56 ± 1.11	1.75 ± 0.13
	OA	11.23 ± 0.53	0.21 ± 0.010
	HD	9.43 ± 0.53	12.74 ± 0.71
	LP	9.66 ± 0.46	12.54 ± 0.60

5.4.3 Statistical analysis

5.4.3.1 Data pretreatment

To visualize the data, all datasets were normalised and correlated using MS Excel[®] software. The normalization of data was performed to ensure that all the physicochemical descriptors employed had a zero mean with unit variance. Stepwise correlation analysis was performed between the dependent variables (the dependent variables were: flux through membranes, solvent uptake, lag time, permeability coefficient and flux through epidermis) and the independent variables: the molecular descriptors of the permeants, vehicles and membranes (Appendix I). The significance level used was $(-0.8 > r < 0.8)$. This enabled the identification of the significant molecular descriptors affecting penetration of model permeants. An example of a correlation matrix is shown in Table 5.2. Table 5.3 shows an example of a final correlation matrix, indicating the descriptors that were used in the epidermis PCA and QSPR analysis. All correlations are in Appendix II. Since all descriptors used in QSPR and PCA are derived from a correlation analysis, they are independent from one another but related to a dependent variable. Table 5.4 shows the descriptors used for all dependent variables. All permeants and non-porous membranes were employed in the statistical analysis. However, LP as vehicle was removed from the analysis since it is comprised of a mixture of molecularly different components (of poorly defined composition) and there were insufficient descriptors available for it to be included in the subsequent analysis.

Table 5.2 An example of a correlation matrix

	weight ratio	δT vehicle (δ Hildebrand)	δ_{Dexp} vehicle	δ_{Pexp} vehicle	δ_{Hexp} vehicle	Mvol vehicle	Mwt vehicle	Density vehicle	Mpoint vehicle	LogK _{o/w} vehicle
weight ratio	1									
$\delta T/\delta$ Hildebrand vehicle	-0.11361	1								
δ_D vehicle	-0.22941	0.82753	1							
δ_P vehicle	0.00558	0.77548	0.39622	1						
δ_H vehicle	0.03913	0.80810	0.35327	0.95288	1					
Mvol vehicle	0.00792	0.74174	0.36857	0.99800	0.93481	1				
Mwt vehicle	0.00203	0.76862	0.39910	0.99954	0.94325	0.99913	1			
Density vehicle	-0.00382	0.79943	0.43247	0.99918	0.95324	0.99561	0.99863	1		
Mpoint vehicle	-0.21546	0.87561	0.98744	0.52838	0.46551	0.50541	0.53251	0.56132	1	
LogK _{o/w} vehicle	-0.14545	0.29482	0.55170	-0.36753	-0.20809	-0.41910	-0.38100	-0.33308	0.42179	1

The correlation level used was ($-0.8 > r < 0.8$). The numbers noted in red are correlated with each other, and one of them was removed according to the following methodology: the correlation values with the dependent variable (weight ratio) were assessed and descriptors with the highest absolute value of correlation were retained. For example the δ_{Pexp} vehicle was highly correlated with the Mwt of the vehicle (0.99954); since the δ_{Pexp} has a higher correlation to the solvent uptake (0.00558) than Mwt (0.00203), the Mwt was removed from the further analysis.

Table 5.3 The final correlation matrix showing the descriptors that were included in the PCA and QSPR of epidermal permeation.

	<i>normalised Flux</i>	<i>normalised solubility</i>	<i>normalised opr_nring permeant</i>	<i>normalised chi0 permeant</i>	<i>normalised chi0_C permeant</i>	<i>normalised Density vehicle</i>	<i>normalised opr_brigid vehicle</i>	<i>normalised Kier flex vehicle</i>
normalised Flux	1							
normalised solubility	-0.136441149	1						
normalised opr_nring permeant	0.303021372	-0.355178569	1					
normalised chi0 permeant	0.283118962	0.163330809	0.523049	1				
normalised chi0_C permeant	0.044159893	0.50011073	-0.31262	0.646066	1			
normalised Density vehicle	-0.393531438	0.463783616	0	4.76E-18	1.9E-17	1		
normalised opr_brigid vehicle	-0.275673538	0.078625536	0	2.85E-17	-2.6E-17	0.729591786	1	
normalised Kier flex vehicle	-0.83806935	0.209331336	0	1.43E-17	0	0.499356002	0.349131	1

Table 5.4 Physicochemical descriptors used in the PCA of solvent uptake, flux through membranes, permeability coefficient, lag time and flux through epidermis

Dependent variable	Independent variables
Solvent uptake	δ_D vehicle Log $K_{o/w}$ vehicle molecular connectivity index vehicle opr_brigid vehicle chi0_C vehicle HSP distance between the oils and membranes
Flux through membranes	solubility of the permeants in the oils weight ratio of treated: untreated membranes δ_P permeant Log $K_{o/w}$ vehicle lip_acc vehicle lip_don vehicle chi1_C vehicle HSP distance between the oils and membranes
Permeability coefficient	solubility of the permeants in the oils weight ratio of treated: untreated membranes Mpoint permeant Mpoint vehicle Log $K_{o/w}$ vehicle molecular connectivity index vehicle opr_brigid vehicle chi0 vehicle HSP distance between the oils and membranes

Table 5.4 Descriptors used in the PCA of solvent uptake, flux through membranes, permeability coefficient of the permeants in the oils, lag time and flux through epidermis (continued)

Dependent variable	Independent variables
Lag time	solubility weight ratio of treated: untreated membranes δ_T permeant b_count permeant opr_brigid vehicle chi1 vehicle chi0v_C vehicle HSP distance between the oils and membranes
Flux through epidermis	solubility of the permeants in the oils opr_nring permeant chi0 permeant chi0_C permeant density vehicle opr_brigid vehicle Kier flex vehicle

All correlations contained permeant, vehicle and membrane input descriptors. In the solvent uptake correlation the descriptors are mainly related to the lipophilicity, size and flexibility of the vehicle. In the flux, permeability coefficient and lag time correlations the solubility, solvent uptake, shape and size of the oil molecules which constituted the vehicle were important descriptors. The H-bond ability of the vehicle and permeant were found to be important descriptors in determining the flux and permeability through synthetic membranes. The

solubility of the permeant, shape, size and flexibility of the permeant and vehicle are important descriptors to determine flux through the epidermis.

5.4.3.2 Quantitative structure-property relationships

Regression analysis was initially performed for the dependent variable of solvent uptake by synthetic membranes using independent variable descriptors of the vehicle and membrane properties. The results showed that a single equation could not explain the solvent uptake into the range of membranes used. The r^2 value of the multiple regressions was low ($r^2=0.49$) and the p-values were high ($p>0.05$), indicating the model was poor and not robust.

To model the flux through different membranes from the oily (IPM, OA, HD and IHD) vehicles, regression analysis was carried out. Permeant flux was correlated to permeant, vehicle and membrane descriptors. A number of molecular descriptors: the χ_0 permeant, χ_1 -C vehicle and δ_D membrane were found to be highly correlated with the flux. However when they were included in the regression analysis to model the flux, high p-values (i.e. $p>0.05$) were obtained for χ_0 permeant ($p=0.97$) and δ_D membrane ($p=0.87$); whilst the coefficient for χ_1 -C vehicle was zero, therefore these descriptors were removed from the model. A high p-value suggests that changes in the variable may not be associated with changes in the flux response. This suggests that these descriptors do not have a significant effect on the flux model. χ_0 permeant, χ_1 -C vehicle are descriptors related mainly to the molecular shape of the permeant and vehicle respectively.

The solubility of the permeant in the oil variable yielded high p-value ($p=0.37$); however, this factor was not removed since it was clearly an important descriptor for both the vehicle and permeant. Although the p-value of this descriptor is high and not ideal, it is however lower than the p-values of the removed descriptors. The p value depends on the sample size and variability of the data, therefore due

to the limited range of oils and permeants, it is possible that this contributed to the high p-value identified for the solubility of the permeant in the oil. Although the analysis indicates that the solubility in the vehicle is not a significant predictor of permeation, it is well documented that adequate solubility is an important factor of the flux obtained (Hadgraft, 1999; Ceschel et al., 2005), since the permeant has to be in its dissolved state in order to partition into the synthetic membrane. In addition the solubility in the vehicle is important to replenish the amount of permeant lost by diffusion so that the thermodynamic activity of the permeant remains constant. Following the correlation analysis, seven descriptors were highly correlated with the flux: (Appendix II Table A2.1) the solubility of the permeant in the vehicle, weight ratio, δ_P permeant, $\text{Log } K_{o/w}$ vehicle, lip_acc vehicle, lip_don vehicle, δ_H membrane. Therefore these descriptors were employed in the regression analysis to model the flux. The flux of permeants from oily vehicles through the synthetic membranes was modeled by Equation 5.4. The r^2 of the multiple regressions was 0.86 and $N=36$.

$$J_m = 3.22 + 0.39 S_v + 0.69 m_{\text{upt}} - 0.90 \delta_{PP} - 0.63 \text{Log} K_{o/wv} - 1.67 \Sigma \alpha^H + 1.18 \Sigma \beta^H - 1.70 \delta_{Hm}$$

Equation 5.4

Where J_m is the flux of permeants through synthetic membranes, S_v is the solubility of permeant in the oil, m_{upt} is the relative mass uptake of each oil of membrane, which was derived by the difference between the weight of the membrane before and after soaking (Equation 5.5). δ_{PP} the polar component of the HSP for the permeant, $K_{o/wv}$ octanol water partition coefficient for the vehicle, $\Sigma \alpha^H$ is the hydrogen bonding donor ability of the vehicle, $\Sigma \beta^H$ the hydrogen bonding acceptor ability of the vehicle and δ_{Hm} the hydrogen bonding component of HSP for the membrane.

$$m_{\text{upt}} = \frac{m_a - m_b}{m_b}$$

Equation 5.5

m_a is the weight of membrane after soaking and m_b is the weight of membrane before soaking.

It is accepted that the permeability coefficient is a more reliable parameter than simple flux in describing the permeation potential of chemical substances (Wilkinson & Williams 2002; Fitzpatrick et al. 2004); therefore regression analyses were performed to model $\text{Log } K_p$ using permeant, vehicle and membrane descriptors. The descriptors retained in the model after the correlation were (Table A2.3): the (S_v) solubility of the permeant in the oil, MPT_d and MPT_v (i.e. the melting point of the permeant and vehicle respectively), chi0 permeant (which is a descriptor related to the shape of the permeant), $\text{Log } K_{o/wv}$ of the vehicle, opr_brigid vehicle (a descriptor related to the number of rigid bonds, shape and flexibility of the vehicle), δ_{Tm} (the Hildebrand solubility parameter of the membranes) and δ_{Dm} (the dispersion forces component in HSP value of the membranes). Chi0 vehicle and molecular connectivity index for the vehicle were removed from the correlation because these descriptors had a coefficient of zero, while the solvent uptake *per se* was removed due to the high p value ($p=0.23$). Through the construction of the correlation matrices, the extent of solvent uptake was correlated with several other variables. Therefore, despite its removal, the importance of solvent-membrane interactions achieves its impact through the retained descriptors with which it was, itself, correlated. Equation 5.6 models the $\text{Log } K_p$ through the synthetic membranes. The r^2 of the multiple regressions was 0.98 and $N=36$.

$$\begin{aligned} \text{Log } K_p = & 0.34 - 0.30 S_v + 1.10 \text{MPT}_p - 0.44 \text{chi0}_p - 0.43 \text{MPT}_v + 0.38 \text{Log } K_{o/wv} \\ & - 0.54 \text{opr_brigid} - 0.66 \delta_{Tm} + 0.22 \delta_{Dm} \end{aligned} \quad \text{Equation 5.6}$$

The solubility of the permeant in the oil is a descriptor that was found in both QSPRs (Equations 5.4 and 5.6); the value of the coefficient was similar in both QSPRs, however the coefficient was positive with the flux model, which means increasing the solubility led to an increase in the flux, and negative in the $\text{Log } K_p$ model, increasing the solubility decreased the permeability coefficient. This is expected since for a drug to permeate through a membrane it should be in the solubilized form so high solubility will enhance the replenishment of the lost drug

by diffusion. The permeability coefficient is derived from dividing the flux over the solubility in the oil, so increasing the solubility will lead to a decrease in the permeability coefficient value for a constant flux value. Diffusion is a passive process where the permeant moves down its activity gradient. However as the solubility of the permeant in the vehicle increases it means that there is higher affinity and interaction between the permeant and the vehicle and hence the tendency of the permeant to leave the vehicle and partition into the membrane will decrease and therefore the permeability will decrease. High solubility of the permeant in the membrane and low solubility in the vehicle is desired to enhance the permeation. The activity coefficient or the potential of the permeant to be released from the vehicle into the membrane is at maximum when the vehicle is saturated. Since the permeants in this state are in dynamic equilibrium, the molecules are continuously precipitating out of the solution and then re-entering the solution state, they undergo the least degree of vehicle bonding interaction and are most likely to escape from the formulation and enter the membrane.

Log $K_{o/w}$ of the vehicle, which describes the hydrophobicity of the vehicle, is another descriptor which was important in both QSPRs. Equations 5.4 and 5.6 indicate that increasing the Log $K_{o/w}$ of the vehicle leads to a decrease in the flux and increase in the permeability coefficient. This is because, although all systems were originally of unit thermodynamic activity, the permeability coefficient (K_p) being the ratio of flux to actual concentration in the vehicle (Equation 5.3), will differ from system to system. The value of the coefficient for the Log $K_{o/w}$ in the flux model was almost twice its value in the Log K_p model. The vehicles used in this study are all hydrophobic oils; therefore increasing the Log $K_{o/w}$ of the vehicle could lead to a decrease in partition of hydrophobic drug from the oil (or oil-modified membrane phase) and subsequent permeation.

Melting point is a physicochemical property which has also been considered as a determinant of the solubility of the permeant in both the vehicle and membrane; since the value is highly dependent upon hydrogen bonding. Therefore the melting

point and the hydrogen bonding donor and acceptor descriptors introduce the importance of hydrogen bonding on the diffusion process. The melting point of the vehicle and permeant were of importance when modeling the $\text{Log } K_p$, while in the flux model the hydrogen bonding donor and acceptor ability of the vehicles were the highly correlated descriptors. Increasing the number of hydrogen bond donors in the vehicle decreases the flux through the membranes, while increasing the number of hydrogen bond acceptors in the vehicle increase the flux. The hydrogen bonding donor ability is more relevant and contributes more to the flux through synthetic membrane when compared with the hydrogen bonding acceptor. In the membranes used in the modeling, silicone and polyurethane membranes are both capable of interaction and hydrogen bonding with the vehicles, which supports findings of a modification in the flux.

Equation 5.4 indicates the importance of solvent uptake (m_{upt}) on flux; it shows that increasing the amount of solvent sorbed into the membrane leads to higher flux. According to the analysis carried out χ_0 of the permeant is correlated to δ_p of the permeant, therefore one of these descriptors encodes the other in the model. In equation 5.4 there is a negative correlation between the δ_p of the permeant and flux. Since all the vehicles are hydrophobic increasing δ_p of the permeant means that the permeant is becoming more polar and this would be expected to lower the solubility of the permeant; in addition, it would lead to a lower partitioning into the hydrophobic membranes, therefore the flux would be predicted to decrease. However since solubility depends on all molecular interactions, in some situations even should δ_p increase and the molecule become more polar, it is the value of δ_H that might determine the high molecular interaction between the polar compound and the hydrophobic oil, therefore high solubility values might be achieved. For example the solubility of CF in OA is similar to the solubility of MP in OA despite CF being considered a polar compound. In Equation 5.6 there is also a negative correlation between χ_0 permeant and the $\text{Log } K_p$. The χ_0 descriptor encodes the importance of the molecular size of the permeant and this means that

increasing the molecular size of the permeant decreases its permeation through synthetic membranes.

Increasing the number of rigid bonds in the vehicles (opr_brigid) leads to a decrease in the permeability coefficient. The lower number of rigid bonds leads to higher flexibility of the vehicle, which in turn increases the uptake and interaction of the vehicle with the membrane therefore it enhances the flux.

The membrane descriptors were also important when modeling the flux and $\text{Log } K_p$. Increasing the δ_H of the membrane led to lower flux. In addition increasing the δ_T of the membrane decreased the permeability coefficient. On the other hand increasing δ_D led to an increase in the $\text{Log } K_p$. As mentioned earlier the vehicles are hydrophobic; therefore increasing δ_H and δ_T of the membranes means that the membrane is becoming more hydrophilic. In general, this will decrease the level of interactions between the vehicle and membrane and hence the flux and K_p are decreased for hydrophobic penetrants such as MP or BP. In contrast as δ_D of the membrane is increased, then the membrane becomes more hydrophobic, which decreases the flux of more hydrophilic compounds such as CF.

In both models there were descriptors related to the permeant vehicle and membrane indicating the importance of all three in the diffusion process. In the flux model the membrane descriptor δ_H had the highest coefficient in the model followed the hydrogen bond donor and acceptor descriptors for the vehicles respectively. In the $\text{Log } K_p$ model the melting point of the permeant had the highest coefficient, as indicated previously this descriptor is related to the hydrogen bonding ability of the permeant and the solubility of the permeant. These results demonstrate that the permeation through synthetic membrane is controlled primarily by the hydrogen bonding ability of the vehicle and permeant with the membrane.

Since it proved possible to perform QSPR on the flux and Log K_p of permeants through synthetic membranes, a correlation and regression of the permeant and vehicle descriptors against the flux through epidermis was carried out. However due to the limited data $N=12$, the descriptors could not be fitted to one equation. Therefore despite the r^2 value of the multiple regressions being 0.91, the p-values associated with the descriptors proved to be high (i.e. $p>0.05$).

5.4.3.3 Principal component analysis

A PCA score plot is useful in finding the clustering of samples, whilst a loading plot is useful in identifying important variables. PCA analysis loading plots show which variables are influential, and also how the variables are correlated. Positively correlated variables are the variables close to each other on the same side of the plot. When the numerical value of a variable increases or decreases the numerical value of the correlated variable has a tendency to change in the same way. When variables are negatively (“inversely”) correlated they are positioned on opposite sides of the plot origin, in diagonally opposed quadrants. Furthermore, the distance to the origin also conveys important information. The further away from the plot origin a variable lays, the stronger impact that variable has on the model (Eriksson et al., 2006).

To ensure data quality, the absence of outliers was assessed employing Hotelling’s test (Jackson, 1991; Tracy et al., 1992). This statistic is a multivariate generalization of Student’s t-test, and provides a check for observations adhering to multivariate normality. Strong outliers are found in the score plots. They have high leverage on the model, i.e. strong “power” to pull the PCA model toward them, and may “consume” one principal component (PC) just because of their existence. The term leverage derives from the Archimedean principle that anything can be lifted out of balance as long as the lifter has a long enough lever. Leverage is a measure of the influence of an observation and is proportional to the distance of the observation from the center of the data (Eriksson et al., 2006).

Hotelling's test was employed with 95% confidence limit and no outlier data in the score plots were found.

PCA for the solvent uptake and interaction with membranes was used to provide an overview of trends in the data, with the results being displayed in bi-plot graphics (Figure 5.11). The descriptors of both the vehicle and membrane were used to perform the solvent uptake PCA. The first two PCs describe 76% of the total variance in the data. δ_{Dm} and δ_{Tm} were removed from the analysis because they skewed the data. They contributed very little to describing the variance captured by either PC1 or PC2. First δ_{Dm} was removed and the plots were regenerated, but the data were still skewed by δ_{Tm} , and the latter term was also found not to contribute to the description of the variance captured by both PC1 and PC2; therefore δ_{Tm} was removed from the analysis. The PCA plots were regenerated again and then all of the available descriptors were found to contribute to the description of variance captured by PC1 and PC2. When a descriptor skews the data it pulls the PC strongly toward itself because its influence is enhanced; its influence is enhanced because it is so far from the mean. It is similar to undertaking PCA without centering the data. δ_{Dm} and δ_{Tm} were the only descriptors relevant to the characteristics of the membrane and since the membrane descriptors cannot be ignored in the analysis, then the distance between the HSP values of the membranes and vehicles (which is a derived descriptor; Table 4.13), was introduced instead. The distance represents a measure of the degree of matching (i.e. similarity) between the solubility parameters of the vehicles and the membranes. Therefore it represents a descriptor relating the vehicle to the membrane.

As mentioned previously LP as vehicle was removed from all the analysis since it is comprised of a mixture of molecularly different components (of poorly defined composition) therefore the available descriptors were insufficient for it to be included. In the PCA of solvent uptake (Figure 5.11), the score plot shows that

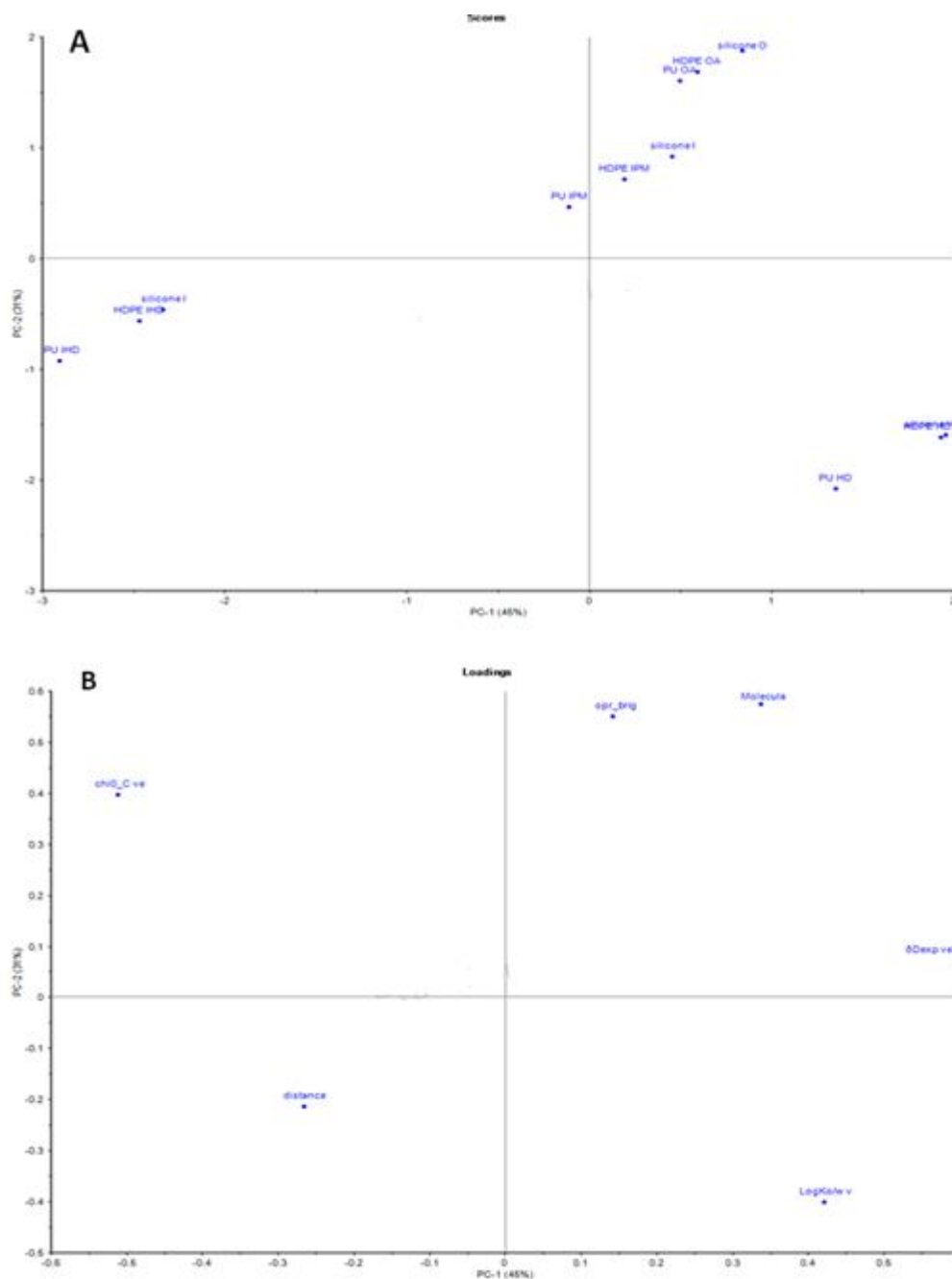


Fig. 5.11 (A) Score plot from the PCA of solvent uptake of vehicles into membranes showing the grouping of scores representing different vehicles. The two displayed PCs explain 76% of the total variability; 45% and 31% of the variability are explained by PC1 and PC2 respectively. (B) Loading plots from the PCA of the solvent uptake of vehicles into membranes showing descriptors explaining the solvent uptake.

there is no special clustering for the membranes; each membrane was found in all the groups. The clustering was more related to the vehicle; IPM and OA were close to each other on the plot. OA and IPM have heteroatoms, compared with IHD and HD which are simply hydrocarbons; this could indicate that the same descriptors are related to their behaviors. Although HD is the linear counterpart of IHD, they were on the opposite sides of the plot; this indicates that the combination of descriptors which make up the PCs separates the behaviour of these two oils. In general silicone membrane was closer to HDPE membrane compared with PU. This might be due to the more hydrophilic properties of PU compared with the other membranes. There are three distinct groups, and although in each group the behaviour of the solvent uptake is described by the same descriptors, the descriptors are different between different groups. A QSPR model could not be developed for the solvent uptake, because each group was explained by different descriptors, and therefore the terms cannot be combined into a single linear relationship.

The six descriptors, (δ_D vehicle, Log $K_{o/w}$ vehicle, molecular connectivity index vehicle, opr_brigid vehicle, chi0_C vehicle, distance) found in the loading plot (Figure 5.11) are responsible for the changes in the solvent uptake into membranes. The descriptors are distributed across the loading plot. δ_D of the vehicles appears to have the biggest effect on describing the variance of the data captured by PC1, OA and IPM had the same value of δ_D (16 MPa)^{1/2} while HD has the highest value of δ_D (16.3 MPa)^{1/2} and IHD has the lowest value of δ_D (14.7 MPa)^{1/2}. Chi0_C also describes the variance of the data explained by PC1. OA and IPM has similar values of chi0_C, while IHD has the highest value and HD the lowest value. The molecular connectivity index has the greatest effect on the variance described by PC2. IPM and OA have close values of molecular connectivity index. These descriptors which were found to be highly loaded on both PC1 and PC2 were able to describe the variance between IHD and HD, but they were not involved in describing the variance between OA and IPM to the same extent, because OA and IPM have similar values of these descriptors.

Therefore, IPM and OA were found to lie close to each other on the plot, while IHD and HD were separated on different sides of the plot.

A similarity of molecular behaviour is expected between molecules which have similar properties than molecules with dissimilar characteristics. However in PCA plots, molecules behave in the same way when they have similar values of the dominating descriptor. This is the descriptor that is highly loaded on either PC1 or PC2. Therefore in some instances molecules will have the same value of some descriptors but they will be located on opposite sides of the plot, if these descriptors were not the main descriptors contributing to explaining the variance either on PC1 or PC2. For example HD and IHD have more than one descriptor in common but are located on opposite sides of the plot because they differ in the dominating descriptor. In Figure 5.11 IPM, IHD and HD have the same value of opr-brigid while OA has a different value, if this descriptor was dominant IPM and OA will be separated from each other and HD, IPM and HD will be closer, however since it is not a dominant descriptor it did not affect the clustering.

PCA analysis was also carried out using the data obtained for the flux, permeability coefficient and the lag time of permeant diffusion through synthetic membranes. Descriptors of the permeant, vehicle and membranes were used in the correlation analysis. As in the analysis of the solvent uptake, δ_{Dm} , δ_{Hm} and δ_{Tm} polarized the data and did not contribute to explain the variance captured by PC1 and PC2, since only three membranes were employed and the differences in their properties was not sufficient. Accordingly these descriptors were omitted from the analyses and the HSP-distance was introduced instead.

The score plot for the flux and K_p (Figures 5.12 and 5.13) shows that the data are distributed across the plot. In Figure 5.12 the data in the score plot of the flux are distributed in four groups. The groups were clustered according to the vehicle used regardless of the membrane and permeant. Within vehicle clusters (e.g. IPM and OA clustered groups) the clustering was according to the permeant identity

(e.g. in the OA cluster in the lower left quadrant, clusters of CF, BP or MP were identifiable). On the other hand in the HD and IHD groups MP and BP from the same membrane were closer to each other compared to CF

In the loading plot of the flux (Figure 5.12) each descriptor has a unique position on the PC1 and PC2 axes. The H-bond acceptor of the vehicle has the greatest effect in describing the variance of the data accounted for PC1. The H-bond acceptor of the vehicle has a positive correlation with the solubility of the model permeants in the oil. Both OA and IPM have two H-bond acceptor groups, in general the solubility of the model permeants in these oils was higher, when compared with HD and IHD. The Log $K_{o/w}$ vehicle and solubility are the main descriptors which contribute to the variance captured by PC2. HD and IPM have the highest and lowest values of Log $K_{o/w}$ respectively. Chi1_C is also highly loaded on PC1. Chi1_C is a descriptor relating to localized branching within a molecule indicating its importance to the overall topology of the oil. The descriptor relates the effect of branching in the molecule to its overall shape by considering the connectivity between two carbon atoms.

In the studied vehicles, OA had the highest value of localized hydrocarbon branching (chi1_C) owing to its alkene-bond and it is the only vehicle that contains a H-bond donor group. These descriptors were able to separate the behaviour of the four vehicles across the plot. Although OA and IPM have H-bond acceptor groups, the variance in their behaviour was separated by the chi1_C and Log $K_{o/w}$ effect on the plot. In addition the HD and IHD behaviour was separated mainly by the $K_{o/w}$ and chi1_C. Since the main descriptors influencing PC1 and PC2 were related to the vehicle, the variances in the permeant and membrane behaviours were not explained as sufficiently as those associated with the vehicles.

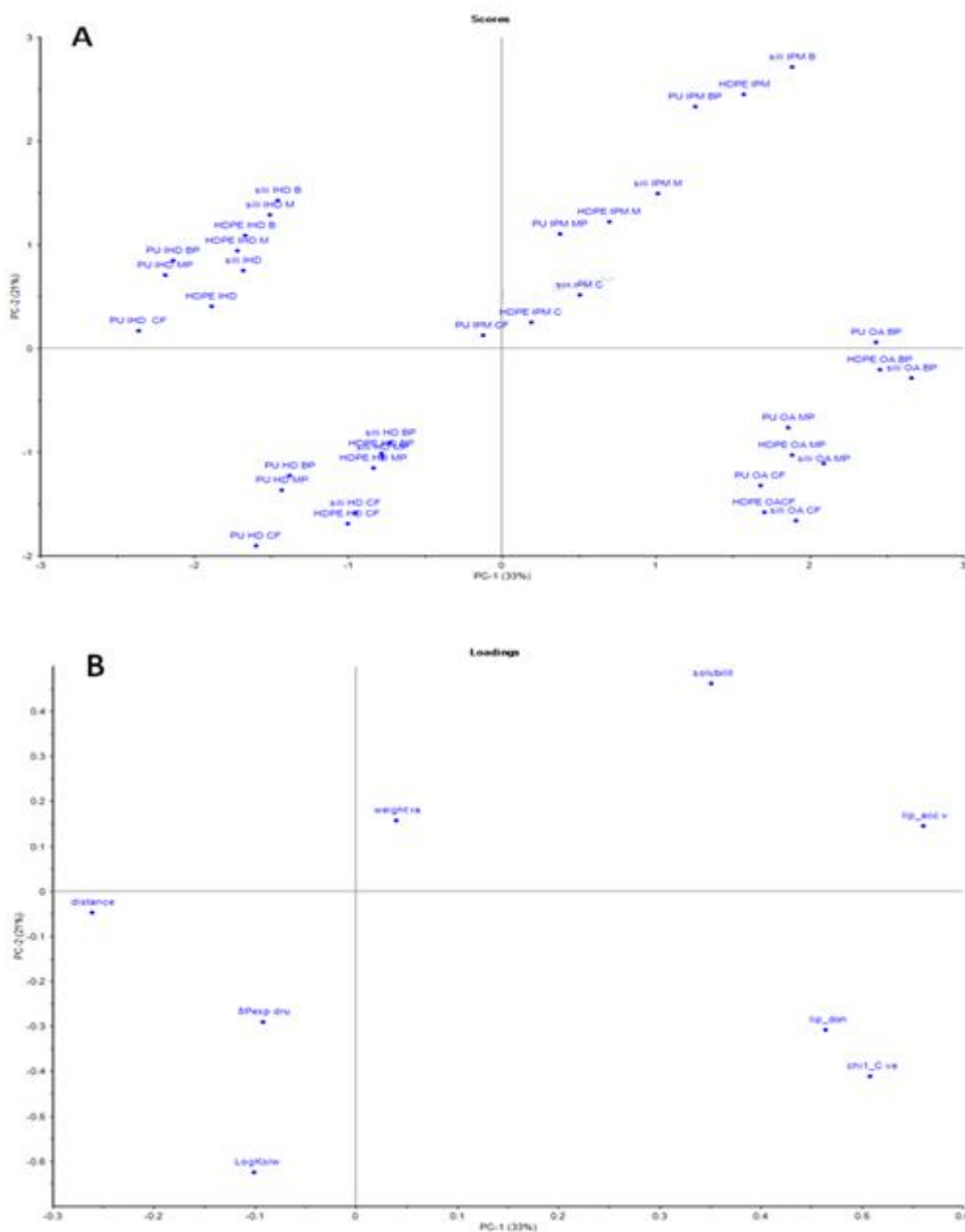


Fig. 5.12 (A) Score plot from PCA showing the relationship between permeant-oily vehicle –membrane descriptors with flux. The two displayed PCs explain 54 % of the total variability; 33% and 21% of the variability are explained by PC1 and PC2 respectively. (B) Loading plots from PCA showing the relationship between permeant-oily vehicle-membrane descriptors with flux.

The K_p score plot (Figure 5.13) shows that the data are arranged in three distinct groups, one group consists of IPM and OA data, while HD and IHD are found in two groups separately. In the HD group HDPE and silicone membrane data were closer to each other compared to PU. While in the IHD group the grouping was according to the membrane regardless of the permeant. In contrast, when the IPM and OA groups are considered, the separation was according to permeant, where MP and CF were closer to each other compared to BP.

In the K_p loading plot (Figure 5.13) the descriptors were scattered across the plot. The molecular connectivity index had the biggest effect in explaining the variance of the data which is captured by PC1, while the variance captured by PC2 was mainly described by Log $K_{o/w}$. Chi0 vehicle also contributes to explaining the variance captured by PC1. As mentioned previously, IPM and OA have similar values for the molecular connectivity index and chi0, therefore these descriptors are unable to extract and capture the variance between OA and IPM. On the other hand these descriptors are different for IHD and HD, therefore the behaviour of both oils is separated from each other and also separated from OA and IPM. The main descriptors involved in explaining the variance captured by PC1 and PC2 are related to the vehicle; consequently the membrane and permeants were clustered together.

Comparing Figures 5.12 and 5.13: The same amount of variance is explained in both plots, PC1 and PC2 described 54% of the total variance in the data for both the flux and K_p analysis. The molecular connectivity index is the descriptor related to the position and influence of heteroatom patterns of adjacency, these atoms are responsible for the hydrogen bond acceptor ability of the molecule. This means that similar descriptors are influencing the flux and K_p loading plots. Furthermore Log $K_{o/w}$ was the main descriptor affecting PC2 in both plots. These results indicate that the lipophilicity, in addition to the hydrogen bond ability of the vehicle were the major determinants of the diffusion across synthetic membranes. This might explain the clustering of IPM and OA in the K_p loading

plot, and also the finding that OA and IPM were closer to each other in the flux loading plot, while HD and IHD were on the opposite side of the latter plot.

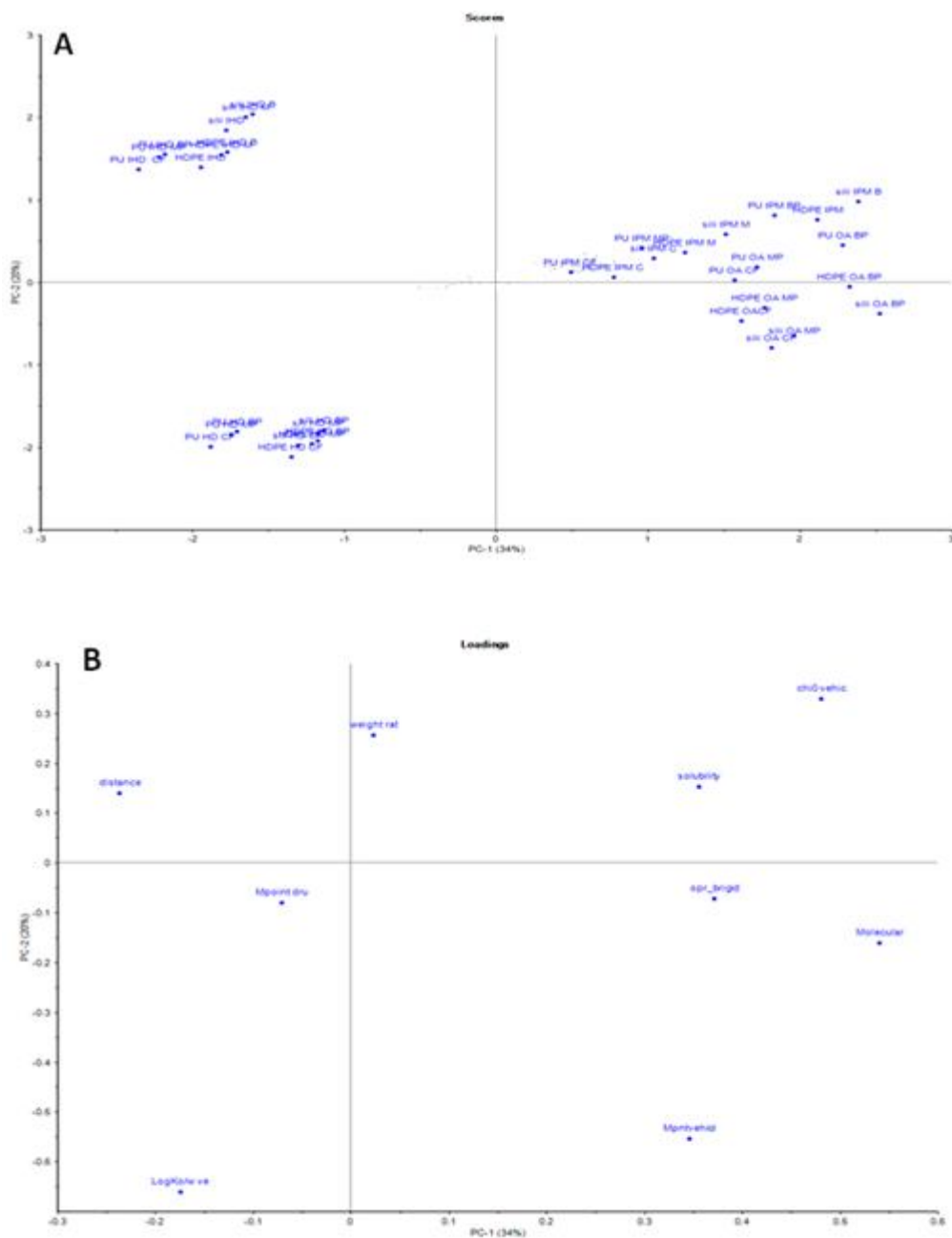


Fig. 5.13 (A) Score plot from PCA showing the relationship between permeant-oily vehicle –membrane descriptors with K_p . The two displayed PCs explain 54 % of the total variability; 34% and 20% of the variability are explained by PC1 and PC2 respectively. (B) Loading plots from PCA showing the relationship between permeant-oily vehicle–membrane descriptors with K_p .

The score plot for the permeant-vehicle –membrane descriptors correlated with lag time (Figures 5.14) shows that the data are scattered across the plot. PC1 and PC2 described 55% of the variance in the data. Generally CF and MP are clustered together in the plot. HDPE and silicone membrane were closer to each other compared to PU. In the loading plot Figure 5.14, χ_1 vehicle and the solubility of the permeant in the oils has the greatest effect in describing the variance in the data obtained by PC1, while δ_T of the permeant and b_{count} of the permeant provided the biggest contribution to the description of the variance captured by PC2. The solubility of the permeant in the vehicle is negatively correlated with the Hildebrand solubility parameter of the permeant, which means a permeant that has high δ_T will have low solubility in the vehicle. Such a relationship may be expected since the vehicles used are oils and hydrophobic, and increasing the δ_T means that the permeant is becoming more hydrophilic. Since the permeant descriptors are contributing to explaining the variance of the data, the clustering was both related to the permeant and vehicle. The used descriptors were able to separate the behaviour of BP more readily than that of MP from CF.

The clustering and behaviour of the score plot in the lag time is different when compared with the flux and K_p score plots. In the flux and K_p plots the same vehicle was clustered together while in the lag time the scattering is dependent upon the vehicle, permeant and membrane descriptors. Furthermore, in the flux and K_p plots the vehicle descriptors have the biggest effect in describing the variance captured by both PC1 and PC2, which means most of the 54% of the variance was described by the vehicle descriptors. However in the lag time plots both the vehicle and permeant descriptors, combined, to describe 55% of the variance.

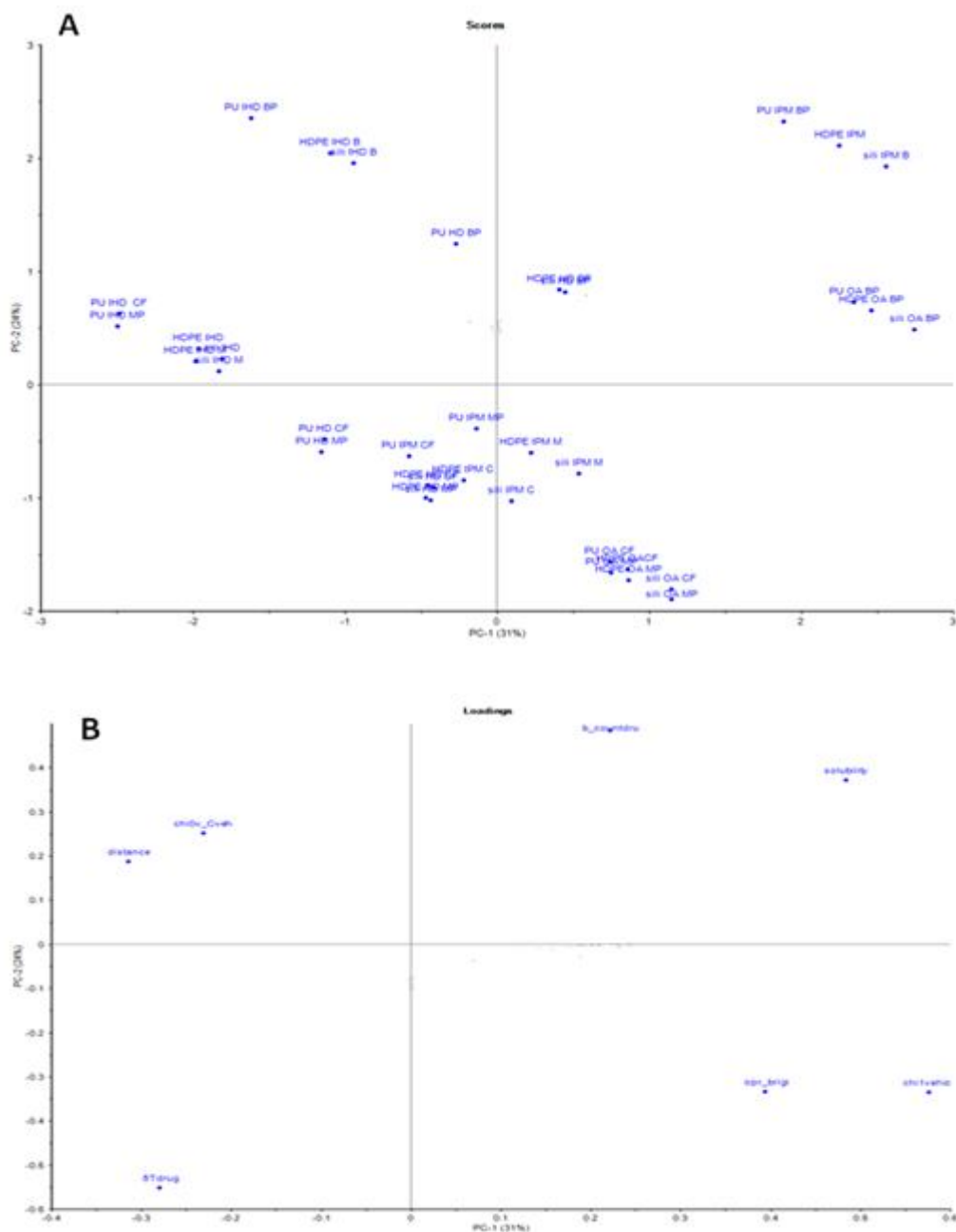


Fig. 5.14 (A) Score plot from PCA showing the relationship between permeant-oily vehicles – membrane descriptors with lag time. The two displayed PCs explain 55 % of the total variability; 31% and 24% of the variability are explained by PC1 and PC2 respectively. (B) Loading plots from PCA showing the relationship between permeant-oily vehicle–membrane descriptors with lag time.

The PCA was carried out on the permeant and vehicle descriptors for the flux through epidermis (Figure 5.15). The first two PCs describe 59% of the variance in the data. The PCA score plot shows that, unlike the synthetic membranes flux data, there is no specific clustering according to the oil or permeant, data are distributed across the score plot. However there is a notable trend in the distribution of the oils and permeants. The permeants from the same vehicle are distributed in a curved shape. This trend is broken by the flux of BP from IPM; this might be a consequence of the comparatively high solubility of BP in IPM relative to the other oils.

The descriptors in the loading plot are distributed on the positive side of PC1 except for opr_nring of the permeant, which is located on the negative side of PC1; in addition it is only described by PC1. All the descriptors have unique positions on the PC1 and PC2 axes. Kier flex and opr_brigid of the vehicle are positively related to each other, the more rigid the bonds in the compound, the less flexible it is. The Kier flex descriptor is related to the flexibility and shape of the molecule; the lower the value, the higher the flexibility of the compound. The density of the vehicle, the solubility and opr-brigid were found to have the greatest effect on the variance in the data captured by PC1. In contrast, the Chi0_C and chi0 values of the permeant were shown to induce the highest variance in the data captured by PC2. This indicated that both the permeant itself and the vehicle are important in determining the overall diffusion of the compound through epidermis studies.

The descriptors used were able to separate the behaviour of the three permeants; each permeant having different values of these descriptors. OA and IPM possess similar density values (0.62 and 0.61 g/cm^3 respectively), whilst IHD and HD have the same density (0.56 g/cm^3). Hence it is the differences in the permeant solubility in these oils along with the difference in the values of the chi0_C and chi0 of the permeants that lead to the distribution of the permeants across the plot.

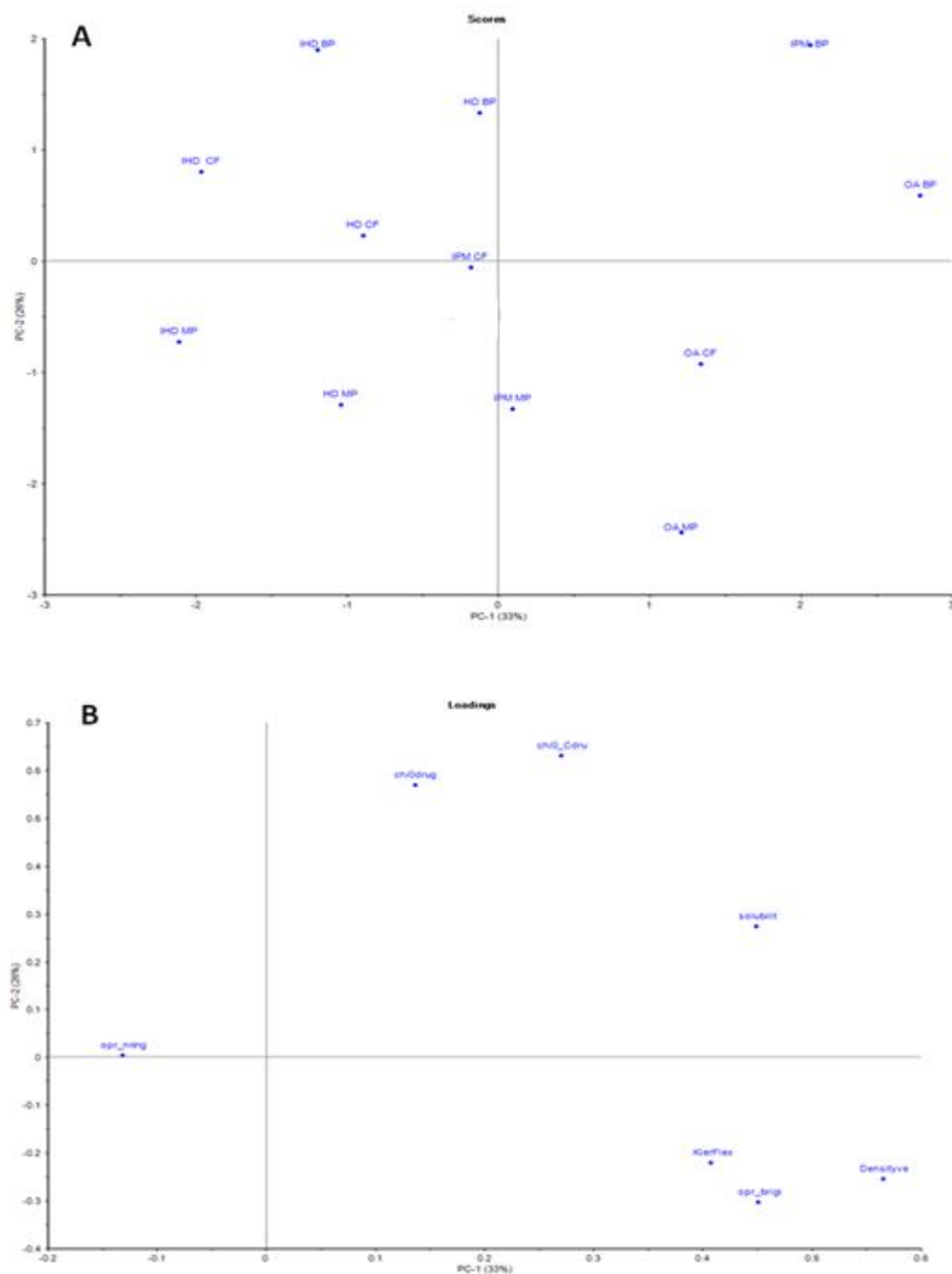


Fig. 5.15 (A) Score plot from PCA showing the relationship between permeant-oily vehicles descriptor with epidermis flux. The two displayed PCs explain 33% and 26% of the variance, respectively. (B) Loading plots from PCA showing the relationship between permeant-oily vehicle descriptors with epidermis flux.

5.5 Discussion

In order for any permeant to reach its target receptor it must cross a number of different body membranes. As discussed previously in section 1.7.1 the passage of compounds through a biological membrane after topical application is divided into four main stages. First the drug has to be liberated from the formulation. Next it penetrates into the outermost skin layer and then it permeates (or partitions) from one layer into the other, and finally it reaches the vascular system. Most biological membranes are lipophilic and they are composed of one or more layers and this generally leads to slow drug diffusion (Camenisch et al., 1996). However, biological membranes are generally complex and variable and therefore in order to study the permeation of different model penetrants it can be advantageous to use less complex membranes such as synthetic polymers (Watkinson et al., 1995; Feldstein et al., 1996, 1998; Rousseau et al., 2009). In this study human epidermis was used as a biological membrane and silicone, HDPE and PU membranes were selected as examples of different synthetic membranes. The selected membranes possess different solubility parameters and different chemical characteristics.

The vehicles used in these studies were all saturated and in all cases contained sufficient excess solute to maintain a constant donor concentration during the experimental time frame. Under equilibrium conditions flux will be at a maximum when the outer layer of a membrane is saturated and this will occur when the vehicle is a saturated solution of the solute with excess permeant in suspension. In an ideal situation all saturated solutions of the same permeant in any solvent system should produce an equal flux through a membrane that is independent of solute concentration (Higuchi, 1960). Examination of the flux results shows that flux of permeants from different vehicles through all membranes was not constant. The direct implication of this result is that all of the situations investigated were not ideal, i.e. there was some interaction between the vehicle and the membrane. Such an interaction may involve diffusion of the solvent into

the membrane where it may increase or decrease the partition and/or diffusion coefficient of the solute. Alternatively, it is possible the vehicle may act as an extraction solvent and remove some components of the membrane, e.g. a plasticizer, thus modifying its resistance to permeation of the solute in the membrane. In addition, any sorbed vehicle component(s) may increase the solubility of the incorporated drug in the membrane (Crawford & Esmerian, 1971; Amnuaikit et al., 2005; Alexander et al., 2012). The differences in the cumulative amount of a given permeant diffusing across the different membranes are therefore likely to be a consequence of the different physicochemical properties of the membranes.

CF is the most hydrophilic model permeant therefore it has a relatively low solubility in the oils but a higher solubility in the buffer (Table 3.1). The diffusion of CF from the buffer through silicone and HDPE membranes was comparatively low. This is likely to be due to the low partitioning of the buffer and CF into the hydrophobic membranes. However that was not the case when the PU membrane was employed. The diffusion of CF from the buffer was significantly higher than from any of the oils ($p \leq 0.05$). The more relatively hydrophilic properties of the PU membrane, particularly following its solvation with the aqueous buffer could have enhanced partitioning and diffusion of CF through the membrane, compared to both CF from oils through HDPE or silicone membranes. In addition, CF with its higher solubility in the buffer relative to the other permeants might diffuse concurrently with the buffer through the (comparatively) hydrophilic PU membrane. CF has been reported previously to diffuse through a hydrophilic Carbosil[®] membrane with a rate that was very similar to the diffusion of water, therefore concurrent diffusion of the compound with water was proposed to occur (Russeau et al., 2009).

The highest amounts of CF that permeated from oily vehicles through all model membranes were achieved when IPM was the vehicle. IPM was sorbed by the model membranes therefore it might alter the overall structure of the membrane,

consequently enhancing the diffusion of CF through the membrane, and subsequently when CF reaches the receptor compartment it will readily partition into, and dissolve in the buffer. Despite the low solubility of CF in IHD, high flux values were achieved when IHD was the vehicle. This could be due to the high amount of IHD sorbed by the hydrophobic membranes (Table 4.4), which presumably does modify the membrane properties. Although higher amounts of IHD were sorbed into the HDPE and silicone membranes, the flux of CF from IPM was higher because IPM has higher solvation capacity for CF compared to IHD. Therefore, it follows that: (a) the amount lost by diffusion will be replenished quickly when IPM is the vehicle; and (b) the solubility of CF in the membrane is most likely higher in the IPM-modified membrane, compared to an IHD-modified membrane.

OA has the greatest capacity to dissolve CF. However the lowest amount of CF that permeated through silicone membrane was when OA was the vehicle. This could be due to the low interaction between OA and silicone membrane (Table 4.3). Although the results presented in Section 5.4 identified multiple physicochemical properties of both vehicle and permeant those determine the extent of oil-membrane interaction, the 'kinked' shape of OA compared to other oils is perceived to play a role in restricting the diffusion of OA into the membrane. On the other hand, OA behaved as a plasticizer for PU changing the membrane properties and rendering it 'sticky' by the end of the experiments. Thus the resistance of the membrane to penetration would have been modified. Comparing the results of the model permeant (i.e. CF) diffusion from OA through the three membranes, the diffusion through PU was the highest. However the diffusion of CF from OA through PU was significantly lower than its diffusion from the buffer.

CF was similarly soluble in all of the hydrocarbon vehicles, but the amount of IHD sorbed by HDPE and silicone was greater than the other oils. Therefore the amount of CF permeating through the membranes from an IHD vehicle proved to

be significantly higher. The viscosity of LP is higher than HD or IHD and the higher viscosity may decrease diffusivity of the permeant, both within the vehicle and in a vehicle-modified membrane. LP viscosity is approximately 30 mPas, whilst the viscosities of HD and IHD are 3.34 mPas at 25°C and 5.2 mPas at 20°C respectively, as supplied by the suppliers. In addition the amount of HD sorbed by silicone and HDPE was higher than LP, thus leading to a lower amount of CF permeating from LP compared with HD.

MP was chosen as a model permeant as being representative of a compound having intermediate lipophilicity, and it also demonstrated it has intermediate solubility in the oils and buffer (Table 3.1). The amount of MP that permeated through silicone membrane when the buffer was the vehicle was higher than BP and CF. Its moderate solubility and partitioning between hydrophilic and lipophilic regions aids in its ability to partition and diffuse through the lipophilic membrane and later become solubilised in the receptor compartment. The flux of MP through PU membrane was lower than CF, due to the higher lipophilicity of MP, when compared with CF. HDPE membrane posed the highest resistance to MP permeation from the buffer, this might be due to the structure of HDPE since it is not a branched cross-linked membrane, and therefore it has a more compact structure while also being poorly solvated by an aqueous solvent phase.

MP permeated faster through all membranes when presented in IPM (Figure 5.4). Since IPM was sorbed by all membranes, it tended to improve the partitioning and diffusion of all permeants. The oil sorbed by the membrane might therefore promote the permeation of the model permeant molecules through the modified matrix. IPM is therefore, likely to enhance the penetration of the model permeant across the membrane because the oil was taken up well into the membranes (Table 4.5), and the solubility of the permeants in IPM is relatively high. Therefore the high permeation through the membrane could be correlated with the solvent uptake of IPM (Tables 4.4 and 4.5). The confirmation of the importance of solvent uptake was demonstrated by the QSPR model; in

the flux model (Equation 5.4) it was shown that increasing the amount of oil sorbed (m_{upt}) by the membrane will lead to an increase in the flux. IPM has been reported previously to act as a good penetration enhancer for different drugs through silicone membrane (Dias et al., 2007; Liu et al., 2009; McAuley et al., 2009). A particularly novelty of the current study has been the study of alternative membranes of differing structure and physicochemical properties (e.g. solubility parameters) to silicone membrane. This was effected with a view to seeking to identify any parameters of the membrane that might be employed in a capacity to achieve parameterization during in vitro experiments to predict the diffusion of topically applied compounds to the more-difficult to acquire (and experimentally manipulated) skin.

As discussed previously HD, IHD and LP are oils constituted mainly of hydrocarbon chains, therefore there is no special interaction with the model permeants, and this is confirmed by the solubility results, since similar solubility values were achieved in the three vehicles (Table 3.1). The main difference between these oils was in their ability to interact with the membrane, described by the amount of oil sorbed into membranes (Table 4.4). The amount of oils sorbed by silicone membrane was in the order of IHD>HD>LP which was the same ranking for MP flux through silicone membrane from these oils. This identifies the existence of a correlation between the amount of oil sorbed by the membrane and amount of drug permeating through it, even if the compound demonstrates a similar solubility in both oils. The latter finding is compatible with the theory of a vehicle modifying the properties of a barrier membrane due to preferential uptake. Vehicles which are taken up by the membranes occupy a larger solvent fraction in the membrane and accordingly a larger overall amount of permeant might be expected to diffuse through the membrane. Also the properties of the membrane would change (a decrease in the resistance by providing a more extended molecular structure due to swelling) and this might also enhance the flux. Therefore higher fluxes of the permeant were determined when IHD was employed, when comparing only the hydrocarbon vehicles. A

positive correlation between the amount of drug in the membrane and the corresponding uptake of the vehicle has been previously reported (Oliveira et al., 2012b).

There was no significant difference in the amount of HD and IHD sorbed by PU membrane, and the flux results for MP from these vehicles through PU were similar. However, although there was also no significant difference in the amount of LP sorbed by the membrane (in comparison to IHD and HD), the fluxes of the permeants from LP were significantly lower than from the other oils. It is possible that the higher viscosity of LP compared to IHD and HD was a factor contributing to this difference. The LP viscosity is also hypothesized to affect the amount of MP permeating through HDPE membrane, where a lower amount of MP permeated through the membrane from LP even though the uptake of LP into HDPE was higher compared to HD.

BP was the most lipophilic of the model permeants that was employed, and therefore generally oily vehicles enhanced the permeation of BP through silicone and HDPE membranes compared to the buffer. This is likely to be due to the interaction of the oily vehicles with the hydrophobic membranes which leads to an enhancement in the BP flux. CF and MP are more likely to exhibit enhanced partitioning and diffusion through the relatively more hydrophilic PU membrane compared to BP. BP diffused markedly slower than MP and CF probably as a consequence of the low solubility of BP in buffer compared with the other two compounds. The comparatively greater lipophilicity of BP results in its lower affinity to the PU membrane, particularly following membrane hydration.

The highest amount of BP that permeated through silicone membranes was when IHD was the vehicle. The primary factor contributing to this enhancement is the high solvent uptake of IHD into silicone membrane. As described previously the relatively large amount of IHD that was sorbed by the membranes might lead to an opening-up of the polymer chains within the silicone membrane structure and

this could lead to an enhanced diffusivity of the permeant through the membrane. In addition since BP is a lipophilic permeant it could partition favourably into the lipophilic silicone membrane, especially following extensive uptake of the hydrocarbon vehicle.

IPM also provided a marked enhancement of BP diffusion through different membranes. BP has high solubility in IPM, and IPM was sorbed into different membranes, therefore it would have changed the properties of the membrane, leading to enhanced partitioning of the permeant from the donor into the membrane phase. The results of BP diffusion through HDPE and PU membranes show that although BP has higher solubility in IPM there was no significant difference between the flux of this permeant whether it is suspended in IPM or IHD. The importance of uptake of the vehicle into the membrane has been demonstrated previously, using ATR-FTIR spectroscopy (McAuley et al., 2010). In the latter study, permeation of the model permeant through silicone membrane was similar for two solvents. The greater extent of IPM uptake into the membrane enhanced the flux to overcome the effect of the greater solubility of the permeant in decanol. Similarly, the fluxes of BP from IPM and IHD through HDPE are significantly higher than from OA, LP and HD.

There was no significant difference between rate of diffusion of BP from OA through HDPE and PU membranes. This was attributed to the relatively high lipophilicity of BP and despite OA clearly modifying the properties of the PU membrane, BP did not partition favorably into the oil-modified membrane. All model permeants were highly soluble in OA compared with other vehicles; however the low OA sorption by the membranes correlated with lower diffusion rates; whilst there appeared less of an effect imposed by the increased solubility. Clearly both the solvent uptake and the solubility of permeant in the membrane affect the concentration of the permeant in the membrane at equilibrium (McAuley et al., 2010).

In an attempt to understand the effects of permeant-vehicle-membrane interactions in relation to the specific molecular properties of vehicles, permeants and membranes, multivariate data analysis was applied. Regression analysis was used to build a QSPR model and PCA was used to extract the important information from a set of data.

Since the variables used in the analysis have different numerical ranges. Before the analysis, the data were normalised and mean centered to confirm that all variables make the same contribution to the model. This improves the interpretability of the model. Then the descriptors were correlated to the dependent variable. In the QSPR and PCA some descriptors were removed in the correlation, for example the parameters relating to molecular volume and size; this was because the retained descriptors proved to be more correlated to the dependent variable. In addition, the excluded descriptors were correlated and explained by the descriptors used in the analysis. Therefore an effect relating to the original descriptors are still present in (and therefore making an impact upon) the analysis.

QSPR models were constructed for the flux of the permeants through membranes and Log K_p . An acceptable r^2 of the multiple regressions was achieved and the P-values were below 0.05. Each QSPR consisted of permeant descriptor, vehicle descriptor and combined vehicle-permeant or vehicle membrane descriptors. However due to the limited data size the QSPR of the solvent uptake failed. Most QSPR models are generated from data taken from different laboratories. Accordingly, unlike these earlier QSPR models, the data used in this study were consistent; all the experiments being conducted in the same laboratory under the same conditions, and this might decrease the error if the number of permeants were to be increased.

The generated QSPR models showed that the permeant, vehicle and membrane descriptors are important in determining the flux through synthetic membranes.

Therefore all of them should be taken into consideration when predicting permeation of topically applied compounds. A limitation of most of the previously generated models is that they only consider the permeant descriptors and ignore the effect of the physicochemical properties of the vehicle or the membrane under study on the permeant diffusion process (Potts and Guy 1992 & 1995; Lien & Gao, 1995; Pugh et al., 1996; Moss & Cronin, 2002; Lam et al., 2010). Such a restriction may impact upon the ability to develop representative models based on in-vitro experimental data.

Equations 5.4 and 5.6 shows that the hydrogen bond ability of the vehicle and membrane are important descriptors to predict the flux through synthetic membranes. The Log K_p model showed that the melting point of the permeant, which is related to the hydrogen bond ability of the permeant, has the highest coefficient (1.10 MPT_d) in determining the permeability coefficient through synthetic membranes. Also the melting point of the vehicle was one of the descriptors to determine the Log K_p . This indicated the importance of the hydrogen bonding of the vehicle, permeant and membrane in influencing the diffusion of permeants through synthetic membranes. The hydrogen bond donor ability of the vehicle ($-1.67 \sum \alpha^H$) was more important than the hydrogen bond acceptor ability ($-1.18 \sum \beta^H$). The importance of the hydrogen bond donor of the drug has been reported previously in human skin and silicone (Cronin et al., 1999; Geinoz et al., 2002). The present study confirms its importance for the drug, however, unlike previous studies, it has been shown here that the H-bonding behaviour of the vehicle is also a determinant of permeant flux across a barrier membrane.

In the current analysis the lipophilicity and hydrogen bonding were important determinants of diffusion through the synthetic membranes. However it is well documented that the Mwt is also important (Potts & Guy, 1992; Cronin et al., 1999) but this was a factor that was not investigated here because of the limited range of molecules employed in this study where compounds within a narrow

range of Mwt but with different lipophilicities were deliberately selected. This was a deliberate component of the initial experimental and hypothesis design in an attempt to effect a degree of consistency during, what was an attempt to pilot multivariate analytical methods for application to dermal permeation processes.

The amount of solvent sorbed into the membrane (m_{upt}) was positively correlated with the flux through membranes. This was also confirmed by the diffusion results, since as mentioned previously a correlation was found between the amount of vehicle sorbed and the flux. The lipophilicity of the vehicle was an important descriptor in determining both the flux and permeability coefficient of a permeant from a vehicle donor across barrier membranes.

The shape and size of the permeant and vehicle (χ_0 permeant and opr-brigid vehicle) were also important descriptors for determining $\log K_p$. The coefficients were -0.44 χ_0 permeant and -0.54 opr-brigid vehicle, respectively. The negative sign indicates that increasing the size or number of rigid bonds would lead to lower permeability of a permeant. Therefore the smaller flexible molecules will permeate the membranes more easily than large, rigid permeants. High flexibility leads to higher mobility and rotational freedom (Lemont & Kier, 1989), and it should be borne in mind that the size and flexibility of vehicle molecular components will also determine the degree to which vehicles can partition into (and modify the properties of) barrier membranes. This might elucidate the preferential uptake of IHD into synthetic membranes when compared with HD.

In order to understand the effect of the descriptors on the solvent uptake and diffusion through membranes, PCA was conducted examining solvent uptake, flux, K_p and lag time of the diffusion of model permeants through membranes. In addition it was performed on the diffusion of model permeants through the epidermis.

In all correlations, the solubility of the permeant in the oil was an important descriptor (Table 5.5). This was expected since the permeant must have sufficient solubility in order to diffuse through the membranes, and particularly so in the case of a vehicle-modified membrane. Previous studies have shown the importance of the drug solubility in the vehicles which are sorbed by the membrane (Dias et al., 2001; McAuley et al. 2010). The $\text{Log } K_{o/w}$ of the vehicle has been reported to be an important descriptor for describing the solvent uptake and K_p and previous QSPR models have also used $\text{Log } K_{o/w}$ of the permeants as a descriptor for $\text{Log } K_p$ (Potts & Guy, 1992; Lien & Gao, 1995; Moss & Cronin, 2002). The hydrogen bonding ability of the vehicle and the δ_H of the membranes play a role in the flux of the selected permeants through the different membranes. Generally the oils used had a wide range of values for δ_H (0-6.2) $\text{MPa}^{1/2}$ compared with δ_D (14.7-16) $\text{MPa}^{1/2}$ and δ_P . (0-2.8) $\text{MPa}^{1/2}$. Cronin and others have developed a QSPR model for the prediction of the maximum steady state flux through the silicone membrane ($\text{Log } J$), in which the number of hydrogen bond acceptor and donor groups for the permeant were important descriptors in their model (Cronin et al., 1998).

Six vehicle descriptors described the behaviour of the solvent uptake and K_p , five of them were identical in the solvent uptake and K_p : ($\text{Log } K_{o/w}$, molecular connectivity index, opr_brigid , distance and chi0 descriptors). This might indicate that the behaviour of the vehicle in solvent uptake is similar to it in the K_p . The difference in the general distributions in the two plots is due to the existence of the permeant descriptors in the case of K_p .

In the PCA plots of solvent uptake and K_p (Figures 5.11 and 5.13 respectively) OA and IPM were clustered together and exhibited similar behaviour in terms of influencing membrane uptake and K_p . HD and IHD each displayed unique behaviour with the descriptors that are highly loaded on PC1 and PC2 being able to separate the two oils. This finding could be because although OA and IPM have similar values of the molecular descriptors that influence both solvent uptake

and K_p , they are different for IHD and HD. The descriptors in question were δ_D and molecular connectivity index for solvent uptake; and molecular connectivity index and $\text{Log } K_{o/w}$ for K_p . Since the main descriptors that were highly loaded on PC1 and PC2 are only related to the vehicle no special separation for the membranes or permeants was seen in the score plot.

In the flux score plot (Figure 5.12) there were four main groups. The main descriptors that explained the variance were able to separate the behaviour of each vehicle. As mentioned previously this is because the combination of the values of each vehicle was different for the main descriptors. The descriptors were H-bond acceptor ability, solubility and $\text{Log } K_{o/w}$. In the PCA of lag time (Figure 5.14), the data were scattered across the plot. Both χ_{i1} and δ_T permeant were the main descriptors contributing to the explanation of the variance captured by both PC1 and PC2. Since the latter descriptors are inherently related to both the vehicle and permeant, the clustering that was found was attributable to both of these components. However although the descriptors were able to separate the behaviour of BP, the descriptors for MP and CF were clustered together. In the case of permeant flux analysis, therefore, the PCA accommodated both permeant and vehicle properties in explaining the complex interactions during permeation across the membranes.

Diffusion studies of model permeants through the epidermis were conducted to study the effect of the oily vehicle on the diffusion through skin. Molecules are thought to transverse the skin by one of the three main pathways: the polar, non-polar or polar/non-polar pathways, the relative importance of each being dependent upon their physicochemical properties (Section 1.2). The molecular weight and the $\text{Log } K_{o/w}$ can be used to predict its distribution within a biological system (Potts & Guy, 1992). The diffusion law predicts an inverse relationship between membrane diffusivity and permeant size (Lieb & Stein, 1971). Since the three permeants selected for this study have similar molecular weights, their rates of permeation through skin might be expected to correlate with their $\text{Log } K_{o/w}$

values. An ideal candidate for transdermal delivery should ideally possess Log $K_{o/w}$ values between 1 and 3 in order for high fluxes through the skin to be achieved (Yano et al., 1986; Potts & Francoeur, 1991; Lee et al., 1994). Therefore MP would be expected to be the best candidate in this context (with its Log $K_{o/w}$ being 1.96), since BP is more hydrophobic, in terms of its Log $K_{o/w}$ (3.57) and CF more hydrophilic Log $K_{o/w}$ (-0.07). However, in light of the analysis using a range of model membranes, permeants and vehicles above, it was deemed appropriate to also perform multivariate analysis accommodating a wider range of physicochemical parameters in estimating permeant flux across epidermis.

The flux of the model permeants (MP>BP>CF) from the buffer across human epidermis, reflected the differences in lipophilicity of each of the permeant and the ease of the compounds in traversing the skin barrier. The physicochemical properties of MP promote its ability to traverse the lipophilic and hydrophilic regions of the stratum corneum as well as the more hydrophilic components of the underlying epidermis (Soni et al., 2002). Despite its moderate hydrophilicity, its principal diffusion pathway is presumed to be through the relatively non-polar lipid route of the stratum corneum. BP is also expected to penetrate the skin by this route. Previous studies involving the use of normal (intact) and de-lipidised guinea pig skin concluded that penetration of parabens tended to occur primarily via the lipoidal pathway obeying a parabolic relationship as a function of lipophilicity (Kitagawa et al. 1997). The trend of parabens flux in this study was consistent with the previous findings.

Treffel et al. (1992), suggested the main route of CF permeation through skin was via the transcellular keratin matrix, due to the inability of occlusion to enhance CF skin absorption. However, CF has also been proposed to traverse the skin via the lipoidal pathway (Dias et al., 1999). These findings could suggest that CF permeation across skin involves multiple pathways. The slower permeation profiles of CF, compared with the parabens, would be expected, due

to the difficulties associated with hydrophilic compounds traversing the lipophilic stratum corneum. This is confirmed by the results obtained in the current studies which demonstrated the lower fluxes obtained for CF from the vehicles compared to those found for the two other permeants.

All oily vehicles enhanced the permeation of the model permeants through the human epidermis relative to the buffer. The factors affecting the diffusion of permeants from these vehicles may include differences in either (i) vehicle–skin effects and/or (ii) permeant–vehicle affinity. Using a cellulose acetate nitrate membrane (non-rate limiting), it was shown that all permeants were readily released from the vehicles (Figure 3.2, 3.3 Table 3.3). This may imply that differences in diffusion are likely to be attributable to the interaction of the oily components with the membrane; since saturated systems were used in all cases (Barry et al., 1985; Twist & Zatz, 1986). The highest permeation was attained using IHD. IHD is highly branched molecule which is more flexible than other vehicles (Kier, 1989). Such results support the hypothesis that shape and size of the vehicle is a key determinant in any modification of epidermal structure brought about by sorption of the oil. Such modification may enhance the permeation of all permeants including the more hydrophilic CF.

Among the possible effects of hydrocarbons on the skin is the increased fluidity that might be imparted to the intercellular lipid layer by their presence and the possible extraction of lipids and/or other components that could occur (Rahman et al., 1992). Without the specific effects of the vehicle on the skin, the equivalent thermodynamic activity produces very similar permeation rates of the drug across skin (Barry et al., 1985; Twist & Zatz 1986). Diffusion would appear therefore to be highly dependent on the uptake of the vehicle and solubility of the permeant in that sorbed vehicle. However in the current study all permeants have a poorer solubility in IHD compared with OA and IPM. Nevertheless IHD was highly taken up to a greater extent by the hydrophobic synthetic membranes employed in this study, although the HSP distance between IHD and the

membranes was the highest comparatively. However, since all factors should be taken into consideration, IHD might have been taken up in greater amounts because of its high flexibility, small size and spherical shape. The enhanced flux of the model permeants with different lipophilicity indicated that IHD might be affecting the structure of the stratum corneum and reducing its resistance.

LP which is also a hydrocarbon (a mixture of liquid hydrocarbons from petroleum) appeared to have the least interaction with the human epidermis; this is consistent with the lower flux values of the permeants from this vehicle. LP has been reported to interact weakly with mouse skin compared with other vehicles (Roberts et al., 1975; Rahman et al., 1992). The fluxes of MP and CF were similar from LP to those from HD; whereas BP diffusion from HD was significantly higher than from LP. This indicates that HD might improve the flux of the lipophilic compounds. HD and IHD were used together in this study in order to investigate the effect of structure, ovality and flexibility of the vehicle on the penetration. Since all permeants have similar solubility and interaction with both vehicles, the difference in the flux is most likely due to the difference in interaction of the vehicles with the skin. It is interesting that the fluxes of all permeants were greater from IHD than from HD. Both vehicles are hydrocarbons and, as a consequence, do not have specific functional groups that could interact with the skin differently. This might suggest again that the interaction between IHD and skin is mainly attributed to its structure, flexibility and shape. This assumption was confirmed by the PCA of the flux of model permeants through the epidermis where *kier flex* and *opr-birgid* were explaining part of the total variance explained by both PC1 and PC2. In addition the chi descriptors, which are related to the size and shape of the molecule, were also correlated with the flux through synthetic membranes.

The distance between the HSP values of the skin and OA or IPM is smaller compared with IHD. This suggests that these two oils might be expected to be better vehicles for the skin when compared with IHD. However IPM and OA are

less flexible comparatively and have two hydrogen bonding acceptor groups (and OA also has a hydrogen donor group). In addition the molecular volumes of these two oils are greater than molecular volume of IHD. Therefore taking all these factors into consideration IHD appeared to act as a better enhancer for the diffusion of the model permeants through the epidermis.

OA enhanced the permeation of the three model permeants through the epidermis compared with that from the buffer. However IPM and IHD were comparatively better enhancers than OA for MP diffusion through epidermis. Although all permeants yielded higher flux values from IPM through synthetic membranes compared with from OA, there proved to be no significant difference between the fluxes of CF from IPM and OA through the epidermis. The same behaviour was seen with BP, however this was not the case with MP, the flux of MP from IPM as a vehicle was significantly higher than from OA. OA has been reported to function by partitioning into the lipid regions of the stratum corneum, disrupting the structure and lipid fluidity of the stratum corneum (Kim et al., 1993). Barry (1987) explored the mechanism of OA as a penetration enhancer using differential scanning calorimetry of human stratum corneum. OA was demonstrated to 'melt' the lipid chain portion buried within the bilayer structure together with some non-polar material. It is also thought to break associations between lipid polar groups together with disruption of cholesterol-stiffened regions. It is hypothesized that the *cis* double bond at C9 on OA causes a kink in the alkyl chain, which is likely to disrupt the ordered array of the predominantly saturated straight chain skin lipids and increase the fluidity of the lipid regions (Barry, 1987; Golden et al., 1987). In order for long-chained fatty acids including OA to induce the maximum disruption of lipids, they should be applied in a hydrophilic polar vehicle such as propylene glycol (Wang et al., 2004). OA has also been blended with ethanol and the maximum lipid disorder occurred at 1% OA and no additional disorder was induced by increasing the OA concentration to 10% (Mak et al., 1990). However in this study OA was not blended with any

other hydrophilic vehicle, only the effect of the pure oily vehicle structure, and the characteristics and descriptors of the oil itself are being studied.

IPM has been widely used as a penetration enhancer in previous studies and has shown to be superior when compared with other vehicles (Gwak & Chun, 2002; Dias et al., 2007; Rhee et al., 2007; Oliveira, et al., 2012b; Santos et al., 2012). The sorption of IPM by the stratum corneum has been reported also (Oliveira, et al., 2012b). Since the permeation of any drug through different membranes depends on the interaction of the vehicle with the membrane; therefore IPM is a good vehicle for the selected permeants. High fluxes of MP and BP have been achieved from IPM due to its ability to modify the membrane after the sorption of the oil. Previous studies found a linear correlation between the amount of drugs partitioning into the membranes, solvent uptake and the concentration of the solute in the vehicle (Twist & Zatz, 1988 & 1990; Shah et al., 1993; Dias et al., 2001; Dias et al., 2004). Despite the proven capacity of IPM to enhance permeation through skin, and the weaker ability of LP, both vehicles increased the permeation of CF to a similar extent. Similar results have been noted previously by other authors (Dias et al., 2007).

When CF was suspended in IPM, OA, HD and LP similar results were obtained for its diffusion through epidermis, while CF diffusion from IHD was significantly higher. However when model membranes were used the flux of CF from IPM was significantly enhanced compared to the flux from all other vehicles. Such a contrast in the results obtained using the model membranes and epidermis was also apparent for CF diffusion from OA. OA enhanced the permeation of the model permeants through the skin but it was less effective using the model membranes. This could be due to its shape since as outlined above; OA can disturb the lipids of the skin whilst it is relatively poorly sorbed into the synthetic membranes. Cross-linked polymers chains are joined by strong covalent bonds. The solvent can intercalate between the macromolecular chains and solvate the polymer, leading to membrane swelling. Since OA has a

relatively large structure it might not easily enter into these spaces, between the polymer molecules. On the other hand it more readily enters between the skin lipids, which are formed mainly from: ceramides, cholesterol, and saturated long chain free fatty acids which are packed together (Section 1.1.2.2). As discussed above OA (which shows molecular structure similarity to stratum corneum lipids) can then integrate into the highly ordered packing of the lipid bilayers and the central position of the double bond can lead to an increase in its potential in lipid order disruption. Other authors have noted the non-specificity of the effect of some vehicles on the model membranes and skin (Cross et al., 2001; Dias et al., 2007).

Multivariate data analysis was also applied to the epidermis diffusion data to understand the effects of permeant-vehicle-epidermis interaction. Regression analysis was used to build a QSPR model but because of the limited data size the development of a QSPR model of permeant flux through epidermis failed.

Some key descriptors used to account for the permeation of compounds through epidermis proved to be different to those identified for synthetic membranes. For example, chi descriptors remained after the correlation of synthetic membrane dependent variables, while Kier flex remained after the correlation with the epidermis flux; therefore the chi descriptors were found in the PCA of the membranes while the Kier flex descriptor was found in the epidermis PCA. Both descriptors are related to each other, both of them are topological descriptors related to the shape and branching of the structure. The chi descriptors do also encode the size of the molecule, whilst the Kier flex values (Kier molecular flexibility index) account for the structural features aiding in the flexibility of the molecules, which are: (i) few atoms, (ii) the presence of cycles (iii) the presence of branching.

The behaviour of the data presented in the score plot of the flux through epidermis (Figure 5.15) was different to those derived using synthetic

membranes. A typified trend was seen for each vehicle and membrane, however this trend was broken by BP in IPM; this might be as a consequence of the high solubility of BP in this oil. The scattering of the data was because the main descriptors to describe the variance (density, solubility, Chi_C permeant) were able to separate the behavior of vehicles and permeants.

The vehicle descriptors were the dominant terms in explaining the variance of the diffusion through the synthetic membranes as compared with the epidermis PCA. Also in the PCA score plots of the data relating to synthetic membranes, clustering is apparent according to the specific vehicle employed, regardless the membrane and permeant used. However this was not the case with the epidermis PCA plots. The data were distributed along the plot and no special clustering was seen and therefore both the permeant and vehicle descriptors were of importance.

The chi descriptors (chi0 and chi0_C) and the opr_nring descriptors for the permeant were important defining the flux of the compounds through epidermis. The chi descriptors were also correlated to the K_p of synthetic membranes, and this might indicate that the permeant shape, size and flexibility is an important factor in the diffusion through epidermis in the limited number of permeants used. Three descriptors related to the vehicle were important in the epidermis flux, density, opr_brigid and Kier flex, two of these being related to the flexibility of the vehicle. These results indicate that, for the permeants and vehicles that were employed in the current study, the flexibility of the molecules was an important factor to consider in molecules capable of traversing the human epidermis. However this tentative conclusion requires further study using a wider dataset, to confirm the results and produce a more robust model.

The highest flux values for all model permeants were obtained when the compounds were suspended in IHD. Branched molecules are smaller and more compact in size and they have higher flexibility (lower Kier flex) which might increase their mobility and ease their uptake into different membranes, this will

have a positive effect on promoting the diffusion of different permeants. The diffusion of model permeants through the membranes was in most instances correlated with the solvent uptake into the different membranes. IHD was sorbed into different membranes enhancing the diffusion of permeants, the high fluxes of model permeants through the epidermis when IHD was the vehicle, indicates that it might be sorbed by the epidermis and in turn modify the properties of the membrane. However a wider range of branched vehicles need to be studied in order to confirm whether molecular branching truly has an effect on membrane permeation.

It is well established that the preferential diffusion of one drug over the other is dependent upon the lipophilicity, size and hydrogen bond ability of the drug. The PCA of the epidermis flux (Figure 5.15) showed that the chi descriptors (chi0 and chi0_C) and the opr_nring descriptors for the permeant were important descriptors in explaining the variance in the flux results obtained using epidermis. These descriptors encode the size, shape and flexibility of the permeant. The shape and flexibility have not been taken into consideration in previous models. Including these descriptors with the lipophilicity and hydrogen bonding ability in QSPR models might improve the correlations obtained in future developed QSPR models.

In conclusion, these results show that the use of synthetic membranes to determine the flux of permeants from oils should be treated with care. This is because the oils can interact differently with each of the membranes and alter the diffusion of each compound. The shape of the oil molecule affects its uptake into the membrane and the subsequent interaction with either synthetic or epidermal membrane. The diffusion results showed that the vehicles containing the highest molecular branching tended to promote the permeability of the model compounds employed. Molecular branching leads to a more spherical molecular shape with a higher flexibility, and ultimately sorption in high amounts by the membranes. The fluxes of concomitantly applied permeants were then modified.

Multivariate analysis confirms that the vehicle, the membrane and the permeant should be considered when determining permeability. This strategy of monitoring the diffusion of permeant across synthetic membranes might prove useful in selecting the optimum vehicle for delivery, after the model here is more fully developed.

CHAPTER SIX
GENERAL DISCUSSION

6.1. General Discussion

Transdermal delivery offers a number of potential advantages over more traditional drug delivery methods (Hadgraft & Guy, 1989; Smith & Maibach, 1995; Guy, 1996). However the skin is an efficient barrier, which prevents both excessive water loss from the body and the ingress of xenobiotics (Hadgraft, 2001). The first transdermal patch, which contained scopolamine, was granted a licence by the FDA in 1979 (Langer, 2004). It comprised a small reservoir type patch where the drug was dispersed in liquid and this suspension sealed between an impermeable backing layer and a rate-controlling membrane. The membrane was adhered directly to the skin surface and was responsible for the sustained delivery of the drug. However, since then fewer than two dozen of drugs have been approved by the regulatory authorities for transdermal administration (Gratieri et al., 2013). This short list of “deliverable” drugs highlights the physicochemical restrictions imposed on skin delivery.

In order to fully explore the potential benefits of the transdermal route for drug delivery, the number of potential drug candidates that might reach the circulation in sufficient amounts so as to attain therapeutic efficacy has to be increased. Accordingly, various enhancement strategies designed to overcome the permeability barrier of stratum corneum have begun to emerge, and these can be categorised into passive and active methods. The passive approach relies upon optimising the formulation in order to provide an improved driving force to increase the rate of transport and the permeability of the skin to the agent (i.e. modify the formulation in some way) (Gratieri et al., 2013). Examples of this strategy include the use of penetration enhancers, prodrugs, lipid vesicles and supersaturated systems. Active methods normally involve physical or mechanical methods of enhancing delivery, and they aim to modify the properties of the microenvironment through which permeation must occur (i.e. act on the stratum corneum) (Gratieri et al., 2013). Active strategies include the use of iontophoresis, electroporation, radio frequency and needleless injection.

Drug permeation through membranes will often be dependent upon both the physicochemical properties of the drug and those of the vehicle comprising the formulation. The use of vehicles that are sorbed by the membrane, which might also interact with components of the membrane, might induce changes in the physicochemical properties of the membrane. Such an action might be expected to modulate the transport rate of permeants, and is a common strategy when seeking to improve dermal delivery (Williams & Barry, 2004). Additionally, penetration-enhancing chemical agents are often co-formulated in the vehicle, which serve to improve the permeability of the epidermal barrier to xenobiotics. The understanding of vehicle-membrane interactions is therefore a critical step not only in the selection of an optimal penetration enhancer but also a prime factor affecting formulation design. Investigation of possible membrane-vehicle interaction, using solvent uptake, and then seeking to correlate this with the effect on drug permeation, has been employed by a number of previous workers, although almost exclusively employing aqueous- and alcoholic-based vehicles. Their findings have shown that high solvent sorption can alter the physicochemical properties of the membrane and result in changes to the partition and diffusion properties of the drug, leading to a modified permeation (Most, 1972; Twist & Zatz, 1988 & 1990; Cross et al., 2001; Dias et al., 2007; McAuley et al., 2010; Oliveira et al., 2010; Zhang et al., 2011). Nevertheless, oily vehicles have received little attention despite their inclusion as vehicle components in many topical formulations.

Oils have been incorporated into transdermal and cosmetic preparations since ancient times. In most preparations oils are thought to be inert, being integrated for the purpose of providing a matrix or medium for the formulation, although sometimes they are used to dissolve the drug or act as phase modifiers for organoleptic properties. The effect of combining two oils within a vehicle, applying that vehicle topically to the membrane and then considering the interaction of those oils with membranes and the possible effects on permeants

presented in the formulation has not previously been studied, despite the common practice (especially within cosmetic formulations) to blend oily vehicles to enhance organoleptic properties. Little attention has also been given to the ability of the oils included in cosmetic and topical products to enhance the unwanted permeation of formulation ingredients for example preservatives.

The vehicles investigated in this present study are oils which have been used previously either in transdermal delivery or cosmetic products and are generally regarded as safe (GRAS). Oleic acid (OA) and isopropyl myristate (IPM) have been previously used in transdermal formulations to enhance drug delivery whereas although hexadecane (HD) and isohexadecane (IHD) have both been used in cosmetic products, their ability to enhance drug permeation has not been studied previously. Liquid paraffin (LP) has been used in both transdermal and cosmetic preparations. The potential of these selected oily vehicles to promote the diffusion of model solutes with different physicochemical properties through synthetic and human epidermis was investigated in this present study. Equal thermodynamic activity of the incorporated permeant was maintained in the Franz cell donor chamber in all experiments. This was to ensure that effects associated with the enhancement could be solely attributed to the effect of the vehicle on the membrane, rather than to changes in the activity of the permeant within the vehicle.

The use of human skin for studying the effect of formulation components is associated with several difficulties and limitations, the biological nature of the skin is complex compared with membranes, and furthermore there is extremely large inter- and intra-individual variability of skin samples. Artificial model membranes can be used as simple and reproducible alternatives to study the effect of vehicles on the mechanisms of drug permeation, when seeking to understand the basic phenomenon of possible vehicle interaction with, and drug permeation through, human skin. The use of membrane models to screen transdermal formulations and assess their possible contribution to the overall

mechanisms of drug transport across human skin is well documented in the literature (Nakano & Patel, 1970; Twist & Zatz, 1988; Pellett et al., 1997; Cross et al., 2001; Yang et al., 2004; Chen et al., 2007; Dias et al., 2007a; Watkinson et al., 2009 a&b; Oliveira et al., 2010; Santos et al., 2011).

With a view to investigating the release of model permeants, from an oil or oil blend, cellulose acetate nitrate membrane was used. In models using such a porous membrane, the permeants would be expected to partition from the oily vehicle into the receptor compartment through the buffer filled pores. Since this comprises a partitioning process the difference in the amount of drug released from the different blends is attributed to the difference in the activity coefficient (γ) of the drugs in the different vehicles, and the difference of the solubility and partitioning properties of the drug between the oil and buffer. However this outline of the diffusion process might be simplistic since it is possible: 1) that the oils (such as OA and IPM) might interact with the buffer filling the pores of the membrane, 2) the oil might displace some or all of the buffer bound to the pores, or 3) an interaction might occur between the membrane matrix and oily vehicle changing the pore size of the membrane. Since sink conditions were maintained throughout the experiment the partitioning process of the parabens did not reach equilibrium and the amount released continued to increase with time and would have been expected to be relatively unaffected by previous diffused compound. However in contrast to the parabens, CF release stopped after approximately three hours, and this was attributed to the high solubility of CF in the buffer compared with its low dissolution in the oily donor compartment, therefore the amount lost by release may not have been quickly restored from the particles suspended within the oil.

In order to investigate any interaction between the oily vehicles and the membranes, diffusion studies were conducted through non-porous membranes employing saturated solution of the model permeants. The fluxes of a permeant from saturated solutions, despite the permeants displaying different solubilities,

are expected to be the same unless the vehicle interacts with the membrane. Different flux values were obtained for each of the permeants from the different vehicles, confirming that there might be some interaction of the different vehicles with the membrane. The use of IHD which has a branched structure was found to produce high penetrant flux values when compared with HD, which is its linear counterpart. These latter two oils were blended with IPM and LP in different ratios to study the effect of structure on the diffusion of model permeants through silicone membrane. In all formulations IHD blends yielded higher flux values compared with HD blends. In addition blends containing IPM yielded higher flux values. The flux of BP was increased as the ratio of IHD was increased when the latter was blended with any other oil. This relationship was found to be the same for MP and CF in IHD blends containing HD, LP and OA; whereas in contrast when IPM was blended with IHD, as the content of IHD decreased then the fluxes of MP and CF increased.

Since all formulations had the same thermodynamic activity, the difference in the flux values might be attributed to the solvent being sorbed by the membrane leading to the properties of the latter being modified. Oil uptake by the membranes was determined gravimetrically; the oils being sorbed in different amounts into the different membranes. When blends of oils were applied it was hypothesised that preferential sorption of one of the oily components over the other might occur. If this were the case, then, the diffusion of a penetrant would depend on the nature of the membrane and the solvent within that membrane, therefore permeation might be affected by one vehicle more than the other. Furthermore, in some cases if one vehicle permeates the membrane more than the other, the thermodynamic activity of the drug in the donor compartment might be altered. Therefore silicone membrane was soaked in different oil blends and subsequently the sorbed oils were extracted and quantified by an appropriate gas chromatographic method. The results showed that in some cases the ratio of oils in the silicone membrane was not the same as the ratio in the original solution i.e. one vehicle was preferentially sorbed at the expense of the other.

However in other cases both oils were sorbed in the same ratio as in the original applied solution. The amount of oil sorbed into silicone from simulated Franz cell diffusion experiment, using different oil blends was also quantified, by assessing changes to the ratio of HD:IHD in the donor oil phase. The results of these experiments indicated that the oils (IHD and HD) were sorbed in different ratios during diffusion studies and hence would likely affect the partition and diffusion of model permeants through the modified membrane. The effect of oil sorbed to the membrane on the diffusion of a model permeant (MP) was also studied, by conducting a diffusion study of the permeant from buffer as a vehicle through silicone membrane soaked (i.e. pre-treated) with oils. The enhanced permeation of MP confirmed that the membrane had been modified by the oils.

In order to investigate the parameters that might affect the uptake and diffusion process through synthetic membranes, and also the diffusion of the model permeants through human epidermis, multivariate analysis (QSPR and PCA) on the available data were performed. Previous studies (Flynn, 1990; Potts & Guy, 1992; Wilschut et al., 1995; Pugh et al., 1996; Moss et al., 2002) have highlighted a range of permeant molecular properties that can be predictive of the extent of molecular transport across epidermal membranes. The current study has demonstrated the need to consider physicochemical properties of vehicle components, to understand vehicle uptake into the barrier membrane and consequent alteration of barrier properties. Therefore investigation of permeant flux requires an understanding of the physicochemical factors influencing interactions between vehicles, membranes (or vehicle-modified membranes) and permeants such as drug molecules. Multivariate statistics are statistical techniques that allow examination of the relationship between several variables simultaneously. Therefore it aids to obtain an overview of the relationship between different independent variables and a dependent variable. In this study the vehicle, permeant, membrane descriptors and interactions between different combinations of all three were analysed against different dependents. The results showed that the diffusion process was influenced by the drug, vehicle and

membrane descriptors. All factors which were identified as having an effect were found to be related to each other and should be considered when a formulation is designed. The interpretation of diffusion results involving the placing of weight on any one individual descriptor cannot provide an understanding of the uptake and diffusion behaviour.

The solubility of the permeant in the vehicle and the size, branching and flexibility of the oil were identified as important descriptors that can contribute to the process of permeant diffusion through both the synthetic membranes and human epidermis. The branching and flexibility descriptors were also of importance when considering the vehicle uptake into membranes, permeability coefficient and lag time. These results indicate that the shape and flexibility should be taken into consideration either in formulation design or in choosing a vehicle for the formulations.

The amount of solvent sorbed to the membrane affected the diffusion, permeability coefficient and lag time of permeants through the synthetic membranes. The diffusion, QSPR and PCA results confirmed the correlation between the diffusion and solvent uptake, therefore when the drug is intended to permeate the skin it may be advantageous to use a vehicle that is sorbed by the skin. On the other hand care should be taken when preparing topical and cosmetic formulations designed for localized function or use.

The key descriptor related to the membrane was the distance between the Hansen solubility parameter values; this descriptor was important in determining the solvent uptake, diffusion, permeability coefficient and lag time. The smaller the value of the distance then the higher uptake and interaction between the vehicle and membrane, could predispose an enhancement in the diffusion of the permeant. However, since the diffusion and uptake is related to all descriptors, of the drug, vehicle and membrane, such a 'distance rule' was not obeyed in all vehicle-membrane interactions.

The QSPR of solvent uptake failed due to the limited data size, therefore a single equation could not describe the data. This was not the case with Log K_p and flux where an equation was found describing the available data. The data used in the QSPR were consistent since all experiments were made in the same laboratory under the same conditions. This would be expected to decrease the chances of the experimental errors in the QSPR data. The multivariate analysis technique could not be applied to the blends, since (as was proven by the solvent uptake experiments) there was preferential uptake of some oils from an applied blend and therefore the oil sorbed would modify the membrane in a non-linear way.

Further studies to include a wider range of permeants and vehicles are needed to produce more data which would lead to a more robust modeling and QSPR. In addition, a wider range of membranes is needed in order to probe further a more robust correlation with that obtained using human epidermis diffusion. The drug and vehicle descriptors should be taken into consideration when preparing future formulations, in order to identify the most appropriate vehicle combination. Further studies should be carried out using topically relevant drugs such as steroids, incorporating the further use of synthetic membrane(s) and human stratum corneum. In due course it might then be possible to conduct *in vivo* trials employing the most promising formulations identified on the basis of these *in vitro* studies.

In summary it is concluded that the novel approach of using multivariate analysis was found to be promising in understanding the interaction and diffusion behaviour of permeants from oily vehicles through synthetic membranes and human epidermis. The diffusion through synthetic membranes was found to be dependent upon the amount of oil sorbed by the membranes. Some of the oils that are currently widely used in cosmetics were found to enhance parabens permeation, which are currently used as preservatives in topical formulations. However, these preservatives have been reported to have a degree of associated

carcinogenicity (Darbre et al., 2004), if they permeate into the skin in sufficient quantities. In addition, should the vehicle contain a blend of oils in the formulation then these may be sorbed in different quantities to those present in the applied vehicle. Therefore some care should be exercised when developing blended products. Further PCA analysis is expected to improve the understanding of drug-vehicle-membrane interaction but clearly drug, vehicle and membrane descriptors have to be taken into account when modeling the permeability of membranes to drug and other xenobiotic molecules.

APPENDICES

Appendix I: Definitions of molecular descriptors used in PCA analysis

The molecular descriptors used in PCA analysis were determined using Molecular Operating Environment 2012, produced by Chemical Computing Group Inc., Montreal, Canada. and by HSPiP software version 4.0.04

Table A1.1 Descriptions of PCA and QSPR descriptors

Code	Description
Solvent uptake	Amount of oil sorbed by membrane
solubility	Solubility of the permeants in the oil
density	Molecular mass density: Weight divided by vdw_vol (amu/Å ³).
Weight	Molecular weight (including implicit hydrogens) in atomic mass units with atomic weights taken from (Lide.& Frederikse, 1994).
Mpoint	Melting point
δ_D	The dispersive component of HSP
δ_P	The polar component of HSP
δ_H	The hydrogen bond component of HSP
δ_T	Hildebrand solubility parameter
LogP(o/w)	Log of the octanol/water partition coefficient (including implicit hydrogens). This property is calculated from a linear atom type model with $r^2 = 0.931$, RMSE=0.393 on 1,827 molecules.
SlogP	Log of the octanol/water partition coefficient (including implicit hydrogens). This property is an atomic contribution model that calculates LogP from the given structure; i.e., the correct protonation state (washed structures). Results may vary from the LogP(o/w) descriptor. The training set for SlogP was ~7000 structures.
ovality	A measure of how the shape of a molecule approaches an oval shape

Table A1.1 Descriptions of PCA and QSPR descriptors (continued)

Mwt	Molecular weight
Mvol	Molecular volume
TPSA	Polar surface area (\AA^2) calculated using group contributions to approximate the polar surface area from connection table information only. The parameterization is that of Ertl et al. [Ertl 2000].
vdw_vol	van der Waals volume (\AA^3) calculated using a connection table approximation.
vdw_area	Area of van der Waals surface (\AA^2) calculated using a connection table approximation.
a_nH	Number of hydrogen atoms (including implicit hydrogens). This is calculated as the sum of h_i over all non-trivial atoms i plus the number of non-trivial hydrogen atoms.
a_nC	Number of carbon atoms: $\#\{Z_i \mid Z_i = 6\}$.
a_nO	Number of oxygen atoms: $\#\{Z_i \mid Z_i = 8\}$.
b_1rotN	Number of rotatable single bonds. Conjugated single bonds are not included (e.g., ester and peptide bonds).
b_1rotR	Fraction of rotatable single bonds: b_{1rotN} divided by b_{heavy} .
b_ar	Number of aromatic bonds.
b_count	Number of bonds (including implicit hydrogens). This is calculated as the sum of $(d_i/2 + h_i)$ over all non-trivial atoms i .
b_double	Number of double bonds. Aromatic bonds are not considered to be double bonds.
b_rotN	Number of rotatable bonds. A bond is rotatable if it has order 1, is not in a ring, and has at least two heavy neighbors.
b_rotR	Fraction of rotatable bonds: b_{rotN} divided by b_{heavy} .
b_single	Number of single bonds (including implicit hydrogens). Aromatic bonds are not considered to be single bonds.
lip_acc	The number of O and N atoms.
lip_don	The number of OH and NH atoms.
opr_brigid	The number of rigid bonds from [Oprea 2000].

A1.1 Descriptions of PCA and QSPR descriptors (continued)

opr_nring	The number of ring bonds from [Oprea 2000].
opr_nrot	The number of rotatable bonds from [Oprea 2000].
chi0	Atomic connectivity index (order 0) from [Hall 1991] and [Hall 1977]. This is calculated as the sum of $1/\sqrt{d_i}$ over all heavy atoms i with $d_i > 0$.
chi0_C	Carbon connectivity index (order 0). This is calculated as the sum of $1/\sqrt{d_i}$ over all carbon atoms i with $d_i > 0$.
chi1	Atomic connectivity index (order 1) from [Hall 1991] and [Hall 1977]. This is calculated as the sum of $1/\sqrt{d_i d_j}$ over all bonds between heavy atoms i and j where $i < j$.
chi1_C	Carbon connectivity index (order 1). This is calculated as the sum of $1/\sqrt{d_i d_j}$ over all bonds between carbon atoms i and j where $i < j$.
chi0v	Atomic valence connectivity index (order 0) from [Hall 1991] and [Hall 1977]. This is calculated as the sum of $1/\sqrt{v_i}$ over all heavy atoms i with $v_i > 0$.
chi0v_C	Carbon valence connectivity index (order 0). This is calculated as the sum of $1/\sqrt{v_i}$ over all carbon atoms i with $v_i > 0$.
Kier1	First kappa shape index: $(n-1)^2 / m^2$ [Hall 1991].
Kier2	Second kappa shape index: $(n-1)^2 / m^2$ [Hall 1991].
Kier3	Third kappa shape index: $(n-1)(n-3)^2 / p^2$ for odd n , and $(n-3)(n-2)^2 / p^2$ for even n [Hall 1991].
KierFlex	Kier molecular flexibility index: $(KierA1) (KierA2) / n$ [Hall 1991].
balabanJ	Balaban's connectivity topological index [Balaban 1982].
Q_VSA_HYD PEOE_VSA_H YD	Total hydrophobic van der Waals surface area. This is the sum of the v_i such that $ q_i $ is less than or equal to 0.2. The v_i are calculated using a connection table approximation.

A1.1 Descriptions of PCA and QSPR descriptors (continued)

Q_VSA_FPOL PEOE_VSA_FPOL	Fractional polar van der Waals surface area. This is the sum of the v_i such that $ q_i $ is greater than 0.2 divided by the total surface area. The v_i are calculated using a connection table approximation.
Q_VSA_FHYD PEOE_VSA_FHYD	Fractional hydrophobic van der Waals surface area. This is the sum of the v_i such that $ q_i $ is less than or equal to 0.2 divided by the total surface area. The v_i are calculated using a connection table approximation.
Q_VSA_POL PEOE_VSA_POL	Total polar van der Waals surface area. This is the sum of the v_i such that $ q_i $ is greater than 0.2. The v_i are calculated using a connection table approximation.

Table A2.1 The final correlation matrix showing the descriptors that will be included in the flux through synthetic membranes

PCA and QSPR

[illegible]

Table A2.2 The final correlation matrix showing the descriptors that will be included in the solvent uptake into synthetic membranes PCA and QSPR

	normalized weight ratio	normalized δ Dexp vehicle	normalized LogKo/w vehicle	normalized Molecular connectivity index vehicle	normalized opr_brigid vehicle	normalized chi0_C vehicle	normalized δ T/ δ Hildebrand membrane	normalized δ Dexp membrane
normalized weight ratio	1							
normalized δ Dexp vehicle	-0.2294124	1						
normalized LogKo/w vehicle	-0.1454454	0.551700643	1					
normalized Molecular connectivity index vehicle	-0.0881439	0.673488942	-0.15646	1				
normalized opr_brigid vehicle	0.0805219	0.233380014	0.053972	0.583410084	1			
normalized chi0_C vehicle	0.2495684	-0.78383731	-0.79916	-0.08222289	0.28106091	1		
normalized δ T/ δ Hildebrand membrane	-0.2988566	0	0	-6.3441E-18	1.26883E-17	-6.3413E-18	1	
normalized δ Dexp membrane	-0.4129002	0	0	3.17207E-18	1.90324E-17	-1.0324E-17	0.712492	1

Table A2.3 The final correlation matrix showing the descriptors that will be included in the permeability coefficient PCA and QSPR

[illegible]

Table A2.4 The final correlation matrix showing the descriptors that will be included in the lag time PCA and QSPR

[illegible]

REFERENCES

References

- Abdi, H. & Williams, L. J. 2010. Principal component analysis. *Wiley Interdisciplinary Reviews: Computational Statistics*, 2, 433–459.
- Abbott, S. 2012. An integrated approach to optimizing skin delivery of cosmetic and pharmaceutical actives. *International Journal of Cosmetic Science*, 34, 217-222.
- Abraham, M. H., Martins, F. & Mitchell, R. C. 1997. Algorithms for skin permeability using hydrogen bond descriptors: the problem of steroids. *Journal of Pharmacy and Pharmacology*, 49, 858-865.
- Adams, E., De Maesschalck, R., De Spiegeleer, B., Vander Heyden, Y., Smeyers-Verbeke, J. & Massart, D. L. 2001. Evaluation of dissolution profiles using principal component analysis. *International Journal of Pharmaceutics*, 212, 41-53.
- Adams, E., Walczak, B., Vervaet, C., Risha, P. G. & Massart, D. L. 2002. Principal component analysis of dissolution data with missing elements. *International Journal of Pharmaceutics*, 234, 169-178.
- Agero, A. L. C. & Verallo-Rowell, V. M. 2004. A randomized double-blind controlled trial comparing extra virgin coconut oil with mineral oil as a moisturizer for mild to moderate xerosis. *Dermatitis : contact, atopic, occupational, drug*, 15, 109-16.
- Agner, T. & Serup, J. 1993. Time Course Of Occlusive Effects On Skin Evaluated By Measurement Of Transepidermal Water-Loss (TEWL) - Including Patch Tests With Sodium Lauryl Sulfate And Water. *Contact Dermatitis*, 28, 6-9.
- Aithal, U. S. & Aminabhavi, T. M. 1990. Measurement Of Diffusivity Of Organic Liquids Through Polymer Membranes - A Simple And Inexpensive Laboratory Experiment. *Journal of Chemical Education*, 67, 82-85.
- Akomeah, F., Nazir, T., Martin, G. P. & Brown, M. B. 2004. Effect of heat on the percutaneous absorption and skin retention of three model penetrants. *European Journal of Pharmaceutical Sciences*, 21, 337-345.
- Alberti, I., Kalia, Y. N., Naik, A., Bonny, J. D. & Guy, R. H. 2001. In vivo assessment of enhanced topical delivery of terbinafine to human stratum corneum. *Journal of Controlled Release*, 71, 319-327.
- Albery, W. J. & Hadgraft, J. 1979. Percutaneous absorption - Invivo experiments. *Journal of Pharmacy and Pharmacology*, 31, 140-147.

- Alexander, A., Dwivedi, S., Ajazuddin, Giri, T. K., Saraf, S., Saraf, S. & Tripathi, D. K. 2012. Approaches for breaking the barriers of drug permeation through transdermal drug delivery. *Journal of Controlled Release*, 164, 26-40.
- Alvarez-Figueroa, M. J. & Blanco-Mendez, J. 2001. Transdermal delivery of methotrexate: iontophoretic delivery from hydrogels and passive delivery from microemulsions. *International Journal of Pharmaceutics*, 215, 57-65.
- Aminabhavi, T. M. & Khinnavar, R. S. 1993. Diffusion and sorption of organic liquids through polymer membranes .10. Polyurethane, nitrile-butadiene rubber and epichlorohydrin versus aliphatic-alcohols (C1-C5). *Polymer*, 34, 1006-1018.
- Amnuait, C., Ikeuchi, I., Ogawara, K., Higaki, K. & Kimura, T. 2005. Skin permeation of propranolol from polymeric film containing terpene enhancers for transdermal use. *International Journal of Pharmaceutics*, 289, 167-178.
- Amusquivar, E., Schiffner, S. & Herrera, E. 2011. Evaluation of two methods for plasma fatty acid analysis by GC. *European Journal of Lipid Science and Technology*, 113, 711-716.
- Anigbogu, A. N. C., Williams, A. C., Barry, B. W. & Edwards, H. G. M. 1995. Fourier-transform raman-spectroscopy of interactions between the penetration enhancer dimethyl-sulfoxide and human stratum-corneum. *International Journal of Pharmaceutics*, 125, 265-282.
- Archer, D. F., Cullins, V., Creasy, G. W. & Fisher, A. C. 2004. The impact of improved compliance with a weekly contraceptive transdermal system (Ortho Evra (R)) on contraceptive efficacy. *Contraception*, 69, 189-195.
- Artusi, M., Nicoli, S., Colombo, P., Bettini, R., Sacchi, A. & Santi, P. 2004. Effect of chemical enhancers and iontophoresis on thiocolchicoside permeation across rabbit and human skin in vitro. *Journal of Pharmaceutical Sciences*, 93, 2431-2438.
- Aungst, B. J., Blake, J. A. & Hussain, M. A. 1990. Contributions of drug solubilization, partitioning, barrier disruption, and solvent permeation to the enhancement of skin permeation of various compounds with fatty-acids and amines. *Pharmaceutical Research*, 7, 712-718.
- Aungst, B. J., Rogers, N. J. & Shefter, E. 1986. Enhancement of naloxone penetration through human-skin invitro using fatty-acids, fatty alcohols, surfactants, sulfoxides and amides. *International Journal of Pharmaceutics*, 33, 225-234.

- Babar, A., Bhandari, R. D. & Plakogiannis, F. M. 1991. Invitro release studies of chlorpheniramine maleate from topical bases using cellulose membrane and hairless mouse skin. *Drug Development and Industrial Pharmacy*, 17, 1027-1040.
- Babita, K. & Tiwary, A. K. 2005. Transcutaneous delivery of levodopa: Enhancement by fatty acid synthesis inhibition. *Molecular Pharmaceutics*, 2, 57-63.
- Badran, M., Shalaby, K. & Al-Omrani, A. 2012. Influence of the flexible liposomes on the skin deposition of a hydrophilic model drug, carboxyfluorescein: dependency on their composition. *The Scientific World Journal*, ID 134876, 1-9.
- Balaban, A. T. 1982. Highly discriminating distance-based topological index. *Chemical Physics Letters*, 89, 399-404.
- Barbe, A. M., Hogan, P. A. & Johnson, R. A. 2000. Surface morphology changes during initial usage of hydrophobic, microporous polypropylene membranes. *Journal of Membrane Science*, 172, 149-156.
- Barcelo, D. & Petrovic, M. 2011. *Handbook of Environmental Chemistry. The Ebro River Basin*. Berlin: Springer., pp. 1-300.
- Baroli, B., Lopez-Quintela, M. A., Delgado-Charro, M. B., Fadda, A. M. & Blanco-Mendez, J. 2000. Microemulsions for topical delivery of 8-methoxsalen. *Journal of Controlled Release*, 69, 209-218.
- Baron, J. M., Holler, D., Schiffer, R., Frankenberg, S., Neis, M., Merk, H. F. & Jugert, F. K. 2001. Expression of multiple cytochrome P450 enzymes and multidrug resistance-associated transport proteins in human skin keratinocytes. *Journal of Investigative Dermatology*, 116, 541-548.
- Barry, B. W. 1984. *Drugs and the pharmaceutical sciences. Dermatological formulations percutaneous absorption*. Barry, B. W. *Drugs and the Pharmaceutical Sciences*, Vol. 18. *Dermatological Formulations: Percutaneous Absorption*. Marcel Dekker, Inc.: New York, N.Y., USA; Basel, Switzerland. ISBN-13: 978-0824717292.
- Barry, B. W. 1987. Mode of action of penetration enhancers in human skin. *Journal of Controlled Release*, 6, 85-98.
- Barry, B. W. 1988. Action of skin penetration enhancers - the lipid protein partitioning theory. *International Journal of Cosmetic Science*, 10, 281-293.

- Barry, B. W. 1991. Lipid-protein-partitioning theory of skin penetration enhancement. *Journal of Controlled Release*, 15, 237-248.
- Barry, B. W. & Bennett, S. L. 1987. Effect of penetration enhancers on the permeation of mannitol, hydrocortisone and progesterone through human-skin. *Journal of Pharmacy and Pharmacology*, 39, 535-546.
- Barry, B. W., Harrison, S. M. & Dugard, P. H. 1985. Correlation of thermodynamic activity and vapor diffusion through human-skin for the model-compound, benzyl alcohol. *Journal of Pharmacy and Pharmacology*, 37, 84-90.
- Beastall, J. C., Hadgraft, J., Palin, K. J. & Washington, C. 1987. Interaction of azone with lipid bilayers and its significance in percutaneous absorption. *Journal of Pharmacy and Pharmacology*, 39, pp 23.
- Beastall, J. C., Hadgraft, J. & Washington, C. 1988. Mechanism of action of azone as a percutaneous penetration enhancer - lipid bilayer fluidity and transition-temperature effects. *International Journal of Pharmaceutics*, 43, 207-213.
- Behl, C. R., Flynn, G. L., Kurihara, T., Smith, W., Gatmaitan, O., Higuchi, W. I., Ho, N. F. H. & Pierson, C. L. 1980. Permeability of thermally damaged skin .1. Immediate influences of 60-degrees-C scalding on hairless mouse skin. *Journal of Investigative Dermatology*, 75, 340-345.
- Benaouda, F., Brown, M. B., Ganguly, S., Jones, S. A. & Martin, G. P. 2012a. Discriminating the molecular identity and function of discrete supramolecular structures in topical pharmaceutical formulations. *Molecular Pharmaceutics*, 9, 2505-2512.
- Benaouda, F., Brown, M. B., Martin, G. P. & Jones, S. A. 2012b. Triggered in situ drug supersaturation and hydrophilic matrix self-assembly. *Pharmaceutical Research*, 29, 3434-3442.
- Bendas, B., Schmalfuss, U. & Neubert, R. 1995. Influence of propylene-glycol as cosolvent on mechanisms of drug transport from hydrogels. *International Journal of Pharmaceutics*, 116, 19-30.
- Benowitz, N. L. 1990. Clinical-pharmacology of caffeine. *Annual Review of Medicine*, 41, 277-288.
- Benson, H. A. E. 2005. Transdermal drug delivery: Penetration enhancement techniques. *Current Drug Delivery*, 2, 23-33.

- Bensouilah, J. & Buck, P. 2006. Aromadermatology : aromatherapy in the treatment and care of common skin conditions, Abingdon, Radcliffe Publishing.
- Berdick, M. 1972. Role of fats and oils in cosmetics. *Journal of the American Oil Chemists Society*, 49, 406-408.
- Berins M. L., 1991. Polymer Chemistry. In Berins M. L editors. *Plastics engineering handbook of the Society of the Plastics Industry, Inc*, New York, Van Nostrand Reinhold. 33-45
- Berner, B., Mazzenga, G. C., Otte, J. H., Steffens, R. J., Juang, R. H. & Ebert, C. D. 1989. Ethanol water mutually enhanced transdermal therapeutic system .2. Skin permeation of ethanol and nitroglycerin. *Journal of Pharmaceutical Sciences*, 78, 402-407.
- Bertin, C., Zunino, H., Pittet, J. C., Beau, P., Pineau, P., Massonneau, M., Robert, C. & Hopkins, J. 2001. A double-blind evaluation of the activity of an anti-cellulite product containing retinol, caffeine, and ruscogenine by a combination of several non-invasive methods. *Journal of Cosmetic Science*, 52, 199-210.
- Biedermann, M., Fiselier, K. & Grob, K. 2009. Aromatic hydrocarbons of mineral oil origin in foods: method for determining the total concentration and first results. *Journal of Agricultural and Food Chemistry*, 57, 8711-8721.
- Blank, I. H. & McAuliffe, D. J. 1985. Penetration of benzene through human-skin. *Journal of Investigative Dermatology*, 85, 522-526.
- Blank, I. H., Scheuple.RJ & Macfarla.DJ 1967. Mechanism of percutaneous absorption .3. Effect of temperature on transport of non-electrolytes across skin. *Journal of Investigative Dermatology*, 49, 582-589.
- Blanken, R., Vanvilsteren, M. J. T., Tupker, R. A. & Coenraads, P. J. 1989. Effect of mineral-oil and linoleic-acid-containing emulsions on the skin vapor loss of sodium-lauryl-sulfate-induced irritant skin reactions. *Contact Dermatitis*, 20, 93-97.
- Bodde, H. E., Kruithof, M. A. M., Brussee, J. & Koerten, H. K. 1989. Visualization of normal and enhanced HgCl₂ Transport through human-skin in vitro. *International Journal of Pharmaceutics*, 53, 13-24.
- Bock, U., Limberger, M., Schmitz, S. & Haltner, E. 2002. In vitro systems to characterize dermal permeation and penetration. *Proceeding 4th World meeting on Pharmaceutics Biopharmaceutics Pharmaceutical Technology*. 1223-1224.

- Bogusz, M. J., El Haj, S. A., Ehaideb, Z., Hassan, H. & Al-Tufail, M. 2004. Rapid determination of benzo(a)pyrene in olive oil samples with solid-phase extraction and low-pressure, wide-bore gas chromatography-mass spectrometry and fast liquid chromatography with fluorescence detection. *Journal of Chromatography A*, 1026, 1-7.
- Bolzinger, M.-A., Briancon, S., Pelletier, J. & Chevalier, Y. 2012. Penetration of drugs through skin, a complex rate-controlling membrane. *Current Opinion in Colloid & Interface Science*, 17, 156-165.
- Bommannan, D., Potts, R. O. & Guy, R. H. 1991. Examination of the effect of ethanol on human stratum-corneum invivo using infrared-spectroscopy. *Journal of Controlled Release*, 16, 299-304.
- Bonina, F. P., Carelli, V., Dicolo, G., Montenegro, L. & Nannipieri, E. 1993. Vehicle effects on in-vitro skin permeation of and stratum-corneum affinity for model-drugs caffeine and testosterone. *International Journal of Pharmaceutics*, 100, 41-47.
- Bonina, F. P., Puglia, C., Barbuzzi, T., De Caprariis, P., Palagiano, F., Rimoli, M. G. & Saija, A. 2001. In vitro and in vivo evaluation of polyoxyethylene esters as dermal prodrugs of ketoprofen, naproxen and diclofenac. *European Journal of Pharmaceutical Sciences*, 14, 123-134.
- Borgia, S. L., Schupp, P., Mehnert, W. & Schaefer-Korting, M. 2008. In vitro skin absorption and drug release - A comparison of six commercial prednicarbate preparations for topical use. *European Journal of Pharmaceutics and Biopharmaceutics*, 68, 380-389.
- Bos, J. D. & Meinardi, M. 2000. The 500 Dalton rule for the skin penetration of chemical compounds and drugs. *Experimental Dermatology*, 9, 165-169.
- Bouwstra, J. A., De Graaff, A., Gooris, G. S., Nijssse, J., Wiechers, J. W. & Van Aelst, A. C. 2003. Water distribution and related morphology in human stratum corneum at different hydration levels. *Journal of Investigative Dermatology*, 120, 750-758.
- Bouwstra J. A., Gooris G. S. & Ponc M. 2008. Skin lipid organization, composition and barrier function. *International Journal of Cosmetic Science*; 30, 388-390
- Bragagni, M., Mennini, N., Maestrelli, F., Cirri, M. & Mura, P. 2012. Comparative study of liposomes, transfersomes and ethosomes as carriers for improving topical delivery of celecoxib. *Drug Delivery*, 19, 354-361.

- Breitkreutz, D., Mirancea, N. & Nischt, R. 2009. Basement membranes in skin: unique matrix structures with diverse functions? *Histochemistry and Cell Biology*, 132, 1-10.
- Brinkmann, I. & Muller-Goymann, C. C. 2003. Role of isopropyl myristate, isopropyl alcohol and a combination of both in hydrocortisone permeation across the human stratum corneum. *Skin Pharmacology and Applied Skin Physiology*, 16, 393-404.
- Brinkmann, I. & Muller-Goymann, C. C. 2005. An attempt to clarify the influence of glycerol, propylene glycol, isopropyl myristate and a combination of propylene glycol and isopropyl myristate on human stratum corneum. *Pharmazie*, 60, 215-220.
- Bronaugh, R. L. & Stewart, R. F. 1985. Methods for invitro percutaneous-absorption studies .5. Permeation through damaged skin. *Journal of Pharmaceutical Sciences*, 74, 1062-1066.
- Brown, M. B. & Jones, S. A., 2007. Topical Formulations. Patent. WO2007031753.
- Brown, M. B., Martin, G. P., Jones, S. A. & Akomeah, F. K. 2006. Dermal and transdermal drug delivery systems: Current and future prospects. *Drug Delivery*, 13, 175-187.
- Brufau, G., Codony, R., Canela, M. A. & Rafecas, M. 2006. Rapid and quantitative determination of total sterols of plant and animal origin in liver samples by gas chromatography. *Chromatographia*, 64, 559-563.
- Bucks D. & Maibach H.I. 2005. Occlusion does not uniformly enhance penetration in vivo. In Bronaugh R.L. & Maibach H.I editors. *Percutaneous Absorption: Drugs, Cosmetics, Mechanism, Methods*. Informa healthcare, Hoboken. ISBN: 9780849359033, 65–83.
- Camenisch, G., Folkers, G. & Van De Waterbeemd, H. 1996. Review of theoretical passive drug absorption models: historical background, recent developments and limitations. *Pharmaceutica acta Helvetiae*, 71, 309-27.
- Campbell, R. L. & Bruce, R. D. 1981. Comparative dermatotoxicology .1. Direct comparison of rabbit and human primary skin irritation responses to isopropylmyristate. *Toxicology and Applied Pharmacology*, 59, 555-563.
- Cappel, M. J. & Kreuter, J. 1991. Effect of nonionic surfactants on transdermal drug delivery .1. Polysorbates. *International Journal of Pharmaceutics*, 69, 143-153.
- Corbo M., Schultz T.W., Wong G.K. & Van Buskirk G.A. 1993. Development and validation of in vitro release testing methods for semisolid formulations. *Pharmaceutical Technology*, 9, 112–128.

- Cardoso, V. M., Reis Solano, A. G., Fontes Prado, M. A. & Nunan, E. D. A. 2006. Investigation of fatty acid esters to replace isopropyl myristate in the sterility test for ophthalmic ointments. *Journal of Pharmaceutical and Biomedical Analysis*, 42, 630-634.
- Carmichael, A. J. 1994. Skin sensitivity and transdermal drug-delivery - a review of the problem. *Drug Safety*, 10, 151-159.
- Caspers, P. J., Lucassen, G. W., Bruining, H. A. & Puppels, G. J. 2000. Automated depth-scanning confocal Raman microspectrometer for rapid in vivo determination of water concentration profiles in human skin. *Journal of Raman Spectroscopy*, 31, 813-818.
- Caspers, P. J., Lucassen, G. W., Wolthuis, R., Bruining, H. A. & Puppels, G. J. 1998. In vitro and in vivo Raman spectroscopy of human skin. *Biospectroscopy*, 4, S31-S39.
- Catz, P. & Friend, D. R. 1990. Transdermal delivery of levonorgestrel .10. Effect of cosolvents on ethyl-acetate enhanced percutaneous-absorption of levonorgestrel. *Journal of Controlled Release*, 12, 171-180.
- Celia, C., Cilurzo, F., Trapasso, E., Cosco, D., Fresta, M. & Paolino, D. 2012. Ethosomes (R) and transfersomes (R) containing linoleic acid: physicochemical and technological features of topical drug delivery carriers for the potential treatment of melasma disorders. *Biomedical Microdevices*, 14, 119-130.
- Ceschel, G., Bergamante, V., Maffei, P., Borgia, S. L., Calabrese, V., Biserni, S. & Ronchi, C. 2005. Solubility and transdermal permeation properties of a dehydroepiandrosterone cyclodextrin complex from hydrophilic and lipophilic vehicles. *Drug Delivery*, 12, 275-280.
- Cevc, G. 1996. Transfersomes, liposomes and other lipid suspensions on the skin: Permeation enhancement, vesicle penetration, and transdermal drug delivery. *Critical Reviews in Therapeutic Drug Carrier Systems*, 13, 257-388.
- Cevc, G. 2004. Lipid vesicles and other colloids as drug carriers on the skin. *Advanced Drug Delivery Reviews*, 56, 675-711.
- Cevc, G. & Blume, G. 2001. New, highly efficient formulation of diclofenac for the topical, transdermal administration in ultradeformable drug carriers, Transfersomes. *Biochimica Et Biophysica Acta-Biomembranes*, 1514, 191-205.
- Cevc G., Schatzlein A., Gebauer D. & Blume G. 1993. Ultra-high means of novel drug carriers, transferosomes. In: Brain KR, James VA, Walters KA, editors. *Prediction of Percutaneous Penetration* (vol 3b). Cardiff: STS Publishing, 226-234.

- Cevc, G., Schatzlein, A. & Richardsen, H. 2002. Ultradeformable lipid vesicles can penetrate the skin and other semi-permeable barriers unfragmented. Evidence from double label CLSM experiments and direct size measurements. *Biochimica et Biophysica Acta-Biomembranes*, 1564, 21-30.
- Chen, L., Han, L. & Lian, G. 2013. Recent advances in predicting skin permeability of hydrophilic solutes. *Advanced Drug Delivery Reviews*, 65, 295-305.
- Chen, Y., Liu, Y., Fan, H., Li, H., Shi, B., Zhou, H. & Peng, B. 2007. The polyurethane membranes with temperature sensitivity for water vapor permeation. *Journal of Membrane Science*, 287, 192-197.
- Chi, S. C., Park, E. S. & Kim, H. 1995. Effect of penetration enhancers on flurbiprofen permeation through rat skin. *International Journal of Pharmaceutics*, 126, 267-274.
- Chien, Y. W., Valia, K. H. & Doshi, U. B. 1985. Long-term permeation kinetics of estradiol .5. Development and evaluation of transdermal bioactivated hormone delivery system. *Drug Development and Industrial Pharmacy*, 11, 1195-1212.
- Chilcott, R. P., Barai, N., Beezer, A. E., Brain, S. I., Brown, M. B., Bunge, A. L., Burgess, S. E., Cross, S., Dalton, C. H., Dias, M., Farinha, A., Finnin, B. C., Gallagher, S. J., Green, D. M., Gunt, H., Gwyther, R. L., Heard, C. M., Jarvis, C. A., Kamiyama, F., Kasting, G. B., Ley, E. E., Lim, S. T., McNaughton, G. S., Morris, A., Nazemi, M. H., Pellett, M. A., Du Plessis, J., Quan, Y. S., Raghavan, S. L., Roberts, M., Romonchuk, W., Roper, C. S., Schenk, D., Simonsen, L., Simpson, A., Traversa, B. D., Trotter, L., Watkinson, A., Wilkinson, S. C., Williams, F. M., Yamamoto, A. & Hadgraft, J. 2005. Inter- and intralaboratory variation of in vitro diffusion cell measurements: An international multicenter study using quasi-standardized methods and materials. *Journal of Pharmaceutical Sciences*, 94, 632-638.
- Clarys, P., Alewaeters, K., Jadoul, A., Barel, A., Manadas, R. O. & Preat, V. 1998. In vitro percutaneous penetration through hairless rat skin: influence of temperature, vehicle and penetration enhancers. *European Journal of Pharmaceutics and Biopharmaceutics*, 46, 279-283.
- Cleary G. W. 1993. Transdermal delivery systems: a medical rationale. Shah, V. P. & Maibach, H. I. Topical drug bioavailability, bioequivalence, and penetration, New York, Plenum Press. 17-68.

- Clement, L. M., Hansen, S. L., Costin, C. D. & Perri, G. L. 2010. Quantitation of Sterols and Steryl Esters in Fortified Foods and Beverages by GC/FID. *Journal of the American Oil Chemists Society*, 87, 973-980.
- Clement, P., Laugel, C. & Marty, J. P. 2000. Influence of three synthetic membranes on the release of caffeine from concentrated W/O emulsions. *Journal of Controlled Release*, 66, 243-254.
- Coldman, M. F., Poulsen, B. J. & Higuchi, T. 1969. Enhancement of percutaneous absorption by use of volatile – non-volatile systems as vehicles. *Journal of Pharmaceutical Sciences*, 58, 1098-1102.
- Conradi, R. A., Hilgers, A. R., Ho, N. F. H. & Burton, P. S. 1991. The influence of peptide structure on transport across CACO-2 cells. *Pharmaceutical Research*, 8, 1453-1460.
- Cooper, E. R. 1984. Increased skin permeability for lipophilic molecules. *Journal of Pharmaceutical Sciences*, 73, 1153-1156.
- Cooper, E. R., Merritt, E. W. & Smith, R. L. 1985. Effect of fatty-acids and alcohols on the penetration of acyclovir across human-skin invitro. *Journal of Pharmaceutical Sciences*, 74, 688-689.
- Cork, M. J. 1997. The importance of skin barrier function. *Journal of Dermatological Treatment*, 8, S7-S13.
- Cramer, M. P. & Saks, S. R. 1994. Translating safety, efficacy and compliance into economic value for controlled-release dosage forms. *Pharmacoeconomics*, 5, 482-504.
- Crawford, R. R. & Esmerian, O. K. 1971. Effect of plasticizers on some physical properties of cellulose acetate phthalate films. *Journal of pharmaceutical sciences*, 60, 312-4.
- Lide D. R. & Frederikse H. P. R 1994. *Handbook of Chemistry and Physics* 75th ed. CRC Press.
- Cronin, M. T. D., Dearden, J. C., Gupta, R. & Moss, G. P. 1998. An investigation of the mechanism of flux across polydimethylsiloxane membranes by use of quantitative structure-permeability relationships. *Journal of Pharmacy and Pharmacology*, 50, 143-152.
- Cronin, M. T. D., Dearden, J. C., Moss, G. P. & Murray-Dickson, G. 1999. Investigation of the mechanism of flux across human skin in vitro by quantitative structure-permeability relationships. *European Journal of Pharmaceutical Sciences*, 7, 325-330.

- Cross, S. E., Pugh, W. J., Hadgraft, J. & Roberts, M. S. 2001. Probing the effect of vehicles on topical delivery: Understanding the basic relationship between solvent and solute penetration using silicone membranes. *Pharmaceutical Research*, 18, 999-1005.
- Cross, S. E. & Roberts, M. S. 2000. The effect of occlusion on epidermal penetration of parabens from a commercial allergy test ointment, acetone and ethanol vehicles. *Journal of Investigative Dermatology*, 115, 914-918.
- Cullander, C. & Guy, R. H. 1992. Penetration enhancement for polypeptides through epithelia .D. routes of delivery - case-studies .6. Transdermal delivery of peptides and proteins. *Advanced Drug Delivery Reviews*, 8, 291-329.
- Curry, S. E. & Finkel, J. C. 2007. Use of the Synera (TM) patch for local anesthesia before vascular access procedures: A randomized, double-blind, placebo-controlled study. *Pain Medicine*, 8, 497-502.
- Damien, F. & Boncheva, M. 2010. The extent of orthorhombic lipid phases in the stratum corneum determines the barrier efficiency of human skin in vivo. *Journal of Investigative Dermatology*, 130, 611-614.
- Darbre, P. D., Aljarrah, A., Miller, W. R., Coldham, N. G., Sauer, M. J. & Pope, G. S. 2004. Concentrations of parabens in human breast tumours. *Journal of Applied Toxicology*, 24, 5-13.
- Davis, A. F., Gyurik, R. J., Hadgraft, J., Pellett, M. A. & Walters, K. A. 2002. Formulation strategies for modulating skin permeation. *Drugs and the Pharmaceutical Sciences. Dermatological and transdermal formulations*, 119, 271-317.
- Davis, A. F. & Hadgraft, J. 1991. Effect of supersaturation on membrane-transport .1. Hydrocortisone acetate. *International Journal of Pharmaceutics*, 76, 1-8.
- Dayan, N. & Touitou, E. 2000. Carriers for skin delivery of trihexyphenidyl HCl: ethosomes vs. liposomes. *Biomaterials*, 21, 1879-1885.
- Degim, I. T., Pugh, W. J. & Hadgraft, J. 1998. Skin permeability data: anomalous results. *International Journal of Pharmaceutics*, 170, 129-133.
- Degim, I. T., Uslu, A., Hadgraft, J., Atay, T., Akay, C. & Cevheroglu, S. 1999. The effects of Azone and capsaicin on the permeation of naproxen through human skin. *International Journal of Pharmaceutics*, 179, 21-25.

- Dias, M., Farinha, A., Faustino, E., Hadgraft, J., Pais, J. & Toscano, C. 1999. Topical delivery of caffeine from some commercial formulations. *International Journal of Pharmaceutics*, 182, 41-47.
- Dias, M., Hadgraft, J. & Lane, M. E. 2007a. Influence of membrane-solvent-solute interactions on solute permeation in model membranes. *International Journal of Pharmaceutics*, 336, 108-114.
- Dias, M., Hadgraft, J. & Lane, M. E. 2007b. Influence of membrane-solvent-solute interactions on solute permeation in skin. *International Journal of Pharmaceutics*, 340, 65-70.
- Dias, M., Hadgraft, J., Raghavan, S. L. & Tetteh, J. 2004. The effect of solvent on permeant diffusion through membranes studied using ATR-FTIR and chemometric data analysis. *Journal of Pharmaceutical Sciences*, 93, 186-196.
- Dias, M., Raghavan, S. L. & Hadgraft, J. 2001. ATR-FTIR spectroscopic investigations on the effect of solvents on the permeation of benzoic acid and salicylic acid through silicone membranes. *International Journal of Pharmaceutics*, 216, 51-59.
- Dick, I. P. & Scott, R. C. 1992. Pig ear skin as an invitro model for human skin permeability. *Journal of Pharmacy and Pharmacology*, 44, 640-645.
- Dingler, A., Hildebrand, G., Niehus, H. & Müller, R. H. 1998. Cosmetic anti-aging formulation based on vitamin E-loaded solid lipid nanoparticles. *Controlled Release Society, International Symposium on Control Release Bioact Mater*, 25, 433-434.
- Downing, D. T., Stewart, M. E., Wertz, P. W., Colton, S. W., Abraham, W. & Strauss, J. S. 1987. Skin lipids - An update. *Journal of Investigative Dermatology*, 88, S2-S6.
- Dreher, F., Walde, P., Walther, P. & Wehrli, E. 1997. Interaction of a lecithin microemulsion gel with human stratum corneum and its effect on transdermal transport. *Journal of Controlled Release*, 45, 131-140.
- Du Plessis, J., Pugh, W. J., Judefeind, A. & Hadgraft, J. 2001. The effect of hydrogen bonding on diffusion across model membranes: consideration of the number of H-bonding groups. *European Journal of Pharmaceutical Sciences*, 13, 135-141.
- Du Plessis, J., Pugh, W. J., Judefeind, A. & Hadgraft, J. 2002. The effect of the nature of H-bonding groups on diffusion through PDMS membranes saturated with octanol and toluene. *European Journal of Pharmaceutical Sciences*, 15, 63-69.

- Edwards, D. A., Prausnitz, M. R., Langer, R. & Weaver, J. C. 1995. Analysis of enhanced transdermal transport by skin electroporation. *Journal of Controlled Release*, 34, 211-221.
- Egbaria, K., Ramachandran, C., Kittayanond, D. & Weiner, N. 1990. Topical delivery of liposomally encapsulated interferon evaluated by invitro diffusion studies. *Antimicrobial Agents and Chemotherapy*, 34, 107-110.
- Egelrud, T., Brattsand, M., Kreutzmann, P., Walden, M., Vitzithum, K., Marx, U. C., Forssmann, W. G. & Magert, H. J. 2005. HK5 and HK7, two serine proteinases abundant in human skin, are inhibited by LEKTI domain 6. *British Journal of Dermatology*, 153, 1200-1203.
- Elias, P. M. 1983. Epidermal lipids, barrier function, and desquamation. *Journal of Investigative Dermatology*, 80, S44-S49.
- Elias, P. M., Cooper, E. R., Korc, A. & Brown, B. E. 1981. Percutaneous transport in relation to stratum-corneum structure and lipid-composition. *Journal of Investigative Dermatology*, 76, 297-301.
- Elias, P. M., Feingold, K. R., Tsai, J., Thornfeldt, C. & Menon, G. 2003. Metabolic approach to transdermal drug delivery. In: Guy RH, Hadgraft J, editors. *Transdermal drug delivery*. New York: Marcel Dekker, pp. 285-304.
- Elias, P. M., Tsai, J., Menon, G. K., Holleran, W. M. & Feingold, K. R. 2002. The potential of metabolic interventions to enhance transdermal drug delivery. *Journal of Investigative Dermatology Symposium Proceedings*, 7, 79-85.
- Elmoslemny, R. M., Abdallah, O. Y., El-Khordagui, L. K. & Khalafallah, N. M. 2012. Propylene glycol liposomes as a topical delivery system for miconazole nitrate: comparison with conventional liposomes. *AAPS Pharmscitech*, 13, 723-731.
- Eltayar, N., Tsai, R. S., Testa, B., Carrupt, P. A., Hansch, C. & Leo, A. 1991. Percutaneous penetration of drugs - A quantitative structure permeability relationship study. *Journal of Pharmaceutical Sciences*, 80, 744-749.
- Embery, G. & Dugard, P. H. 1971. Isolation of dimethyl sulfoxide soluble components from human epidermal preparations - Possible mechanism of action of dimethyl sulfoxide in effecting percutaneous migration phenomena. *Journal of Investigative Dermatology*, 57, 308-311.

- Engblom, J., Engstrom, S. & Jonsson, B. 1998. Phase coexistence in cholesterol fatty acid mixtures and the effect of the penetration enhancer Azone. *Journal of Controlled Release*, 52, 271-280.
- Eriksson L., Johansson E., Kettaneh-Wold N., Trygg J., Wikström C. & Wold S.. 2006. Multi- and megavariable data analysis, Umeå, Umetrics AB Sweden. ISBN-13-978-91-973730-2-9.
- Ertl, P., Rohde, B. & Selzer, P. 2000. Fast calculation of molecular polar surface area as a sum of fragment-based contributions and its application to the prediction of drug transport properties. *Journal of Medicinal Chemistry*, 43, 3714-3717.
- Escribano, E., Calpena, A. C., Queralt, J., Obach, R. & Domenech, J. 2003. Assessment of diclofenac permeation with different formulations: anti-inflammatory study of a selected formula. *European Journal of Pharmaceutical Sciences*, 19, 203-210.
- European Food Safety Authority (EFSA) 2012. Panel on Contaminants in the Food Chain (CONTAM); scientific opinion on mineral oil hydrocarbons in food. *European Food Safety Authority Journal*, 10, 2704. 1-185.
- Evans, C.R.G., Traynor, M.J., Lim, S.T., Turner, R.B. & Brown, R.B. 2010. A Phase II study of the efficacy, tolerability and consumer acceptability of topical MedSpray 1%w/w/terbinafine (TerbiMed) versus Lamisil Once in the treatment of Tinea pedis. In: Brain, K.R., Walters, K.A. (Eds.), In: *Perspectives in Percutaneous Penetration*, vol. 12. STS Publishing, Cardiff, p. 101.
- Fagan, P., Wijesundera, C. & Watkins, P. 2004. Determination of mono- and di-acylglycerols in milk lipids. *Journal of Chromatography A*, 1054, 251-259.
- Fang, J. Y., Fang, C. L., Sung, K. C. & Chen, H. Y. 1999. Effect of low frequency ultrasound on the in vitro percutaneous absorption of clobetasol 17-propionate. *International Journal of Pharmaceutics*, 191, 33-42.
- Fang, L., Kobayashi, Y., Numajiri, S., Kobayashi, D., Sugibayashi, K. & Morimoto, Y. 2002. The enhancing effect of a triethanolamine-ethanol-isopropyl myristate mixed system on the skin permeation of acidic drugs. *Biological & Pharmaceutical Bulletin*, 25, 1339-1344.
- Feldstein, M. M., Raigorodskii, I. M., Iordanskii, A. L. & Hadgraft, J. 1998. Modeling of percutaneous drug transport in vitro using skin-imitating Carbosil membrane. *Journal of Controlled Release*, 52, 25-40.

- Feldstein, M. M., Tohmakhchi, V. N., Malkhazov, L. B., Vasiliev, A. E. & Plate, N. A. 1996. Hydrophilic polymeric matrices for enhanced transdermal drug delivery. *International Journal of Pharmaceutics*, 131, 229-242.
- Fitzpatrick, D., Corish, J. & Hayes, B. 2004. Modelling skin permeability in risk assessment - the future. *Chemosphere*, 55, 1309-1314.
- Fitzpatrick, F. A., Summa, A. F. & Cooper, A. D. 1975. Quantitative-analysis of methyl and propylparaben by high-performance liquid-chromatography. *Journal of the Society of Cosmetic Chemists*, 26, 377-387.
- Flynn G. L. 1990. Physicochemical determinants of skin absorption. In: Gerrity TR, Henry CJ, editors. *Principles of route-to-route extrapolation in risk assessment*. New York: Elsevier Science Publishing, 93-127.
- Flynn, G. L. & Roseman, T. J. 1971. Membrane diffusion .2. Influence of physical adsorption on molecular flux through heterogeneous dimethylpolysiloxane barriers. *Journal of Pharmaceutical Sciences*, 60, 1788-1796.
- Flynn, G. L., Shah, V. P., Tenjarla, S. N., Corbo, M., Demagistris, D., Feldman, T. G., Franz, T. J., Miran, D. R., Pearce, D. M., Sequeira, J. A., Swarbrick, J., Wang, J. C. T., Yacobi, A. & Zatz, J. L. 1999. Assessment of value and applications of in vitro testing of topical dermatological drug products. *Pharmaceutical Research*, 16, 1325-1330.
- Flynn, T. C., Petros, J., Clark, R. E. & Viehman, G. E. 2001. Dry skin and moisturizers. *Clinics in Dermatology*, 19, 387-392.
- Foerster, M., Bolzinger, M.-A., Fessi, H. & Briancon, S. 2009. Topical delivery of cosmetics and drugs. Molecular aspects of percutaneous absorption and delivery. *European Journal of Dermatology*, 19, 309-323.
- Forchielli, M. L., Bersani, G., Tala, S., Grossi, G., Puggioli, C. & Masi, M. 2010. The spectrum of plant and animal sterols in different oil-derived intravenous emulsions. *Lipids*, 45, 63-71.
- Forster, S., Buckton, G. & Beezer, A. E. 1991. The importance of chain-length on the wettability and solubility of organic homologs. *International Journal of Pharmaceutics*, 72, 29-34.
- Fox, L. T., Gerber, M., Du Plessis, J. & Hamman, J. H. 2011. Transdermal drug delivery

enhancement by compounds of natural origin. *Molecules*, 16, 10507-10540.

Francoeur, M. L., Golden, G. M. & Potts, R. O. 1990. Oleic-acid - its effects on stratum-corneum in relation to (trans)dermal drug delivery. *Pharmaceutical Research*, 7, 621-627.

Franz, T. J. 1975. Percutaneous absorption - Relevance of invitro data. *Journal of Investigative Dermatology*, 64, 190-195.

Fresta, M. & Puglisi, G. 1997. Corticosteroid dermal delivery with skin-lipid liposomes. *Journal of Controlled Release*, 44, 141-151.

Friebe, K., Effendy, I. & Loffler, H. 2003. Effects of skin occlusion in patch testing with sodium lauryl sulphate. *British Journal of Dermatology*, 148, 65-69.

Friend, D. R. 1991. Transdermal delivery of levonorgestrel. *Medicinal Research Reviews*, 11, 49-80.

Friend, D. R., Phillips, S. J. & Hill, J. R. 1991. Transdermal delivery of levonorgestrel .6. Cutaneous effects of transdermal levonorgestrel. *Food and Chemical Toxicology*, 29, 639-646.

Gabbanini, S., Lucchi, E., Carli, M., Berlini, E., Minghetti, A. & Valgimigli, L. 2009. In vitro evaluation of the permeation through reconstructed human epidermis of essential oils from cosmetic formulations. *Journal of Pharmaceutical and Biomedical Analysis*, 50, 370-376.

Gabrielsson, J., Lindberg, N. O., Palsson, M., Nicklasson, F., Sjostrom, M. & Lundstedt, T. 2004. Multivariate methods in the development of a new tablet formulation: Optimization and validation. *Drug Development and Industrial Pharmacy*, 30, 1037-1049.

Gabrielsson, J., Nystrom, A. & Lundstedt, T. 2000. Multivariate methods in developing an evolutionary strategy for tablet formulation. *Drug Development and Industrial Pharmacy*, 26, 275-296.

Gallarate, M., Carlotti, M. E., Trotta, M. & Bovo, S. 1999. On the stability of ascorbic acid in emulsified systems for topical and cosmetic use. *International Journal of Pharmaceutics*, 188, 233-241.

Ganga, S., Ramarao, P. & Singh, J. 1996. Effect of Azone on the iontophoretic transdermal delivery of metoprolol tartrate through human epidermis in vitro. *Journal of Controlled Release*, 42, 57-64.

- Garcia-Munoz, S. & Carmody, A. 2010. Multivariate wavelet texture analysis for pharmaceutical solid product characterization. *International Journal of Pharmaceutics*, 398, 97-106.
- Garrett, E. R. & Chemburk, P. B. 1968. Evaluation control and prediction of drug diffusion through polymeric membranes .2. Diffusion of aminophenones through silastic membranes - a test of ph-partition hypothesis. *Journal of Pharmaceutical Sciences*, 57, 949-959
- Geinoz, S., Rey, S., Boss, G., Bunge, A. L., Guy, R. H., Carrupt, P. A., Reist, M. & Testa, B. 2002. Quantitative structure-permeation relationships for solute transport across silicone membranes. *Pharmaceutical Research*, 19, 1622-1629.
- Geladi, P. & Kowalski, B. R. 1986. Partial least-squares regression - a tutorial. *Analytica Chimica Acta*, 185, 1-17.
- Ghafourian, T., Samaras, E. G., Brooks, J. D. & Riviere, J. E. 2010a. Modelling the effect of mixture components on permeation through skin. *International Journal of Pharmaceutics*, 398, 28-32.
- Ghafourian, T., Samaras, E. G., BROOKS, J. D. & Riviere, J. E. 2010b. Validated models for predicting skin penetration from different vehicles. *European Journal of Pharmaceutical Sciences*, 41, 612-616.
- Ghanem, A. H., Mahmoud, H., Higuchi, W. I., Liu, P. C. & Good, W. R. 1992. The effects of ethanol on the transport of lipophilic and polar permeants across hairless mouse skin - methods validation of a novel-approach. *International Journal of Pharmaceutics*, 78, 137-156.
- Godin, B. & Touitou, E. 2003. Ethosomes: New prospects in transdermal delivery. *Critical Reviews in Therapeutic Drug Carrier Systems*, 20, 63-102.
- Godwin, D. A. & Michniak, B. B. 1999. Influence of drug lipophilicity on terpenes as transdermal penetration enhancers. *Drug Development and Industrial Pharmacy*, 25, 905-915.
- Goldbergcettina, M., Liu, P. C., Nightingale, J. & Kuriharabergstrom, T. 1995. Enhanced transdermal delivery of estradiol in-vitro using binary vehicles of isopropyl myristate and short-chain alkanols. *International Journal of Pharmaceutics*, 114, 237-245.
- Golden, G. M., Mckie, J. E. & Potts, R. O. 1987. Role of stratum-corneum lipid fluidity in transdermal drug flux. *Journal of Pharmaceutical Sciences*, 76, 25-28.

- Gorukanti, S. R., Li, L. L. & Kim, K. H. 1999. Transdermal delivery of antiparkinsonian agent, bztropine. I. Effect of vehicles on skin permeation. *International Journal of Pharmaceutics*, 192, 159-172.
- Gratieri, T., Alberti, I., Lapteva, M. & Kalia, Y. N. 2013. Next generation intra- and transdermal therapeutic systems: Using non- and minimally-invasive technologies to increase drug delivery into and across the skin. *European Journal of Pharmaceutical Sciences*, 50, 609-622.
- Green, P. G., Guy, R. H. & Hadgraft, J. 1988. Invitro and invivo enhancement of skin permeation with oleic and lauric acids. *International Journal of Pharmaceutics*, 48, 103-111.
- Green, P. G., Hadgraft, J. & Miller, A. 1987. The use of derivative spectroscopy to measure the percutaneous absorption of oxprenolol. *Journal of Pharmacy and Pharmacology*, 39, 26P-26P.
- Grubauer, G., Feingold, K. R., Harris, R. M. & Elias, P. M. 1989. Lipid-content and lipid type as determinants of the epidermal permeability barrier. *Journal of Lipid Research*, 30, 89-96.
- Gulati, M., Grover, M., Singh, S. & Singh, M. 1998. Lipophilic drug derivatives in liposomes. *International Journal of Pharmaceutics*, 165, 129-168.
- Guy, R. H. 1996. Current status and future prospects of transdermal drug delivery. *Pharmaceutical Research*, 13, 1765-1769.
- Gwak, H. S. & Chun, I. K. 2002. Effect of vehicles and penetration enhancers on the in vitro percutaneous absorption of tenoxicam through hairless mouse skin. *International Journal of Pharmaceutics*, 236, 57-64.
- Hadgraft, J. 1991. Structure-activity-relationships and percutaneous-absorption. *Journal of Controlled Release*, 15, 221-226.
- Hadgraft, J. 1999. Passive enhancement strategies in topical and transdermal drug delivery. *International Journal of Pharmaceutics*, 184, 1-6.
- Hadgraft, J. 2001a. Modulation of the barrier function of the skin. *Skin Pharmacology and Applied Skin Physiology*, 14, 72-81.
- Hadgraft, J. 2001b. Skin, the final frontier. *International Journal of Pharmaceutics*, 224, 1-18.
- Hadgraft, J. 2004. Skin deep. *European Journal of Pharmaceutics and Biopharmaceutics*, 58,

291-299.

Hadgraft, J. & Lane, M. E. 2009. Transepidermal water loss and skin site: A hypothesis. *International Journal of Pharmaceutics*, 373, 1-3.

Hadgraft, J., Peck, J., Williams, D. G., Pugh, W. J. & Allan, G. 1996. Mechanisms of action of skin penetration enhancers retarders: Azone and analogues. *International Journal of Pharmaceutics*, 141, 17-25.

Hadgraft, J. & Pugh, W. J. 1998. The selection and design of topical and transdermal agents: a review. *The journal of investigative dermatology. Symposium proceedings / the Society for Investigative Dermatology, Inc. [and] European Society for Dermatological Research*, 3, 131-135.

Hadgraft, J., Williams, D. G. & Allan, G. 1993: Azone: Mechanisms of action and clinical effect. In *Pharmaceutical Skin Penetration Enhancement* Edited by: Walters K, Hadgraft J. New York: Marcel Dekker; 175-198.

Hafeez, F. & Maibach, H. 2013. Occlusion effect on in vivo percutaneous penetration of chemicals in man and monkey: partition coefficient effects. *Skin Pharmacology and Physiology*, 26, 85-91.

Hall, L.H. & Kier, L.B. 1991. The Molecular Connectivity Chi Indices and Kappa Shape Indices in Structure-Property Modeling. In Lipkowitz, K.B. & Boyd B.D. editors *Reviews of Computational Chemistry 2*, ISBN:9780471188100, 367-422

Hamuy, R. & Berman, B. 1998a. Topical antiviral agents for herpes simplex virus infections. *Drugs of Today*, 34, 1013-1025.

Hamuy, R. & Berman, B. 1998b. Treatment of herpes simplex virus infections with topical antiviral agents. *European Journal of Dermatology*, 8, 310-319.

Han, Y. M., Du, P. X., Cao, J. J. & Posmentier, E. S. 2006. Multivariate analysis of heavy metal contamination in urban dusts of Xi'an, Central China. *Science of the Total Environment*, 355, 176-186.

Hansen, C.M. 1967. The Three Dimensional Solubility Parameter - Key to Paint Component Affinities II. - Dyes, Emulsifiers, Mutual Solubility and Compatibility, and Pigments. *Journal of Paint Technology*. 39, 505-510.

- Harada, S., Nakada, Y., Yamashita, F. & Hashida, M. 2005. Biopharmaceutical considerations on antihistamine effects of topically administered emedastine. *Journal of Pharmaceutical Sciences*, 94, 17-24.
- Harper, C. A., Baker, A.-M. M., Mead, J., Wright, R. E., Margolis, J. M., Peters, S. T., Zweben, C., Izzo, C. P., Petrie, E. M., Hull, J. L., Hernandez, R. J. & Selke, S. E. 2002. *Handbook of plastics, elastomers, and composites*. 4th ed. New York: McGraw-Hill. ISBN: 9780071384766
- Harrison, J. E., Groundwater, P. W., Brain, K. R. & Hadgraft, J. 1996a. Azone(R) induced fluidity in human stratum corneum. A Fourier transform infrared spectroscopy investigation using the perdeuterated analogue. *Journal of Controlled Release*, 41, 283-290.
- Harrison, J. E., Watkinson, A. C., Green, D. M., Hadgraft, J. & Brain, K. 1996b. The relative effect of Azone(R) and Transcutol(R) on permeant diffusivity and solubility in human stratum corneum. *Pharmaceutical Research*, 13, 542-546.
- Harvey, P. W. & Everett, D. J. 2004. Significance of the detection of esters of p-hydroxybenzoic acid (parabens) in human breast tumours. *Journal of Applied Toxicology*, 24, 1-4.
- Hatanaka, T., Inuma, M., Sugibayashi, K. & Morimoto, Y. 1990. Prediction of skin permeability of drugs .1. Comparison with artificial membrane. *Chemical & Pharmaceutical Bulletin*, 38, 3452-3459.
- Hatanaka, T., Inuma, M., Sugibayashi, K. & Morimoto, Y. 1992. Prediction of skin permeability of drugs .2. Development of composite membrane as a skin alternative. *International Journal of Pharmaceutics*, 79, 21-28.
- Hathout, R. M. 2014. Using principal component analysis in studying the transdermal delivery of a lipophilic drug from soft nano-colloidal carriers to develop a quantitative composition effect permeability relationship. *Pharmaceutical Development and Technology*, 19, 598-604.
- Haware, R. V., Tho, I. & Bauer-Brandl, A. 2009. Application of multivariate methods to compression behavior evaluation of directly compressible materials. *European Journal of Pharmaceutics and Biopharmaceutics*, 72, 148-155.
- Henmi, T., Fujii, M., Kikuchi, K., Yamanobe, N. & Matsumoto, M. 1994. Application of an oily gel formed by hydrogenated soybean phospholipids as a percutaneous absorption-type

ointment base. *Chemical & Pharmaceutical Bulletin*, 42, 651-655.

Henzl, M. R. & Loomba, P. K. 2003. Transdermal delivery of sex steroids for hormone replacement therapy and contraception - A review of principles and practice. *Journal of Reproductive Medicine*, 48, 525-540.

Higuchi, T. 1960. Physical chemical analysis of percutaneous absorption process from creams and ointments. *Journal Society of Cosmetic Chemists* 11, 70-82.

Higuchi, T. 1961. Rate of release of medicaments from ointment bases containing drugs in suspension. *Journal of Pharmaceutical Sciences*, 50, 874-875.

Higuchi, W. I., Ho, N.F.H., Park, J.Y. & Komiya, I. 1981. Rate limiting steps and factors in drug absorption. In: eds. L.F. Nimmo and W.S. Prescott. *Drug Absorption*. MTP Press, Lancaster, 35-60.

Hikima, T., Tojo, K. & Maibach, H. I. 2005. Skin metabolism in transdermal therapeutic systems. *Skin Pharmacology and Physiology*, 18, 153-159.

Hildebrand, J. H. & Scott, R. L. 1950. *The solubility of nonelectrolytes*, New York, Reinhold Pub. Corp. pp 497.

Hiranita, T., Nakamura, S., Kawachi, M., Courrier, H. N., Vandamme, T. F., Krafft, M. P. & Shibata, O. 2003. Miscibility behavior of dipalmitoylphosphatidylcholine with a single-chain partially fluorinated amphiphile in Langmuir monolayers. *Journal of Colloid and Interface Science*, 265, 83-92.

Hirvonen, J., Rajala, R., Vihervaara, P., Laine, E., Paronen, P. & Urtti, A. 1994. Mechanism and reversibility of penetration enhancer action in the skin - A DSC study. *European Journal of Pharmaceutics and Biopharmaceutics*, 40, 81-85.

Hogan, D. J. & Maibach, H. I. 1990. Adverse dermatological reactions to transdermal drug delivery systems. *Journal of the American Academy of Dermatology*, 22, 811-814.

Holzner, C. 1963. The use of isopropyl fatty esters in cosmetic formulations. *American Perfumer. Cosmetics*, 78, 89-93.

Hope, M. J. & Kitson, C. N. 1993. Liposomes - A perspective for dermatologists. *Dermatologic Clinics*, 11, 143-154.

- Hori, M., Satoh, S., Maibach, H. I. & Guy, R. H. 1991. Enhancement of propranolol hydrochloride and diazepam skin absorption invitro - Effect of enhancer lipophilicity. *Journal of Pharmaceutical Sciences*, 80, 32-35.
- Hotchkiss, S. A. M., Miller, J. M. & Caldwell, J. 1992. Percutaneous-absorption of benzyl acetate through rat skin invitro .2. Effect of vehicle and occlusion. *Food and Chemical Toxicology*, 30, 145-153.
- Houk, J. & Guy, R. H. 1988. Membrane models for skin penetration studies. *Chemical Reviews*, 88, 455-471.
- Howes, D., Guy, R., Hadgraft, J., Heylings, J., Hoeck, U., Kemper, F., Maibach, H., Marty, J. P., Merk, H., Parra, J., Rekkas, D., Rondelli, I., Schaefer, H., Tauber, U. & Verbiere, N. 1996. Methods for assessing percutaneous absorption - The report and recommendations of ECVAM workshop 13. *Atla-Alternatives to Laboratory Animals*, 24, 81-106.
- Huang Z., Fenglou Z., Eric L., Julian Y. Zuo & Dan Z. 2012. Gas Chromatograph Applications in Petroleum Hydrocarbon Fluids, *Advanced Gas Chromatography - Progress in Agricultural, Biomedical and Industrial Applications*, Dr. Mustafa Ali Mohd (Ed.), ISBN: 978-953-51-0298-4, InTech, DOI: 10.5772/34074.
- Huang, M. T., Xie, J. G., Wang, Z. Y., Ho, C. T., Leu, Y. R., Wang, C. X., Hard, G. C. & Conney, A. H. 1997. Effects of tea, decaffeinated tea, and caffeine on UVB light-induced complete carcinogenesis in SKH-1 mice: Demonstration of caffeine as a biologically important constituent of tea. *Cancer Research*, 57, 2623-2629.
- ICH Harmonised tripartite guideline, 2005. Validation of analytical procedures: Text and methodology Q2(R1). www.ich.org
- Idborg-Bjorkman, H., Edlund, P. O., Kvalheim, O. M., Schuppe-Koistinen, I. & Jacobsson, S. P. 2003. Screening of biomarkers in rat urine using LC/electrospray ionization-MS and two-way data analysis. *Analytical Chemistry*, 75, 4784-4792.
- Iervolino, M., Raghavan, S. L. & Hadgraft, J. 2000. Membrane penetration enhancement of ibuprofen using supersaturation. *International Journal of Pharmaceutics*, 198, 229-238.
- Iozzo, R. V. 2005. Basement membrane proteoglycans: From cellar to ceiling. *Nature Reviews Molecular Cell Biology*, 6, 646-656.

- Irwin, W. J., Sanderson, F. D. & Po, A. L. W. 1990. Percutaneous-absorption of ibuprofen - Vehicle effects on transport through rat skin. *International Journal of Pharmaceutics*, 66, 193-200.
- Isidorov, V. A. & Szczepaniak, L. 2009. Gas chromatographic retention indices of biologically and environmentally important organic compounds on capillary columns with low-polar stationary phases. *Journal of Chromatography A*, 1216, 8998-9007.
- Jackson, J. E. 1991. *A user's guide to principal components*, New York, Wiley. 1-18
- Jain, A. K., Thomas, N. S. & Panchagnula, R. 2002. Transdermal drug delivery of imipramine hydrochloride. I. Effect of terpenes. *Journal of Controlled Release*, 79, 93-101.
- Jarupanich, T., Lamlertkittikul, S. & Chandeying, V. 2003. Efficacy, safety and acceptability of a seven-day, transdermal estradiol patch for estrogen replacement therapy. *Journal of the Medical Association of Thailand*, 86, 836-45.
- Jee, J.-P., Lim, S.-J., Park, J.-S. & Kim, C.-K. 2006. Stabilization of all-trans retinol by loading lipophilic antioxidants in solid lipid nanoparticles. *European Journal of Pharmaceutics and Biopharmaceutics*, 63, 134-139.
- Jenning, V. & Gohla, S. H. 2001. Encapsulation of retinoids in solid lipid nanoparticles (SLN (R)). *Journal of Microencapsulation*, 18, 149-158.
- Jenning, V., Gysler, A., Schafer-Korting, M. & Gohla, S. H. 2000a. Vitamin A loaded solid lipid nanoparticles for topical use: occlusive properties and drug targeting to the upper skin. *European Journal of Pharmaceutics and Biopharmaceutics*, 49, 211-218.
- Jenning, V., Schafer-Korting, M. & Gohla, S. 2000b. Vitamin A-loaded solid lipid nanoparticles for topical use drug release properties. *Journal of Controlled Release*, 66, 115-126.
- Jiang, R. Y., Benson, H. A. E., Cross, S. E. & Roberts, M. S. 1998. In vitro human epidermal and polyethylene membrane penetration and retention of the sunscreen benzophenone-3 from a range of solvents. *Pharmaceutical Research*, 15, 1863-1868.
- Johnson, M. E., Blankschtein, D. & Langer, R. 1995. Permeation of steroids through human skin. *Journal of Pharmaceutical Sciences*, 84, 1144-1146.
- Jones, S. A., Reid, M. L. & Brown, M. B. 2009. Determining degree of saturation after application of transiently supersaturated metered dose aerosols for topical delivery of corticosteroids. *Journal of Pharmaceutical Sciences*, 98, 543-554.

- Jorgensen, A. C., Miroshnyk, I., Karjalainen, M., Jouppila, K., Siiria, S., Antikainen, O. & Rantanen, J. 2006. Multivariate data analysis as a fast tool in evaluation of solid state phenomena. *Journal of Pharmaceutical Sciences*, 95, 906-916.
- Joshi, V., Brewster, D., & Colonero, P. 2012. Transdermal diffusion. In vitro diffusion studies in transdermal research: a synthetic membrane model in place of human skin. *Drug Development & Delivery* 12, 40-42.
- Joshi, M. & Patravale, V. 2006. Formulation and evaluation of nanostructured lipid carrier (NLC)-based gel of Valdecocix. *Drug Development and Industrial Pharmacy*, 32, 911-918.
- Kaliszan, R. 1992. Quantitative structure-retention relationships. *Analytical Chemistry*, 64, 619A-631A.
- Kamo, J., Hirai, T. & Kamada, K. 1992. Solvent-induced morphological change of microporous hollow fiber membranes. *Journal of Membrane Science*, 70, 217-224.
- Kandimalla, K., Kanikkannan, N., Andega, S. & Singh, M. 1999. Effect of fatty acids on the permeation of melatonin across rat and pig skin in-vitro and on the transepidermal water loss in rats in-vivo. *Journal of Pharmacy and Pharmacology*, 51, 783-790.
- Kang, S. H. & Kim, H. 1997. Simultaneous determination of methylparaben, propylparaben and thimerosal by high-performance liquid chromatography and electrochemical detection. *Journal of Pharmaceutical and Biomedical Analysis*, 15, 1359-1364.
- Karande, P., Jain, A. & Mitragotri, S. 2006. Insights into synergistic interactions in binary mixtures of chemical permeation enhancers for transdermal drug delivery. *Journal of Controlled Release*, 115, 85-93.
- Karande, P. & Mitragotri, S. 2009. Enhancement of transdermal drug delivery via synergistic action of chemicals. *Biochimica et Biophysica Acta-Biomembranes*, 1788, 2362-2373.
- Karpanen, T. J., Conway, B. R., Worthington, T., Hilton, A. C., Elliott, T. S. J. & Lambert, P. A. 2010. Enhanced chlorhexidine skin penetration with eucalyptus oil. *BMC Infectious Diseases*, 10.
- Katz, M. & Poulsen, B. J. 1971. Absorption of drugs through the skin. Brodie, B.B. and J.R. Gillette (Edited by). *Handbuch Der Experimentellen Pharmakologie*. Band Xxviii. Teil 1. (Handbook of Experimental Pharmacology. Vol. Xxviii. Part 1: Concepts in Biochemical Pharmacology. Illus. Springer-Verlag: Berlin, West Germany; New York, N.Y., U.S.A, pp. 103-174.

- Keister, J. C. & Kasting, G. B. 1986. The use of transient diffusion to investigate transport pathways through skin. *Journal of Controlled Release*, 4, 111-118.
- Kemken, J., Ziegler, A. & Muller, B. W. 1992. Influence of supersaturation on the pharmacodynamic effect of bupranolol after dermal administration using microemulsions as vehicle. *Pharmaceutical Research*, 9, 554-558.
- Khanna, S. & Darbre, P. D. 2013. Parabens enable suspension growth of MCF-10A immortalized, non-transformed human breast epithelial cells. *Journal of Applied Toxicology*, 33, 378-382.
- Kier, L. B. & Hall, L. H. 1977. Nature of structure-activity-relationships and their relation to molecular connectivity. *European Journal of Medicinal Chemistry*, 12, 307-312.
- Kiptoo, P. K., Paudel, K. S., Hammell, D. C., Pinninti, R. R., Chen, J., Crooks, P. A. & Stinchcomb, A. L. 2009. Transdermal Delivery of Bupropion and its Active Metabolite, Hydroxybupropion: A Prodrug Strategy as an Alternative Approach. *Journal of Pharmaceutical Sciences*, 98, 583-594.
- Kirjavainen, M., Monkkonen, J., Saukkosaari, M., Valjakka-Koskela, R., Kiesvaara, J. & Urtti, A. 1999a. Phospholipids affect stratum corneum lipid bilayer fluidity and drug partitioning into the bilayers. *Journal of Controlled Release*, 58, 207-214.
- Kirjavainen, M., Urtti, A., Jaaskelainen, I., Suhonen, T. M., Paronen, P., Valjakkakoskela, R., Kiesvaara, J. & Monkkonen, J. 1996. Interaction of liposomes with human skin in vitro - The influence of lipid composition and structure. *Biochimica et Biophysica Acta-Lipids and Lipid Metabolism*, 1304, 179-189.
- Kirjavainen, M., Urtti, A., Valjakka-Koskela, R., Kiesvaara, J. & Monkkonen, J. 1999b. Liposome-skin interactions and their effects on the skin permeation of drugs. *European Journal of Pharmaceutical Sciences*, 7, 279-286.
- Kitagawa, S., Li, H. & Sato, S. 1997. Skin permeation of parabens in excised guinea pig dorsal skin, its modification by penetration enhancers and their relationship with n-octanol/water partition coefficients. *Chemical & Pharmaceutical Bulletin*, 45, 1354-1357.
- Knutson, K., Potts, R. O., Guzek, D. B., Golden G. M., McKie, J. W., Lambert, W.J. & Higuchi, W.I. 1985. Macro- and molecular physicochemical considerations in understanding drug transport in the stratum corneum. *Journal of Controlled Release* 2: 67-87.

- Koelega, H. S. 1993. Stimulant-drugs and vigilance performance - A review. *Psychopharmacology*, 111, 1-16.
- Kogan, A. & Garti, N. 2006. Microemulsions as transdermal drug delivery vehicles. *Advances in Colloid and Interface Science*, 123, 369-385.
- Kogermann, K., Aaltonen, J., Strachan, C. J., Pollanen, K., Heinamaki, J., Yliruusi, J. & Rantanen, J. 2008. Establishing Quantitative In-Line Analysis of Multiple Solid-State Transformations During Dehydration. *Journal of Pharmaceutical Sciences*, 97, 4983-4999.
- Kogermann, K., Aaltonen, J., Strachan, C. J., Pollanen, K., Veski, P., Heinamaki, J., Yliruusi, J. & Rantanen, J. 2007. Qualitative in situ analysis of multiple solid-state forms using spectroscopy and partial least squares discriminant modeling. *Journal of Pharmaceutical Sciences*, 96, 1802-1820.
- Kokubo, T., Sugibayashi, K. & Morimoto, Y. 1991. Diffusion of drug in acrylic-type pressure-sensitive adhesive matrices .1. Influence of physical property of the matrices on the drug diffusion. *Journal of Controlled Release*, 17, 69-77.
- Komatsu, N., Saijoh, K., Toyama, T., Ohka, R., Otsuki, N., Hussack, G., Takehara, K. & Diamandis, E. P. 2005. Multiple tissue kallikrein mRNA and protein expression in normal skin and skin diseases. *British Journal of Dermatology*, 153, 274-281.
- Kondo, S., Yamasakikonishi, H. & Sugimoto, I. 1987. Enhancement of transdermal delivery by superfluous thermodynamic potential .2. Invitro-invivo correlation of percutaneous nifedipine transport. *Journal of Pharmacobio-Dynamics*, 10, 662-668.
- Kornick, C. A., Santiago-Palma, J., Moryl, N., Payne, R. & Obbens, E. 2003. Benefit-risk assessment of transdermal fentanyl for the treatment of chronic pain. *Drug Safety*, 26, 951-973.
- Koszinowski, J. 1986. Diffusion and solubility of hydroxy compounds in polyolefines. *Journal of Applied Polymer Science*, 31, 2711-2720.
- Kreilgaard, M. 2002. Influence of microemulsions on cutaneous drug delivery. *Advanced Drug Delivery Reviews*, 54, S77-S98.
- Kriwet, K. & Mullergoymann, C. C. 1995. Diclofenac release from phospholipid drug systems and permeation through excised human stratum-corneum. *International Journal of Pharmaceutics*, 125, 231-242.

- Kushnir, M., Yaar, A., Reichman, A. & Heldman, E. 2008. Transdermal delivery of a levodopa prodrug; a pilot clinical trial. *Movement Disorders*, 23, S196-S196.
- Kvalheim, O. M. 1988. Interpretation of direct latent-variable projection methods and their aims and use in the analysis of multicomponent spectroscopic and chromatographic data. *Chemometrics and Intelligent Laboratory Systems*, 4, 11-25.
- Lademann, J., Richter, H., Schanzer, S., Knorr, F., Meinke, M., Sterry, W. & Patzelt, A. 2011. Penetration and storage of particles in human skin: Perspectives and safety aspects. *European Journal of Pharmaceutics and Biopharmaceutics*, 77, 465-468.
- Laitinen, N., Antikainen, O., Rantanen, J. & Yliruusi, J. 2004. New perspectives for visual characterization of pharmaceutical solids. *Journal of Pharmaceutical Sciences*, 93, 165-176.
- Lam, L. T., Sun, Y., Davey, N., Adams, R., Prapopoulou, M., Brown, M. B. & Moss, G. P. 2010. The application of feature selection to the development of Gaussian process models for percutaneous absorption. *Journal of Pharmacy and Pharmacology*, 62, 738-749.
- Lane, M. E. 2013. Skin penetration enhancers. *International Journal of Pharmaceutics*, 447, 12-21.
- Langer, R. 2004. Transdermal drug delivery: past progress, current status, and future prospects. *Advanced Drug Delivery Reviews*, 56, 557-558.
- Larrucea, E., Arellano, A., Santoyo, S. & Ygartua, P. 2001. Combined effect of oleic acid and propylene glycol on the percutaneous penetration of tenoxicam and its retention in the skin. *European Journal of Pharmaceutics and Biopharmaceutics*, 52, 113-119.
- Lau, H. L. N., Puah, C. W., Choo, Y. M., Ma, A. N. & Chuah, C. H. 2005. Simultaneous quantification of free fatty acids, free sterols, squalene, and acylglycerol molecular species in palm oil by high-temperature gas chromatography-flame ionization detection. *Lipids*, 40, 523-528.
- Lauer, A. C., Lieb, L. M., Ramachandran, C., Flynn, G. L. & Weiner, N. D. 1995. Transfollicular drug-delivery. *Pharmaceutical Research*, 12, 179-186.
- Lee, C. K., Uchida, T., Kitagawa, K., Yagi, A., Kim, N. S. & Goto, S. 1994. Relationship between lipophilicity and skin permeability of various drugs from an ethanol/water/lauric acid system. *Biological & Pharmaceutical Bulletin*, 17, 1421-1424.
- Lee, J. N., Park, C. & Whitesides, G. M. 2003. Solvent compatibility of poly(dimethylsiloxane)-based microfluidic devices. *Analytical Chemistry*, 75, 6544-6554.

- Lehman, P. A., Raney, S. G. & Franz, T. J. 2011. Percutaneous Absorption in Man: In vitro-in vivo Correlation. *Skin Pharmacology and Physiology*, 24, 224-230.
- Leichtnam, M.-L., Rolland, H., Wuethrich, P. & Guy, R. H. 2007. Impact of antinucleants on transdermal delivery of testosterone from a spray. *Journal of Pharmaceutical Sciences*, 96, 84-92.
- Leichtnam, M.-L., Rolland, H., Wuthrich, P. & Guy, R. H. 2006. Formulation and evaluation of a testosterone transdermal spray. *Journal of Pharmaceutical Sciences*, 95, 1693-1702.
- Lemont B & Kier 1989. An Index of Flexibility from Kappa Shape Values. *Quantitative Structure-Activity Relationships*, 8, 221 -224.
- Leopold, C. S. & Lippold, B. C. 1995. An attempt to clarify the mechanism of the penetration enhancing effects of lipophilic vehicles with differential scanning calorimetry (DSC). *Journal of Pharmacy and Pharmacology*, 47, 276-281.
- Lien, E. J. & Gao, H. 1995. QSAR analysis of skin permeability of various drugs in man as compared to in-vivo and in-vitro studies in rodents. *Pharmaceutical Research*, 12, 583-587.
- Lippold, B. C. & Schneemann, H. 1984. The influence of vehicles on the local bioavailability of betamethasone-17-benzoate from solution-type and suspension-type ointments. *International Journal of Pharmaceutics*, 22, 31-43.
- Liron, Z. & Cohen, S. 1984. Percutaneous-absorption of alkanolic acids .2. Application of regular solution theory. *Journal of Pharmaceutical Sciences*, 73, 538-542.
- Liu, J., Hu, W., Chen, H., Ni, Q., Xu, H. & Yang, X. 2007. Isotretinoin-loaded solid lipid nanoparticles with skin targeting for topical delivery. *International Journal of Pharmaceutics*, 328, 191-195.
- Liu, P., Cettina, M. & Wong, J. 2009. Effects of isopropanol-isopropyl myristate binary enhancers on in vitro transport of estradiol in human epidermis: A mechanistic evaluation. *Journal of Pharmaceutical Sciences*, 98, 565-572.
- Liu, P. C., Kuriharabergstrom, T. & Good, W. R. 1991. Cotransport of estradiol and ethanol through human skin invitro - Understanding the permeant enhancer flux relationship. *Pharmaceutical Research*, 8, 938-944.
- Liu, P. C., Nightingale, J. A. S. & Kuriharabergstrom, T. 1993. Variation of human skin permeation invitro - Ionic vs neutral compounds. *International Journal of Pharmaceutics*, 90, 171-176.

- Loden, M. 2003. Role of topical emollients and moisturizers in the treatment of dry skin barrier disorders. *American Journal of Clinical Dermatology*, 4, 771-788.
- Loden, M. & Lindberg, M. 1991. The influence of a single application of different moisturizers on the skin capacitance. *Acta Dermato-Venereologica*, 71, 79-82.
- Long, C. C. 2002. Common skin disorders and their topical treatment. *Drugs and the Pharmaceutical Sciences. Dermatological and transdermal formulations*, 119, 41-60.
- Lopez, V. C., Hadgraft, J. & Snowden, M. J. 2005. The use of colloidal microgels as a (trans)dermal drug delivery system. *International Journal of Pharmaceutics*, 292, 137-147.
- Lopez, V. C., Raghavan, S. L. & Snowden, M. J. 2004. Colloidal microgels as transdermal delivery systems. *Reactive & Functional Polymers*, 58, 175-185.
- Lotte C. 1997. A reconstructed skin model for permeation studies. In: Brian K, James VJ, Walters KA, editors. *Perspectives in Percutaneous Absorption*. Cardiff: STS Publishing, 61-70.
- Lotte, C., Patouillet, C., Zanini, M., Messenger, A. & Roguet, R. 2002. Permeation and skin absorption: Reproducibility of various industrial reconstructed human skin models. *Skin Pharmacology and Applied Skin Physiology*, 15, 18-30.
- Lu, Y.-P., Lou, Y.-R., Peng, Q.-Y., Xie, J.-G., Nghiem, P. & Conney, A. H. 2008. Effect of caffeine on the ATR/Chk1 pathway in the epidermis of UVB-irradiated mice. *Cancer Research*, 68, 2523-2529.
- Lu, Y. P., Lou, Y. R., Lin, Y., Shih, W. C. J., Huang, M. T., Yang, C. S. & Conney, A. H. 2001. Inhibitory effects of orally administered green tea, black tea, and caffeine on skin carcinogenesis in mice previously treated with ultraviolet B light (high-risk mice): Relationship to decreased tissue fat. *Cancer Research*, 61, 5002-5009.
- Maggio, R. M., Castellano, P. M. & Kaufman, T. S. 2008. A new principal component analysis-based approach for testing "similarity" of drug dissolution profiles. *European Journal of Pharmaceutical Sciences*, 34, 66-77.
- Maggio, R. M., Castellano, P. M. & Kaufman, T. S. 2009. PCA-CR analysis of dissolution profiles. A chemometric approach to probe the polymorphic form of the active pharmaceutical ingredient in a drug product. *International Journal of Pharmaceutics*, 378, 187-193.

- Magnusson, B. M., Anissimov, Y. G., Cross, S. E. & Roberts, M. S. 2004. Molecular size as the main determinant of solute maximum flux across the skin. *Journal of Investigative Dermatology*, 122, 993-999.
- Mahjour, M., Mauser, B. E. & Fawzi, M. B. 1989. Skin permeation enhancement effects of linoleic-acid and azone on narcotic analgesics. *International Journal of Pharmaceutics*, 56, 1-11.
- Maitani, Y., Sato, H. & Nagai, T. 1995. Effect of ethanol on the true diffusion-coefficient of diclofenac and its sodium-salt in silicone membrane. *International Journal of Pharmaceutics*, 113, 165-174.
- Majumdar, S., Mueller-Spaeth, M. & Sloan, K. B. 2012. Prodrugs of Theophylline Incorporating Ethyleneoxy Groups in the Promoiety: Synthesis, Characterization, and Transdermal Delivery. *Aaps Pharmscitech*, 13, 853-862.
- Mak, V. H. W., Potts, R. O. & Guy, R. H. 1990. Oleic-acid concentration and effect in human stratum-corneum - Noninvasive determination by attenuated total reflectance infrared-spectroscopy invivo. *Journal of Controlled Release*, 12, 67-75.
- Mak, V. H. W., Potts, R. O. & Guy, R. H. 1991. Does hydration affect intercellular lipid organization in the stratum-corneum. *Pharmaceutical Research*, 8, 1064-1065.
- Malzfeldt, E., Lehmann, P., Goerz, G. & Lippold, B. C. 1989. Influence of drug solubility in the vehicle on clinical efficacy of ointments. *Archives of Dermatological Research*, 281, 193-197.
- Mao, Y.-T., Hua, H.-Y., Zhang, X.-G., Zhu, D.-X., Li, F., Gui, Z.-H. & Zhao, Y.-X. 2013. Ethosomes as delivery system for transdermal administration of vinpocetine. *Pharmazie*, 68, 381-382.
- Marrink, S. J. & Berendsen, H. J. C. 1996. Permeation process of small molecules across lipid membranes studied by molecular dynamics simulations. *Journal of Physical Chemistry*, 100, 16729-16738.
- Martin, Y. C. 1981. A practitioners perspective of the role of quantitative structure-activity analysis in medicinal chemistry. *Journal of Medicinal Chemistry*, 24, 229-237.
- Masunaga, T. 2006. Epidermal basement membrane: Its molecular organization and blistering disorders. *Connective Tissue Research*, 47, 55-66.

- Mcauley, W. J., Lad, M. D., Mader, K. T., Santos, P., Tetteh, J., Kazarian, S. G., Hadgraft, J. & Lane, M. E. 2010. ATR-FTIR spectroscopy and spectroscopic imaging of solvent and permeant diffusion across model membranes. *Eur J Pharm Biopharm*, 74, 413-9.
- Mcauley, W. J., Mader, K. T., Tetteh, J., Lane, M. E. & Hadgraft, J. 2009. Simultaneous monitoring of drug and solvent diffusion across a model membrane using ATR-FTIR spectroscopy. *European Journal of Pharmaceutical Sciences*, 38, 378-383.
- McNair, H. M. & Miller, J. M. 1998. *Basic gas chromatography*, New York ; Chichester, John Wiley. pp193
- Megrab, N. A., Williams, A. C. & Barry, B. W. 1995. Estradiol permeation across human skin, silastic and snake skin membranes - the effects of ethanol-water cosolvent systems. *International Journal of Pharmaceutics*, 116, 101-112.
- Meidan, V. M., Bonner, M. C. & Michniak, B. B. 2005. Transfollicular drug delivery - Is it a reality? *International Journal of Pharmaceutics*, 306, 1-14.
- Menon, G. K., Cleary, G. W. & Lane, M. E. 2012. The structure and function of the stratum corneum. *International Journal of Pharmaceutics*, 435, 3-9.
- Menon, G. K. & Lee, S. H. 1998. Ultrastructural effects of some solvents and vehicles on the stratum corneum and other skin components: evidence for an "extended mosaic-partitioning model of the skin barrier. In Roberts, M. S. & Walters, K. A. *Dermal absorption and toxicity assessment*, New York London, Informa Healthcare ; Taylor & Francis.
- Michaels, A. S., Chandrasekaran, S. K. & Shaw, J. E. 1975. Drug permeation through human skin - Theory and invitro experimental measurement. *Aiche Journal*, 21, 985-996.
- Miller, J. N. & Miller, J. C. 2010. *Statistics and chemometrics for analytical chemistry*, Harlow, England ; New York, Prentice Hall/Pearson.
- Milosovich, S. M., Hussain, A. A., Hussain, M. & Dittert, L. 1989. The utilization of prodrugs to enhance transdermal absorption of testosterone, deoxycorticosterone & indomethacin. *Progress in clinical and biological research*, 292, 273-7.
- Mitragotri, S. 2000. Synergistic effect of enhancers for transdermal drug delivery. *Pharmaceutical Research*, 17, 1354-1359.
- Mitragotri, S. 2003. Modeling skin permeability to hydrophilic and hydrophobic solutes based on four permeation pathways. *Journal of Controlled Release*, 86, 69-92.

- Mitragotri, S., Anissimov, Y. G., Bunge, A. L., Frasc, H. F., Guy, R. H., Hadgraft, J., Kasting, G. B., Lane, M. E. & Roberts, M. S. 2011. Mathematical models of skin permeability: An overview. *International Journal of Pharmaceutics*, 418, 115-129.
- Moghimi, S. M. & Patel, H. M. 1993. Durrent progress and future-prospects of liposomes in dermal drug delivery. *Journal of Microencapsulation*, 10, 155-162.
- Mondello, L., Casilli, A., Tranchida, P. Q., Costa, R., Dugo, P. & Dugo, G. 2004. Fast GC for the analysis of citrus oils. *Journal of Chromatographic Science*, 42, 410-416.
- Mondello, L., Casilli, A., Tranchida, P. Q., Furukawa, M., Komori, K., Miseki, K., Dugo, P. & Dugo, G. 2006. Fast enantiomeric analysis of a complex essential oil with an innovative multidimensional gas chromatographic system. *Journal of Chromatography A*, 1105, 11-16.
- Moser, K., Kriwet, K., Naik, A., Kalia, Y. N. & Guy, R. H. 2001. Passive skin penetration enhancement and its quantification in vitro. *European Journal of Pharmaceutics and Biopharmaceutics*, 52, 103-112.
- Moss, G. P. & Cronin, M. T. D. 2002. Quantitative structure-permeability relationships for percutaneous absorption: re-analysis of steroid data. *International Journal of Pharmaceutics*, 238, 105-109.
- Moss, G. P., Gullick, D. R., Cox, P. A., Alexander, C., Ingram, M. J., Smart, J. D. & Pugh, W. J. 2006. Design, synthesis and characterization of captopril prodrugs for enhanced percutaneous absorption. *Journal of Pharmacy and Pharmacology*, 58, 167-177.
- Moss, G. P., Sun, Y., Wilkinson, S. C., Davey, N., Adams, R., Martin, G. P., Prapopopolou, M. & Brown, M. B. 2011. The application and limitations of mathematical modelling in the prediction of permeability across mammalian skin and polydimethylsiloxane membranes. *J Pharm Pharmacol*, 63, 1411-27.
- Mossa, G. P., Sun, Y., Wilkinson, S. C., Davey, N., Adams, R., Martin, G. P., Prapopopolou, M. & Brown, M. B. 2011. The application and limitations of mathematical modelling in the prediction of permeability across mammalian skin and polydimethylsiloxane membranes. *Journal of Pharmacy and Pharmacology*, 63, 1411-1427.
- Most, C. F. 1970. Some filler effects on diffusion in silicone rubber. *Journal of Applied Polymer Science*, 14, 1019-1024.
- Most, C. F. 1972. Co-permeant enhancement of drug transmission rates through silicone-rubber. *Journal of Biomedical Materials Research*, 6, 3-14.

- Mueller, R. H., Petersen, R. D., Hornmoss, A. & Pardeike, J. 2007. Nanostructured lipid carriers (NLC) in cosmetic dermal products. *Advanced Drug Delivery Reviews*, 59, 522-530.
- Mulder, M. H. V., Franken, T. & Smolders, C. A. 1985. Preferential sorption versus preferential permeability in pervaporation. *Journal of Membrane Science*, 22, 155-173.
- Müller, B. & Kreuter, J. 1999. Enhanced transport of nanoparticle associated drugs through natural and artificial membranes - a general phenomenon? *International Journal of Pharmaceutics*, 178, 23-32.
- Müller, R. H., Immig, H. & Hommoss, A. 2007. Prolonged release of perfumes by nano lipid carriers (NLC) technology. *Euro cosmetics* 15, 10-15.
- Mullerplathe, F. 1991. Diffusion of penetrants in amorphous polymers - a molecular-dynamics study. *Journal of Chemical Physics*, 94, 3192-3199.
- Murphy, M. & Carmichael, A. J. 2000. Transdermal drug delivery systems and skin sensitivity reactions. Incidence and management. *American Journal of Clinical Dermatology*, 1, 361-8.
- Naik, A., Kalia, Y. N. & Guy R.H. 2000. Transdermal drug delivery: overcoming the skin's barrier function. *Pharmaceutical Science & Technology Today*. 3, 318-326.
- Naik, A., Pechtold, L., Potts, R. O. & Guy, R. H. 1995. Mechanism of oleic acid-induced skin penetration enhancement in vivo in humans. *Journal of Controlled Release*, 37, 299-306.
- Nakano, M. & Patel, N. K. 1970. Release, uptake, and permeation behavior of salicylic acid in ointment bases. *Journal of Pharmaceutical Sciences*, 59, 985-8.
- Nanayakkara, G. R., Bartlett, A., Forbes, B., Marriott, C., Whitfield, P. J. & Brown, M. B. 2005. The effect of unsaturated fatty acids in benzyl alcohol on the percutaneous permeation of three model penetrants. *International Journal of Pharmaceutics*, 301, 129-139.
- Nardello, W., Chailloux, N., Poprawski, J., Salager, J. L. & Aubry, J. M. 2003. HLD concept as a tool for the characterization of cosmetic hydrocarbon oils. *Polymer International*, 52, 602-609.
- Nastruzzi, C., Esposito, E., Pastesini, C., Gambari, R. & Menegatti, E. 1993. Comparative-study on the release kinetics of methyl-nicotinate from topic formulations. *International Journal of Pharmaceutics*, 90, 43-50.

- Neudecker B. A., Csóker, A. B., Kazuhiro. M., Maibach, H. I. & Stern, R. 2000. Hyaluronan: the natural moisturizer. In: Elsner P. & Maibach H. I. editors. Cosmeceuticals: drugs vs. cosmetics. New York: Marcel Dekker, 319-357.
- Nisbet, K., 1977. Structure–solubility parameter relationships in alcohols. In Harris, F. W., Seymour, R. B. & American chemical society. meeting . Structure-solubility relationships in polymers, New York, Academic Press.
- Ng, S.-F., Rouse, J. J., Sanderson, F. D. & Eccleston, G. M. 2012. The relevance of polymeric synthetic membranes in topical formulation assessment and drug diffusion study. Archives of Pharmacal Research, 35, 579-593.
- Ng, S.-F., Rouse, J. J., Sanderson, F. D., Meidan, V. & Eccleston, G. M. 2010. Validation of a Static Franz Diffusion Cell System for In Vitro Permeation Studies. AAPS Pharmscitech, 11, 1432-1441.
- OECD, 2004 guidelines for testing of chemicals: Guidance document for the conduct of skin absorption studies. OECD series on testing and assessment No. 28. Organisation for economic co-operation and development, Paris. www.oecd.org
- Oesch, F., Fabian, E., Oesch-Bartlomowicz, B., Werner, C. & Landsiedel, R. 2007. Drug-metabolizing enzymes in the skin of man, rat, and pig. Drug Metabolism Reviews, 39, 659-698.
- Ogiso, T., Iwaki, M. & Paku, T. 1995. Effect of various enhancers on transdermal penetration of indomethacin and urea, and relationship between penetration parameters and enhancement factors. Journal of Pharmaceutical Sciences, 84, 482-488.
- Oh, H. J., Oh, Y. K. & Kim, C. K. 2001. Effects of vehicles and enhancers on transdermal delivery of melatonin. International Journal of Pharmaceutics, 212, 63-71.
- Oh, S. Y., Jeong, S. Y., Park, T. G. & Lee, J. H. 1998. Enhanced transdermal delivery of AZT (Zidovudine) using iontophoresis and penetration enhancer. Journal of Controlled Release, 51, 161-168.
- Oishi, S. 2002a. Effects of butyl paraben on the male reproductive system in mice. Archives of Toxicology, 76, 423-429.
- Oishi, S. 2002b. Effects of propyl paraben on the male reproductive system. Food and Chemical Toxicology, 40, 1807-1813.

- Okamoto, H., Hashida, M. & Sezaki, H. 1991. Effect of 1-alkyl- or 1-alkenylazacycloalkanone derivatives on the penetration of drugs with different lipophilicities through guinea-pig skin. *Journal of Pharmaceutical Sciences*, 80, 39-45.
- Okamoto, H., Muta, K., Hashida, M. & Sezaki, H. 1990. Percutaneous penetration of acyclovir through excised hairless mouse and rat skin - Effect of vehicle and percutaneous penetration enhancer. *Pharmaceutical Research*, 7, 64-68.
- Oliveira, G., Beezer, A. E., Hadgraft, J. & Lane, M. E. 2010. Alcohol enhanced permeation in model membranes. Part I. Thermodynamic and kinetic analyses of membrane permeation. *International Journal of Pharmaceutics*, 393, 61-67.
- Oliveira, G., Beezer, A. E., Hadgraft, J. & Lane, M. E. 2011. Alcohol enhanced permeation in model membranes. Part II. Thermodynamic analysis of membrane partitioning. *International Journal of Pharmaceutics*, 420, 216-222.
- Oliveira, G., Hadgraft, J. & Lane, M. E. 2012a. The influence of volatile solvents on transport across model membranes and human skin. *International Journal of Pharmaceutics*, 435, 38-49.
- Oliveira, G., Hadgraft, J. & Lane, M. E. 2012b. The role of vehicle interactions on permeation of an active through model membranes and human skin. *International Journal of Cosmetic Science*, 34, 536-545.
- Olsen, L. O. & Jemec, G. B. E. 1993. The influence of water, glycerin, paraffin oil and ethanol on skin mechanics. *Acta Dermato-Venereologica*, 73, 404-406.
- Olszynska-Janus, S., Gasior-Glogowska, M., Szymborska-Malek, K., Komorowska, M., Witkiewicz, W., Pezowicz, C., Szotek, S. & Kobielarz, M. 2012. Spectroscopic techniques in the study of human tissues and their components. Part II: Raman spectroscopy. *Acta of Bioengineering and Biomechanics*, 14, 121-133.
- Ongpipattanakul, B., Burnette, R. R., Potts, R. O. & Francoeur, M. L. 1991. Evidence that oleic-acid exists in a separate phase within stratum-corneum lipids. *Pharmaceutical Research*, 8, 350-354.
- Oprea, T. I. 2000. Property distribution of drug-related chemical databases. *Journal of Computer-Aided Molecular Design*, 14, 251-264.
- Organisation For Economic Co-Operation And Development. 2004. Guidance Document for the Conduct of Skin Absorption Studies. OECD Series on Testing and Assessment, Paris: OECD Publishing.

Ostrenga, J., Steinmet.C & Poulsen, B. 1971. Significance of vehicle composition .1. Relationship between topical vehicle composition, skin penetrability, and clinical efficacy. *Journal of Pharmaceutical Sciences*, 60, 1175-1179.

Ottaviani, G., Martel, S. & Carrupt, P. A. 2006. Parallel artificial membrane permeability assay: A new membrane for the fast prediction of passive human skin permeability. *Journal of Medicinal Chemistry*, 49, 3948-3954.

Pant, P. V. K. & Boyd, R. H. 1993. Molecular-dynamics simulation of diffusion of small penetrants in polymers. *Macromolecules*, 26, 679-686.

Paolino, D., Ventura, C. A., Nisticion, S., Puglisi, G. & Fresta, M. 2002. Lecithin microemulsions for the topical administration of ketoprofen: percutaneous adsorption through human skin and in vivo human skin tolerability. *International Journal of Pharmaceutics*, 244, 21-31.

Pardeike, J., Hommoss, A. & Mueller, R. H. 2009. Lipid nanoparticles (SLN, NLC) in cosmetic and pharmaceutical dermal products. *International Journal of Pharmaceutics*, 366, 170-184.

Pardeike, J. & Müller, R. H. 2007. Coenzyme Q10 loaded NLCs: preparation, occlusive properties and penetration enhancement. *Pharmaceutical Technology Europe*. 19, 46–49.

Pardeike, J., Schwabe, K. & Mueller, R. H. 2010. Influence of nanostructured lipid carriers (NLC) on the physical properties of the Cutanova Nanorepair Q10 cream and the in vivo skin hydration effect. *International Journal of Pharmaceutics*, 396, 166-173.

Park, S. N., Lee, H. J. & Gu, H. A. 2014. Enhanced skin delivery and characterization of rutin-loaded ethosomes. *Korean Journal of Chemical Engineering*, 31, 485-489.

Paudel, K. S., Hammell, D. C., Agu, R. U., Valiveti, S. & Stinchcomb, A. L. 2010. Cannabidiol bioavailability after nasal and transdermal application: effect of permeation enhancers. *Drug Development and Industrial Pharmacy*, 36, 1088-1097.

Payne, R., Mathias, S. D., Pasta, D. J., Wanke, L. A., Williams, R. & Mahmoud, R. 1998. Quality of life and cancer pain: Satisfaction and side effects with transdermal fentanyl versus oral morphine. *Journal of Clinical Oncology*, 16, 1588-1593.

Peck, K. D., Ghanem, A. H. & Higuchi, W. I. 1994. Hindered diffusion of polar-molecules through and effective pore radii estimates of intact and ethanol-treated human epidermal membrane. *Pharmaceutical Research*, 11, 1306-1314.

- Pellett, M. A., Castellano, S., Hadgraft, J. & Davis, A. F. 1997a. The penetration of supersaturated solutions of piroxicam across silicone membranes and human skin in vitro. *Journal of Controlled Release*, 46, 205-214.
- Pellett, M. A., Davis, A. F. & Hadgraft, J. 1994. Effect of supersaturation on membrane-transport .2. Piroxicam. *International Journal of Pharmaceutics*, 111, 1-6.
- Pellett, M. A., Roberts, M. S. & Hadgraft, J. 1997b. Supersaturated solutions evaluated with an in vitro stratum corneum tape stripping technique. *International Journal of Pharmaceutics*, 151, 91-98.
- Pilgram, G. S. K., Engelsma-Van Pelt, A. M., Bouwstra, J. A. & Koerten, H. K. 1999. Electron diffraction provides new information on human stratum corneum lipid organization studied in relation to depth and temperature. *Journal of Investigative Dermatology*, 113, 403-409.
- Pillai, O., Nair, V. & Panchagnula, R. 2004. Transdermal iontophoresis of insulin: IV. Influence of chemical enhancers. *International Journal of Pharmaceutics*, 269, 109-120.
- Plewig, G., Scheuber, E., Reuter, B. & Waidelich, W. 1983. Thickness of corneocytes in stratum corneum, In Mark, R. & Plewig, G editors *Stratum Corneum*, Springer, Berlin, pp. 171-174.
- Postnov, V.V., Gafarova, N. A., Serikov, Zh. S., Nauruzov, M. Kh. & Malenko, E. V. 1972. Composition of liquid paraffinic hydrocarbons from Mangyshlak crude. *Chemistry and Technology of Fuels and Oils*, 8, 260-262.
- Potts, R. O. & Francoeur, M. L. 1991. The influence of stratum-corneum morphology on water permeability. *Journal of Investigative Dermatology*, 96, 495-499.
- Potts, R. O. & Guy, R. H. 1992. Predicting skin permeability. *Pharmaceutical Research*, 9, 663-669.
- Potts, R. O. & Guy, R. H. 1995. A predictive algorithm for skin permeability - The effects of molecular-size and hydrogen-bond activity. *Pharmaceutical Research*, 12, 1628-1633.
- Poucher, W. A. 1959. *Perfumes, cosmetics and soaps, with a special reference to synthetics*, London, Chapman and Hall.
- Poulsen, B. J., Young, E., Coquilla, V. & Katz, M. 1968. Effect of topical vehicle composition on in vitro release of fluocinolone acetonide and its acetate ester. *Journal of Pharmaceutical Sciences*, 57, 928-933.

- Pugh, W. J., Roberts, M. S. & Hadgraft, J. 1996. Epidermal permeability - Penetrant structure relationships .3. The effect of hydrogen bonding interactions and molecular size on diffusion across the stratum corneum. *International Journal of Pharmaceutics*, 138, 149-165.
- Raghavan, S. L., Kieper, B., Davis, A. F., Kazarian, S. G. & Hadgraft, J. 2001a. Membrane transport of hydrocortisone acetate from supersaturated solutions; the role of polymers. *International Journal of Pharmaceutics*, 221, 95-105.
- Raghavan, S. L., Trividic, A., Davis, A. F. & Hadgraft, J. 2001b. Crystallization of hydrocortisone acetate: influence of polymers. *International Journal of Pharmaceutics*, 212, 213-221.
- Rahman, M. S., Gallo, M. A., Umbreit, T. H. & Zatz, J. L. 1992. Investigation of the invitro interaction of various vehicles with hairless mouse skin. *Journal of the Society of Cosmetic Chemists*, 43, 251-258.
- Rane, S. S. & Anderson, B. D. 2008. What determines drug solubility in lipid vehicles: Is it predictable? *Advanced Drug Delivery Reviews*, 60, 638-656.
- Rastogi, S. K. & Singh, J. 2004. Iontophoretic enhancement of leuprolide acetate by fatty acids, limonene, and depilatory lotions through porcine epidermis. *Pharmaceutical Development and Technology*, 9, 341-348.
- Rawlings, A. V. & Harding, C. R. 2004. Moisturization and skin barrier function. *Dermatologic therapy*, 17 Suppl 1, 43-8.
- Rawlings, A. V. & Matts, P. J. 2005. Stratum corneum moisturization at the molecular level: An update in relation to the dry skin cycle. *Journal of Investigative Dermatology*, 124, 1099-1110.
- Rawlings, A. V., Scott, I. R., Harding, C. R. & Bowser, P. A. 1994. Stratum corneum moisturization at the molecular level. *Journal of Investigative Dermatology*, 103, 731-740.
- Raykar, P. V., Fung, M. C. & Anderson, B. D. 1988. The role of protein and lipid domains in the uptake of solutes by human stratum-corneum. *Pharmaceutical Research*, 5, 140-150.
- Reid, M. K. & Spencer, K. L. 2009. Use of principal components analysis (PCA) on estuarine sediment datasets: The effect of data pre-treatment. *Environmental Pollution*, 157, 2275-2281.
- Reid, M. L., Benaouda, F., Khengar, R., Jones, S. A. & Brown, M. B. 2013. Topical corticosteroid delivery into human skin using hydrofluoroalkane metered dose aerosol sprays. *International Journal of Pharmaceutics*, 452, 157-165.

- Reid, M. L., Brown, M. B. & Jones, S. A. 2008a. Manipulation of corticosteroid release from a transiently supersaturated topical metered dose aerosol using a residual miscible co-solvent. *Pharmaceutical Research*, 25, 2573-2580.
- Reid, M. L., Brown, M. B., Moss, G. P. & Jones, S. A. 2008b. An investigation into solvent-membrane interactions when assessing drug release from organic vehicles using regenerated cellulose membranes. *Journal of Pharmacy and Pharmacology*, 60, 1139-1147.
- Reid, M. L., Jones, S. A. & Brown, M. B. 2009. Transient drug supersaturation kinetics of beclomethasone dipropionate in rapidly drying films. *International Journal of Pharmaceutics*, 371, 114-119.
- Rencher, A. C. 2001. *Methods of multivariate analysis*, New York, Wiley.
- Rencher, A. C. 2002. *Methods of multivariate analysis*, New York, J. Wiley.
- Rhee, Y.-S., Huh, J.-Y., Park, C.-W., Nam, T.-Y., Yoon, K.-R., Chi, S.-C. & Park, E.-S. 2007. Effects of vehicles and enhancers on transdermal delivery of clebopride. *Archives of Pharmacal Research*, 30, 1155-1161.
- Rhee, Y. S., Choi, J. G., Park, E. S. & Chi, S. C. 2001. Transdermal delivery of ketoprofen using microemulsions. *International Journal of Pharmaceutics*, 228, 161-170.
- RiemmaPierre, M. B. & Miranda Costa, I. D. S. 2011. Liposomal systems as drug delivery vehicles for dermal and transdermal applications. *Archives of Dermatological Research*, 303, 607-621.
- Roberts, M. S. & Anderson, R. A. 1975. Percutaneous absorption of phenolic compounds - effect of vehicles on penetration of phenol. *Journal of Pharmacy and Pharmacology*, 27, 599-605.
- Roberts, M. S., Cross, S. E. & Pellett, M. A. 2002. Skin transport. *Drugs and the Pharmaceutical Sciences. Dermatological and transdermal formulations*, 119, 89-195.
- Roberts, M. S. & Horlock, E. 1978. Effect of repeated skin application on percutaneous absorption of salicylic-acid. *Journal of Pharmaceutical Sciences*, 67, 1685-1687.
- Roberts, M.S. & Walker, M. 1993. Water the most natural penetration enhancer. In: Walters, K. A. & Hadgraft, J. editors. *Pharmaceutical Skin Penetration Enhancement*. New York: Marcel Dekker, 1-30.

- Romonchuk, W. J. & Bunge, A. L. 2006. Permeation of 4-cyanophenol and methyl paraben from powder and saturated aqueous solution through silicone rubber membranes and human skin. *Journal of Pharmaceutical Sciences*, 95, 2526-2533.
- Rosado, C., Cross, S. E., Pugh, W. J., Roberts, M. S. & Hadgraft, J. 2003. Effect of vehicle pretreatment on the flux, retention, and diffusion of topically applied penetrants in vitro. *Pharmaceutical Research*, 20, 1502-1507.
- Rossmill, J.D. & Hoekstra, W. G. 1966. Hexadecane-induced hyperkeratinization of guinea pig skin .3. Cutaneous penetration of topically applied hexadecane-1-c-14. *Journal of Investigative Dermatology*, 47, 39-43.
- Rougier, A., Lotte, C. & Maibach, H. I. 1987. In vivo percutaneous penetration of some organic-compounds related to anatomic site in humans - predictive assessment by the stripping method. *Journal of Pharmaceutical Sciences*, 76, 451-454.
- Rowe, R. C., Sheskey, P. J. & OWEN, S. C. 2006. Handbook of pharmaceutical excipients, London ; Greyslake, IL Washington, DC, Pharmaceutical Press, American Pharmacists Association.
- Roy, S. D. & Flynn, G. L. 1989. Transdermal delivery of narcotic analgesics - Comparative permeabilities of narcotic analgesics through human cadaver skin. *Pharmaceutical Research*, 6, 825-832.
- Russeau, W., Mitchell, J., Tetteh, J., Lane, M. E. & Hadgraft, J. 2009. Investigation of the permeation of model formulations and a commercial ibuprofen formulation in Carbosil (R) and human skin using ATR-FTIR and multivariate spectral analysis. *International Journal of Pharmaceutics*, 374, 17-25.
- Sabisz, M. & Skladanowski, A. 2008. Modulation of cellular response to anticancer treatment by caffeine: Inhibition of cell cycle checkpoints, DNA repair and more. *Current Pharmaceutical Biotechnology*, 9, 325-336.
- Santos, P., Machado, M., Watkinson, A. C., Hadgraft, J. & Lane, M. E. 2009. The effect of drug concentration on solvent activity in silicone membranes. *International Journal of Pharmaceutics*, 377, 70-75.
- Santos, P., Watkinson, A. C., Hadgraft, J. & Lane, M. E. 2010. Oxybutynin permeation in skin: The influence of drug and solvent activity. *International Journal of Pharmaceutics*, 384, 67-72.

- Santos, P., Watkinson, A. C., Hadgraft, J. & Lane, M. E. 2011. Formulation issues associated with transdermal fentanyl delivery. *International Journal of Pharmaceutics*, 416, 155-159.
- Santos, P., Watkinson, A. C., Hadgraft, J. & Lane, M. E. 2012. Influence of penetration enhancer on drug permeation from volatile formulations. *International Journal of Pharmaceutics*, 439, 260-8.
- Santus, G. C. & Baker, R. W. 1993. Transdermal enhancer patent literature. *Journal of Controlled Release*, 25, 1-20.
- Sarkaria, J. N., Busby, E. C., Tibbetts, R. S., Roos, P., Taya, Y., Karnitz, L. M. & Abraham, R. T. 1999. Inhibition of ATM and ATR kinase activities by the radiosensitizing agent, caffeine. *Cancer Research*, 59, 4375-4382.
- Saroj, S., Baby, D. A. & Sabitha, M. 2012. Current trends in lipid based delivery systems and its applications in drug delivery. *Asian Journal of Pharmaceutical and Clinical Research*, 5, 4-9.
- Sarraguca, M. C. & Lopes, J. A. 2009. Quality control of pharmaceuticals with NIR: From lab to process line. *Vibrational Spectroscopy*, 49, 204-210.
- Sawyer, J., Febbraro, S., Masud, S., Ashburn, M. A. & Campbell, J. C. 2009. Heated lidocaine/tetracaine patch (Synera (TM), Rapydan (TM)) compared with lidocaine/prilocaine cream (EMLA (R)) for topical anaesthesia before vascular access. *British Journal of Anaesthesia*, 102, 210-215.
- Schaefer, H. & Redelmeier, T. E. 1996. Skin barrier: Principles of percutaneous absorption. *Skin barrier: Principles of percutaneous absorption*. ISBN: 978-3-8055-6326-0.
- Schatzlein, A. & Cevc, G. 1998. Non-uniform cellular packing of the stratum corneum and permeability barrier function of intact skin: a high-resolution confocal laser scanning microscopy study using highly deformable vesicles (Transfersomes). *British Journal of Dermatology*, 138, 583-592.
- Scheuple.RJ 1967. Mechanism of percutaneous absorption .2. Transient diffusion and relative importance of various routes of skin penetration. *Journal of Investigative Dermatology*, 48, 79-88.
- Scheuple.RJ & Blank, I. H. 1971. Permeability of skin. *Physiological Reviews*, 51, 702-747.
- Scheuple.RJ, Blank, I. H., Brauner, G. J. & Macfarla.DJ 1969. Percutaneous absorption of steroids. *Journal of Investigative Dermatology*, 52, 63-70.

- Scheuplein, R. 1978. Skin as a barrier. In Jarrett, A. editors: *The Physiology and Pathophysiology of Skin* (Vol. 5). New York: Academic Press, pp. 1693-1730.
- Schmook, F. P., Meingassner, J. G. & Billich, A. 2001. Comparison of human skin or epidermis models with human and animal skin in in-vitro percutaneous absorption. *International Journal of Pharmaceutics*, 215, 51-56.
- Schmook, F. P., Stutz, A. & Reinhardt, J. 1993. Penetration of sandimmune (cyclosporine-a) in rat skin in-vitro - effects of penetration enhancers and solvents. *Skin Pharmacology*, 6, 116-124.
- Schreier, H. & Bouwstra, J. 1994. Liposomes and niosomes as topical drug carriers - dermal and transdermal drug-delivery. *Journal of Controlled Release*, 30, 1-15.
- Schuckler, F. & Lee, G. 1992. Relating the concentration-dependent action of azone and dodecyl-l-pyroglytamate on the structure of excised human stratum-corneum to changes in drug diffusivity, partition-coefficient and flux. *International Journal of Pharmaceutics*, 80, 81-89.
- Schwarb, F. P., Imanidis, G., Smith, E. W., Haigh, J. M. & Surber, C. 1999. Effect of concentration and degree of saturation of topical fluocinonide formulations on in vitro membrane transport and in vivo availability on human skin. *Pharmaceutical Research*, 16, 909-915.
- Scott, R. C., Batten, P. L., Clowes, H. M., Jones, B. K. & Ramsey, J. D. 1992. Further validation of an invitro method to reduce the need for invivo studies for measuring the absorption of chemicals through rat skin. *Fundamental and Applied Toxicology*, 19, 484-492.
- Scott, R. C., Walker, M. & Dugard, P. H. 1986. A comparison of the invitro permeability properties of human and some laboratory-animal skins. *International Journal of Cosmetic Science*, 8, 189-194.
- Selzer, D., Abdel-Mottaleb, M. M. A., Hahn, T., Schaefer, U. F. & Neumann, D. 2013. Finite and infinite dosing: Difficulties in measurements, evaluations and predictions. *Advanced Drug Delivery Reviews*, 65, 278-294.
- Sethna, N. F., Verghese, S. T., Hannallah, R. S., Solodiuk, J. C., Zurakowski, D. & Berde, C. B. 2005. A randomized controlled trial to evaluate S-Caine Patch (TM) for reducing pain associated with vascular access in children. *Anesthesiology*, 102, 403-408.

- Shah, J. C. 1993. Analysis of permeation data - evaluation of the lag time method. *International Journal of Pharmaceutics*, 90, 161-169.
- Shah, K. A., Date, A. A., Joshi, M. D. & Patravale, V. B. 2007. Solid lipid nanoparticles (SLN) of tretinoin: Potential in topical delivery. *International Journal of Pharmaceutics*, 345, 163-171.
- Shah, V. P. 1994. Skin penetration enhancers: Scientific perspectives. *Drugs and the Pharmaceutical Sciences; Drug permeation enhancement: Theory and applications*, 62, 19-23.
- Shah, V. P., Elkins, J., Lam, S. Y. & Skelly, J. P. 1989. Determination of invitro drug release from hydrocortisone creams. *International Journal of Pharmaceutics*, 53, 53-59.
- Shakeel, F. & Ramadan, W. 2010. Transdermal delivery of anticancer drug caffeine from water-in-oil nanoemulsions. *Colloids and Surfaces B-Biointerfaces*, 75, 356-362.
- Sharata, H. & Burnette, R. R. 1989. Percutaneous absorption of electron-dense ions across normal and chemically perturbed skin. *Journal of Pharmaceutical Sciences*, 77, 27-32.
- Sherry, M., Charcosset, C., Fessi, H. & Greige-Gerges, H. 2013. Essential oils encapsulated in liposomes: a review. *Journal of Liposome Research*, 23, 268-275.
- Shi, J., Wang, Y. & Luo, G. 2012. Ligustrazine Phosphate Ethosomes for Treatment of Alzheimer's Disease, In Vitro and in Animal Model Studies. *Aaps Pharmscitech*, 13, 485-492.
- Shi, S., Ashley, E. S. D., Alexander, B. D. & Hickey, A. J. 2009. Initial Characterization of Micafungin Pulmonary Delivery via Two Different Nebulizers and Multivariate Data Analysis of Aerosol Mass Distribution Profiles. *AAPS Pharmscitech*, 10, 129-137.
- Shin, S. C. & Byun, S. Y. 1996. Controlled release of ethinylestradiol from ethylene-vinyl acetate membrane. *International Journal of Pharmaceutics*, 137, 95-102.
- Shiyab, S., Shatnawi, M., Shibli, R., Alzweiri, M., Akash, M. & Aburjai, T., 2012. Influence of developmental stage on yield and composition of *Origanum syriacum* L. oil by multivariate analysis. *Journal of Medicinal Plants Research*, 6, 2985-2994.
- Siepmann, J. & Peppas, N. A. 2011. Higuchi equation: Derivation, applications, use and misuse. *International Journal of Pharmaceutics*, 418, 6-12.
- Silva, C. L., Nunes, S. C. C., Eusebio, M. E. S., Pais, A. & Sousa, J. J. S. 2006. Thermal behaviour of human stratum corneum - A differential scanning calorimetry study at high scanning rates. *Skin Pharmacology and Physiology*, 19, 132-139.

- Singh, S. & Singh, J. 1993. Transdermal drug-delivery by passive diffusion and iontophoresis - A review. *Medicinal Research Reviews*, 13, 569-621.
- Singh, S., Zhao, K. & Singh, J. 2002. In vitro permeability and binding of hydrocarbons in pig ear and human abdominal skin. *Drug and Chemical Toxicology*, 25, 83-92.
- Sinico, C., Manconi, M., Peppi, M., Lai, F., Valenti, D. & Fadda, A. M. 2005. Liposomes as carriers for dermal delivery of tretinoin: in vitro evaluation of drug penetration and vesicle-skin interaction. *Journal of Controlled Release*, 103, 123-136.
- Sinko, B., Garrigues, T. M., Balogh, G. T., Nagy, Z. K., Tsinman, O., Avdeef, A. & Takacs-Novak, K. 2012. Skin-PAMPA: A new method for fast prediction of skin penetration. *European Journal of Pharmaceutical Sciences*, 45, 698-707.
- Sinko, B., Koekoesi, J., Avdeef, A. & Takacs-Novak, K. 2009. A PAMPA Study of the Permeability-Enhancing Effect of New Ceramide Analogues. *Chemistry & Biodiversity*, 6, 1867-1874.
- Sintov, A. C. & Shapiro, L. 2004. New microemulsion vehicle facilitates percutaneous penetration in vitro and cutaneous drug bioavailability in vivo. *Journal of Controlled Release*, 95, 173-183.
- Sloan, K. B., Dellavecchia, S. A., Estes, J. V. & Roberts, W. J. 2000. 7-alkylcarbonyl and 7-alkyloxycarbonyl prodrugs of theophylline. *International Journal of Pharmaceutics*, 205, 53-63.
- Sloan, K. B., Koch, S. A. M., Siver, K. G. & Flowers, F. P. 1986a. Use of solubility parameters of drug and vehicle to predict flux through skin. *Journal of Investigative Dermatology*, 87, 244-252.
- Sloan, K. B., Siver, K. G. & Koch, S. A. M. 1986b. The effect of vehicle on the diffusion of salicylic acid through hairless mouse skin. *Journal of Pharmaceutical Sciences*, 75, 744-749.
- Sloan, K. B., Synovec, J. & Ketha, H. 2013. A surrogate for topical delivery in human skin: silicone membranes. *Therapeutic delivery*, 4, 203-24.
- Sloan, K. B. & Wasdo, S. 2003. Designing for topical delivery: Prodrugs can make the difference. *Medicinal Research Reviews*, 23, 763-793.

- Sloan, K. B., Wasdo, S., Ezike-Mkparu, U., Murray, T., Nickels, D., Singh, S., Shanks, T., Tovar, J., Ulmer, K. & Waranis, R. 2003. Topical delivery of 5-fluorouracil and 6-mercaptopurine by their alkylcarbonyloxymethyl prodrugs from water: Vehicle effects on design of prodrugs. *Pharmaceutical Research*, 20, 639-645.
- Smith, C. K. & Hotchkiss, S. A. M. 2001. Allergic contact dermatitis : chemical and metabolic mechanisms, London, Taylor & Francis.
- Smith, E. W. & Maibach, H. I. 1995. Percutaneous penetration enhancers, Boca Raton ; London, CRC Press.
- Song, C. J. & Liu, S. X. 2005. A new healthy sunscreen system for human: Solid lipid nanoparticles as carrier for 3,4,5-trimethoxybenzoylchitin and the improvement by adding Vitamin E. *International Journal of Biological Macromolecules*, 36, 116-119.
- Soni, M. G., Taylor, S. L., Greenberg, N. A. & Burdock, G. A. 2002. Evaluation of the health aspects of methyl paraben: a review of the published literature. *Food and Chemical Toxicology*, 40, 1335-1373.
- StamataS, G. N., De Sterke, J., Hauser, M., Von Stetten, O. & VanDer Pol, A. 2008. Lipid uptake and skin occlusion following topical application of oils on adult and infant skin. *Journal of Dermatological Science*, 50, 135-142.
- Steinstrasser, I. & Merkle, H. P. 1995. Dermal metabolism of topically applied drugs: pathways and models reconsidered. *Pharmaceutica acta Helvetiae*, 70, 3-24.
- Storm, J. E., Collier, S. W., Stewart, R. F. & Bronaugh, R. L. 1990. Metabolism of xenobiotics during percutaneous penetration - Role of absorption rate and cutaneous enzyme-activity. *Fundamental and Applied Toxicology*, 15, 132-141.
- Strasinger, C. L., Scheff, N. N. & Stinchcomb, A. L. 2008. Prodrugs and codrugs as strategies for improving percutaneous absorption. *Expert Reviews Dermatology*, 3, 221–233.
- Su, J. T., Duncan, P. B., Momaya, A., Jutila, A. & Needham, D. 2010. The effect of hydrogen bonding on the diffusion of water in n-alkanes and n-alcohols measured with a novel single microdroplet method. *Journal of Chemical Physics*, 132, 044506,1-044506,9.
- Suhonen, T. M., Bouwstra, J. A. & Urtti, A. 1999. Chemical enhancement of percutaneous absorption in relation to stratum corneum structural alterations. *Journal of Controlled Release*, 59, 149-161.

- Swanson, H. I. 2004. Cytochrome P450 expression in human keratinocytes: an aryl hydrocarbon receptor perspective. *Chemico-Biological Interactions*, 149, 69-79.
- Swarbrick, B. 2001. *Multivariate Data Analysis. CAMO® Software Special Edition* Oslo, Norway.
- Swarbrick, J., Lee, G. & Brom, J. 1982. Drug permeation through human-skin .1. Effect of storage-conditions of skin. *Journal of Investigative Dermatology*, 78, 63-66.
- Takahashi, A., Suzuki, S., Kawasaki, N., Kubo, W., Miyazaki, S., Loebenberg, R., Bachynsky, J. & Attwood, D. 2002. Percutaneous absorption of non-steroidal anti-inflammatory drugs from in situ gelling xyloglucan formulations in rats. *International Journal of Pharmaceutics*, 246, 179-186.
- Takeuchi, H. 1990. A jump motion of small molecules in glassy-polymers - a molecular-dynamics simulation. *Journal of Chemical Physics*, 93, 2062-2067.
- Tanojo, H., Bouwstra, J. A., Junginger, H. E. & Bodde, H. E. 1997. In vitro human skin barrier modulation by fatty acids: Skin permeation and thermal analysis studies. *Pharmaceutical Research*, 14, 42-49.
- Taylor, H. E. & Sloan, K. B. 1998. 1-alkylcarbonyloxymethyl prodrugs of 5-fluorouracil (5-FU): Synthesis, physicochemical properties, and topical delivery of 5-FU. *Journal of Pharmaceutical Sciences*, 87, 15-20.
- Testa, B., Carrupt, P. A., Gaillard, P., Billois, F. & Weber, P. 1996. Lipophilicity in molecular modeling. *Pharmaceutical Research*, 13, 335-343.
- Thomas, J. D., Majumdar, S. & Sloan, K. B. 2009. Soft alkyl ether prodrugs of a model phenolic drug: the effect of incorporation of ethyleneoxy groups on transdermal delivery. *Molecules*, 14, 4231-4245.
- Thomas, N. S. & Panchagnula, R. 2003. Transdermal delivery of zidovudine: effect of vehicles on permeation across rat skin and their mechanism of action. *European Journal of Pharmaceutical Sciences*, 18, 71-79.
- Tojo, K., Valia K. H. & Chien, Y. W. 1986. Transdermal drug delivery by prodrug bioconversion. *Proc 3rd World Congress of Chem Eng Tokyo*, 1085-1088.
- Tojo, K. & Lee, A. R. C. 1991. Penetration and bioconversion of drugs in the skin. *Journal of Chemical Engineering of Japan*, 24, 297-300.

- Tokudome, Y. & Sugibayashi, K. 2003. The synergic effects of various electrolytes and electroporation on the in vitro skin permeation of calcein. *Journal of Controlled Release*, 92, 93-101.
- Tomita, K. & Tsuchiya, H. 1989. Caffeine enhancement of the effect of anticancer agents on human sarcoma-cells. *Japanese Journal of Cancer Research*, 80, 83-88.
- Toole, J., Silagy, S., Maric, A., Fath, B., Quebe-Fehling, E., DePalacios, P. I., Laurin, L. & Giguere, M. 2002. Evaluation of irritation and sensitisation of two 50 microg/day oestrogen patches. *Maturitas*, 43, 257-263.
- Touitou, E., Dayan, N., Bergelson, L., Godin, B. & Eliaz, M. 2000. Ethosomes - novel vesicular carriers for enhanced delivery: characterization and skin penetration properties. *Journal of Controlled Release*, 65, 403-418.
- Touitou, E., Godin, B., Dayan, N., Weiss, C., Piliponsky, A. & Levi-Schaffer, F. 2001. Intracellular delivery mediated by an ethosomal carrier. *Biomaterials*, 22, 3053-3059.
- Touitou, E., Junginger, H. E., Weiner, N. D., Nagai, T. & Mezei, M. 1994. Liposomes as carriers for topical and transdermal delivery. *Journal of Pharmaceutical Sciences*, 83, 1189-1203.
- Tracy, N. D., Young, J. C. & Mason, R. L. 1992. Multivariate control charts for individual observations. *Journal of Quality Technology*, 24, 88-95.
- Treffel, P., Muret, P., Muretdaniello, P., Coumesmarquet, S. & Agache, P. 1992. Effect of occlusion on invitro percutaneous-absorption of 2 Compounds with different physicochemical properties. *Skin Pharmacology*, 5, 108-113.
- Trotta, M., Ugazio, E., Peira, E. & Pulitano, C. 2003. Influence of ion pairing on topical delivery of retinoic acid from microemulsions. *Journal of Controlled Release*, 86, 315-321.
- Tsai, J. C., Guy, R. H., Thornfeldt, C. R., Gao, W. N., Feingold, K. R. & Elias, P. M. 1996. Metabolic approaches to enhance transdermal drug delivery .1. Effect of lipid synthesis inhibitors. *Journal of Pharmaceutical Sciences*, 85, 643-648.
- Tsai, J. C., Lin, C. Y., Sheu, H. M., Lo, Y. L. & Huang, Y. H. 2003. Noninvasive characterization of regional variation in drug transport into human stratum corneum in vivo. *Pharmaceutical Research*, 20, 632-638.

- Tsong, Y., Hammerstrom, T. & Chen, J. J. 1997. Multipoint dissolution specification and acceptance sampling rule based on profile modeling and principal component analysis. *Journal of Biopharmaceutical Statistics*, 7, 423-39.
- Twist, J. N. & Zatz, J. L. 1986. Influence of solvents on paraben permeation through idealized skin model membranes. *Journal of the Society of Cosmetic Chemists*, 37, 429-444.
- Twist, J. N. & Zatz, J. L. 1988a. Characterization of solvent-enhanced permeation through a skin model membrane. *Journal of the Society of Cosmetic Chemists*, 39, 324-324.
- Twist, J. N. & Zatz, J. L. 1988b. Membrane solvent solute interaction in a model permeation system. *Journal of Pharmaceutical Sciences*, 77, 536-540.
- Twist, J. N. & Zatz, J. L. 1990. A model for alcohol-enhanced permeation through polydimethylsiloxane membranes. *Journal of Pharmaceutical Sciences*, 79, 28-31.
- Vaddi, H. K., Banks, S. L., Chen, J., Hammell, D. C., Crooks, P. A. & Stinchcomb, A. L. 2009. Human Skin Permeation of 3-O-Alkyl Carbamate Prodrugs of Naltrexone. *Journal of Pharmaceutical Sciences*, 98, 2611-2625.
- Vaddi, H. K., Ho, P. C. & Chan, S. Y. 2002. Terpenes in propylene glycol as skin-penetration enhancers: Permeation and partition of haloperidol, fourier transform infrared spectroscopy, and differential scanning calorimetry. *Journal of Pharmaceutical Sciences*, 91, 1639-1651.
- Valenta, C., Siman, U., Kratzel, M. & Hadgraft, J. 2000. The dermal delivery of lignocaine: influence of ion pairing. *International Journal of Pharmaceutics*, 197, 77-85.
- Van De Sandt, J. J. M., Van Burgsteden, J. A., Cage, S., Carmichael, P. L., Dick, I., Kenyon, S., Korinth, G., Larese, F., Limasset, J. C., Maas, W. J. M., Montomoli, L., Nielsen, J. B., Payan, J. P., Robinson, E., Sartorelli, P., Schaller, K. H., Wilkinson, S. C. & Williams, F. M. 2004. In vitro predictions of skin absorption of caffeine, testosterone, and benzoic acid: a multi-centre comparison study. *Regulatory Toxicology and Pharmacology*, 39, 271-281.
- Van Der Merwe, D. & Riviere, J. E. 2005. Comparative studies on the effects of water, ethanol and water/ethanol mixtures on chemical partitioning into porcine stratum corneum and silastic membrane. *Toxicology in Vitro*, 19, 69-77.
- Van Ravenzwaay, B. & Leibold, E. 2004. A comparison between in vitro rat and human and in vivo rat skin absorption studies. *Human & Experimental Toxicology*, 23, 421-430.

Vasile M., Iulian C. & Anca-Florentina B. 2012. Stationary Phases, Advanced Gas Chromatography - Progress in Agricultural, Biomedical and Industrial Applications, Dr. Mustafa Ali Mohd (Ed.), Chapter Two. ISBN: 978-953-51-0298-4.

Venkatraman, S. & Gale, R. 1998. Skin adhesives and skin adhesion 1. Transdermal drug delivery systems. *Biomaterials*, 19, 1119-1136.

Wang, M. Y., Yang, Y. Y. & Heng, P. W. S. 2004a. Role of solvent in interactions between fatty acids-based formulations and lipids in porcine stratum corneum. *Journal of Controlled Release*, 94, 207-216.

Wang, R., ;Li, D. F., Zhou, C., Liu, M. & Liang, D. T. 2004b. Impact of DEA solutions with and without CO₂ loading on porous polypropylene membranes intended for use as contactors. *Journal of Membrane Science*, 229, 147-157.

Wang, Y. P., Fan, Q. X., Song, Y. F. & Michniak, B. 2003. Effects of fatty acids and iontophoresis on the delivery of midodrine hydrochloride and the structure of human skin. *Pharmaceutical Research*, 20, 1612-1618.

Waranis, R. P., Siver, K. G. & Sloan, K. B. 1987. The solubility parameter of vehicles as a predictor of relative vehicle effects on the diffusion of 6-mercaptopurine. *International Journal of Pharmaceutics*, 36, 211-222.

Warner, R. R., Myers, M. C. & Taylor, D. A. 1988. Electron-probe analysis of human-skin - determination of the water concentration profile. *Journal of Investigative Dermatology*, 90, 218-224.

Wasdo, S. C., Juntunen, J., Devarajan, H. & Sloan, K. B. 2009. A correlation of flux through a silicone membrane with flux through hairless mouse skin and human skin in vitro. *International Journal of Pharmaceutics*, 373, 62-67.

Watkinson, A. C., Joubin, H., Green, D. M., Brain, K. R. & Hadgraft, J. 1995. The influence of vehicle on permeation from saturated solutions. *International Journal of Pharmaceutics*, 121, 27-36.

Watkinson, R. M., Guy, R. H., Hadgraft, J. & Lane, M. E. 2009a. Optimisation of Cosolvent Concentration for Topical Drug Delivery - II: Influence of Propylene Glycol on Ibuprofen Permeation. *Skin Pharmacology and Physiology*, 22, 225-230.

- Watkinson, R. M., Herkenne, C., Guy, R. H., Hadgraft, J., Oliveira, G. & Lane, M. E. 2009b. Influence of Ethanol on the Solubility, Ionization and Permeation Characteristics of Ibuprofen in Silicone and Human Skin. *Skin Pharmacology and Physiology*, 22, 15-21.
- Weerheim, A. & Ponc, M. 2001. Determination of stratum corneum lipid profile by tape stripping in combination with high-performance thin-layer chromatography. *Archives of Dermatological Research*, 293, 191-199.
- Wertz, P. W. 1992. Epidermal lipids. *Seminars in Dermatology*, 11, 106-113.
- Wertz, P. W. 2000. Lipids and barrier function of the skin. *Acta Dermato-Venereologica*, 7-11.
- Wester, R. C., Christoffel, J., Hartway, T., Poblete, N., Maibach, H. I. & Forsell, J. 1998. Human cadaver skin viability for in vitro percutaneous absorption: Storage and detrimental effects of heat-separation and freezing. *Pharmaceutical Research*, 15, 82-84.
- Wiechers, J. W., Drenth, B. F. H., Jonkman, J. H. G. & Dezeuw, R. A. 1987. Percutaneous-absorption and elimination of the penetration enhancer azone in humans. *Pharmaceutical Research*, 4, 519-523.
- Wilkinson, S. C. & Williams, F. M. 2002. Effects of experimental conditions on absorption of glycol ethers through human skin in vitro. *International Archives of Occupational and Environmental Health*, 75, 519-527.
- Williams, A. 2003. *Transdermal and topical drug delivery: from theory to clinical practice*, London, Pharmaceutical Press.
- Williams, A. C. & Barry, B. W. 2004. Penetration enhancers. *Advanced Drug Delivery Reviews*, 56, 603-618.
- Williams, A. C. & Barry, B. W. 2012. Penetration enhancers. *Advanced Drug Delivery Reviews*, 64, 128-137.
- Williams, A. C., Cornwell, P. A. & Barry, B. W. 1992. On the non-gaussian distribution of human skin permeabilities. *International Journal of Pharmaceutics*, 86, 69-77.
- Williams, F. M. 2006. In vitro studies - how good are they at replacing in vivo studies for measurement of skin absorption? *Environmental Toxicology and Pharmacology*, 21, 199-203.

- Wilschut, A., Tenberge, W. F., Robinson, P. J. & Mckone, T. E. 1995. Estimating skin permeation - The validation of 5 mathematical skin permeation models. *Chemosphere*, 30, 1275-1296.
- Wissing, S. A. & Mueller, R. H. 2001. A novel sunscreen system based on tocopherol acetate incorporated into solid lipid nanoparticles. *International Journal of Cosmetic Science*, 23, 233-243.
- Wissing, S. A. & Muller, R. H. 2002. The development of an improved carrier system for sunscreen formulations based on crystalline lipid nanoparticles. *International Journal of Pharmaceutics*, 242, 373-375.
- Wohlrab, J., Beck, G. M., Neubert, R. H. H., Sischka, U. & Kreft, B. 2010. Hydrocortisone Aceponate Activity and Benefit/Risk Ratio in Relation to Reference Topical Glucocorticoids. *Skin Pharmacology and Physiology*, 23, 177-182.
- Wold, S., Esbensen, K. & Geladi, P. 1987. Principal component analysis. *Chemometrics and Intelligent Laboratory Systems*, 2, 37-52.
- Wold, S. & Sjostrom, M. 1998. Chemometrics, present and future success. *Chemometrics and Intelligent Laboratory Systems*, 44, 3-14.
- Wold, S. & Sjöström, M. 1998. Chemometrics, present and future success. *Chemometrics and Intelligent Laboratory Systems*.
- Wood, D. G., Brown, M. B. & Jones, S. A. 2012. Understanding heat facilitated drug transport across human epidermis. *European Journal of Pharmaceutics and Biopharmaceutics*, 81, 642-649.
- Wotton, P. K., Mollgaard, B., Hadgraft, J. & Hoelgaard, A. 1985. Vehicle effect on topical drug delivery .3. Effect of azone on the cutaneous permeation of metronidazole and propylene-glycol. *International Journal of Pharmaceutics*, 24, 19-26.
- Xie, L., Wu, H., Shen, M., Augsburger, L. L., Lyon, R. C., Khan, M. A., Hussain, A. S. & Hoag, S. W. 2008. Quality-by-design (QbD): Effects of testing parameters and formulation variables on the segregation tendency of pharmaceutical powder measured by the ASTM D 6940-04 segregation tester. *Journal of Pharmaceutical Sciences*, 97, 4485-4497.
- Yamada, M., Uda, Y. & Tanigawara, Y. 1987. Mechanism of enhancement of percutaneous-absorption of molsidomine by oleic-acid. *Chemical & Pharmaceutical Bulletin*, 35, 3399-3406.

- Yamashita, F. & Hashida, M. 2003. Mechanistic and empirical modeling of skin permeation of drugs. *Advanced Drug Delivery Reviews*, 55, 1185-1199.
- Yang, F.-K., Zhang, Z.-T. & Chen, F. 2008. The method for analysis of hydrocarbon mixtures C-1-C-5 by capillary column gas chromatography. *Journal of the Chinese Chemical Society*, 55, 675-677.
- Yang, S. I., Park, H. Y., Lee, S. H., Lee, S. J., Han, O. Y., Lim, S. C., Jang, C. G., Lee, W. S., Shin, Y. H., Kim, J. J. & Lee, S. Y. 2004a. Transdermal eperisone elicits more potent and longer-lasting muscle relaxation than oral eperisone. *Pharmacology*, 71, 150-156.
- Yang, Y. R., Huang, Y. M., Wang, D. N., Lu, H. L. & Hu, C. P. 2004b. Sorption and diffusion of ethanol vapor in polybutadiene/acrylonitrile, polybutadiene/styrene and polybutadiene based polyurethanes. *European Polymer Journal*, 40, 855-863.
- Yano, T., Nakagawa, A., Tsuji, M. & Noda, K. 1986. Skin permeability of various nonsteroidal anti-inflammatory drugs in man. *Life Sciences*, 39, 1043-1050.
- Yener G., Dal, Ö. & Üner, M. 2009. Effect of vehicles on release meloxicam from various of topical formulations. *The Open Drug Delivery Journal*, 3, 19-23.
- Yi, Z.-B., Yu, Y., Liang, Y.-Z. & Zeng, B. 2007. Evaluation of the antimicrobial mode of berberine by LC/ESI-MS combined with principal component analysis. *Journal of Pharmaceutical and Biomedical Analysis*, 44, 301-304.
- Yosipovitch, G., Maayan-Metzger, A., Merlob, P. & Sirota, L. 2000. Skin barrier properties in different body areas in neonates. *Pediatrics*, 106, 105-108.
- Young, R. C., Mitchell, R. C., Brown, T. H., Ganellin, C. R., Griffiths, R., Jones, M., Rana, K. K., Saunders, D., Smith, I. R., Sore, N. E. & Wilks, T. J. 1988. Development of a new physicochemical model for brain penetration and its application to the design of centrally acting h-2-receptor histamine-antagonists. *Journal of Medicinal Chemistry*, 31, 656-671.
- Zadeh, B. S. M., Moghimi, H., Santos, P., Hadgraft, J. & Lane, M. E. 2008. A comparative study of the in vitro permeation characteristic of sulphadiazine across synthetic membranes and eschar tissue. *International Wound Journal*, 5, 633-638.
- Zellmer, S., Pfeil, W. & Lasch, J. 1995. Interaction of phosphatidylcholine liposomes with the human stratum-corneum. *Biochimica Et Biophysica Acta-Biomembranes*, 1237, 176-182.

Zhai, H. & Maibach, H.I. 2005. Effects of occlusion: Percutaneous absorption: (Percutaneous Absorption: Drugs, Cosmetics, Mechanism, Methods, Bronaugh R.L& Maibach H.I Informa healthcare, Hoboken, ISBN: 9780849359033, 235–243.

Zhang, Q., Grice, J. E., Li, P., Jepps, O. G., Wang, G.-J. & Roberts, M. S. 2009. Skin Solubility Determines Maximum Transepidermal Flux for Similar Size Molecules. *Pharmaceutical Research*, 26, 1974-1985.

Zhang, Q., Li, P. & Roberts, M. S. 2011. Maximum transepidermal flux for similar size phenolic compounds is enhanced by solvent uptake into the skin. *Journal of Controlled Release*, 154, 50-57.